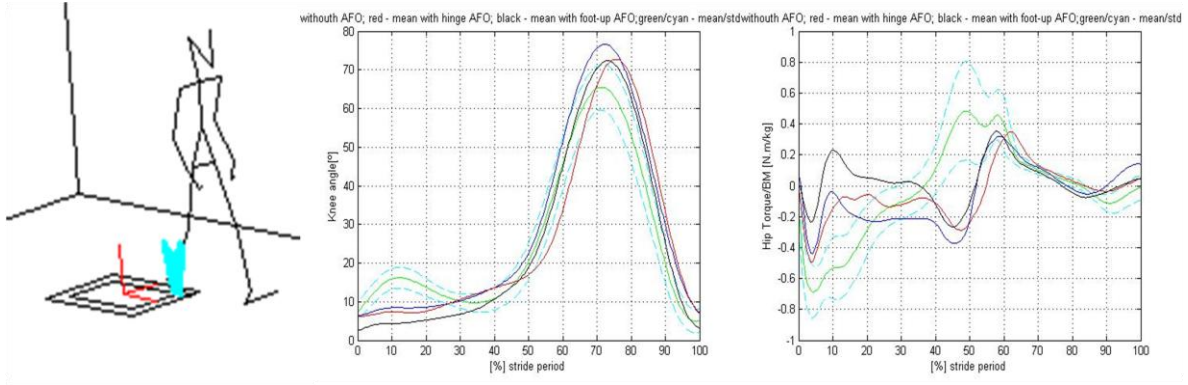INSTITUTO SUPERIOR TÉCNICO
Universidade Técnica de Lisboa

FACULDADE DE MEDICINA
Universidade de Lisboa

Advanced Computer Methods for Pathological and Non-Pathological Human Movement Analysis

Sérgio Miguel Barroso Gonçalves

Dissertação para obtenção do Grau de Mestre em

Engenharia Biomédica

Júri

Presidente: Prof. Doutor Hélder Rodrigues
Orientadores: Prof. Doutor Miguel Pedro Tavares da Silva
                     Prof. Doutor Jorge Manuel Mateus Martins
                     Prof. Doutor Mamede Carvalho
Vogais: Prof. Doutor Jorge Alberto Cadete Ambrósio
                     Prof. Doutor João Nuno Marques Parracho Guerra da Costa

Outubro 2010

Agradecimentos

II

Resumo

O objectivo principal deste trabalho passou por estudar os padrões da marcha humana não-patológica e patológica. Desta forma, foi necessário desenvolver um protocolo de análise da marcha humana, projectado para analisar uma grande variedade de parâmetros biomecânicos do movimento humano. O protocolo desenvolvido consistiu numa metodologia eficaz e eficiente para preparação do paciente e do ambiente laboratorial, permitindo a análise dos parâmetros, cinemáticos, cinéticos, electromiográficos, temporais e espaciais. A metodologia desenvolvida incluiu um protocolo de colocação de marcadores, de electromiografia e de aquisição de ensaios. Foram também desenvolvidas uma série de rotinas que permitiram automatizar o processamento de dados, com a finalidade de gerar uma base de dados de marcha não-patológica. A análise cinética recorreu ao uso de um software de análise dinâmica multicorpo – Apollo.

Seguidamente, a metodologia desenvolvida foi aplicada na aquisição de padrões de marcha de três grupos não-patológicos representativos da população portuguesa (crianças, adultos do sexo masculino e adultos do sexo feminino). Os resultados obtidos foram comparados com trabalhos anteriores, observando-se resultados concordantes com estes. Desta forma, a metodologia utilizada foi validada, obtendo-se uma base de dados de padrões de marcha para utilização em futuros estudos, como em reabilitação física e análise clínica.

Por fim, foram estudados dois sujeitos com patologias de marcha e comparados os seus resultados com a população padrão. Esses estudos incluíram ensaios com e sem as suas ortóteses. Uma vez mais, esta análise permitiu comprovar a boa aplicabilidade da metodologia desenvolvida, uma vez que os resultados obtidos encontravam-se concordantes com a literatura.

Palavras-chave: Análise da marcha humana não-patológica, análise da marcha humana marcha patológica, análise cinemática e dinâmica da marcha, análise electromiográfica da marcha, protocolos de análise de marcha, biomecânica

Abstract

The main objective of this work was to analyze the main human patterns of non-pathological and pathological gait. In order to achieve this objective, it was necessary to develop a protocol of gait analysis designed to withstand a vast range of biomechanical aspects of the human motion. The protocol's desiderata consists of an effective and efficient methodology for subject instrumentation and laboratory setup, enabling the study of time-distance, kinematic, kinetic and electromyographic parameters. The proposed methodology includes a marker set protocol, a superficial electromyographic protocol and a trial acquisition protocol. Moreover, in order to automate the data processing and generate a database of non-pathological patterns a set of routines was developed. The kinetic analysis recurred to the use of the multibody dynamics software – Apollo.

In a second part, the developed methodology was applied in the analysis of the gait parameters of three non-pathological groups representing the Portuguese population – children, male adult and female adult. The obtained results were compared with previous works, presenting the expected pattern. Thus, the used methodology was approved, but also allowed obtaining the gait patterns for a sample of the Portuguese population, which can be used in future studies, such as clinical analysis and physical rehabilitation.

Lastly, two pathological subjects were analyzed and their results compared with the normal obtained patterns. In these studies, it was studied the subjects' gait with and without their orthoses. Once more, the developed methodology was approved, since the obtained results were in concordance with literature.

Keywords: Analysis of non-pathological human gait, analysis of pathological human gait, kinematic and kinetic analysis of gait, electromyographic analysis of gait, gait acquisition protocols, biomechanics

Contents

X

List of Figures

List of Tables

List of Symbols

$\boldsymbol{\theta_a}$ – ankle angle

$\boldsymbol{\theta_{ft}}$ – foot angle

$\boldsymbol{\theta_h}$ – hip angle

$\boldsymbol{\theta_k}$ – knee angle

$\boldsymbol{\theta_{lg}}$ – leg angle

$\boldsymbol{\theta_{th}}$ – thigh angle

F_X – anterior-posterior component of GRFs

F_Y – medial-lateral component of GRFs

F_Z – vertical component of GRFs

W_{lead} – work of leading leg

W_{trail} – work of trailing leg

$\boldsymbol{q}$ – vector of generalized coordinates

$\dot{\mathbf{q}}$ – vector of generalized velocities

$\ddot{\mathbf{q}}$ – vector of generalized accelerations

$\boldsymbol{\Phi}$ – kinematic constraints expressions

$\boldsymbol{\Phi_q}$ – jaciobian matrix of in order to q

$\boldsymbol{v}$ – Right-hand-side of the velocity equation

$\boldsymbol{\gamma}$ – Right-hand-side of the acceleration equation

P^* - virtual power produced by the external forces

$\mathbf{f}$ – vector of all forces that produce virtual power (external and inertial forces)

$\mathbf{g}$ – vector of generalized force

$\mathbf{g}^*$ – vector of the generalized forces that contains the internal constraint forces

$\boldsymbol{\lambda}$ – vector of Lagrange multipliers

$\mathbf{M}$ – global mass matrix

α, β – parameters of the Baumgarte method

$\boldsymbol{\rho}$ – rigid body density

Ω – rigid body volume

$\mathbf{r}$ – global coordinates of point P

$\dot{\mathbf{r}}$ – virtual velocity of the generic point P

$\ddot{\mathbf{r}}$ – virtual acceleration of the generic point P

$\mathbf{u}, \mathbf{v}, \mathbf{w}$ – two non-coplanar unit vectors

$\mathbf{c}$ – vector containing previous coefficients c_1, c_2 and c_3

$\mathbf{C}$ – coordinate transformation matrix

$\overline{\mathbf{X}}$ - matrix containing the components of the vector $(\overline{\mathbf{r}} - \overline{\mathbf{r_i}})$

$\mathbf{I}$ – identity matrix

θ_i - angle of the ith body segment

$\mathbf{o}$ – unit vector

$\mathbf{p}_i$ – vector which defines the orientation of the body segment i

ω – angular velocity

M_j – moment-of-joint of jth joint

P_j – mechanical power of jth joint

W^+ – positive work

W^+ – negative work

Glossary

3D – Three-dimensional

AFO – Ankle-foot orthosis

ASIS – Anterior Superior Iliac Spine

BW – Body Weight

CNS – Central nervous system

COM – Center of Mass

COP – Center of Pressure

CGPs – Central Pattern Generating Networks

DOF – Degrees-of-Freedom

EC – End of Contact

EMG – Electromyography

EMSP – Extensive Marker Set Protocol

FF – Foot Flat

GC – Gait Cycle

GRF – Ground Reaction Force

HAT – Head Arms and Trunk

HC – Heel Contact

HH – Helen Hayes maker set

HO – Heel Off

IC – Initial Contact

ISB – International Society of Biomechanics

ISEK – International Society of Electrophysiology and Kinesiology

LBL – Laboratório Biomecânico de Lisboa

LIC – Left Iliac Crest

MR – Metabolic Rate

MS – Mid Stance

MSP – marker set protocol

MSw – Mid Swing

NR – Newton-Raphson

PNS – Peripheral Nervous System

PO – Push-Off

PSIS – Posterior Superior Iliac Spine

QTM – Qualisys Track Manager

RIC – Right Iliac Crest

sEMG – Superficial Electromyography

SENIAN - Surface ElectroMyoGraphy for the Non-Invasive Assessment of Muscles

SEP – Superficial Electromyography Protocol

SESP – Superficial Electronyograophy set protocol

TO – Toe-Off

WA – Weight Acceptance

Chapter I

Introduction

1.1. Motivation

Doubtless, the twentieth century was marked by several important advances in the scientific area and gait analysis followed this tendency. The study of human locomotion reached the pinnacle with the great number of works published throughout this century and the application of the acquired knowledge to clinical analyses and diagnose. Defining gait is not easy, although almost all humans perform this motion every day. It is characterized by a set of movement patterns, whose understanding becomes essential not only to comprehend the walking mechanisms but also to allow the study of different pathologies. Sutherland stated that the application of gait in clinical brought a new approach in the treatment of subjects with neuropathologies, such as cerebral palsy (Sutherland 2001).

The clinical application of gait analysis allowed the development of new operations for neuropathological subjects as well as the development of biomedical devices such as prostheses and orthoses, which besides to the anatomo-physiological function that these confer, are more effective in the improvement of the quality of life of patients. These devices have increasingly been customized to the needs of each subject, taking into account their comfort and ergonomics. The field of gait analysis makes possible the better understanding of these problems using quick and noninvasive analysis methods. Essentially, the study of human gait considers four different areas: 1) Time-distance parameters – provide the temporal and distance information such as the stride/step time, step/stride length, velocity, cadence, etc. 2) Kinematic analysis – studies the movement without considering the forces underlying its origin – displacement of body members, angular displacement of joints, etc. 3) Kinetic analysis – studies the forces and torques that originate the gait movements. 4) EMG analysis – studies the activation of a certain muscle or muscular group. The technological progresses occurred in the twentieth century make it possible the development of accurate acquisition systems, which permit the quick analysis of these four different areas.

The numbers of the last Portuguese census (2001) shows that 6.1% of the Portuguese population has at least one deficiency, from which 24,6% of these individuals have motor deficiencies and 2.4% have cerebral palsy (Gonçalves 2003). These numbers are concerning. However, some of these subjects can significantly improve their life style using adapted prostheses/orthoses. For instance, in

the US, amongst children with cerebral palsy approximately 53.000 ankle-foot orthoses (AFO) are prescribed each year (Lam, Leong et al. 2005). It is important to refer that these devices do not cure these neuropathologies, but instead help individuals improving their quality of life, which is essential to their welfare, while the scientific community pursues a solution for the pathologies.

1.2. Objectives

The main objective of the present work is the development of a database with kinematic, kinetic, and electromyographic gait results for a non-pathological Portuguese population. In this sense, the implementation of a protocol is intended, as well as the automation of all the analysis process, for the purpose of application not only at the academic but also at the clinical level. Since normal gait patterns vary with patient's age and gender, the database should contain the principal groups studied in bibliography – children, adult male, adult female and elderly.

Firstly a marker set protocol is required, which allows obtaining all the kinematic and kinetic results with interest in gait analysis, and it also enables subsequent processing with two distinct software – Visual3D^{TM} (c-motion 2010) and the academic software Apollo (Silva 2003). It should also be developed a sEMG protocol for the acquisition of muscular activation signals of the muscular groups of interest in gait analysis. Since it is intended for both protocols to be clinically applied, it is necessary to take in account the robustness and speed of assembly, as well as the capability to detect gait disorders.

Then, a set of gait acquisitions should be performed for all the considered groups, except elderly. The kinematic results should be treated firstly with the Qualisys acquisition software – QTM^{TM} (QUALYSIS 2010) and the electromyographic results with the *EMGWorks3.7*^{TM} (Delsys 2010) After that, a set of user-friendly routines should be developed that allow preparing the inputs for the Apollo software.

In what concerns the development of the database, additional routines should be developed for the analysis and management of the Apollo and *EMGWorks3.7*^{TM} results, generating a user-friendly interaction platform, which makes possible a comprehensive consultation of the principal kinematic, kinetic and electromyographic results, as well as the comparison of a given subject (non-pathological or pathological) with the subject group normal pattern.

Lastly, the developed protocol and analyzing should allow a deeper study of pathological subjects. These results should be compared with the respective normal population pattern. These would be conclusive, allowing to understand the anatomo-phisiology characteristics underlying the pathology, significantly contributing to the future design of corrective biomedical devices, adapted to each subject, which are comfortable, ergonomic and aesthetically acceptable.

1.3. State of the art

Although Human movements seem rather simple, these are the result of a highly complex process, involving a composite interaction between the skeletal system, the muscle system and the central nervous system (CNS). The human gait can be defined as the natural way of the body to transport itself safely and efficiently (Winter 1991). Each movement of gait cycle is controlled by a synergistic combination of muscular contractions (Stein and Mushahwar 2005). This intrinsic relation between

CNS and musculoskeletal system results in a well defined pattern of movements. The analyses of these patterns are interlinked with the development of biomechanics. Although "biomechanics" is a term adopted in 70's to describe the scientific area that studies the mechanical analysis of biological systems, the first studies are much older (Hall 2003).

Essentially, the study of human walking is generally divided in four different types of analyses: 1) Time-distance parameters 2) Kinematic analysis 3) Kinetic Analysis 4) Muscular Activation (Sutherland, Olshen et al. 1980; Winter 1991; Perry 1992; Vaughan, Davis et al. 1999). These types of analyses will be briefly described thereafter.

1.3.1. Kinematic Analysis

As stated before the kinematic analysis concerns the study of bodies' motions without considering the forces that causes them. This field comprises the displacement, velocity and acceleration of body members and angular displacements of joints (Sutherland 1997). The accurate measurement of these parameters is critical to understand the normal mechanism of human gait, and posteriorly to allow the detection and correction of gait disorders (Sutherland 2002).

The first scientific description of a stride cycle dates back to 4th century BC, when Aristotle wrote *De motu animalium* (on the motion of animals). This study was based solely on visual analysis of the motion – descriptive study (Nussbaum 1985; Nigg and Herzog 1994). The descriptive study of gait appeared again in renaissance and subsequent periods (scientific revolution, the age of enlightenment). da Vinci, Galileo and Newton performed useful walking descriptions (Whittle 2002). However, the first scientific gait analysis is attributed to Borelli's treatise *De Motu Animalium* (1682)*.* In this work Borelli used geometry to describe gait, running, jumping and muscular contraction, and also measured the center of gravity of the body, describing the mechanisms of balance during walking (Borelli, Bernoulli et al. 1743). In 1836, the Weber brothers published *Mechanik der menschlichen Gehwerkzeuge: Eine anatomisch-physiologische Untersuchung* which contained the first clear description of the gait cycle. These authors also measured with precision the pendulum mechanisms of the leg during the swing phase and the time distance-parameters – stride time, stride length, step time, step length, etc. (Weber and Weber 1836).

The first kinematic publications of human locomotion (second half of the nineteenth century) using specific tools for the acquisition of motion is reported to two contemporary scientists – Marey and Muybridge. Both recurred to photographic techniques to quantify several patterns of human gait. In brief, these authors used a set of cameras to take multiple photos of human and animal motion. Marey still developed a specific tool, that he named as chronophotographic gun, which allow to take several photos in one second (Muybridge 1979; Marey 1994).

Years later, in an attempt to improve the efficiency of troops, Braune and Fisher studied several subjects to determine not only the kinematics of locomotion but also the joint forces and energy expenditures. In a series of papers published between 1899 and 1904, they calculated the joint angles and displacements of body segments (Braune and Fischer 1887; Braune and Fischer 1889; Braune and Fischer 1890; Fischer and Braune 1899). These authors developed a method that they called *two-chronophotography*, which consisted in a series of Geissler tubes attached to the limbs segments. When stimulated with a high voltage pulse, these tubes emitted a short flash of light. The subjects

were asked to perform a certain movement while they were being photographed in total darkness. In their works Braune and Fisher also calculated trajectories, velocities and accelerations of body segments, which have revealed to be in concordance with the most recent studies. However, the method took a long time to prepare the subject (6-8 hours) and additional several weeks of work to treat the data and calculate kinematic measures (Braune, Fischer et al. 1987).

After the II world war, on an attempt of understanding the locomotion for the purpose of treating war veterans, Eberhart, Inman and their teams of California University provided a great source of knowledge concerning the human movement. These studies also included the use of photographic cameras and bulbs (interrupted light) attached to several anatomical points of interest, as the hip, knee and the ankle. In some studies Inman et al. used drilled pins in the principal bones and a camera over the subject to enable the analysis of movements in the horizontal plane (Eberhart and Inman 1947; Inman, Ralston et al. 1981).

Until reaching the present methods, other techniques were used. Murray et al. used a series of reflective targets attached to the anatomical interest positions; the subject was photographed while walking illuminated with a strobe light. These studies in men, women, elderly and pathological subjects allow recognizing some of the main patterns of human gait for these groups (Murray, Drought et al. 1964; Murray, Kory et al. 1969; Murray, Kory et al. 1970). The introduction of electrogoniometers by the Karpovich brothers allowed the quick study of joint angular displacements, since this technique did not require the time-consuming data treatment that other methods demanded. There are several papers concerning the study of normal patterns of human gait (Kettelkamp, Johnson et al. 1970) and gait disorders (Stauffer, Chao et al. 1977) using this tool. However, Sutherland reported some problems related to difficulties in avoiding the cross-talking between the three motion axes, the weight, dimensions of the device and the impossibility of measuring the torque parameter (it required information on the position of joint centers), which led to disuse of this technique (Sutherland 2002).

Recently, with the advancements in instrumentation and computer technologies, the limitations related to the automated capture of motion were progressively eliminated and new methodologies were developed. These new methods allowed the application of kinematic analysis in the clinical context (Mündermann, Corazza et al. 2006). Among others, visual recording systems can be found such as acquisition systems of active and passive markers, as well as magnetic sensors systems (Richards 1999). Since then, many works have been published in this field, the most significant are those presented by Winter, Sutherland and Perry, due to significant contributions they provided to this field (Sutherland, Olshen et al. 1980; Winter 1984; Sutherland, Olshen et al. 1988; Winter 1991; Perry 1992; Sutherland 1997). The perception of normal gait patterns and the possibility of performing fast quantitative studies led to improvements in the treatment of injuries and diseases of the musculoskeletal system. The same authors as well as others (Sutherland 1984; Gage and Society 1991) were also evidenced by their works in the study of gait disorders and other neuropathological diseases.

It is also important to refer to the work of (Kadaba, Ramakrishnan et al. 1991) by its importance in the standardization of marker protocols, presenting the Helen Hayes protocol, still currently used and

the several works from Cappozzo with great improvements in gait analysis methodologies (Cappozzo 1984; Cappozzo, Catani et al. 1995; Cappozzo, Catani et al. 1996).

Lastly, although some of the studies presented in this section are not confined to kinematic analyses, these are mentioned due to their importance and contribution to the advances in this area.

1.3.2. Kinetic analysis

As referred in the previous section, the kinematic analysis enables the study of the motion without considering the forces that originate this motion. The measurement of the biomechanical forces that produce the observed movements is essential to understand the gait mechanisms and the energy expenditure, since this information allows the calculation of parameters such as the internal forces on joints, moments of forces, mechanical power and work (Sutherland 2005).

To perform a kinetic/dynamic analysis, it is necessary to know the location of the joints and the external forces, acting in the mechanical system. The first can be provided by a kinematic analysis, while the second requires measurement (De Jalon and Bayo 1994). Essentially, the main external forces involved in human locomotion are the gravity and the reaction forces between the ground and the foot, and thus the accurate measurement of these parameters is essential to perform such analysis (Sutherland 2005).

The idea of a reaction force is firstly attributed to Aristotle, "…just as the pusher pushes, so the pusher is pushed", though this formulation was only performed by Sir Isaac Newton in 19th century – "for every force applied there is an equal and opposite reaction." (Newton 1833). The first historical reference to a scientific method for recording the ground reaction forces (GRF) dates from the late 19th century, where two Marey students – Carlet and Ampar developed a system using air reservoirs that allowed the measurement of the vertical component of GRF. They obtained a typical "m" curve similar to the ones obtained with modern force plates (Carlet 1872). In the mid-1940s, Elftman presented a model of a force plate with the capacity of measuring the forces in more than one plane. In a series of papers the author studied the distribution of pressure in the human foot, the three components of the GRF and presented some ideas about potential and kinetic energy and angular moments (Elftman 1934; Elftman 1938; Elftman 1939). Although several models of force plates had been developed before Elftman's prototype, the idea of applying the measurement of external forces to the calculation of joint torques was originally conceived by this author in 1939 (Elftman 1939). However, the mathematical formulation lacked technical sophistication and the equations were not clear, though both Winter and Sunderland considered this work as "creative and scientifically splendid" (Sutherland 2005).

A milestone in the development of gait kinetic analysis was the work from Bresler and Frankel, using inverse dynamics, presenting the first correct formulation to calculate moments of forces (Bresler and Frankel 1950).

The major knowledge contribution for gait kinetic analysis was probably done by Winter, with a series of articles studying torque, mechanical power and work patterns of joints for normal and pathological subjects (Winter, Quanbury et al. 1975; Winter, Quanbury et al. 1976; Winter and Robertson 1978; Winter 1979; Winter 1981; Winter 1983; Winter 1984; Winter 1991). Other important works in this area were published by Gage, Davis and their team, focused in the study of kinetic

parameters for children suffering from several neuropathologies (Gage and Society 1991; Ounpuu, Gage et al. 1991; Rose, DeLuca et al. 1993; Gage, Deluca et al. 1995; Ounpuu, Davis et al. 1996; DeLuca, Õunpuu et al. 1998).

1.3.3. Electromyographic analysis

Electromyography (EMG) is an experimental technique that allows the recording and analysis of myoelectric signals, which result from variations in the state of muscle fiber membranes (Basmajian and De Luca 1985). Since muscles are the structures that produce the active movements, the study of their activation patterns is important to understand the human locomotion and especially to detect several neuropathologies (Sutherland 2001).

The first reference to the study of muscle contraction dates from 17th century, in which Swammerdan discovered that stroking the innervating nerve of a frog muscle generated a contraction (Medved 2001). Redi recognized the connection between muscles and generation of electricity, when he observed that electric discharge in electric ray fish were generated by a highly specialized muscle (Redi 1671). Also studying frogs, Galvani showed that electric stimulation of muscular tissue produced contraction and consequently force (Galvani and Green 1953). With the development of the galvanometer in early 1800s, it became possible to measure bioelectric signals. Using this device in animals, Matteucci proved that muscular contraction was related to the existence of bioelectric stimulus (Matteucci and Savi 1844). Few years later, Bois-Reymond, provided the first evidence of electrical activity in human muscles during a voluntary contraction, also using a galvanometer. This author also acknowledged the importance of a good skin preparation in improving the signal magnitude (Du Bois-Reymond 1848). The term electromyography was only applied by Marey in the late 19th century (Medved 2001). Pratt demonstrated that the signal magnitude in EMG is related with the muscle and with the recruitment of individual muscle fibers, rather than the size of the neuronal impulse (Pratt 1917). It is important to refer, that the 20th century has been marked by major developments in this field. In this century some researchers have been evidenced, for instance Jasper constructed the first electromyograph (Medved 2001) and Basmajian and de Luca by the number of papers published in this area (Basmajian and De Luca 1985; De Luca 1997).

The introduction of EMG in gait analysis was applied by Inman and his team, during the study of walking in normal and amputee subjects (1944-1947). However, the protocol could not be applied in clinic since it was too laborious, time-consuming and painful (being an invasive method) (Eberhart and Inman 1947; Inman, Ralston et al. 1952; Ralston, Todd et al. 1976; Inman, Ralston et al. 1981). After Inman's work several researchers studied the normal and pathological patterns of human gait. Close, who had worked with Inman, published several papers studying the muscle phasic activity in normal and poliomyelitis subjects (Close and Todd 1959; Close 1964). A milestone in the development of EMG was the conception of fine-wire EMG electrodes by Basmajian, as these electrodes allowed painless examinations and eliminated the necessity of using intra-dermal local anesthetics. The application of this new method enabled the study of multiple muscles in each analysis (Basmajian and Stecko 1962). Sutherland became notorious by the several papers published in the study of EMG in normal and abnormal subjects (Sutherland, Bost et al. 1960; Sutherland 1966; Sutherland, Schottstaedt et al. 1969; Sutherland, Olshen et al. 1980). Perry studied the differences between fine-

wire and surface electrodes and considered that the superficial electrodes should only be used in the study of muscular groups, though when applied in clinic (neuropathological subjects), Perry considered that the lack of selectivity may have little clinical significance (Perry, Easterday et al. 1981 b)). Finally, it is important to refer all the knowledge provided by Winter in this area. Firstly, this author presented a set of amplitude normalization methods to use in EMG gait analysis. Using these algorithms, the inter-subject variability decreased substantially, significantly improving the sensitivity of the analysis (Yang and Winter 1984). Besides all the contributions Winter provided in the fields of kinematics and kinetic, this author presented several papers studying the intra and inter subject EMG patterns in gait (Yang and Winter 1985; Arsenault, Winter et al. 1986; Arsenault, Winter et al. 1986; Arsenault, Winter et al. 1986; Winter and Yack 1987; Õunpuu and Winter 1989; Winter 1991).

1.3.4. Theories of Human Walking

Although the intrinsic control between CNS and the musculoskeletal system, the human gait can be considered as a passive mechanism. Essentially, literature provides three different models to explain the small energy expenditure in the gait (Kuo 2007). In 1953, Saunders et al. presented the model of six gait determinants, which consist in six gait patterns that help minimizing the horizontal and vertical displacements of the body's center of mass (COM). These determinants are: 1st) Pelvic Rotation, 2nd) Lateral Pelvic Tilt, 3rd) Knee Flexion during the Stance Phase, 4th) and 5th) Foot, Ankle and Knee Mechanisms and 6th) Lateral displacement of the pelvis. During a gait cycle, the COM trajectory presents a smooth regular sinusoidal curve in the plane of progression, oscillating twice in the vertical plane and once in the horizontal plane. Saunders considered that by decreasing the magnitude of these displacements, the energy expenditure would be lower, since the forces necessary to accelerate and decelerate the COM would also be lower (Saunders, Inman et al. 1953).

The second theory, the inverted pendulum, was presented in 1966 by Cavagna and Margaria. It proposes that the stance leg acts like a pendulum describing an arc in progression plane. Essentially, theory considers a conversion of potential energy in kinetic energy and vice-versa, preserving the overall mechanical energy of the system. The model also considers that the swing leg acts entirely by the action of the gravity during the swing phase, as a non-inverted pendulum (Cavagna and Margaria 1963; Cavagna and Margaria 1966).

Both theories have been accepted, despite presenting contradictions. In inverted pendulum, if the leg acts like a pendulum in swing and stance phases, the energy is conserved. This implies a null work and therefore there would be no energetic consumption. On the other hand, walking with a flatten trajectory presents higher energetic expenditure than would be the expected. (Kuo 2007) Kuo et al. presented a new model that was an improvement of the pendulum theory, considering that the leg does not behave passively, rather acting as a forced pendulum with muscular work resulting in acceleration and deceleration. The model yielded metabolic rates in agreement with the expected (Donelan, Kram et al. 2002; Kuo, Donelan et al. 2005; Kuo 2007). Della Croce et al. proposed a new vision of gait's determinants, concluding that the three fist determinants help to reduce the vertical displacement of COM, but the effect is less significant than the one presented by Saunders. Della Croce et al. concluded that the reduction of COM vertical displacement is caused essentially by the 4th and 5th determinants (Della Croce U, Riley P.O. et al. 2001).

1.4. Main Contributions

The contributions of this thesis are:

- To develop an experimental methodology of analysis of the human gait to be applied in Laboratório de Biomecânica de Lisboa, there allows the study of the principal time-distance, kinematic, kinetic and electromyographic parameters. This methodology includes: a protocol for motion acquisition, a protocol for sEMG acquisition a set of routines to process and analyze the obtained results, generating a database of non-pathological subjects.
- The application of the developed methodology, in order to acquire the gait patterns of three non-pathological groups representing the Portuguese population (children, male adult and female adult).
- The application of the developed methodology in the study of pathological subjects.

1.5. Structure and Organization

This thesis is organized in nine chapters:

Chapter I – presents a first approach to the field of this work. It contains the motivation and the objectives that the author proposes to achieve. The state of the art of the different matters of the study is also presented discussed.

Chapter II – provides an overview of the locomotor system, focusing in the study musculoskeletal system. The main objective of this review is present the anatomic concepts behind the gait analysis.

Chapter III – focuses on the detailed study of human gait. The key terms and concepts used in gait analysis are presented. The different phases of gait cycle are described in detail and the biomechanical mechanisms underlying the human locomotion are explored. The relation between the CNS, the muscular action and the skeletal system will be explored in a context of kinematic, kinetic and electromyographic analysis. Different mechanisms of motion and GRF acquisition will be discussed. Other issues, such as the estimation of metabolic costs and the time-distance parameters will be approached.

Chapter IV – will provide an overview of the analysis of gait disorders. Since this thesis inserts in an ample project, which has also the objective of studying pathological subjects, the principal terms used in clinic to describe abnormalities will be presented in this chapter.

Chapter V – addresses the mathematical formulation behind kinematic and kinetic analysis. Using multibody dynamics with fully Cartesian coordinates, motion equations are deduced. The use of these equations in forward and inverse dynamic algorithms is also explained.

Chapter VI – The acquisition protocols developed for the Laboratório de Biomecânica de Lisboa (LBL) are presented. In a first section some considerations about the markers placement are discussed and two marker set protocols will be presented. The sEMG protocol is also explained in this section, as well as a preamble about EMG signals and data treatment. Finally, the designed routines for data treatment and generation of the database will be referred.

Chapter VII – The kinematic, kinetic and electromyographic results obtained for all the groups of analysis (children, adult men and adult women) will be discussed and compared with previous works. Using, the ideas emerging from this analysis, the validity of the designed protocols will be discussed.

Chapter VIII – presents the obtained results for pathological subjects. In a first section, the intra-variability of the subjects will be analyzed. After that, these results will be compared with the non-pathological patterns presented in chapter VII, the principal deviations to these normal patterns will be discussed, taking ideas for future works.

Chapter IX – In this last chapter will be presented the most relevant conclusions of the work, suggesting considerations for future developments in the routines and protocols presented in chapter VI. In this chapter future applications will also be explored, as the utilization of the gait analysis in the development of ergonomic and comfortable biomedical devices.

Chapter II

Locomotor System

The human motion results of a set of complex interactions between muscles, ligaments, bones and joints. In order to introduce the anatomic concepts underlying gait analysis, this chapter will present a small introduction of the body segments with interest in gait analysis – lower limbs and pelvis. The figures illustrating the ideas presented in the following sections can be consulted in Appendix A.

2.1. The Skeletal Anatomy

The Human body is constituted by 206 bones (80 axial skeleton and 126 Appendicular skeleton) which have several functions as support, protection, enabling movement of the body, etc. Figure 59 shows a representation of the human skeleton, with the bones indicated as blue representing the axial skeleton and the yellow representing the appendicular skeleton (Tortora and Grabowsky 2004).

2.1.1. Lower Limb

Each lower limb is composed by 30 bones and can be divided in 3 parts: thigh, leg and foot.

Thigh – corresponds to the structures between the pelvis and knee. It is composed by one bone – femur, which is the longest, heaviest and strongest bone of the body. The proximal end (greater trochanter) articulates with the acetabulum of the hip bone to form the hip joint, and its distal ends expand into the medial condyle and lateral condyle, articulating with the tibia and the patella to form the knee joint. The body of the femur bends medially, and therefore the knee joint is located medially in relation to the hip joint. Since the female pelvis is wider, the femur slope will be greater in women (vide Figure 60) (Tortora and Grabowsky 2004).

Leg – The structures between the knee and ankle joints are designated as the leg. It is constituted by 3 bones (vide Figure 61): 1) Patella – also named as kneecap, is a small triangular bone in front of the joint between the femur and tibia (Knee Joint). Its functions are to increase the leverage of the tendon, maintain the position of the tendon when the knee is flexed and to protect the knee joint. 2) Tibia – is the larger and stronger of the leg bones. Its proximal end expands into the lateral and medial condyles, which articulate with the condyles of the femur to form the knee joint. The distal end of the tibia articulates laterally with the fibula at the fibular notch (inferior tibiofibular articulation) and medially with the talus forming the medial prominence of the ankle – medial malleolus. 3) Fibula **–** is located on the lateral side of the tibia. The proximal end of the tibia (head of fibula) articulates with the lateral

condyle of the tibia (superior tibiofibular articulation). On the other hand, the distal end articulates laterally with the tibia and talus, forming the lateral prominence of the ankle – lateral malleolus (Tortora and Grabowsky 2004).

Foot – represents the body segment distal to the leg. It consists of 24 bones that can be divided in 3 groups: ankle, metatarsals and phalanges (vide Figure 62). The bones of the foot are arranged in three arches, two longitudinal and one transverse, which support the weight of the body and provide an ideal distribution of the body weight on the foot, and leveraging while walking. This last point is very important for the human locomotion, since this arrangement of foot the bones contributes to a lower energy expenditure during walking and running. The longitudinal arches extend from the front to the back of foot and has two parts (medial and lateral). The transverse arch is formed by the navicular, the 3 cuneiforms, and the bases of the five metatarsals. It is important to refer that these arches are flexible, helping to absorb mechanical shocks (Tortora and Grabowsky 2004).

Ankle – or Tarsus is constituted by 7 short bones arranged in two rows. The posterior row is consists in 2 bones – talus and calcaneus. The anterior part of ankle contains the cuboid, navicular and three cuneiform bones (first, second, and third cuneiform). The talus is the only bone that articulates with leg – medially with the medial malleolus of the tibia and laterally with the lateral malleolus of the fibula (Pina 1999).

Metatarsals – consist in a group of 5 bones, numbered I to V from the medial to lateral position from the skeletal of metatarsus. Each metatarsal consists of a proximal base, an intermediate body and a distal head. The base of each metatarsal bone articulates with one or more of the tarsal bones at the tarsometatarsal joints and the head with one of the first row of phalanges at the metatarsophalangeal joints. Their bases also articulates with each others at the intermetatarsal joints (Gray 1918).

Phalanges (of the foot) **–** are constituted by 14 bones arranged in 3 rows. As in the metatarsals bones, each phalange is also composted by a proximal base, an intermediate body and a distal head. The great toe (Hallux) has only two large phalanges (proximal and distal). The remaining toes are constituted by three phalanges (proximal, medial and distal) (Tortora and Grabowsky 2004).

2.1.2. Pelvic Girdle

The pelvic girdle (pelvis) is composed by four bones: the two hip bones, sacrum and coccyx. These four components are united by 3 joints: 1) Pubic symphysis – located in an anterior position, uniting the two hip bones. 2) Two sacroiliac joints – located in a posterior position, these joint are responsible for the union of the two hip bones with the sacrum (vide Figure 63). The pelvic girdle is responsible for providing stable support for the vertebral column, protecting the pelvis viscera and attach the lower limbs to the axial skeleton (Tortora and Grabowsky 2004).

The hip bone is a flat bone composed of three parts: 1) Ilium – located superiorly and the largest of the three subdivisions; 2) Ischium – the lowest and strongest portion of hip bone; 3) Pubis – the lower anterior portion. These three parts are distinct from each other in children, but are fused into one in the adult. The union of these structures takes place in and around a large cup-shaped articular cavity, designated as acetabulum. This cavity is the socket for the head of the femur, constituting the

acetabulofemoral joint, better known as hip joint (vide Figure 64) (Gray 1918; Tortora and Grabowsky 2004).

It is important to refer the two distinct and palpable bone structures of the hip bone, since it will have importance in the placement of markers that will be addressed in chapter VI: 1) Anterior-superior iliac spine (ASIS) 2) Posterior-superior iliac spines (PSIS). These are located respectively in the anterior and posterior position of the iliac crest (superior border of wing of ilium) (vide Figure 64) (Gray 1918).

2.1.3. Differences of female and male skeletons

Some differences can be observed between the skeleton of men and women, which are traduced in variations in weight and proportions of the body segments. Generally male bones are larger and heavier than female bones, and the articular ends are thicker in relation to the shafts. Other differences are observed in points of muscle attachment (tuberosities, lines and ridges), since some male muscles are larger than those of the female. Nonetheless, the overall differences between the skeletons of male and female bodies are rather few when compared with the existing similarities (Riggs, Melton et al. 2004; Tortora and Grabowsky 2004).

The most significant differences between men and women male skeletons are in the pelvis; these differences are related with pregnancy and childbirth. The female pelvis is smaller, lighter, wider and shallower, and is more circular in shape. Other important differences can be found between male and women skeletons, e.g. women tend to have narrower rib cages, smaller teeth, less angular mandibles and less pronounced cranial features (Washburn 1948; Tortora and Grabowsky 2004).

2.2. The Muscular System

The muscular system is the anatomical structure responsible for the generation of human movements. Its control is performed by the nervous system, although the control of some muscles (as the cardiac muscle) is completely autonomous. The human movements are not typically generated by a single muscle, but instead by a muscular group – muscular redundancy, as well as the muscles are arranged in opposing pairs in joints, generating opposing movements (extension-flexion, abduction-adduction) – agonist and antagonists muscles. Agonist muscles are the responsibles for generating a desired action, while the antagonists have the opposite action, i.e. stretch and yield to the movement of the agonist (Tortora and Grabowsky 2004).

In this section, the focus is put only on muscles that can be measured by sEMG and have relevance in the human walking, notwithstanding that many other muscles are active during a gait cycle. The choice of the muscles to be analyzed in this work is based in Winter and Vaughan studies (Winter 1991; Vaughan, Davis et al. 1999).

The muscular analysis in this thesis aims to understand the pattern of activation of the principal lower limb muscular groups, considering that the setup must be rapid and robust. For this reason, the following muscular groups were selected (Merletti, Rau et al. 2010):

- Anterior Leg – Dorsiflexion and assistance in the inversion of the foot;
- Posterior Leg (Triceps Surae) – Plantar Flexion of the ankle joint and assistance in the flexion the knee joint;

- Anterior Thigh – Extension of the knee joint and flexion of the hip joint;
- Posterior Thigh – Flexion and lateral rotation of the knee joint;
- Gluteus – extension and lateral rotation of hip joint.

Since each muscular group is constituted by a different set of muscles, for the development of sEMG protocol, the option was made in choosing the ones with higher importance. Once more, the anatomical figures that help understanding the ideas discussed in this chapter can be found in Appendix A (Figure 65-66).

2.2.1. Anterior Leg

The muscles of anterior leg are responsible for dorsiflexion, inversion and eversion of foot and extension of toes. This muscle group is constituted by 3 muscles: Tibialis anterior, Extensor digitorum longus and Extensor hallucis longus (Pina 1999). In order to analyze the dorsiflexion of foot, only the tibialis anterior was considered.

Tibialis Anterior – has origin in the tibia and insertion at first the metatarsal and first cuneiform. The Tibialis Anterior is responsible for dorsiflexion and inversion of the foot. Its antagonists are the plantar flexors of posterior compartment such the gastrocnemius and soleus (Tortora and Grabowsky 2004).

2.2.2. Posterior Leg

The muscles of the posterior compartment of the leg are responsible for the plantar flexion and inversion of the foot, flexion of the toes and assisting in the flexion of the knee joint. This muscle group is constituted by 6 muscles – Triceps surae, Plantaris, Plopiteus, Flexor digitorum longus, Tibialis posterior and Flexor hallucis longus (Pina 1999). For this analysis, only the 3 muscles, forming the triceps surae – Gastrocnemius Lateralis, Gastrocnemius Medialis and Soleus, were considered. These muscles have interest for the study of plantar flexion and inversion of the foot. Their antagonists are the dorsiflexors of the anterior compartment such as the tibialis anterior (Pina 1999; Tortora and Grabowsky 2004).

Gastrocnemius Lateralis – has its origin in the lateral condyle of the femur. The muscles of the triceps surae have a common insertion – calcaneal tendon or Achilles tendon and insert onto the posterior surface of the calcaneus. This muscle has the function of plantar flexion of the foot and assistance in flexion of the leg at the knee joint (Pina 1999; Tortora and Grabowsky 2004).

Gastrocnemius Medials – has its origin in the medial condyle of the femur and has the same insertion and the same action of Gastrocnemius lateralis (Pina 1999; Tortora and Grabowsky 2004).

Soleus – is a complex multi-pennate muscle, usually having a separate (posterior) aponeurosis from the gastrocnemius muscle. The soleus muscle is divided into marginal, posterior and anterior parts. A majority of soleus muscle fibers originates from each side of the anterior aponeurosis, attached to the tibia and fibula. Other fibers originate from the posterior surfaces of the head of the fibula and its upper quarter, as well as from the middle third border of the tibia. The several fibers of the Soleus are inserted in the calcaneus by means of the calcaneal tendon (Pina 1999; Agur, Ng-Thow-Hing et al. 2003).

2.2.3. Anterior thigh (Anterior external muscles)

This muscle group is constituted by 3 muscles – Sartorius, Tensor fasciae latae and Quadriceps femoris. They have several functions, such as the extension and the flexion of leg at knee joint, and the flexion, abduction and laterally rotation of the thigh at the hip joint (Pina 1999; Tortora and Grabowsky 2004). In order to study the extension of the leg and flexion at the hip joint, only the Quadriceps femoris was choose to analyze.

Quadriceps Femoris – is a bulky muscle group constituted by four portion or heads muscles on the front of the thigh: The Rectus femoris which is the superficial muscle and occupies the middle of the thigh, covering the most of the other three quadriceps muscles. It has origin in the illium and the insertion at the patella by means of the quadriceps tendon, which is common to all of the four heads, and then tibial tuberosity by means of the patellar ligament; The Vastus lateralis which has origin on the lateral side of the femur; Vastus medialis which has origin on the medial side of femur; The Vastus intermedius which has origin between Vastus lateralis and medialis, but deep to the rectus femoris.

The four heads are extensors of the leg at knee the joint. The Rectus femoris is also a flexor of the hip joint (flexes thigh) because it has its origin in the ilium (Pina 1999; Tortora and Grabowsky 2004).

2.2.4. Posterior Thigh (Hamstrings)

The Hamstrings refers to the group of 3 posterior thigh muscles – Biceps Femoris, Semitendinous and Semimembranosus. All have the function of leg flexion at the knee joint and extension of thigh at the hip joint (Tortora and Grabowsky 2004).

In order to study the flexion of the knee joint and the extension of the hip joint, the biceps femoris group was chosen.

Biceps Femoris – is a stretched muscle constituted by 2 heads (long head, short head). The long head has origin in the distal part of sacrotuberous ligament and the posterior part of ischium tuberosity (tendon common with semitendinosus), the short head has origin in the lateral lip of the linea aspera, proximal 2/3 of supracondylar line and lateral intermuscular septum (femur). Both have the same insertion at the head of the fibula which articulates with the back of the lateral tibial condyle. The functions of the Biceps femoris are the flexion and lateral rotation of the knee joint. The long head also extends and assists in lateral rotation of the hip joint. The antagonists of the biceps femoris are the quadriceps muscles (Pina 1999; Tortora and Grabowsky 2004).

2.2.5. Hip

Several muscles can be found in the hip/pelvis region. Essentially, these muscles are divided in four groups according this action and orientation: gluteal, adductor, iliopsoas and lateral rotator group. The thesis will focus on principal flexors and extensors of the hip – respectively Iliopsoas group and Gluteus maximus.

Iliopsoas – The Iliopsoas refers to the combination of 3 muscles (Iliacus, Psoas major and Psoas minor). The muscles of iliopsoas are the strongest of the hip flexors (Rectus femoris, Sartorius and Tensor fasciae latae) and have an important role in the flexion of the thigh at the hip joint during gait.

Their antagonists are the Gluteus maximus and Biceps femoris (long head) (Tortora and Grabowsky 2004; Correa, Crossley et al. 2010).

Psoas Major and Iliacus have the same insertion, attaching at the level of the inguinal ligament that has its insertion in the lesser trochanter. The Iliacus has origin in the iliac fossa, while Psoas major has origin in the thoracic vertebrae XII, lumbar vertebrae I-IV and from neighboring intervertebral discs. Psoas minor has origin in the XII thoracic vertebrae, I lumbar vertebrae and intervertebral discs between T12 and L1. Psoas minor has the insertion in the iliopectineal eminence (Pina 1999; Tortora and Grabowsky 2004).

However, the iliopsoas group is a set of internal muscles, which renders its measurement with sEMG extremely difficult, and as such this muscle group will not be considered in this thesis.

Gluteus Maximus – is the most superficial and the largest of the three gluteus (Gluteus maximus, Gluteus medius and Gluteus minimus). Its origin is situated in the posterior gluteal line of ilium, sacrum, coccyx and aponeurosis of sacrospinalis. Gluteus maximus has its insertion in the gluteal tuberosity of the femur and iliotibial tract of fascia lata. Gluteus Maximus has the function of extension and lateral rotation of the hip joint. The lower and upper fibers also assist in the adduction of the hip joint. By means of its insertion into the iliotibial tract, gluteus maximus helps to stabilize the knee joint when it performs a movement of extension (Pina 1999; Tortora and Grabowsky 2004). Due to its crucial role during gait, as hip extensor, and given also its superficiality, the gluteus maximus has been integrated in the gait analyses performed in this thesis (Correa, Crossley et al. 2010).

2.3. Classification of Joints

The skeleton bones are interlinked between them, and such connections are designated as joints or articulations (Gray 1918). The joint structure determines the direction and range of movement. However, not all joints are flexible, as for instance some have the function of remaining rigid to stabilize the body. These functions determine their classification (Graaff 2001).

The structural classification of joints is based on two criteria – the presence or absence of a space between the articulating bones (synovial cavity) and the type of connective tissue that binds the bones together. As a result, the articulations of the human body are grouped into three principal categories, according to their structure (Graaff 2001; Tortora and Grabowsky 2004):

Fibrous Joints – the bones are held together by fibrous connective tissue. They are also characterized by the absence of joint cavities.

Cartilaginous Joints – In these joints, the bones are held together by cartilage and are also characterized by the absence of joint cavities.

Synovial Joints – the articulating bones are capped with cartilage and often by accessory ligaments. These type of joints are characterized by joint cavities filled with fluid (synovial cavity).

The joints can also be divided by their functions. This functional classification is based on the degree of permitted movement. This classification is usually divided in three groups (Graaff 2001; Tortora and Grabowsky 2004):

Synarthroses – Immovable joints.

Amphiarthyroses – Slightly movable joints.

Diarthroses – Freely movable joints.

Fibrous joints are divided in 3 sub-divisions: (1) suture (synarthroses) –articulation in which contiguous margins of the bones are united by a thin layer of fibrous tissue (only found in the skull); (2) syndesmoses (amphiarthyroses) – are fibrous joints held together by collagenous fibers or sheets of fibrous tissue called interosseous ligaments (distal articulation between fibula and tibia): (3) gomphoses (synarthroses) – it is formed by the insertion of a conical process into a socket. (occurs only between the root of teeth and the supporting bones of the jaws.(Gray 1918; Graaff 2001; Tortora and Grabowsky 2004)

The cartilaginous joints are divided in 2 sub-division: (1) synchondrosis (synarthroses) – the articulating bones are connected by hyaline cartilage; when bone growth ceases, bone replaces the hyaline cartilage (an example is the epiphyseal plates in an elongating bone); (2) symphysis (amphiarthyroses) – is a cartilage joint in which the ends of the articulating bones are covered with hyaline cartilage, but the bones are connected by a broad, flat disc of fibrocartilage (an example is the pubic symphysis) (Gray 1918; Graaff 2001; Tortora and Grabowsky 2004).

Most joints in the human body are of the synovial type (freely movable). This type has the function of provide a wide range of precise, smooth movements, and at same time grant stability, strength and sometimes rigidity of the skeletal system. A synovial joint is characterized by a typical structure, whose unique characteristic is the presence of a space called synovial cavity that allows a free movement (all synovial joints are diarthroses). The articulating bones at a synovial joint are covered by an articular cartilage (hyaline) that reduces friction between bones and helps to absorb mechanical shocks. Synovial joints are enclosed by an articular capsule composed of dense regular connective tissue that encloses the synovial cavity and unites the bones. The articular capsule is composed by 2 layers – a fibrous capsule and a synovial membrane. The synovial membrane is responsible for secreting the synovial fluid. Its functions include reducing friction (lubrification), nutrient supply and removing metabolic waste. The synovial joints can have accessory ligaments in its structure (vide Figure 67) (Gray 1918; Graaff 2001; Tortora and Grabowsky 2004).

Despite having a similar structure, the synovial joints can be classified into six main categories – gliding, hinge, pivot, condyloid, saddle and ball-and-socket. The classification has in consideration the structure and the motion that these enable (vide Figure 68) (Graaff 2001; Tortora and Grabowsky 2004).

Gliding or planar joints – enable side-to-side and back-and-forth movements, with some slight rotation. Examples of these joints are intertarsal, intercarpal, etc.

Hinge Joints – enable angular movements like a hinge of a door (rotation about an axis). This joint is characterized by one concave bone that fits into another convex bone. Examples of hinge joints are the elbow, knee, ankle, etc.

Pivot Joints – are characterized by a limited movement of rotation about a central axis. The joint is formed by a pivot-like process turning within a ring, or a ring on a pivot; the ring being formed partly of bone, and partly of ligament. Examples of these joints are the proximal articulation of the radius and ulna for rotation of the forearm or the atlantoaxial joint (allows the rotation of head).

Condyloid Joints – are characterized by a convex oval-shaped projection of bone that fits into the concave oval shaped depression of another bone. This permits angular movements in two directions,

as in up-and-down and side-to-side motion. The radiocarpal joint of the wrist and metacarpophalangeal joints are examples of this joint.

Saddle Joints **–** there are two places in the human body where this type of joint occurs – Trapezium of carpus with the I metacarpal bone and the articulation between the malleus and incus (ear). The articular surface of a bone is saddle-shaped, and the articular surface of the other bone fits into the saddle (like a rider sitting in a horse). Side-to-side and up-and-down are the movements allowed by this type of joint.

Ball-and-Socket Joints **–** enable movements in several directions. The ball-like surface of the bone fits into a cuplike cavity of the other bone. In the human body, ball-and-socket occurs only in shoulder and hip joints.

2.4. Types of movements at synovial joints

Generally, the movements at synovial joints are divided in four kinds – gliding, angular, circular and special (Gray 1918). The thesis will focus on angular movements, since are the ones with more importance in the description of gait. The figures that help understanding the ideas discussed in this section can be found in Appendix A (Figure 69).

2.4.1. Gliding Movement

Gliding movement is characterized by a simple movement in which one surface glides or moves over another without any angular or rotator movement. It is common in all movable joints, though in some joints (e.g. carpus and tarsus) it is the only motion permitted (Gray 1918). In

2.4.2. Angular Movements

This type of movements occurs only between long bones and it is characterized by an increase or decrease in the angle between these bones. It is usual to consider four types of angular movements – flexion and extension, which characterize movements in the sagittal plane, and abduction and adduction, which occur in the frontal plane (Gray 1918; Graaff 2001).

Flexion **–** is a movement that decreases the joint angle on the anteroposterior plane. Bending the knee or the elbow are examples of this type of movements. It is important to mention two special flexion movements, which occurs in the ankle. The motion that brings the top of the foot towards the lower leg is called dorsiflexion, on the other hand the opposite motion, i.e. pressing the foot downwards is named plantar flexion.

Extension **–** represents an angular movement in which the joint angle is increased. It is the reverse of flexion and, generally, extension returns a body part to its anatomical position. Examples of extension movements are straightening of the elbow and knee. Hyperextension occurs when a part of the body is extended beyond the anatomical position. Examples of hyperextension movements are the backward movement of the humerus during the arm swing that is a characteristic of human walking

Abduction **–** is a movement of a body part away from the midline (sagittal plane) in the frontal plane. Examples of abduction movements include lateral movement of humerus upward, the femur away from the body, etc.

Adduction **–** is the opposite movement of abduction and represents the movement of a bone toward the midline of the body.

2.4.3. Circular Movements

This type of movements occurs when a bone with a rounded or oval surface articulates with a corresponding depression on another bone. Circumduction and rotation are the two basic types of circular movement (Graaff 2001).

Rotation – represents a movement of a body part around its own axis without undergoing any displacement from this axis. Examples are turning the head from side to side (as in answering "no") and twisting the waist (Graaff 2001; Tortora and Grabowsky 2004).

Circumduction – is a movement of a body part so that a cone-shaped airspace is traced. The distal end performs a circular movement while the proximal extremity serves as pivot. Examples of this movement are doing a circle with an arm (humerus at shoulder joint) and doing a circle with a leg (femur at hip joint) (Gray 1918; Tortora and Grabowsky 2004).

2.4.4. Special Movements

This group includes all the other movements that are not included in previous groups. Special movements include elevation/depression, protraction/retraction, inversion/eversion and supination/pronation (Whittle 2002; Tortora and Grabowsky 2004).

Elevation – is the movement that raises a body part, such as closing the mouth by elevating the mandible and lifting the shoulders to shrug.

Depression – is the downward movement of a body part (opposite of elevation). Opening the mouth (depress the mandible) is an example of this movement.

Protraction – represents a movement of the body's part forward, on a plane parallel to the ground. Thrusting the mandible outward is an example of protraction.

Retraction – is the opposite movement of protraction. The mandible is retracted when moved backward.

Inversion – is the movement of the foot sole inward, or medially.

Eversion – represents the movement of the foot sole outward, or laterally.

Supination – is a specialized rotation of the forearm so that the palm of the hand faces forward or upward. The supination of the palms is one of the features that define the anatomical position.

Pronation – is the opposite of supination, representing the movement of the forearm so that the palm is directed to the rear or downward.

Generally, in pathological cases, the terms varus and valgus are also used, in order to describe respectively a permanent angulation of a body part toward or away from the midline.

Chapter III

Human Gait

Walking is probably one of the most common movements in humans, although its definition is not so simple. Walking can be defined as the natural means of transport of the body safely and efficiently from one location to another. Winter considers that to achieve safe and efficient propulsion of the body, five key tasks must occur during each gait cycle (Winter 1991; Perry 1992).

- Maintenance of support of the upper body during stance;
- Maintenance of upright posture and balance of the total body;
- Control foot trajectory to achieve a safe landing;
- Generation of mechanical energy to maintain the present forward velocity or to increase the forward velocity;
- Absorption of the mechanical energy for shock absorption and stability or to decrease the forward velocity of the body

In this chapter, non-pathological gait will be reviewed, with special emphasis to the study of patterns and mechanism, behind these five tasks.

3.1. Gait specific terminology and definitions

In this section the terminology and the concepts most used in gait analysis will be addressed. It is important to refer that this terminology resulted from years of observation and kinematic analyses of non-pathological subjects. In order to enable the effective communication between gait researchers, prosthetist and orthopedists was essential to standardize these concepts, to make their comprehension possible by all (Ayyappa 1997).

3.1.1. Spatial Terminology

Spatial reference system – The spatial reference system often changes among different authors, but all follow the right hand rule to define the three orthogonal vectors. For example Winter uses the X axis to define the direction of progression, Y vertical direction and Z lateral direction; Vaughan uses X to define the direction of progression, Y lateral direction and Z to vertical direction (Winter 1991; Vaughan, Davis et al. 1999). In this thesis the reference system used is the same as Vaughan.

However, in order to avoid errors caused by different spatial reference systems, the gait researchers generally use the terms anterior-posterior, medial-lateral and vertical to refer respectively the X, Y and Z directions.
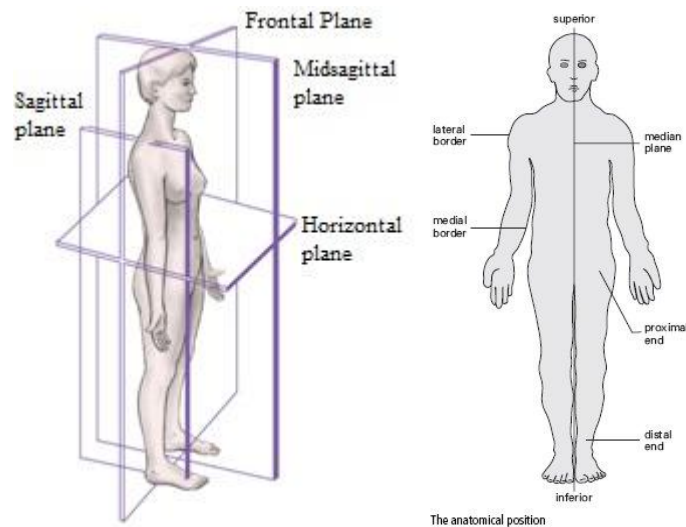
Figure 1– representation of: a) planes of reference b) anatomical position

Planes of reference – in order to visualize and study the structural arrangements of several organs, the body may be sectioned and diagrammed according to three fundamental planes of reference (Figure 1a)):

Sagittal plane – A sagittal plane extends vertically through the body dividing it into right and left portions. Usually it is named midsagittal plane to a sagittal plane that crosses lengthwise through the midplane of the body, dividing it equally.

Coronal plane – also denominated as frontal plane, is a vertical plane that divides the body into anterior (front) and posterior (back) portions.

Transverse plane – also denominated as horizontal plane or cross-sectional plane, divides the body into superior (upper) and inferior (lower) portions.

Ipsilateral – is used to describe the same side of the body.

Contralateral – is used to describe the opposite side of the body.

Anatomical Position – Generally, the movement directions of a body segment are described in relation to an established position – anatomical position. In the anatomical position, the body is erect, the feet are parallel to each other and flat on the floor, the eyes are directed forward, and the arms are at the sides of the body with palms of hands turned forward and the fingers pointed straight down (Figure 1b)) (Graaff 2001).

Mean plane of progression – represents the average vertical plane along which the center of mass of the body moves during a gait cycle (Winter 1991).

3.1.2. Terminology related with contact of feet with the ground

The terminology presented in following sections (3.2.2. until 3.2.7) is based on Winter and Õunpuu work (Winter 1991; Õunpuu 1994).

Initial Contact (IC) – is a term to define the instant when the foot/shoe makes the first contact with the ground. This term is applied independently of how the contact with the ground is made.

Heel Contact (HC) – represents the instant when the heel of the foot/shoe hits the ground (IC for non-pathological subjects).

Ball Contact – is the instant when the ball of the foot/shoe (metatarsal head hits the ground. Generally, this term is used to represent the initial contact of pathological subjects, when the IC is not made by the heel.

Foot Flat (FF) **–** represents the instant during stance phase when the foot/shoe is totally flat on the ground, independently of how the IC was made.

3.1.3. Terminology related with feet leaving the ground

Heel Off (HO) – is the instant during the stance phase when the heel leaves the ground. (Corresponds to the start of push-off event)

Toe Off (TO) – represents the instant when the toe of the foot/shoe leaves the ground. In normal gait, this instant represents the final of the stance phase and the start of swing phase.

End of Contact (EC) – in pathological gait, when the TO is not the end of weight bearing, this term can be used to represent the instant when the last part of foot/shoe leave the ground.

3.1.4. Terminology related with periods during a gait cycle

Stride Period - is the two consecutive steps (left-right or right-left) period of time, in seconds. The stride period is measured from a determined event of one foot to the same event of the same foot. Considering the IC of the foot to analyze as the first event of stride period is an usual procedure. Commonly, in order to compare subjects with different stride periods, or to compare successive strides of the same subject, the stride period is represented as a percentage (0% – first IC to 100% - next IC).

Step Period – is the period of time for one step, in seconds. It is measured from a determined event of one foot to the same event of the other foot. Once more, it is usually consider the IC as the first event of the step period. Both stride and step period usually consider the IC as the foot event.

Single support – represents the period of time, when only one limb is contacting the ground. It is usual express this event in seconds or as a % of stride period.

Double support – represents the period of time, when the two feet are simultaneously in contact with ground. Generally, it is expressed in seconds or as a % of the stride period. In a gait cycle, this event occurs two times:

Right double support – is the time between IC of the left foot and TO of right foot;

Left double support – is the time between IC of right foot and TO of left foot;

Flight Period – represents the period of time when there is no contact of feet with ground (applicable only in running studies).

Stance Period – is a term used to represent the period of time, in which a determined foot is in contact with ground, expressed in seconds or as a % of the stride period. This period is usually sub-divided in 3 sub-events: weight acceptance, mid-stance and push-off.

Weight acceptance**/**Loading response (WA) – represents the time period between IC and maximum knee flexion during stance phase. WA is also expressed in seconds or as a % of the stride period. In

several pathological gaits, when knee flexion does not occur, this term is defined as the time between IC of the ipsilateral limb and TO of contralateral limb. This phase is characterized by the energy absorption by means of ankle, knee and hip muscles. Although the hip and ankle muscles absorb rapidly the energy after IC, the knee muscles continue absorbing the energy until the maximum knee flexion is reached.

Mid Stance (MS) – represents the time period between WA (when the contralateral foot leaves the ground) and terminal stance (when the body weight is aligned over the forefoot), expressed in seconds or as a % of the stride period.

Terminal stance – represents the time period between MS and pre-swing, expressed in seconds or as a % of stride period.

Pre-Swing – begins with the IC of the contralateral foot IC and ends with TO of the ipsilateral foot. Thus, pre-swing corresponds to the second double support phase. This event is expressed in seconds or as a % of the stride period.

Push Off (PO) – is the period of time when the lower limb is pushing away from the ground. The leg muscles perform a powered plantar flexion. PO is usually expressed in seconds or as a % of stride period, it begins shortly after HO and ends with TO.

Swing Period – represents the period of time, in which the foot is not in contact with the ground. This period is expressed in seconds or a % of stride period. Usually, the swing period is sub-divided in three parts – early swing, middle swing and terminal swing. In some pathological cases, were the foot/shoe does not leave the ground, it can be defined as the period of time while all portions of foot are in forward movement.

Early/Initial Swing – represents the period of time between the TO and Middle Swing of the same foot; it is usually expressed in seconds or as a % of stride.

Middle Swing (MSw) – is the instant that represents the midpoint between TO and IC of the same foot.

Terminal/Late Swing –represents the period of time between MSw and IC of the same foot, expressed in seconds or as a % of stride period.

3.1.5. Terminology related with distances during a gait cycle

Step Length – is the horizontal distance measured between a determined point of a foot and the same point of the other foot and is usually expressed in meters. Step length represents the distance traveled forward by a single leg. The term is also used to express the average step length over many strides. Since the step length can presented differences between the two legs, the measurement of this parameter should consider both legs.

Stride Length – is the horizontal distance measured between a determined point of a foot and the same point of the same foot. This parameter represents the distance traveled forward by the two legs and is equal to the sum of the right step length and left step length. Even in presence of marked gait asymmetry, stride length is equal for the two limbs, if the subject is walking in a straight line.

Step Width - represents the mediolateral distance between the heels of the two feet.

3.1.6. Segment and joint angles

In gait analysis, human body segments are generally modeled as rigid bodies and their rotation is assumed to take place about a fixed point in the proximal segment, which is considered to be the center of the joint (Kadaba, Ramakrishnan et al. 1991). Euler angles have been successfully applied to describe a relative rotation of one segment with respect to another segment in 3D space (Chao, Laughman et al. 1983). Other methods can be used, for example Lewis and Lew defined the orthopedic angles that are the same as Euler angles but they are defined according to the clinical terms (flexion, extension, abduction, etc.) (Lewis and Lew 1977).

The definition of joint angles in this thesis follows the convention of Winter and International Society of Biomechanics. The convention states that all segments must be defined as positive in a counter-clockwise direction from the horizontal in order that the first and second time derivatives have the correct polarity (to enable the calculation of joint mechanical power). Thus, the joint angles have a positive value if these are in flexion (dorsiflexion) and negative value if these are in extension (plantar flexion) (Winter 1991; Wu, Siegler et al. 2002; Wu, Helm et al. 2005).

3.1.6.1. Angles in the Sagittal Plane

In the sagittal plane, when a subject progresses from left to right, the view assumed is the right. However, the left limb should have the same convention of right limb, in order to allow the direct comparison between the results of the two legs. It's usually expressed in degrees, though radians can also be used. According to (Winter 1991) and taking in consideration in consideration Figure 2, the sagittal angles are defines as follows:

Foot Angle (θ_{ft}) – the angle between a horizontal line and a line along the bottom of foot measured for the distal end (V metatarsalphalangeal joint).

Leg Angle (θ_{lg}) – represents the angle between a horizontal line and the line defined by knee joint and ankle joint measured from the distal end of leg (ankle joint).

Thigh Angle (θ_{th}) – is the angle between a horizontal line and the line defined by the thigh (hip joint to knee joint) measured from the distal end of thigh (knee joint).

Pelvic Tilt – represents the angle between a horizontal line and the pelvis (line between PSIS iliac and the ASIS)

Trunk Angle (θ_{tr}) – represents the angle between a horizontal line and the line defined by the axis of spine (C7 to L5)

Ankle Angle (θ_a) – represents the angle between the foot and the leg minus 90º. ($\theta_a = \theta_{ft} - \theta_{lg} - 90º$)

Knee Angle (θ_k) – represents the angle between the thigh and the leg. ($\theta_k = \theta_{th} - \theta_{lg}$)

Hip Angle (θ_h) – is the angle measured between the thigh and the trunk. ($\theta_h = \theta_{th} - \theta_{tr}$)

3.1.6.2. Angles in the Frontal Plane

In frontal plane movements as adduction, varus, inversion and foot pronation (defined as inversion of calcaneus with respect to the middle line of the leg) have positive value. Movements as abduction, valgus, eversion and foor supination have negative values. However, it is important

remember that the values of hip abduction/adduction, knee valgus/varus, and ankle inversion/eversion are zero in anatomic position.

Pelvic Obliquity – represents the angle of the pelvis in frontal plane, measured between horizontal and the line defined by right and left ASIS.

Trunk List – represents the angle between horizontal and the line defined by trunk (C7 to L5), with positive value in a counter-clockwise direction.
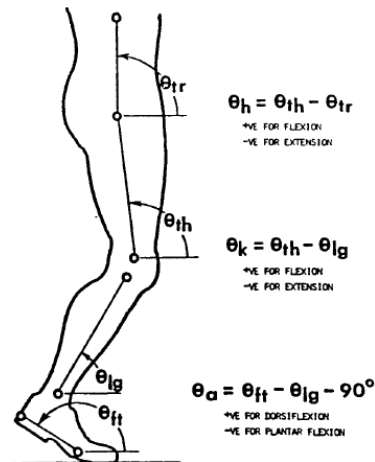
Figure 2 – Definition of joint angles of lower limbs in sagittal plane (Winter 1991)

3.1.6.3. Angles in the Transverse Plane

Pelvic rotation – represents the angle of pelvis in transverse plane. It's reported as rotation towards the right or to the left.

Angle Foot – represents the angle between the line of progression and the line defined by calcaneus and the II Metatarsal.

3.1.7. Terminology related with cadence and velocity

Cadence – is the rate at which a subject walks and is expressed as the number of steps per unit of time, generally steps/min.

Normal/Free Cadence – is the natural cadence of a subject, i.e. the cadence that is voluntarily assumed

Fast/Slow Cadence – is a forced cadence of a subject above/below the natural cadence and must be specified by the researcher.

Gait Velocity – represents the average horizontal speed of the body along the plane of progression measured over one or more stride periods. Generally is reported in $m.s^{-1}$ or $m.min^{-1}$. It is defined as:

$$v_g = \frac{stride\ length * cadence}{120}\ (m.s^{-1}) \qquad 1)$$

3.2. Locomotion Control and Sequence Gait-Related Processes

Understanding the control of automated movements, such as walking, is still under studying. A fact is that the CNS have the capability of to coordinate, which joint, body segment should be moved, the exact time of these movements and the force to apply. Thus, movements like walking need to meet a set of biomechanical requisites. This control is done by patterns of electric signs that are sent along the peripheral nervous system (PNS) – nerves, which activate the appropriate set of muscles. As the

march has to adapt to several obstacles encountered, the body movements are continuously adapting to guarantee a smooth progression – a large flow of sensory input from the periphery of the system have the capability to adapt these movements by selecting the most optimal information (Duysens and Crommert 1998).

Human locomotion results from a set of cyclic events controlled by the central pattern generating networks (CPGs). These unities are located in a large extent within the spinal cord, though its action is controlled by the peripheral and descending signals. CPGs are responsible for the generation of the complex patterns of electric signs addressed in previous paragraph. However, Borghese et al. cited a series of papers, in which is observed differences in time-distance, kinematic and kinetic parameters not only across speeds and subjects, but even from trial to trial (Borghese, Bianchi et al. 1996).

Segers considers that gait pattern is influenced by mechanisms of feedback between the CNS and the networks of PNS, but the collective output is the responsible for the level of performance and control variable. These collective outputs results from an interaction of the system mechanics (muscle mechanics, inertial and material properties, anthropometrics, etc.) and external mechanics (external loads, material properties), which produced the coordinated movement patterns. Using the terminology of the dynamic control systems theory, the behavior of the system can be described by two parameters – 1) the order parameter that reflects the organizational status of the system (collective output of the system) and 2) the control parameter that drives the reorganization of the system (intensity of the graded intentional drive) (Segers 2006).
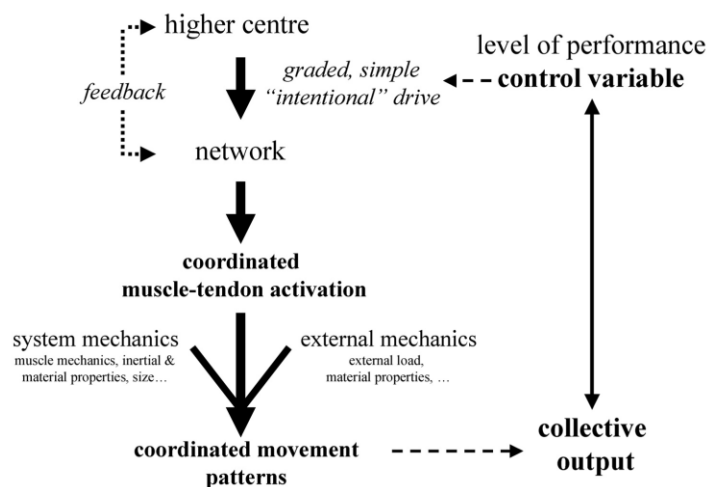
Figure 3 – Simple representation of the control of human locomotion (Segers 2006)

Several studies in postural control try to analyze the human body response to various external perturbations. Although this reflexive approach enables one to examine the input/output characteristics of different closed-loop feedback systems, it does not consider explicitly the stabilizing roles of possible open-lop control schemes or the steady-state behavior of the human body during periods of undisturbed stance (Collins and Luca 1992).

Borghese hypothesized a hierarchy in the neural control, "in which global intersegmental co-ordination is prescribed in terms of general speed-invariant patterns, whereas local variables that pertain to single muscles and joints are defined on the basis of specific task demands". Borghese also suggested that high-order laws of intersegmental co-ordination are defined by "the orientation angles

of each limb segment relatively to the direction of gravity and that of forward progression". This hypothesis follows three considerations (Borghese, Bianchi et al. 1996):

- The locomotion must comply with requirements of postural stability and dynamic equilibrium. The COM position of the body and the geometrical configuration of the legs are accurately controlled relative to the gravity direction in response to perturbation of static posture in man.

- The anticipatory adaptation to changing support conditions during locomotion involves a number of synergies of upper limb, trunk and lower limbs movements. Kinematic constraints as well as position sense for upper limbs in man are normally defined in terms of orientation angles of upper arm and forearm with respect to the vertical and sagittal directions.

- The head is normally stabilized in space during posture and locomotion, and provides an inertial platform for monitoring gravity direction.

Figure 4 shows the various interactions between the CNS, PNS and musculoskeletal effector system that occur in the cycle of human gait, in a simplified way and without taking into account the feedback loops. The sequence of events that must take place during walk are (Vaughan, Davis et al. 1999):

1) Registration and activation of the gait command in the CNS;

2) Transmission of the gait electro-signals by the PNS to the several muscular groups of interest;

3) Contraction of muscles and development of tension;

4) Generation of forces and torques at joints;

5) Regulation of the joint forces and torques by rigid skeletal segments based on the anthropometric characteristics of the subject;

6) Production of movements on the several body segments, which are recognizable as functional gait;

7) Generation of ground reaction forces.
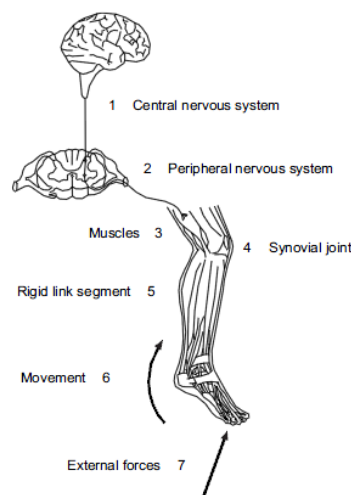
Figure 4 – Functional basis for the way in which we walk (cause-and-effect-model)

3.3. Gait Cycle

Gait presents a cyclic pattern that is repeated stride after stride. Generally, in gait studies, the gait descriptions considers only a single cycle, assuming that all the cycles are equal. However, this fact is

not strictly true, but it is a reasonable approximation (Vaughan, Davis et al. 1999). A gait cycle (GC) corresponds to one complete stride (two steps) and includes all the activities considered between one determined event of one foot and the same event of the same foot (Norkin and Levange 1992). Usually, the IC event is considered the first event of the GC (0%), the same assumption will be followed in this thesis. During a GC two main phases can be considered – Stance phase and Swing phase. Stance phase starts with the IC of one foot and continues while this is on the ground, during approximately 60-62% of the stride period. The swing phase begins with the TO of the same foot; during this phase the foot is not contacting the ground and the leg is swinging in the direction of progression (backward to forward), preparing the next foot strike. Generally swing phase accounts for 38-40% of GC. Both phases are also sub-divided in several sub-phases according the events (Winter 1991; Vaughan, Davis et al. 1999).

3.3.1. Stance Phase sub-phases

Usually, three sub-phases and five events are considered during stance phase. These will be presented in next paragraph by chronological order of events/phases (Vaughan, Davis et al. 1999):

1st phase – first double support – begins with the IC of the ipsilateral foot and ends with the TO of the contralateral foot.

2nd phase – single limb stance – starts with TO of the ipsilateral foot and ends with the IC of the contralateral foot. This phase occurs simultaneously with the swing of the ipsilateral leg.

3rd phase – second double support – occurs when both feet are again in ground. This phase begins with the IC of the contralateral foot and ends with TO of the ipsilateral foot.

1st event – Initial Contact (IC)

2nd event – Foot Flat (FF)

3rd event – Mid stance (MS)

4th event – Heel Off (HO)

5th event – Toe Off (TO)

3.3.2. Swing Phase events

During swing phase is usual consider three distinct events (Vaughan, Davis et al. 1999):

1st event – Acceleration – begins with TO, when the hip flexor muscles activate to accelerate the ipsilateral leg forward.

2nd event – Midswing – occurs when the ipsilateral foot passes along the contralateral foot. This event is coincident with the MS event of the contralateral foot.

3rd event – Deceleration – occurs when the body muscles slow the leg to prepare the next heel contact.

3.3.3. Pathological Gait Events

The nomenclature presented is generally applicable to describe the gait of non-pathological subjects. However, the gait of some pathological individuals cannot be described using this terminology. Therefore, Perry et al. considered the GC divided in 8 events, which are sufficiently general to be applied to any type of gait as represented in (Gage, Deluca et al. 1995; Vaughan, Davis et al. 1999).

Stance Phase

1st event – Initial Contact (0%)

2nd event – Loading Response (0-10%)

3rd event – Mid stance (10-30%)

4th event – Terminal Stance (30-50%)

5th event – Pre-swing (50-60%)

Swing Phase

6th event – Initial Swing (60-70%) – starts with TO of ipsilateral foot, continuing until the maximum knee flexion is reached.

7th event – Midswing (70-85%) – corresponds to the period of time between the initial swing and the terminal swing.

8th event – Terminal Swing (85-100%) – this event begins when the ipsilateral thigh is perpendicular to the ground. Its finish occurs when the ipsilateral foot hits the ground.
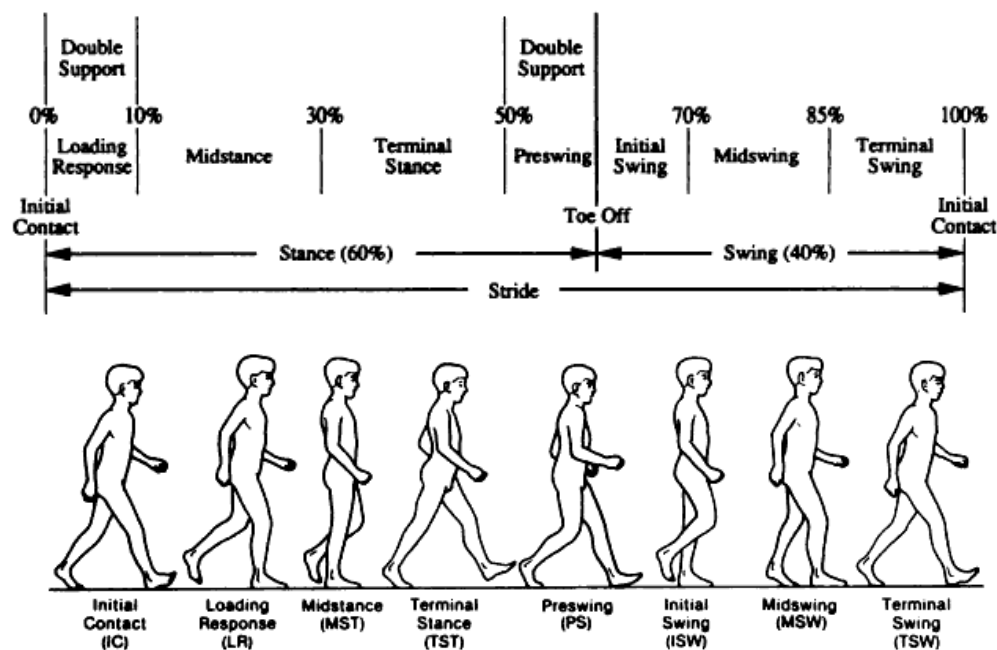
Figure 5 – Schematic representation of a GC using Perry nomenclature (Gage, Deluca et al. 1995)

3.4. Muscle Control Pattern and Detailed Gait Events

Section 3.4 shows the complexity of motion pattern during a stride, which is only possible to achieve due to the existence of a pattern of muscular control. The muscles are the motor units that produce active movements. During gait several muscles are activated according their function. Generally, their activations can be measured by kinesiological electromyography. Although the gait analysis began in 17th century, the study of muscle patterns in gait using EMG was applied only in 1944 by Vern Inman (Sutherland 2001).

The functions of the muscle during the gait are not restricted to the production of motion, other functions as weight bearing stability, shock absorption and progression over the supporting foot are also provided by them (Perry 1992).

The study of the muscle pattern during the normal gait is essential to perceive the complexity of movements. The comparison of these results with pathological gait can help to predict several neuromuscular diseases as well as understand the physiological and anatomical mechanisms of failure. It is important to retain that a profile of EMG can be considered for non pathological gait, although a pattern of EMG activity changes considerably with the subject. Arsenault et al. studied the profile of EMG during activity in gait for five muscles and observed significant differences in amplitude (normalized) to all muscles between subjects. This variability is more significant for muscles with multiple functions; e.g. knee and hip muscles present a high variability, especially during the stance period where their actions have an important role in the control of the body balance and avoid the collapse caused by the gravity action. On the other hand the EMG profiles for the ankle muscles are more consistent, due to the high forces required and the little possibility of adaptation (Arsenault, Winter et al. 1986 a); Winter 1991).

In Figure 7 the EMG profile for non-pathological gait can be consulted. Several papers indicate the presence of co-contractions resulting of activity of antagonist muscles. Its quantification is very difficult, since it is necessary to know the moment-of-force created by them (Winter 1991; Vaughan, Davis et al. 1999).

Several studies referred in Winter, show that the EMG patterns in Children are very similar to adults; small differences are found in rectus femoris and lateral hamstring for two age groups ([4-7] and [8-11]). Other studies showed minor differences in relation to adults pattern to children with 2 and 3 years old and significant differences to one year old children (especially in gastrocnemius) (Winter 1991).

It is important to note that there are few papers analyzing the muscular activation of the upper body (HAT – head, arms and trunk), however its study is important to understand the mechanisms of body balance that are characterized by the CNS's ability to control the acceleration in all involved segments. For example the EMG study of pelvic and trunk muscles shows an important role in the balance stabilization of superior segments (Winter 1991; Winter, MacKinnon et al. 1993).

Winter et al. concluded that, in addition to the function in lower limbs, the hip flexors and hip extensors muscles have also an important function of controlling the dynamic balance of HAT in the plane of progression – passive feedback control. The authors considered that the vestibular system (responsible for the balance, orientation in the space, among other functions) has few influence in the control of dynamic balance. The same idea is shared by Bauby and Kuo. However they concluded that the control of lateral balance is performed by an active visual-vestibular feedback, and a reduction of sensory information has a greater impact in this control. Winter et al. considered two mechanisms (muscular and kinematic) of control of lateral balance: 1) The hip abductors, assisted by the medial acceleration of the hip joint, have an important role in the stabilization of HAT balance during the single support. 2) The position (medial/lateral) and placement of foot also helps to control the total balance of the body in coronal plane, this mechanism is assisted by the medial/lateral acceleration of the subtalar joint (Winter, MacKinnon et al. 1993; Bauby and Kuo 2000).

The swing movement of arms (see 3.4.9) can help optimizing the action of the lower limbs since these coordinate movements minimize the torque loading on the joints and skeletal structure. It is a

fact that the swing motion is not a requisite for a stable walking; however, there is a relation between this motion pattern and the energetic requirement – walking without swing motion implies that the energy cost is greater in lower limbs caused by an increase of reaction moments in the foot (Park 2008).

In the following paragraphs the principal muscular actions in lower limbs and the movements produced by them will be described. The explanation is based in Perry and Winter description (Winter ; Perry 1992).

3.4.1. Initial Contact

During IC the ankle is at neutral dorsiflexion, the knee is totally extended and the hip is flexed (approximately 30º). In non-pathological gait, the impact occurs with the heel creating a floor reaction force that introduces three positions of instability (the alignment of reaction force vector results in a controlled plantar flexion torque at the ankle and a flexor torque at the hip and trunk) and one stable relationship (the alignment of reaction force vector causes a passive stability in knee). To better understanding the relations between GRF vector and the knee and ankle joints, a schematic representation of the evolution of this force during stance period is presented in Figure 6. A more detailed explanation about GRF will be done in section 3.6.2.1.

In muscular activity, this event is marked by the action of hip extensors (hamstring, gluteus maximus and adductor magnus) that maintain the flexion torques presented. The hamstrings also prevent the knee hyperextension.

The combined action of tibialis anterior, extensor digitorium longus and extensor hallucis longus stabilize the ankle and subtalar joints maintaining the foot in neutral position.

3.4.2. Loading Response

This phase is characterized by the absorption of the shock from the impact of foot with ground and by the WA. This phase is characterized by large muscular activity to control them.

Sagittal Plane

The ankle performs a restrained plantar flexion; the foot spins over the calcaneus until being flatted (approximately 10º), this reduces the degree of advancement tibial resulting in a knee flexion. As the GRF vector is being applied in heel (Figure 6), it causes a plantar flexion; however, the Tibialis anterior activates with the objective of decelerating and controlling the ankle motion – controlled plantar flexion.

During WA, the heel rocker action rolls the tibia forward disrupting the knee stability and causing a flexor moment. Due to the passive unlock of the knee, a flexion motion of this joint is performed by the low level of hamstrings action. The fast action of quadriceps limits the flexion to approximately 18º.

The hip continues flexed (30º) to maintain the erect posture; however, this suffers a flexor torque that is countered by the rapid action of hip extensors (Gluteus maximus and Adductor magnus) and assisted by the continuing low level of hamstrings action. The lumbar extensor muscles assisted by the hip extensors prevent the flexion of trunk in the pelvis.

Coronal Plane

Due to the rapid transfer of body weight (BW), a strong adduction torque is produced at the knee and hip, stimulated by the dropping on the unsupported side of pelvis, limited to 5⁰ by the action of the hip abductors (Gluteus medius, Gluteus minimus, Upper gluteus maximus and Tensor fascia lactia). The adductor torque at the knee is countered by the action of the iliotibial tract (insertion of Tensor fascia latae (abductor of tibia at hip joint) and Gluteus maximus). To absorb the shock of the impact, the foot performs a subtalar joint abduction, that is controlled by the action of Tibialis anterior and tibialis posterior (Perry 1992; Graaff 2001).

Transverse plane

The subtalar joint abduction causes an internal rotation of the talus and in turn a rotation of tibia that induces an internal rotation torque in the knee. The deceleration of knee rotation is controlled by the iliotibial tract tension and biceps femoris long head action.

An anterior pelvic rotation can be observed and is restrained by the difference in duration of medial and lateral hamstrings.

3.4.3. Midstance

The MS is characterized by the restrained ankle dorsiflexion, knee extension, and hand hip stabilization in coronal plane. In this phase the intense muscle action is decreased in early middle stance and the vector of GRF becomes posterior to hip joint and anterior to the knee and ankle.

The limb is stabilized by the action of Triceps surae muscles, the knee is extending (controlled by the Soleus muscle). Until the passage of vector of forces to anterior knee position, the quadriceps remains active – the vastus pull the femur forward.

The hip reduces its flexed position (30⁰ to 10⁰), although the action of hip extensor muscles are minimal. In this phase the posterior Gluteus medius is still active.

3.4.4. Terminal Stance

During terminal stance, the body rolls forward over the forefoot causing a 10⁰ dorsiflexion angle at the ankle; the heel rises and the knee extends totally. As a result, a large dorsiflexion torque is produced; however the action of gastrocnemius lateralis, gastrocnemius medialis and soleus counters that and stabilize the tibia at the ankle. The action of soleus in the tibia also helps to stabilize the knee and the hop during this early phase.

At the end of the terminal stance, the interaction between the foot and the ankle causes an advance in the knee, it passes the GRF vector unlocking it and causing its flexion.

3.4.5. Pre-Swing

In this phase starts the second double support event, the counterlateral limb hits the ground beginning the WA and the ipsilateral limb prepares the swing phase.

With the continuous advancement of the GRF vector to the forefoot (metatarsophalangeal joint) and the loss of magnitude of it due to the transfer of BW onto the other limb, the load demands on the foot decreases, causing a high heel rise and a decreasing in the muscular intensity of the triceps surae. The result is the advancement of the tibia for an anterior position to the GRF vector causing an unrestrained flexion of the knee and the advance of the thigh (increasing the hip angle – flexion),

although, in some cases, when the knee flexion is excessive the Rectus femoris is activated to control the movement. The flexion of the hip is followed by the development of an abductor torque (caused by the alignment of the component of the GRF in the coronal plane with hip joint axis) that is restrained by the muscular action of the Adductor longus.
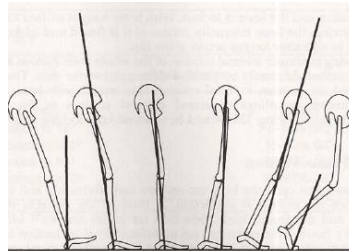
Figure 6 – Sequence of GRF vector (bold vertical lines) and its relations with ankle and knee during stance phase. From left to right IC, WA, early MS, late MS, TS and PS

3.4.6. Initial Swing

This phase is characterized essentially by two events: 1) Increased knee flexion till approximately 60º to lift and prevent the dragging of foot with ground. 2) Hip flexion to advance the limb.

Perry stated that the muscular action during this phase is variable; however some muscles have a consistent activation: the short head of Biceps femoris is responsible for the knee flexion (the long head is also a hip extensor so its activation would result in a flexion restriction at hip), the iliacus performs the flexion and hip and the low action of Sartorius and Gracilis promotes a combined hip and knee flexion.

The ankle angle also varies, the plantar flexion decreases to approximately -10º by the action of the tibialis anterior and the extensor digitorium longus.

3.4.7. Medial Swing

During MSw, the swing limb continues advancing and the hip flexing, although the action of hip flexors is minimal.

In order to avoid the contact of the foot with ground, the Tibialis anterior, Extensor digitorum longus and the Extensor hallucis longus perform a controlled dorsiflexion (low intensity) till neutral position. Passively, the knee flexion decreases to 30º

At the end of this phase, the hamstrings activate to start decelerating the thigh and controlling the hip flexion.

3.4.8. Terminal Swing

The muscular action is again intensive to prepare the stance phase. The knee continues extending passively till neutral position. The hamstrings continue activated to control the hip flexion, decelerating the thigh and avoiding the knee hyperextension. At the end of this phase a reduction in the intensity of the hamstrings is observed then, the quadriceps activated to extend the knee completely. The ankle keeps neutral (in some cases is measured a slightly plantar flexion (-5º)) by the action of the Tibialis anterior and the Extensor digitorium longus.

3.4.9. Upper limbs and Head

As the lower limbs, the upper limbs and the head are characterized by a well defined motion pattern. Both arms act like a pendulum, they extend and flex alternately describing an arc of 30-40º. At IC the ipsilateral shoulder (arm) is at the maximum extension (-24º); with the advancing of the stance period, the arm begins to flex, having a maximum flexion of 8º at the end of terminal stance (45% of GC). After this event, the ipsilateral arm extends till it has a new maximum of extension at the end of the swing phase (IC).

A pattern in the elbow joint can also be observed. At IC, the ispsilateral elbow is at the maximum extension (20º); like the shoulder, with the advancement of stride period, the elbow flexes, though the maximum flexion occurs at the IC of contralateral foot (55% GC), approximately 44º. The elbow reaches again its maximum at MSw.

It is important to retain that the magnitude of total arc is influenced by the velocity of the gait. The fast cadence is accompanied by an enlargement in this arc. It is caused by the increasing of the shoulder extension and elbow flexion while the other arcs remain unchanged.
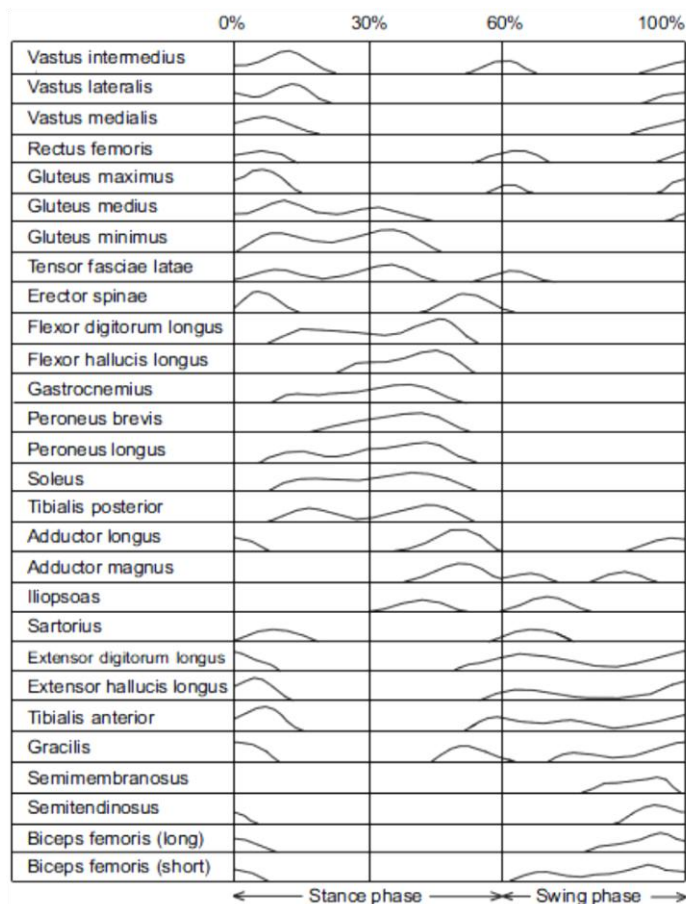
Figure 7 – Normal EMG patterns for the major muscles of lower limbs during a stride period (Vaughan, Davis et al. 1999)

3.4.10. (As)symmetry of Gait

Generally in the study of normal gait, it is assumed that the lower limbs have a symmetrical behaviour and deviations of this symmetry are considered as pathologies, however this assumption is not always valid. The first hypothesis has been accepted for the simplicity of data collecting and processing, some studies cited in Sadeghi et al. present results that support the symmetry. Other

studies cited in Kim and Eng show that the difference between the two limbs using symmetry index for the temporal measures and vertical forces is less than 6% (Sadeghi, Allard et al. 2000; Kim and Eng 2003).

However, more recent works demonstrate that the asymmetrical behavior reflects a natural functional difference between the limbs; Gunderson et al. cite a series of kinematic studies that support this fact (e.g. asymmetries in step length, maximum knee flexion, etc.). These authors also tested the asymmetry of the gait and obtained similar results (Gundersen, Valle et al. 1989).

The asymmetry of lower limbs can also be observed in EMG profiles. Arsenault et al. studied the EMG pattern of soleus and rectus femoris and obtained different EMG amplitudes between the legs. Õunpuu and Winter after analyzed the EMG profile of seven muscles for both legs concluded that the idea of symmetry is not valid for individual subjects and there is a connection between the preferred leg and the EMG profile for the plantar flexors muscles (Arsenault, Winter et al. 1986 b); Õunpuu and Winter 1989).

This asymmetry in lower limbs appears to be related with the functional contributions of each limb to control and propulsion tasks. Sadeghi et al. consider that a subject tends to use the preferred limb to achieve a given objective, while the other limb provides support to that action (Sadeghi, Allard et al. 2000).

3.5. Time-Distance Parameters

In order to analyze the normal and abnormal gait time-distance parameters are usually used – step length, stride length, step time, stride time, step width, cadency and velocity. Sutherland considers that the step length and step frequency for non-pathological subjects are approximately equal and these two parameters can be used to calculate velocity. However, if an asymmetry is observed in these parameters, the calculation of velocity must be performed with stride frequency and stride length. It is important to note that variability is observed in time-distance parameters between the children, adult women, adult men and elderly (Sutherland 1997).

Sutherland et al. studied the differences of these parameters with children (1-7 years), and observed a fast increase in cadence until 2.5-3 years (~180 to ~150) and a stabilization after this age (~140-150). On the other hand the stride length increases rapidly until 4 years (~40cm to ~80cm) and then continues increasing but with a small rate (~100cm to 7years). The gait velocity follows the same pattern of the stride length, increasing rapidly till 4 years (100cm/s) and stabilizing after this age (~110cm/s). Sutherland et al. concluded that there is a linear relationship between the step length and leg length and therefore the gait velocity is also related with this fact (Sutherland, Olshen et al. 1980; Sutherland 1997).

In adult gait a difference between men and women can also be found, as generally men tend to walk with a greater velocity, but with a smaller cadence. The natural cadence in men varies with the studies but all present results between 105 and 120 steps per minute. The results for women present a cadence that is 6-11 steps/min higher than for men (Murray, Drought et al. ; Winter 1991; Öberg, Karsznia et al. 1993).

Murray et al. also studied the velocity for men and women and obtained respectively 1.51m.s^{-1} and 1.30m.s^{-1}. This result is consistent with other studies cited in Waters et al. and Öberg et al. These last

authors studied a total of 233 subjects grouped by the age and sex, in laboratory condition (treadmill with 5.5m of walking distance). They have obtained the same differences between men, women and children to time-distance parameters, but the values were slightly lower than presented before. They concluded that the time-distance parameters vary with the environment of the study (outdoors, short walkways and long walkways), subjects tends to walk slower in short walkways (Murray, Drought et al. 1964; Murray, Kory et al. 1970; Öberg, Karsznia et al. 1993; Waters and Mulroy 1999).

The stride length, the stride width and the foot angle in transverse plane also present small differences between men and women. The average step length, stride length, stride width and foot angle in men and women are respectively 0.79m, 1.58m, 0.081m, 7º, 0.66m, 1.32m, 0.071m and 6º (Murray, Drought et al. 1964; Murray, Kory et al. 1970).

As reported, there is a relation between the step length and leg length for children, the same relationship is also found in adults, though this correlation is smaller (r=0.51-0.59) for natural cadence. However, during fast cadence this relationship plays an important role, the correlation factor increases to 0.71 (Perry 1992).

The studies of time-distance parameters to elderly have showed differences between them. Murray et al., in a study of subjects with ages between 65 and 87, observed a decrease in cadence, stride length and velocity. The same results have been achieved by Öberg et al. and Menz et al. These last authors concluded that the alterations of gait pattern in elderly have the main goal of stabilize the head and pelvis to reduce the risk of falls (Murray, Kory et al. 1969; Öberg, Karsznia et al. 1993; Menz, Lord et al. 2003).

However, Winter et al. performed a kinematic and kinetic study of the gait with 15 healthy elderly subjects and compared with a control group of 12 healthy young adults with similar height, in which they also concluded that the natural walking velocity of such subjects is reduced. The cause relies not in a decrease of cadence (elderly – 110.5 steps/min, adult – 111.0 steps/min), but instead in the reduction of the stride length (elderly – 1.39m, adult – 1.55m) (Winter, Patla et al. 1990).

3.6. Acquisition of Kinematic and Dynamic Data in Gait Analysis

Currently, the gait study is performed by a set of interlinked acquisition systems, which allows analyzing each event of the gait cycle. The acquisition of the kinematic data (instant positions of each body segment, their translations and joint angular rotations) and dynamic data (external forces) became easier, faster and more accurate (Sutherland 2002).

As seen in chapter I, the mechanisms of gait analyses have undergone an evolution across time. The first performed analyzes were a simple description of the observed motion. However, only in the XIX century, also denominated as the gait century, technological devices were applied into the study of human gait, especially in Étienne Marey and Eadweard Muybridge works (Nigg and Herzog 1994).

According to Perry, a complete analysis of gait considers five types of measurement systems. The first three systems study the specific events of walking: 1) Motion analysis – permits the study of a body segment position and their translation movements. It also allows the analysis of the angular movement of joints. 2) Electromyography – allows understanding the period and the relative intensity of muscle action. 3) External forces analysis – allows obtaining the magnitude and direction of reaction forces, which are essential to calculate the torques in the joints. The other two types of measurement

relate the gait mechanics with their effects in the subject: 4) Walking capability – studies the stride characteristics and compares it with a non-pathological pattern. 5) Walking efficiency – studies the efficiency of gait, analyzing its metabolic cost (Perry 1992). For each type of considered measurements, there is not an optimal system to record it. Several techniques can be considered and their choice should take into account the objective of the analysis, its price and application (clinic/science) (Perry 1992). In the following paragraphs, some of the most used techniques in gait analysis and their main characteristics will be presented.

3.6.1. Motion analysis

Several systems can be used to quantify and qualify the motion of human body, from simple photos to complex acquisition systems of movements in 3D. For example, for a qualitative analysis a set of video cameras can be used. However if the main objective of the study is the quantification of gait parameters, a system of marker acquisition is necessary (Hall 2003).

Film Photography – is an older method, which relies on o a large frame camera to record the motion by multiple exposures with an interrupted light (strobe light photography) in a dimly lit room. The subject is clothed with black clothes that have reflective bands/markers in the segments that will be measured. As a result, a series of photos with sticks figures is obtained (Perry 1992; Sutherland 2002).

Video Cameras - generally, a set of video cameras is used for a descriptive analysis, in which is intended to understand the movement without its quantification. These are also used as a support for other systems, e.g. in gait analysis, the video cameras are used simultaneously with the Infrared cameras, providing the researcher a vision of the trial. As the human movement is not constrained to a single plane, it is usual to use a set of cameras to cover different angles. Some advanced systems/software allow calculating general kinematic parameters through image processing (these software have the capability to distinguish high-contrast markers) (Hall 2003).

Goniometers – used in some studies in which the objective is to acquire the joint angular displacements. In gait analysis, an electronic version is generally used (electrogoniometer), since these enable a continuous angle measurement between two segments in real time (Hall 2003). Essentially, two types of goniometers can be considered: 1) single axis – allows the measurement of a joint angle only in one plan, and as such, its use has been discarded. 2) triaxial parallelogram – is the most used in gait analysis, since it allows measuring angles in the three coordinate planes (coronal, sagittal and transverse) (Perry 1992).

Optical motion capture systems – probably the most used system in gait analysis, since these allow the acquisition of the exact 3D position of body segments and the definition of the arcs and the position of joints (Perry 1992). The great advantages of their use are the possibility, not only to acquire the exact positions of segments, but to define the centers of joint rotation, calculate velocities, accelerations, and when associated with a mechanism of external force detection (force plates) this systems allow with the support of a proper biomechanical multibody model to calculate moments in the joints and muscular forces (Perry 1992; Sutherland 2002).

These techniques resort to the use of optical sensors, for example infrared cameras and markers to track human movements. Generally, the markers are placed over the skin or in elastic bands that do

not allow movement. The necessary precautions to a correct placement will be discussed in chapter 6 (Cappozzo, Catani et al. 1996).

Two different types of settings can be performed:

a) **Passive systems** – lies on the use of reflective markers in the anatomical landmarks of segments in study. A set of cameras, strategically placed to cover all the analysis volume, emit an infrared beam that is reflected by the markers, returning to the camera. Each camera measures the 2D position of each marker and combining the data from different cameras with appropriate software, it is possible to reconstruct a 3D model of the movement (Zhou and Hu 2004; QUALYSIS 2010).

b) **Active systems** – utilize markers that are optically active. Contrarily to the passive case, the active markers are the source of the information, emitting a light beam that is captured by a set of cameras. The process of reconstruction is similar to the passive systems. The active markers can make use of LEDs and LASERs (Richards 1999).

For a proper reconstruction is essential that each marker is seen by two cameras at least; thus the number of cameras and their distribution in space is fundamental and must be strategically thought (QUALYSIS 2010). The correct distribution of the cameras is also important to avoid the markers occlusion, typical of a dynamic analysis, due to the movement of some segments that can cause inconsistent and unreliable results (Zhou and Hu 2004).

Although the LED markers provide good results (high contrast with background and only one marker is active at a given time), their use is limited to a certain number of markers (due to the stroboscopic time). To mitigate this problem the use of both passive and active markers at same time is advised (Figueroa, Leite et al. 2003).

The use of passive markers also present some problems, despite having a high contrast with background, the presence of many markers in simultaneous can rise some issues in the 3D reconstruction, especially if the markers have a small distance between them. To avoid this problem, a correct and careful marker placement is essential, as well as a correct calibration of the cameras and adjustment of acquisition parameters (Figueroa, Leite et al. 2003; QUALYSIS 2010).

Non-visual systems – similarly to the motion marker systems, this type also resorts to sensors attached to the analyzed body segment. Several types of sensors can be considered and their use depends on the measurement target. Within this group are found the systems that use mechanical, inertial, acoustic, radio and magnetic sensors (Zhou and Hu 2004).

For example, the inertial motion capture lies on the use of inertial sensor units (IMUs) attached to the body. The great advantage is the portability of the system since it only requires the earth's gravitation force and magnetic fields to function. Associating this fact to the possibility of measuring and treating data in real time, leads to its use in robot controlling (e.g. NASA robonaut) (Miller, Jenkins et al. 2004).

The mechanical systems, also referred to as exoskeleton motion capture systems, use a set of sensors, generally rigid structures of plastic and metal with potentiometers, attached in articular centers with the goal of measuring angular displacements. The advantages of these systems are the

possibility of acquisition and treatment of the data in real time and the absence of occlusion, seen in optical systems. The goniometers are an example of this type of systems (Miller, Jenkins et al. 2004).

The electromagnetic motion systems use transmitters to produce magnetic fields in the surrounding and then resort to sensors to calculate the position and orientation of the body segments based in those magnetic fields. The results obtained are very accurate and each marker has its own sensor data channel (this fact avoids the confusion between markers, which can happen in optical systems when the distance between the markers is small); however, these systems are very sensitive to the metallic interference (transmission source) and the volume of acquisition is relatively small (Gleicher 1999; O'Brien, Bodenheimer et al. 2000; Miller, Jenkins et al. 2004).

3.6.2. Dynamography (Ground Reaction Force)

The study of the Ground Reaction Forces (GRFs) during walking/running allows also the detection of several lower extremity injuries, where some are caused by the repeated impact of the foot on the ground. The study of the variations of GRFs when compared to the normal permits the development of appropriate correctives to each case (Cavanagh and Lafortune 1980).

Sir Isaac Newton has revolutionized the classical mechanics introducing the three laws of motion in XVII century. The third law affirms that forces occur in pairs (Action and Reaction) and these are equal in magnitude and opposite in direction (Sutherland 2005).

During the stance phase, the foot applies a force in the ground that is equally matched by a reaction force of the ground. This reaction force vector is characterized by its application point and three components (three-dimensional) – one vertical component (z) plus two horizontal shear forces - anterior-posterior (corresponds to the direction of progression (x)) and medial-lateral (perpendicular to the other two vectors (y)) (Winter 1990; Sutherland 2005) .

3.6.2.1. Ground Reaction Force during walking

The three components of Ground Reaction Force (GRF) and their application point present distribution curves that are characteristics of the type of movement performed. The GRF components vary slightly with gait speed (slow, normal, fast cadence and running), since for higher cadences the impact on ground and the momentum in the joints articulation will be greater and therefore the GRF will present a higher magnitude (vide Figure 8) (Cavanagh and Lafortune 1980; Winter 1991; Perry 1992).
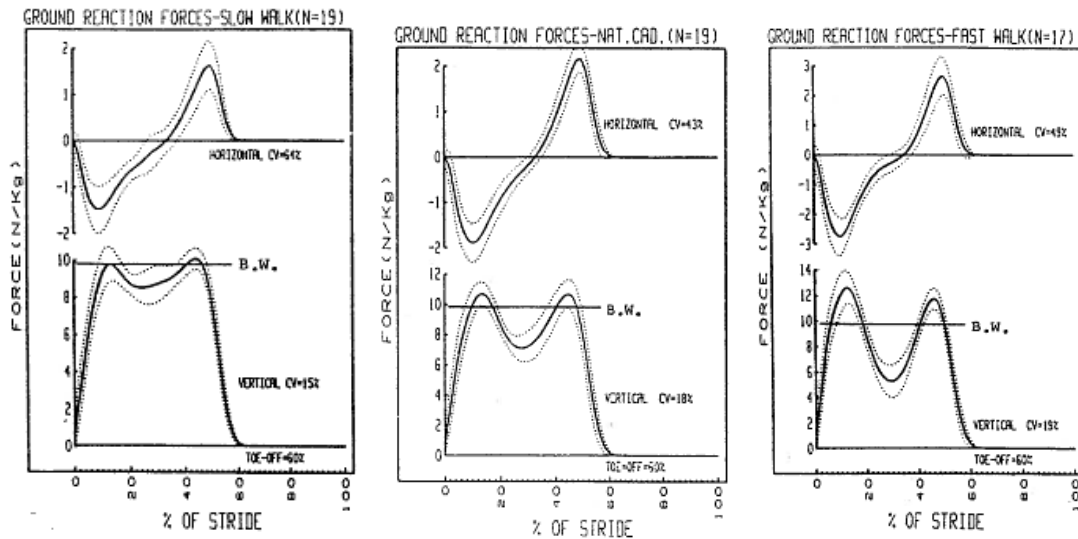
Figure 8 – Non-pathological GFR (antero-posterior shear and vertical force) pattern during a stance for; a) slow Cadence (left) b) normal cadence c) fast cadence (Winter 1991)
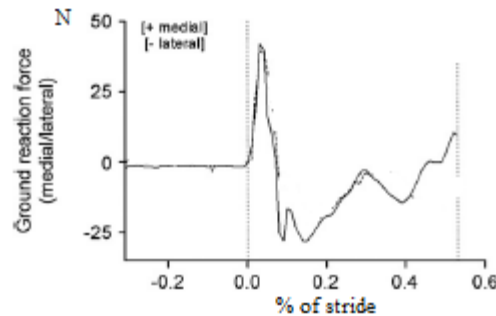
Figure 9 – Non-pathological GFR (medial-lateral shear) pattern during a stance phase normal cadence (Fong, Chan et al. 2008)

Vertical Load – In non-pathological gait, the vertical load for normal cadence presents a characteristic "m" curve; the magnitude value of the F_z component rises quickly, during the WA, having a peak at MS of approximately 110% of the body weight (BW); this phenomenon is caused by the drop of the COM adding the effect of acceleration to BW. With the knee flexion during the MS, the force plate is partially unloaded and the magnitude value decreases to 80% of BW; this decrease is also accentuated by the momentum of the swinging limb. In the terminal stance the value of F_z grows again during the plantar flexion of the ankle causing the second peak, which has a maximum value similar to the first peak. After that, the value decreases to 0% of BW, while the contralateral limb starts the WA phase (Winter 1990; Perry 1992).

Although the vertical load can provide an idea of a possible pathological condition, sometimes this information is less relevant than the change created by the patient's slower gait. The analysis of subjects with painful/weak lower limbs is complicated due to the irregularity of the curve. Perry argues that other measures should be consider when the disability is severe (gait velocity, stance time, etc.) because the measurement of this parameter does not always returns reliable results (Perry 1992).

Horizontal Shear – The horizontal shears represents the two components of GRF in the horizontal plane, being responsible for the interaction between the foot and the ground. These two components

41

have a maximum magnitude value smaller than the vertical component. However they are essential to promote the stability of the stride (avoids sliding) (Perry 1992).

The anterior-posterior shear represents the component of GRF in the direction of progression – the magnitude is positive when the force has the same orientation of the progression (anterior) and a negative value when it is contrary (posterior). The plot of anterior-posterior reaction force is characterized by a quickly decreasing to a minimum value approximately equal to -13% of BW at 10% of stride period. After that, the value starts to become less negative and with the beginning of the HO the magnitude of the force takes a positive value and continues rising until a maximum value of 23% of BW, caused by the forced plantar flexion in the final of PO (Winter 1991; Perry 1992; Fong, Chan et al. 2008).

The exchange of the BW of one limb to the other creates a reaction component that is perpendicular to the direction of progression. Generally, the medial shear is represented as positive and the lateral as negative. During the stance period two peaks can be considered, the first one occurs in mid loading response and has a magnitude of approximately 5% of BW (medial shear). After the first peak the value starts to decrease to a negative value (lateral shear) of approximately -7% of BW in the terminal stance (Perry 1992).

As a result of the three components, the plot of the GRC vector in a sagittal plane during the stance is very characteristic. During the IC event, the high speed of the heel when it contacts the ground causes a momentary vertical force without shear, as can be easily observed in Figure 10.(Perry 1992)
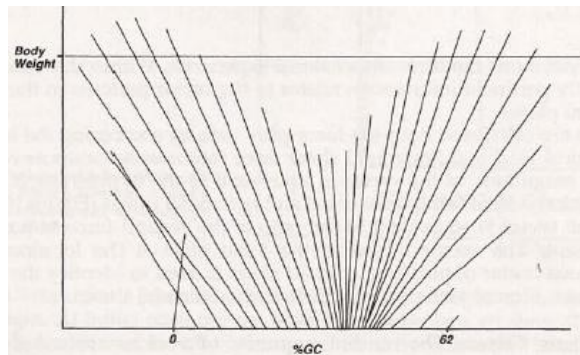
Figure 10 – representation of the vector of GRF in sagittal plane during a stride for normal walking (Perry 1992)

The reaction forces are an algebraic summation of all mass-acceleration products of the body segments. Particularizing to the anterior-posterior shear and vertical shear (Winter 1990; Perry 1992):

$$F_X = \sum_i m_i . a_{xi} \qquad (2)$$

$$F_Z = \sum_i m_i(a_{Zi} + g) \qquad (3)$$

where m_i is the mass of the segment i, a_{xi} is the acceleration of the center of mass in the direction of progression of the segment i, a_{zi} is the acceleration of the center of mass in the vertical direction of the segment i and g is the gravity acceleration. As the g and m_i are constants during the analysis, the value measured in the force plate is a result of variations of the accelerations. For example, for the vertical load, if a = 0, this means that the measured value is the BW, if a > 0 the force will be greater than the BW and vice-versa. However, the F_z can be constant in some cases; e.g. during the gait,

when an arm is accelerating the other is decelerating, thus annulling the force produced. The relation between the gait velocity and the GRF is easily explained by these two equations (2) and (3); when the cadence is increased, the segments accelerations are also increased and thus the components of GRF will have greater magnitudes (Winter 1990; Perry 1992).

Center of Pressure (COP) – represents the origin of the GRF vector, and is related to the plantar outline of the foot. However, its instantaneous location does not necessarily mean that this portion of the foot is the one receiving the greatest pressure. The COP is an average of all forces acting on the foot, not necessarily the site of maximum pressure. For example, during the MS, the pressure is supported by the heel and the forefoot and the respective COP is situated in an area with no/little contact with the ground (Perry 1992).

The COP is essential for a precise dynamic analysis and provides useful information to detect gait pathologies. COP is related with COG and its characterization is important to understand the body balance and dynamic postural control. Thus its recording can be used as a measure for neuropathological subjects and to develop appropriate corrective orthotics (shoes, insoles, orthosis and prosthesis) (Hasan, Robin et al. 1996 b); Jamshidi, Rostami et al. 2010).

For a non-pathological subject, the IC occurs with the heel, and during this event the COP is located approximately in the medial-posterior portion of the heel. With the advance of the stance phase, the COP begins to move to the lateral longitudinal arch of the foot. At the FF event, the COP has a peak of lateral displacement and then continues towards the forefoot (HO event). Finally the COP crosses the forefoot and terminates in I and II metatarsal heads (TO event) (vide Figure 11) (Jamshidi, Rostami et al. 2010).
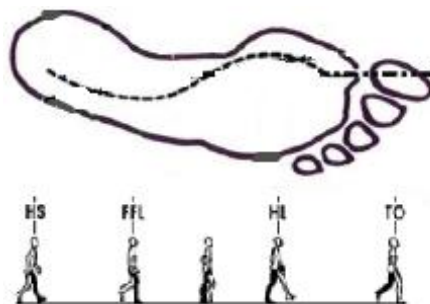
Figure 11- displacement of COP during stance in foot sole

3.6.2.2.   *Ground Reaction Force Recording*

The search of scientific methods to measure the reaction forces started with two students of Marey – Carlet and Ampar. Although the method just had the capacity to measure one dimension (vertical), these authors obtained a typical "m" curve similar to the one obtained with modern force plates. The development of these devices have continued, and in the mid-1940s, Elftman presented a force plate with the capacity of measuring forces in more than one plan (vertical force and dynamic pressure) (Elftman 1934; Sutherland 2005). In our days, essentially two types of force plates can be considered (Winter 1990):

1) **Flat plate supported by four triaxial transducers (Kistler force plates)** – this type of force plates is characterized by four piezoelectric transducers located in its corners (vide Figure 12). Kistler force plates output eight channels of force data – four F_Z, two F_X and two Fy.

Representing F_{00}, F_{0z}, F_{x0}, and F_{xz} as the vertical forces measured in each transducer, the total vertical force is equal to the sum of these four components. It is also possible to estimate the COP through these four components, where the x and z coordinates are represented by the equations (4) and(5) (Winter 1990):

$$x = \frac{X}{2}\left[1 + \frac{(F_{X0} + F_{XZ}) - (F_{00} + F_{0Z})}{F_Y}\right] \qquad 4)$$

$$z = \frac{Z}{2}\left[1 + \frac{(F_{0Z} + F_{XZ}) - (F_{00} + F_{0Z})}{F_Y}\right] \qquad 5)$$
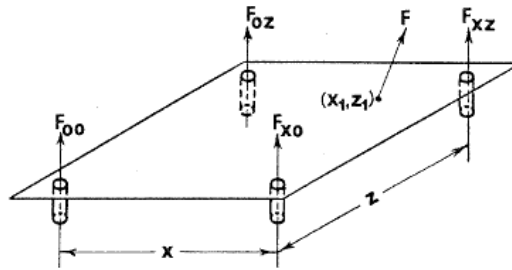
Figure 12 – Schematic representation of a Kistler force plate

2) **Flat plate supported by a pillar (AMTI force plates) –** in this case the plate is supported by a pillar as represented in Figure 13; a series of transducers measure the three orthogonal force components along the X, Y and Z axes as well as the moments on the three axis in relation to a central point in the column. The deduction of the COP is presented in equations [(6)-(11)] (Hasan, Robin et al. 1996 a)):

$$\sum M_x = 0 \qquad 6)$$

$$M_X - y.F_Z + D_Z.F_Y = 0 \qquad 7)$$

$$y = \frac{M_X + D_Z.F_Y}{F_Z} \qquad 8)$$

$$\sum M_Y = 0 \qquad 9)$$

$$M_Y + x.F_Z - D_Z.F_x = 0 \qquad 10)$$

$$x = \frac{-M_Y + D_Z.F_X}{F_Z} \qquad 11)$$

It is important to have some caution, especially when F_z<2% Body Weight, because small errors in the F_z measurement causes large errors in the calculation of the COP (Winter 1990) .

In order to analyze a complete stride with maximum rigor, it is necessary to use at least three plates; each foot should step on only one plate and the whole sole should contact the force plate. To minimize the errors, the plates must be securely fastened to prevent slippage and vibrations, and thus the force plate montages are often fixed and are not easily adapted to each subject. These two factors can restrict the stride for some subjects since they are conditioned to hit the plates (Perry 1992; Fong, Chan et al. 2008).
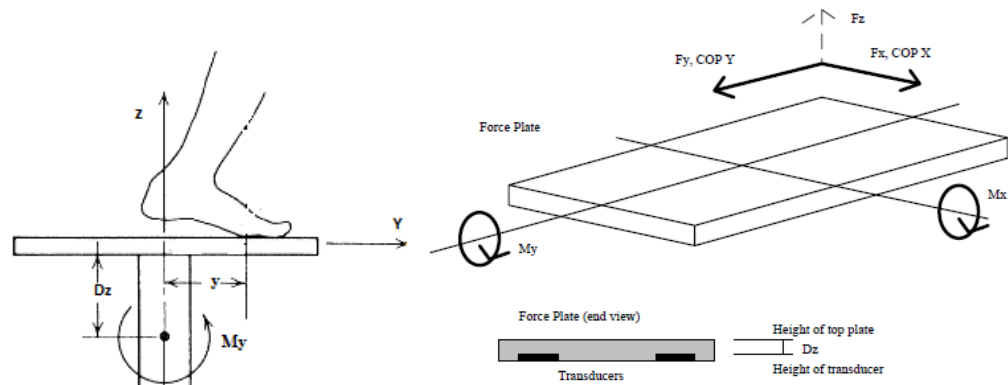
Figure 13 – a) representation schematic of AMTI force plate (left) b) AMTI Force plate axes for force and moment measurement

To avoid the problems of measuring consecutive steps with no constraint on foot placement, in recent years, several research teams have developed algorithms to estimate the ground reaction forces and their application point through the record of the pressure distribution under the foot sole. The measure of the pressure distribution is easily performed by pressure insoles. It consists of an array of pressure sensors spread in an insole. Cordero et al. developed a method to calculate the three components of the ground reaction force and obtained results which were very close to the expected. Nevertheless, the algorithm needs kinematic data and thus still cannot be used in an external environment (Forner Cordero, Koopman et al. 2004). Posteriorly, Fong et al. also developed an algorithm to estimate the ground reaction forces. The obtained results are not as good as the Cordero's. However, the method has the advantage of not requiring kinematic data, hence possibly used outdoors (Fong, Chan et al. 2008).

Although the use of pressure insole avoids the problems of constrained foot placement, it presents some disadvantages. Fong et al. consider the possibility of a change of the interface between shoe sole and the ground for an interface between the mounting frames and the ground, which probably cause an alteration in the friction between the contact interface and in the geometry (increasing the height and weight of the effective sole). The limitation of the pressure insole to a determined foot size and the high cost of the sensors make this technology expensive and not sufficiently robust to be applied in clinical analysis (Fong, Chan et al. 2008).

The use of pressure platforms also allows the measurement of the GRF components as well as the evolution of the COP during the stance phase. The mechanisms are similar to the pressure insole; however it is restricted to a laboratory environment (Hall 2003; Fong, Chan et al. 2008).

3.7. Estimation of Metabolic Costs of Human Gait

It is essential to understand that walking requires metabolic cost; to perform mechanical work, muscles need to spend energy. In some studies is showed that there is a proportional relationship between mechanical work and metabolic cost (Hill 1938).

The human gait is characterized by several complex interactions between the muscular and skeletal system, as well as interactions between human body and the ground. These interactions

result in a mechanical energy loss, that has to be compensated by controlled muscle actions (Donelan, Kram et al. 2002).

A metabolic energy cost is a measurement off effort required to execute a given task. Two types of methods can be considered to perform this measure – experimental and non-experimental. The experimental method involves measuring changes in gas concentration during respiration with metabolic gas analysis systems or metabolic measurement charts (Waters and Mulroy 1999; Macfarlane 2001). The second method recurs to the use of models/algorithms to estimate this value. Some simplistic models estimate the metabolic costs as a value proportional to the external work of the joints moment, however erroneous estimations can be done, since this two variables are poorly correlated and this model cannot consider the isometric contractions (Schiehlen and Ackermann 2005).

Some improvements, like associate models of heat production in the muscles to models of musculoskeletal systems, can perform better estimates that the first model referred. An example of this model is the work developed by (Anderson and Pandy 2001). Other models, as the (Umberger, Gerristen et al. 2003), recurs to the Hill's model of the muscle and permit predict reliable characteristics of human walking with simulation results obtained by dynamic optimization, which allows the minimization of the metabolic costs of transport (Schiehlen and Ackermann 2005).

As already mentioned, the main objective of locomotion is to transport the body with the lowest possible metabolic cost. During a steady motion, there two types of work can be considered: 1) Positive Work – representing the work done by concentric muscles and is equal to the time integral of the mechanical power during the time that the muscle is shortening. 2) Negative Work – which is the work done by eccentric muscles and it is also equal to the time integral of the mechanical power, but during muscle lengthening (Winter 1991). The muscular efficiency (work divided by the expended energy) for this type of motions differs; for a positive work the value is approximately 25% while for a negative work the value is approximately -120%. Due to this fact, the body has to expend positive energy in motions. However, these conditions do not apply to the complex contractions of walking (Donelan, Kram et al. 2002). This fact occurs, because in human walking the muscles maintain a near-constant length, generating minimal power with minimal energetic cost. The tendons execute a stretch recoil cycle, in each step, that generates elastic strain and helps to reduce the energy costs of walking (Fukunaga, Kubo et al. 2001).

Kuo stated that it is relatively easy to quantify the energy expended during a task, because the cost is proportional to the positive work of the muscles. However quantify the energy cost needs to consider the negative work. The author defended that "the negative work of walking comes from the body, not the environment, because the negative work done by aerodynamic drag and friction is almost null at normal walking speed" (Kuo 2007).

Donovan et al. has determined a net metabolic rate (MR) of 150 (MR=0.076)W, to a subject with 66 Kg walking with a speed of $1.25 m.s^{-1}$ (Donelan, Kram et al. 2002). Note that net metabolic rate is considered as the average rate at which metabolic energy is expended and the term net refers to the total energy cost subtracting that for the quiet standing (Kuo 2007).

3.8. Theories of Human Walking

During several years, multiple studies have been performed in order to understand gait patterns and to quantify its major parameters. The latter include moments and torques in joints, external forces, electromyography signs, and so on. However, only in 1953 Saunders et al. proposed the first accepted theory for human walking – The six determinants of gait (Saunders, Inman et al. 1953). Years later, Cavagna et al. proposed a second theory for human gait with different contours – The inverted pendulum model (Cavagna and Margaria 1963; Cavagna and Margaria 1966).

The theory of inverted pendulum and the theory of six determinants of gait have been accepted over the years; however both clash in some aspects. The reason of their acceptance is related to the fact that both consider the same objective of reducing energetic cost.

In recent years, another theory has been developed – dynamic walk. It is an extension of the inverted pendulum theory and tries to eliminate some of the problems pointed to the first theory (Kuo 2007).

3.8.1. Center of Gravity of the Body

To better understand the two theories, it is essential to understand the displacement of the COM during locomotion. Croskey has determined the COM of the body in its mid line, at a distance from the ground corresponding to about 55% of the height of the subject. Thus, the COM occupies a position just anterior to the second sacral vertebra (Croskey, Dawson et al. 1922; Saunders, Inman et al. 1953).

In non-pathologic gait, the COM describes a smooth regular sinusoidal curve in the plane of progression. The COM, during a GC, oscillates twice in the vertical plane and once in the horizontal plane, as can be seen in Figure 14.
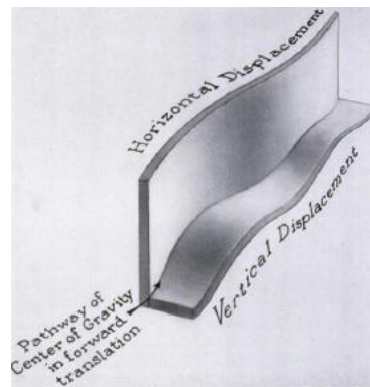
Figure 14 – the horizontal and vertical displacements of the COM during a gait cycle. The first instant corresponds to the IC of one foot and the last instant corresponds to the subsequent IC of the same foot (Saunders, Inman et al. 1953)

The total amount of vertical COM displacement in a normal adult is about 2-2.5 cm. The maximum value of vertical displacement occurs at 25% and 75 % of stride period and corresponds to each mid-stance event of a stride; the height of these peaks is limited by the lateral pelvic tilt (2nd determinant) and the knee flexion during the early support phase (3rd determinant). On the other hand the minimum value occurs at 0%, 100% and 50% of stride period and corresponds to double support phases. The

depth of the troughs is limited by pelvic rotation (1st determinant) and knee-ankle-foot-interactions (4th and 5th determinant) (Saunders, Inman et al. 1953).

The value of horizontal displacement is approximately 4.5 cm, measured from the extremes of the deviation from right to left. The greatest lateral displacement of the COM occurs at the MS event. The amplitude of this lateral displacement is limited by the lateral displacement of the pelvis (6th determinant) (Saunders, Inman et al. 1953).

The study of the COM displacement importance lies in the fact that allows relating the gait with the energy expenditure. The best way, in terms of energy expenditure is to transport the body in a straight line, since according to Newton's 2ª Law is not necessary to apply forces to accelerate and decelerate the COM; however, this is quite impossible to achieve in a bipedal gait. The smooth sinusoidal pathway, with a low amplitude may be considered the best viable alternative with least energy expenditure. As abrupt changes do not exist, only small forces are necessary to guide the COM along the trajectory and hence the energy consumption is lower. This type of translations also permits to conserve the mechanical energy due to conversions of potential energy in kinematic energy and vice-versa (Saunders, Inman et al. 1953). Figure 15 show a summary diagram of the relation between the locomotion efficiency and the COM displacement.
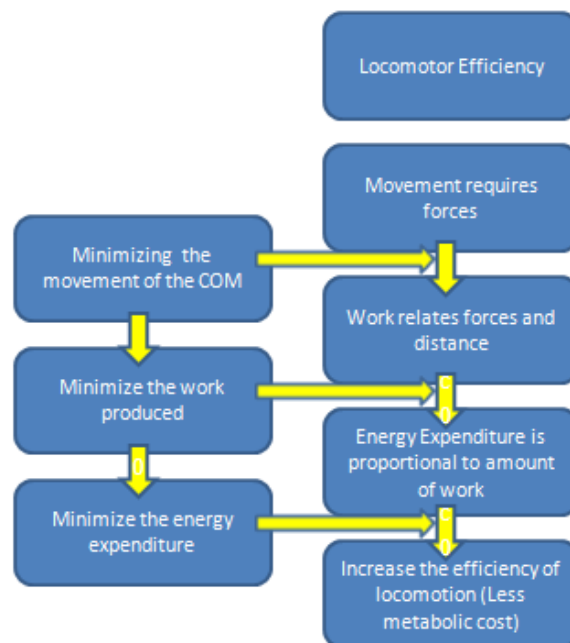
Figure 15 – Summary diagram representing the relation between locomotion's efficiency and the COM displacement

3.8.2. Inverted Pendulum Theory

The inverted pendulum theory, presented in 1966, proposes that the stance leg acts like a pendulum, describing an arc in the plane of progression. This fact helps to understand the less metabolic cost of gait. The kinetic energy is converted in potential energy and vice-versa, preserving mechanical energy (Cavagna and Margaria 1963; Cavagna and Margaria 1966).

During single support, the ipsilateral leg acts like an inverted pendulum, conserving the mechanical energy, and thus the COM can be supported with no muscle force. The center of mass (COM) velocity

is directed perpendicular to the ground reaction force and, as a result no work is performed on the COM during the arch trajectory (vide Figure 16) (Kuo, Donelan et al. 2005; Kuo 2007).
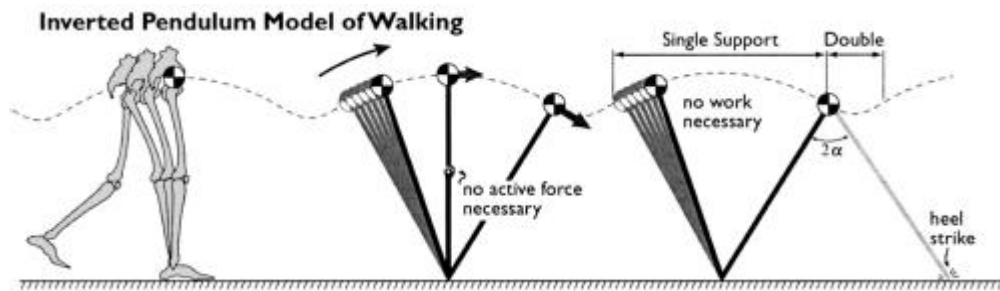
Figure 16 – representation of the simple inverted pendulum model of walk (Kuo, Donelan et al. 2005)

The model of the inverted pendulum also considers that the swing leg moves entirely by the action of the gravity during the swing phase, behaving like a non-inverted pendulum. The stance leg remains at full extension with minimal muscle force – the passive mechanical stop of the leg prevents the hyperextension, and it is not necessary to spend energy in the muscles to maintain the leg extended (Kuo, Donelan et al. 2005; Kuo 2007). So, if the stance leg acts like an inverted pendulum and the swing leg acts as a pendulum, the energy would be conserved in both movements (no work) (Mochon and McMahon 1980). However, this fact is a paradox, since normal walking is characterized by energy consumption – the efficiency of transference between kinetic and potential energy is not 100% efficient, but has instead only a maximum of 70%. One reason is the fact that fluctuations in potential and kinetic energy are not matched in magnitude. During a fast walk, it is normal that fluctuations in potential energy are smaller than the fluctuations in kinetic energy. Hence, in order to maintain the movement an energy expenditure is necessary (Lee and Farley 1998). Kuo suggest that one possible explanation is that the stance leg does not behave passively, acting instead as a forced pendulum with muscular work performed to accelerate and decelerate it. These are the basic principles of the dynamic walking model presented in 3.8.4 (Kuo, Donelan et al. 2005; Kuo 2007).

3.8.3. Determinants of Gait

The theory of the six determinants of gait was proposed firstly by Saunders et al. in 1953, after the study of the behavior of the center of gravity of the body during gait. It consists of a series of six patterns that helps to minimize the displacement of the COM during each GC, so as to achieve a smooth sinusoidal trajectory of the COM (vide 3.8.1) (Saunders, Inman et al. 1953). When Saunders et al. proposed such theory, the authors did not present a tested hypothesis. However, due to the attractive character of the theory, the scientific community has accepted it, and an example of that are the several papers citing it. Recently, there has been a concern to validate the theory, although the concept of minimizing the displacement of the COM is generally accepted as one the main objectives in human walking (Orendurff, Segal et al. 2004).

3.8.3.1. 1st determinant - Pelvic rotation

During normal walking, the pelvis rotates alternately in a horizontal plane. It rotates forward on the swing side, and then rotates relatively backward during stance. The magnitude of this rotation is approximately 8 degrees, 4 degrees to each side of the central axis (Saunders, Inman et al. 1953).

The objective of this rotation is to permit a flatten arc of the passage of the COM, since it elevates the extremities of that arc. Hence, the forward rotation of the pelvis on the swing side prevents an excessive drop in the COM during periods of double limb support; the angles of inflection at the successive arcs are less abrupt. Due to this fact the loss of potential energy is not so abrupt, and the force required to change the direction of the COM is lower. The pelvic rotation is the mechanism that allows the pelvis to rotate over a vertical axis, permitting the advance of the hip that goes into flexion and retreat of the hip that goes into extension. Such characteristics reduce the energy expenditure, because the angle of extension and flexion at the hip joints needed to step is decreased. The pelvic rotation also increases the step length (Saunders, Inman et al. 1953).
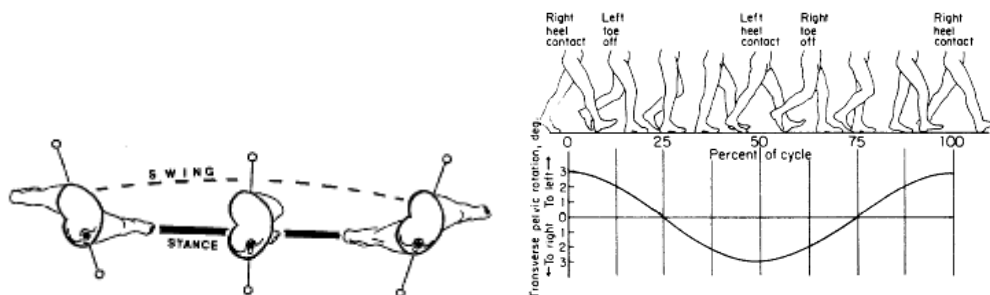
Figure 17 – a) representation of pelvic rotation during a swing event (left) b) variation of pelvic rotation angle along a stride period (Herr 2009)

3.8.3.2.   *2nd determinant – Lateral Pelvic Tilt (pelvic obliquity)*

In normal walking, during the flexion and extension of the hip joint, the pelvis is tilted in relation to the horizontal plane. As can be seen in Figure 18, during swing phase, the pelvis tilts downward to the side of the swing leg (positive "trendelenburg"). Pelvic tilt produces a relative adduction on the stance leg and a relatively abduction in the swing leg. The average value of this angular displacement is approximately 5 degrees. The lateral pelvic tilt during the swing phase associated with the flexion of the knee of the swing leg (condition to occur pelvic tilt) prevents an excessive rise of the body's COM, reducing the COM arcs and the energy expended.(Saunders, Inman et al. 1953)
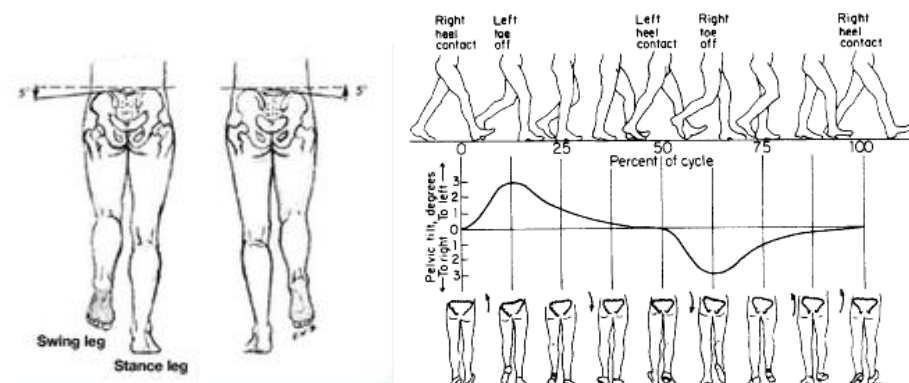
Figure 18 – a) representation of pelvic tilt during the swing phase (left) b) evolution of angular displacement during a stride period (Herr 2009)

3.8.3.3.   *3rd Determinant – Knee Flexion during the Stance Phase*

At the end of the swing phase, the knee is fully extended. At the beginning of the stance phase the knee begins to flex until FF (approximately 0-10% of stride period) – corresponds to the period of WA. After FF the knee joint begins to extend until TO. The maximum value achieved is approximately 20

degrees (vide Figure 19 b)). This movement, allows to absorb not only the weight and part of energy resulting from the impact of foot with the ground, but also to reduce the vertical displacement of the COM (Saunders, Inman et al. 1953).
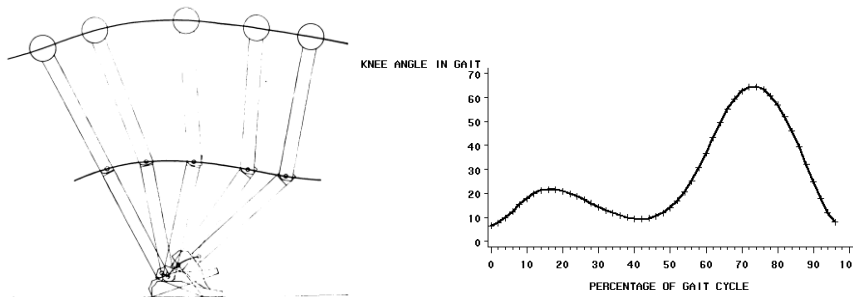
Figure 19 – a) representation of COM arc and knee arc during stance phase (left) b) evolution of knee angle during a stride.

3.8.3.4. 4th and 5th Determinants – Foot, Ankle and Knee Mechanisms

The angular displacements of foot and knee during the stance phase are closely related, and contribute to minimize the COM displacement, and because of that these two determinants are usually considered together (4th – Controlled Plantar flexion and 5th Powered Plantar flexion). Saunders et al. consider the existence of two intersecting arcs of rotation during the stance period. The first is defined by the rotation of the ankle during the controlled plantar flexion (HC until FF; center of rotation in calcaneus; see Figure 20). The second arc is defined by the rotation over the forefoot (FF till TO) and corresponds to the powered plantar flexion event (Propulsion). These two arcs, associated with the initiation of the knee flexion in the stance leg prevent an abrupt rise of the COM trajectory (Saunders, Inman et al. 1953).
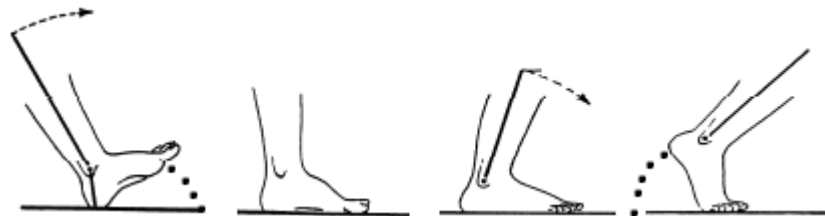
Figure 20 –Representation of four instants of the stance phase. In the left figure is represented the first arc, the foot is dorsiflexed and the knee is extended. In the second picture the foot is flatted, after the controlled plantar flexion. In the right picture is represented the second arc, representing the trajectory of the heel after the powered plantar flexion.

3.8.3.5. 6th Determinant – Lateral Displacement of the Pelvis

As explained in 3.8.1, the COM is characterized in gait by a sinusoidal displacement in the horizontal plane, produced by a relative adduction at the hip and by the horizontal shift of the pelvis. However since the two legs are parallel to each other, the horizontal displacement would be characterized by relatively high values. To avoid this fact, the existence of a tibiofemoral angle is considered, which related the relative adduction, allows the decrease of the value of this displacement (approximately 7.5 cm to 4.5 cm).

51
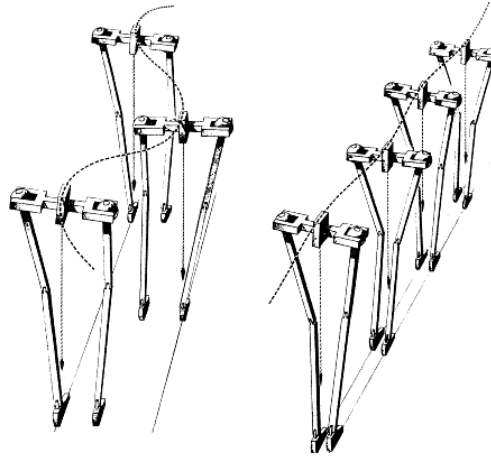
Figure 21 – representation of the lateral displacement COM, a) considering the two limbs parallel (left) b) considering a tibiofemoral angle (knees are medial to the hips) and the adduction of the hip (Saunders, Inman et al. 1953)

This model is sometimes criticized; although it tries to explain the low energy expenditure, the predicted value is more than the double of the estimate for humans (MR=0.18). Some studies cited by Kuo also present results with subjects walking with a flatten trajectory, and the obtained WR data also shows higher values than those observed for normal gait (Kuo 2007).

3.10.3.6 Other Determinants

In a recent study, Herr considered the existence of three other gait determinants (Herr 2009):

- **7th determinant** - Inversion-Eversion-Inversion sequence at the subtalar joint – Herr indicates the existence of a normal pattern of inversion-eversion-inversion of the foot. This mechanism causes the flattening of the longitudinal arch, which helps to absorb the shock during WA. It also enables the rotation of the tibia (from IC to FF, the tibia rotates medially (approximately 10^0) and from FF till TO, the tibia rotates laterally approximately 20^0).

- **8th determinant –** lateral flexion of the trunk – Herr indicates the existence of an ipsilateral flexion of the trunk in a coronal plane, which helps to control the angular momentum in the anterior-posterior direction.

- **9th determinant –** Antero-posterior flexion of the trunk – the author considers that during a GC the trunk angle in a sagittal plane varies according to a certain pattern. It has a maximum backward flexion at the beginning of the support phase and a maximum forward flexion at IC of the contralateral foot.
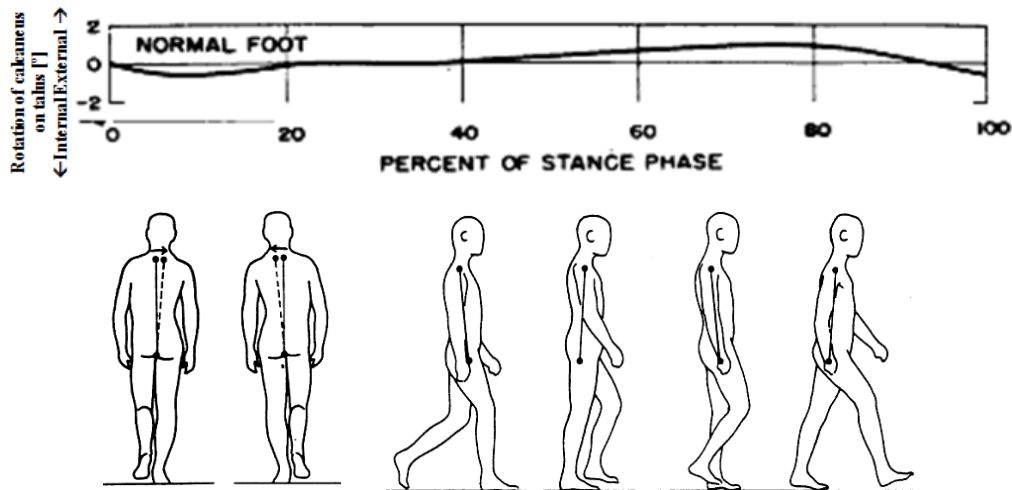
Figure 22 – other gait determinants presented by Herr: a) 7th determinant – representation of the rotation of calcaneus on talus (+ eversion, - inversion) b) 8th determinant – lateral displacement of trunk c) 9th determinant – antero-posterior flexion of the trunk

3.8.4. Dynamic Walking

The idea of dynamic walking was firstly applied in the development of mechanical legs, by McGeer, and afterwards applied to human walking. This model is based in the inverted pendulum theory and permits to eliminate part of the paradox of the model presented in 3.8.2. The dynamic walking varies essentially in the double limb support phases, presenting a model for step-to-step transition, where the motion is controlled by passive dynamics of the legs themselves (Kuo 2007).

The essential principles are based on the fact that the leg acts like a forced pendulum, rather than an inverted pendulum. The conservation of the mechanical energy of single support is disturbed by the collision of the foot with the ground during the IC. Essentially, the large energy loss is caused by the sudden stop of the foot during the impact, although some energy can also be dissipated through noise and deformation of the ground. These facts change the velocity of the legs and consequently of the COM (Kuo 2007). The COM trajectory, during step-to-step transition, is redirected to a new pendular arc (v^{-}_{COM} to v^{+}_{COM} (see Figure 23 a)). In Figure 23 b) the COM work during double support can be observed. The leading leg will perform a negative work and the trailing leg a positive work – the two forces are assumed to be directed along the legs. The rate of work is equal to the dot product of force and velocity vectors (Kuo, Donelan et al. 2005).
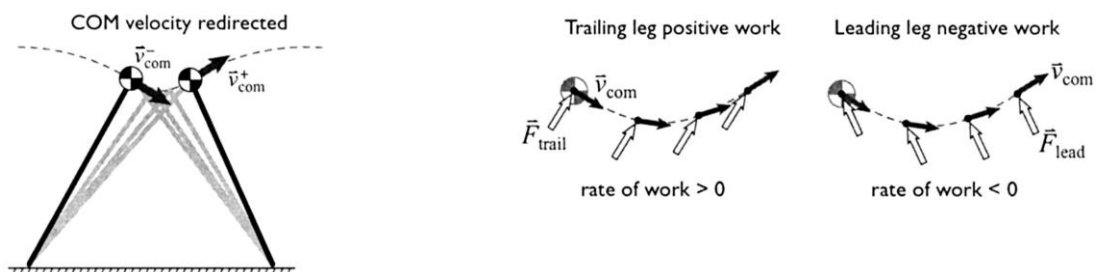
Figure 23 – a) left – schematic diagram of double support: step-to-step transition b) right – representation of the double support COM work (Kuo, Donelan et al. 2005)

Then, to maintain the COM velocity constant, it is necessary that the positive work surpasses the negative work. The negative work performed by the leading leg and the positive work performed by

trailing leg are proportional to the difference in squared velocities, as can be seen in equations (12) and (13) (Kuo, Donelan et al. 2005).

$$W_{trail} = \frac{1}{2} M (v_{COM}^- \tan(\alpha))^2 \tag{12}$$

$$W_{lead} = -\frac{1}{2} M (v_{COM}^- \tan(\alpha))^2 \tag{13}$$

Step-to-step transition is optimal when the magnitude of negative work (collision) and the magnitude of positive work (PO) have the same value and short duration (see Figure 24 a)); in this case, the amount of work (positive and negative) is minimized and the velocity of the COM will be maintained (no energy expenditure is necessary during single support). Other two cases can occur, in Figure 24 b) is represented the case when the magnitude of negative work is smaller than the positive work, which causes the velocity of the COM to decrease in order to avoid the necessity of an energy expenditure for performing a positive work during single support. The last case occurs when the magnitude of positive work is greater than negative work; in this case, negative work is required, so as to decrease the velocity of the pendulum (Kuo, Donelan et al. 2005).
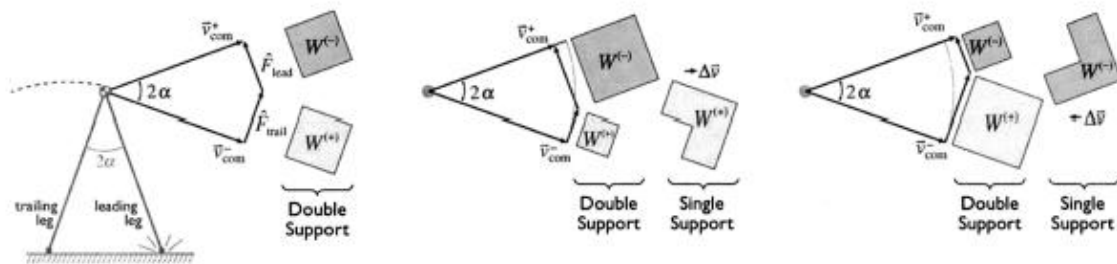
Figure 24 – geometric diagram of COM velocity redirection of step-to-step model. a) Represents the optimal case, when the positive work (PO) is equal to negative work (collision) (left)) b) represents the case when the magnitude of negative work is greater than positive work, in this case the next step will start with a smaller velocity (middle) c) represents the case, when the magnitude of negative work is smaller than positive work, in this case it will be necessary spend more energy to decelerate the pendulum and maintain the velocity (Kuo, Donelan et al. 2005).

During step-step transitions, the value obtained for the work is considerately smaller than that predicted by the six determinants theory, and has a value of MR similar to the obtained for human walking (Kuo 2007). This model also gives an explanation to understand other parameters of gait like step length, width and frequency. As can be seen in Figure 25 a), for the same step frequency, if the step length increases, the magnitude of positive work also increases (more expenditure of energy during the PO). Such need to increase the positive work is the result of greater speed of the COM, as well as of a larger angle of redirection (more work is needed to change the velocity direction). In Figure 25 b) is represented the effect of the step width on PO work. For the same frequency and step length, the increase of the step width results in more positive work done during PO. Although the major responsible for the loss of energy in collision is the velocity, the magnitude of this effect has a smaller contribution. This fact can be observed in Figure 25 c), where the predicted work rate is showed in function of the step length and the step width (Kuo, Donelan et al. 2005).
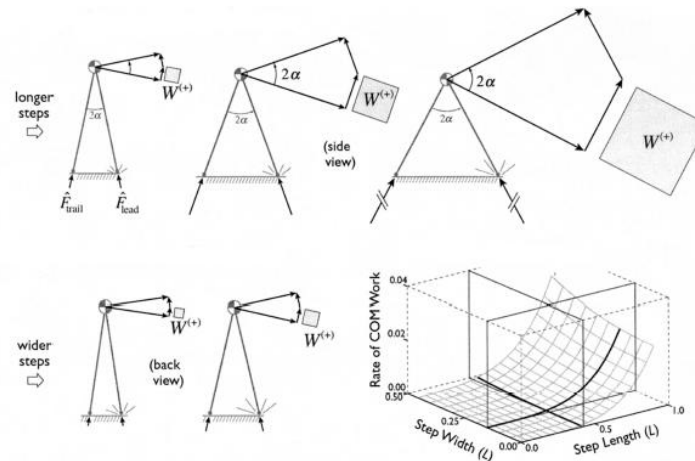
Figure 25 – Variation on COM work, during step-to-step transition, by changing: a) step length (above) b) step width (below left) c) predicted work rate for both variables (Kuo, Donelan et al. 2005).

3.8.5. Comparisons between presented Models (Revision)

The main objective of these three theories is to explain the expenditure of energy during gait. However, these theories present contradictions. The six determinants of gait are based in the premise that the COM displacement is energetically costly. On the other hand, the inverted pendulum theory defends that the stance leg acting like an inverted pendulum is more energetically economic (Saunders, Inman et al. 1953; Cavagna and Margaria 1963).

The six determinants gait have been generally accepted, even though this theory does not present experimental validation (Orendurff, Segal et al. 2004). The predicted metabolic rate is much higher than the observed in normal gait and some studies show that walking with a flatter COM trajectory implies higher expenditure energy (Kuo 2007).

Della Croce et al. have proposed a new vision of gait's determinants, they proved that the three first gait determinants are the most important mechanisms in reducing the vertical displacement of COM (Della Croce U, Riley P.O. et al. 2001). They also proved the idea presented by Gard and Childress that the effect of pelvic list in the displacement of the COM is less significant than the one presented by Saunders et al. (2-4 mm) (Gard and Childress 1997). Gard and Childress have also studied the 3rd determinant and showed that the knee flexion during stance phase reduces only a few millimeters. The authors advocate that the first goal of this and the 2nd determinant is not reducing the COM displacement, but instead they are a result of a mechanism of shock absorption that occurs in the loading response phase (Gard and Childress 1996; Gard and Childress 2001). Gard and Childress consider that these two determinants have low or no effect, because the timing in which these occur in the gait cycle is not ideal to reduce the vertical displacement of COM. They defend that the parameters that have significant influence in the trajectory of the COM are the leg length, foot rocker radius and step length (Gard and Childress 2001).

To Della Croce, the role of heel rise (4th and 5th determinant) has been considered the principal main pattern of movement that reduces the COM vertical displacement. In Figure 26 the results of the contribution of the gait determinants to the COM vertical displacement can be consulted, using the two models presented by the Della Croce et al. The authors also showed that, when the COM is at its

maximum height, the leg inclination has an important role in reducing the COM vertical displacement (Della Croce U, Riley P.O. et al. 2001).
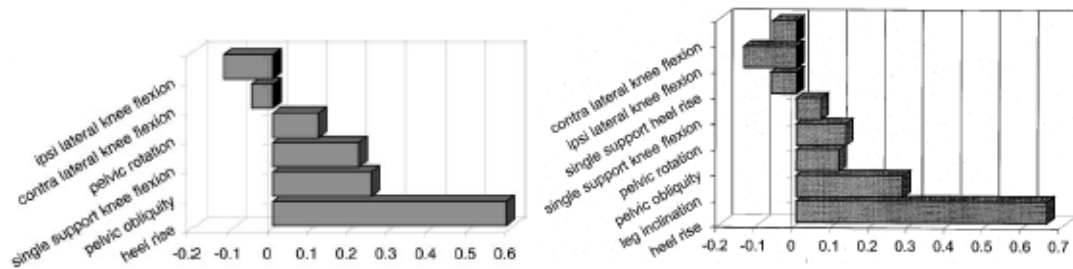
Figure 26 – Average isolated contributions of gait determinants using two models presented by Della Croce ((Della Croce U, Riley P.O. et al. 2001)

Although the inverted pendulum theory also has been criticized, several models have been proposed to resolve some of the problems found. An example of those models is the model of dynamic walk.

Chapter IV

Pathologic Gait

The twentieth century, particularly its second half, was marked by a great number of studies of normal and pathological gait. The evolution of technology allowed the development of accurate and fast methods that calculate kinematic and kinetic parameters for a given subject. Thus, it made possible the creation of biomechanic laboratories specialized in the study of normal and abnormal gait. As a result, several papers can be found which describe the patterns of normal and abnormal gait in different diseases.

A large number of diseases origins gait patterns variations, e.g. cerebral palsy, Spina bifida, neuromuscular diseases. Essentially, these variations are related with: a) Osseous deformations – congenital, traumatic, metabolic, etc. b) Neurological diseases – sensory, motor, spastic, paralytic, etc. c) Muscles/Soft tissues deformations – contractures, fibrosis, metabolic, etc. d) Functional diseases – neuromuscular, lack of coordination, etc. (Fauci, Kasper et al. 2008).

As mentioned before, there are a large number of diseases that cause abnormalities in gait and enumerate them all would be an arduous task. Therefore, in this thesis the option was put is presenting only the clinical terms used in gait analysis, which describe the observed deviations.

4.1. Gait Abnormalities related with Neurological pathologies

Apraxia Gait – in order to understand the apraxia gait is necessary to understand the definition of Apraxia. Apraxia can be described as the "inability to perform certain subjectively purposive movements or movement complexes with conservation of mobility, of sensation and of coordination". Therefore the term "gait apraxia" is generally used in subjects that present abnormal gait not based on upper or lower neuronal lesion or impaired coordination. Apraxia gait is characterized by strange leg and trunk movements, resulting in an ineffective propulsion (Tyrrell 1994; Della Sala, Spinnler et al. 2004).

Ataxia – designates a disabling symptom common in many neurological diseases, which results in the lack of coordination between muscles' movements. Essentially, three causes for ataxia can be considered that result in different gait abnormalities: a) cerebellar ataxia – dysfunction of the cerebellum b) spinal/sensory ataxia –damages on the spine or brainstem c) vestibular disease – dysfunction of vestibular system.

Cerebellar Ataxic Gait – Descriptions of cerebellar ataxic gait include unsteady irregular gait, difficulties in controlling body balance, irregular steps and a wide base of walking. Moreover other kinematic parameters are affecting resulting in a reduced cadency, step and stride length, delays in some events (HO, TO, peak flexion during swing phase) and reduced range of motion of ankle, knee and hip (Palliyath, Hallett et al. 1998; Stolze, Klebe et al. 2002). Mitoma et al. observed significant differences in EMG patterns for patients suffering from cerebellar ataxia. These differences included high activity of triceps surae and tibialis anterior in some periods that in normal EMG pattern are not observed, as well as the ratio ΔEMG/Δangle presented higher values for these muscles during the dorsiflexion and plantar flexion. The same author also observed significant differences in the pattern of GRF and COP (Mitoma, Hayashi et al. 2000).

Sensory Ataxic Gait /Stomping gait – is characterized by a unsteady broad base march with foot slap at foot contact, with the subject having a tendency to look at this feet, as well as a postural instability caused by the loss of proprioception (sensitivity to the position of body segments) (DeLisa and Kerrigan 1998).

Hemiplegic Gait – is a common symptom in the subjects suffering from Hemiplegia – total paralysis of leg, trunk and arm of the same side. This is generally caused by strokes in elderly, although it can also appear in children having, in this case, no identifiable cause. Visually, the hemiplegic gait is characterized by an abnormal swing of the arm, which is flexed, adducted and internally rotated; at the lower limb level, the hip is internally rotated, the knee is in extension and the ankle/foot is plantar flexed and in inversion. While walking the subject tends to sustain the BW on the side not affected, at the same time as drags his affected leg in a semicircle to allow the toe clearance – circumduction. The analysis of time-distance parameters is characterized by an asymmetry in stride length and step period, a decrease of the step length and an increase of swing period of the affected leg. The velocity, cadence and stride length are also reduced (DeLisa and Kerrigan 1998; Pizzi, Carlucci et al. 2007). Kinematically, the absence of knee flexion during swing phase is compensated by several mechanisms such as a hip hiking of the stance phase side (ipsilateral raise of the pelvis), a decreasing on lateral shift of the affected side or a genu recurvatum of the affected knee (pathology characterized by a hyperextension of the knee) (DeLisa and Kerrigan 1998).

Magnetic Gait – is an abnormal gait associated with the most severe cases of normal pressure hydrocephalus. Visually, this type of gait is characterized by a difficult in initiating the swing phase, as if the foot would be magnetically attached to the floor. Other characteristics are the reduced velocity and stride length, slow movements of lower extremities, postural instability and frequent falls (Vanneste 2000; Lee, Yong et al. 2005).

Parkinsonian/Festinating Gait – refers to the typical gait characteristics on subjects suffering from parking disease. Visually, this type of gait is characterized by a shuffling gait with small steps, an anterior flexion of the trunk and lower angular amplitude of movements of the joints (Knutsson 1972). Significant differences were observed in time-distance parameters, such as lower values of speed, and stride length or higher values of stride period and cadence (Morris, Iansek et al. 1996; Cho, Chao et al. 2009). Hughes et al. observed abnormalities on foot strike, as that contact is not as usually made with the heel. In fact parkinsonian gait is characterized by a flat foot strike or, in some cases, the strike

is performed with the forefoot (Hughes, Bowes et al. 1990). Mitoma et al. also studied the differences between EMG and GRF for subjects suffering from Parkinson disease and non-pathological patients. It was observed a lower maximum activity of triceps surae and tibialis anterior muscles, as well as differences in the pattern of GRF and COP (Mitoma, Hayashi et al. 2000). At last, Cioni et al. observed a prolonged activation of quadriceps and hamstrings during the stance phase (Cioni, Richards et al. 1997).

Propulsive Gait – is a gait disturbance common in the festinating gait. In order to avoid a forward fall, during walking, the steps become faster and faster being followed by a decrease in steps' length.

Spastic Gait – is characterized by an unbalanced muscle action of certain muscles, the legs are held together moving in a stiff manner. Other observed symptom is the scissor gait. In order to help maintaining the body balance, this type of gait is associated with tiptoeing, as well as with a great effort to perform the swing of the leg, resulting in an unsteady and fatiguing gait. In some cases, it may be observed an increasing of tone and spasticity of muscles. The kinetic and electromyographic analysis show important differences, especially at the knee joint. The foot contact is done with lateral aspect of foot (DeLisa and Kerrigan 1998; Lin, Guo et al. 2000).

Scissor Gait – is a symptom typical found in subjects suffering from spastic cerebral palsy. This name comes from how subjects walk as they cross the legs similarly to the mechanism of a scissor. It is characterized by a flexion of the knee and an excessive adduction of the leg during swing, which gives the idea of a crouched gait. Other modifications such as rigidity, internal rotation of the hip and equinus or equinovalgus foot are also observed (Yokochi 2001).

4.2.   Gait Abnormalities related with Isolated Motor Weakness

Hip extensor gait (gluteus maximus lurch) – as mentioned in chapter II, the Gluteus maximus is the principal hip extensor, helping to stabilize the trunk, which avoids its forward falling. In the pathological cases in which exists a weakness of this muscle, the hip is supported by the iliofemoral ligament. This type of abnormal gait is characterized by a posterior trunk and arms deviation after the IC of the affected side, in order to maintain the GRF vector behind hip which locks the hip extension (Õunpuu 1994; DeLisa and Kerrigan 1998).

Hip flexor gait – is characterized by a marked limp that starts with the beginning of PO event and continues through the swing phase of the affected side. Visually, a posterior and lateral (affected side) flexion of the trunk is observed from PO till MSw, resulting in the locking of hip joint. The inertia generated by these compensative mechanisms leads to a swing of the affected leg. However, an asymmetry in step length is observed, being clearly lower in the affected side than in the not affected side (DeLisa and Kerrigan 1998).

Quadriceps Gait – is the typical march observed in individuals with quadriceps (knee flexors) weakness. In order to avoid the flexion of the knee after IC, this joint is in hyperextension (genu recurvatum) by action of Gluteus maximus and Soleus which extend, respectively, the femur and the tibia. As result of these compensatory mechanisms the trunk is forward flexed and a knee extension moment is generated. A placement of the hand in thigh can also be observed in some patients, in order to help maintain the extension of knee (DeLisa and Kerrigan 1998).

Steppage gait/Drop Foot – is the characteristic gait in subjects, which suffer from drop foot (the incapability or the difficulty to perform a dorsiflexion and a subtalar eversion caused by neuromuscular lesions). The gait patterns are characterized by a toe catch, pelvic shift and a higher elevation of the swing leg, in order to avoid the foot hitting the ground during swing phase. These mechanisms are achieved by an increased flexion of the knee and hip. A lateral flexion of the trunk in the opposite direction of the swing leg can also be observed, aiming to maintain the body balance (Sabir and Lytlle 1984; Don, Serrao et al. 2007). Significant differences can be observed in the time-distance parameters, such as an increase of stride time, step width, and a decrease in step length, swing velocity and kinetic parameters (Don, Serrao et al. 2007).

Trendelenburg Gait (Gluteus medius) – is a type of gait observed in individuals suffering for neuropathies or closed head traumas. It is caused by a weakness on the abductor muscles of hip – Gluteus medius, causing the hip drop on the opposite side to the abnormal muscle. Visually, this type of gait is characterized by a marked limp, a lateral inclination of the trunk and a drop of shoulder over the affected side. These mechanisms are performed with the intention of maintain the COM over the hip, which results in a decrease of the force required to stabilize the hip. Since the affected leg becomes "functionally longer", increases on knee and hip flexions and the ankle dorsiflexion are observed to allow the toe clearance. These compensative mechanisms can lead to a development of other pathologies in the knee and ankle joints over a period of years (DeLisa and Kerrigan 1998; Petrofsky 2001 a); Petrofsky 2001 b)).

Triceps Surae weakness – results from difficulty in controlling the ankle dorsiflexion. The HO of affected side is delayed and the PO is shortened. These deviations result in a lag of forward movement of pelvis on the not affected side at IC and on the affected side during PO. As a result, differences in time-distance and kinetic parameters are observed, such as a shortening of the step length on the not affected side and a flexion moment behind the knee that can result in other pathologies in this joint (DeLisa and Kerrigan 1998).

Waddling/Myopathic Gait – in this type of gait an excessive alternation of lateral trunk movements is observed, which is followed by an exaggerated elevation of the hip. It occurs in subjects suffering from gluteus muscles weakness. Visually, this type of gait presents similarities with gait of ducks and penguins.

4.3. Gait Abnormalities related with Musculoskeletal Pathologies

Antalgic Gait – is a clinical term used to designate a limp adopted by a patient with the objective to avoid pain caused by weight-bearing. As a result the stance period is shortened and the cadency is increased (with quick, short and soft steps).

Hip pathology (pain) – This gait is a type of antalgic gait characterized by several mechanisms that avoid the weight-bearing on the affected side: during the stance phase of the affected side, which is shortened, the trunk is flexed toward the side of lesion in order to bring the COM over the joint, decreasing the mechanical stress and consequently the pain in this joint. During the swing phase, the hip from the affected side is slightly flexed, abducted and externally rotated, relaxing the ligaments to decrease the joint tension (DeLisa and Kerrigan 1998).

Hip pathology/Coxalgic gait (Osteoarthritis) – The gait of subjects suffering from osteoarthritis is characterized by a decrease on hip range movements, especially an internal rotation and a flexion of hip. An abnormal movement of trunk is observed along with a compensation by the other joints, such as hip hiking on the no affected side and tiptoeing on the affected side (DeLisa and Kerrigan 1998).

Knee pathology (pain) – results in a typical antalgic gait, which is characterized by a slight flexion of the knee during the entire gait cycle.

Knee pathology (ligamentous instability) – the gait patterns varies with the injured knee ligament. The most common abnormality observed is the genu recurvatum – a hyperextension of knee caused by the excessive ligamentous laxity. This abnormality is commonly observed in stance phase, and its correction is essential to avoid future degenerative changes in this articulation.

Knee pathology (contracture) – The typical gait of subjects suffering from knee contracture presents symptoms similar to those observed in short leg limp, both toe walking on the affected side and steppage gait and hip hiking on the no affected side are examples of these deviations.

Ankle-foot pathology (pain) – is also characterized by an antalgic gait. The contact of foot with the ground during the stance phase varies with the location of the lesion, e.g. subjects with lesions in forefoot tends to reduce the plantar flexion during PO, while subjects suffering from lesions in the heel zone tend to walk with a tiptoeing gait (IC is done with the toes). Generally, these abnormal deviations results in shortened stride length and compensative mechanism of the no affected side.

Ankle-foot pathology (ankle instability) – subjects suffering from ankle instabilities also present a antalgic gait, due to difficulties in performing the WA (the instability of ankle leads to a buckling of the ankle)

Ankle-foot pathology (contracture) – the gait pattern for subjects suffering from contractures of ankle varies with the muscle affected, the most usual being the triceps surae muscle or heel cord. For this pathology the subjects' gait is characterized by a steppage gait.

Leg-Length discrepancy – although the leg length discrepancy can have different causes (contractures of hip, knee and ankle, or asymmetries in the length of the femur, tibia and hip), the gait patterns are similar, varying with the value of leg discrepancy. Leg-length discrepancies lower than 2.33 cm do not present compensatory deviations. To higher discrepancies, the gait patterns are characterized by an equimus position of ankle (tiptoeing) and an increase of the knee extension of the short leg. Moreover, are also observed an increased flexion and circumduction of the long limb, a higher vertical displacement of COM and a higher pelvic obliquity with pelvic drop (Liu, Fabry et al. 1998; Walsh, Connolly et al. 2000).

Kinetically, some authors observed an increase in the magnitude of GRF, in energy consumed and in kinetic energy of lower limbs, where other authors present results that are similar with the normal patterns until 6cm of difference (Gurney 2002).

Pigeon-toed/In-toe Gait – is a characteristic gait where the subjects walk with forefoot adduction. This condition is one of the most common problems in childhood, but it is rarely observed in older children or adults. This disturbance is caused by postural disorders of lower limbs, such as an internal femoral rotation, internal tibial torsion, a metatarsus adductus and rothbarts foot (Accardo 1975; Thackeray and Beeson 1996)

Chapter V

Kinematic and Kinetic Analysis

The simple visual analysis of motion only allows the identification of few gait parameters. In order to comprehend all the mechanisms of gait and develop robust routines to detect gait pathologies, it is essential perform a kinematic and kinetic analysis (Sutherland, Olshen et al. 1980).

Kinematics is defined as the study of the movement of bodies and systems without considering the forces causing such motion; a kinematic simulation is of purely geometrical nature and provides the solution for entire the range of motion of the multibody movement. This solution allows, for a given set of considered points, the study of the trajectories, the calculation of joint angles and analysis of the velocity and acceleration (Sutherland, Olshen et al. 1980; De Jalon and Bayo 1994).

Kinetics/dynamics is the term used to study the relation between the motion and its causes – forces and moments of force (torque). The premise behind a kinetic/dynamic problem is to understand the action of these forces and torques in the multibody system and its inertial characteristics – mass, inertia and COM position. Several different dynamic problems can be considered. However, for the study of gait, generally two types of simulations are used – forward dynamic analysis and inverse dynamic analysis (De Jalon and Bayo 1994).

The forward dynamic problem permits simulating the motion of a multibody system, when a set of known forces and moments is applied. Such problems are used to simulate the evolution of a system over a given time interval (De Jalon and Bayo 1994).

On the other hand, the inverse dynamic problem allows calculating the forces and torques that produce a specific motion. The problem requires the position, velocity and acceleration of the systems and all the external forces applied. This type of problem is frequently applied in gait analysis, since the motion and external forces can be measured (vide 3.6.2). The velocity and the acceleration of body parts can be calculated by kinematic analysis, while the external forces can be obtained by direct acquisition of GRFs (Silva 2003).

Before understanding all the concepts behind the kinematic and dynamic analysis, it is necessary to define what is meant by a multibody system. The formulation in multibody dynamics is based in the description of (De Jalon and Bayo 1994; Silva 2003; Ambrósio and Silva 2005). The multibody system is used to simulate the kinematic and dynamic behavior of a system; it is defined as a set of rigid bodies interconnected by kinematic pairs (joints), which allow a relative movement between them, and

are in turn acted by external forces. The complexity of the movement is related with the number of degrees of freedom (DOF) allowed at the joint.

5.1. Fully Cartesian coordinates

The first aspect to be addressed is the type of approach to the multibody system problem, firstly regarding number of dimensions to be considered – either two or three dimensions. The main difference between these approaches relies in the variety of joints, as these increases and allows more than one DOF. The 3D model also requires the introduction of a relative coordinate for each DOF. Relative coordinates define the position of a given element, relating it with the others adjacent elements.

The adoption of fully Cartesian coordinates implies that the position and orientation of a rigid body in the 3D space are represented using the Cartesian coordinates of a set of points and unit vectors. Typically, for a better definition of the multibody system, these points are located strategically in joints and extremities of rigid bodies and the unit vectors are used to define rotational and direction axes of joints. This definition avoids the necessity to introduce angular variables since these are implicit in the model (vide Figure 27).
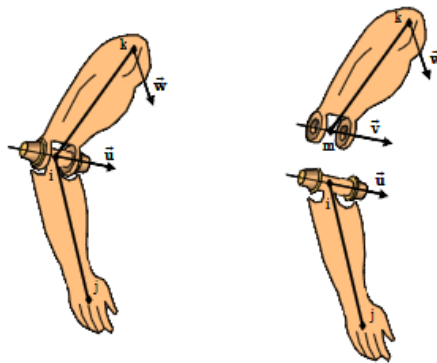
Figure 27 – Schematic representation of a mechanical system with fully Cartesian coordinates: a) the two rigid bodies are assembled sharing the point *i* and the vector **u** (left) b) the same mechanical system of a), however defining the revolute joint with independent points *i* and m and independent vectors **u** and **v** (right) (Silva 2003)

Figure 27 represents two models for the formulation of a mechanical system. On the left, a revolute joint is defined by sharing a point and a unit vector, which reduces both the number of coordinates necessary to define the model and the number of algebraic equations (since the kinematic relations used to define the system's topology (joint) are implicit). This fact brings computational advantages to the kinematic analysis. However, if the objective consists of a dynamic analysis, this model cannot be used, since it does not yield the internal reaction forces in joints (there is no explicit information on how to describe the kinematic pairs). Such problem no longer occurs with the model in Figure 27 on the right, in which an explicit system is used to define the kinematic pairs. Due to this fact, the explicit system must be used to define kinematic pairs in which the internal reaction forces are needed.

The fully Cartesian coordinates of a general mechanical system are represented as a vector **q**. It contains the Cartesian coordinates for every point and every unit vector considered in the definition of the system. The vector *q* is designated as the vector of generalized coordinates, which is an

alternative name for the Cartesian coordinates, as these define the configuration of the system in a unique way at any instant.

$$\boldsymbol{q} = \left\{x_{P_i} y_{P_i} z_{P_i} \dots x_{P_n} y_{P_n} z_{P_n} x_{V_i} y_{V_i} z_{V_i} \dots x_{V_m} y_{V_m} z_{V_m}\right\}^T \qquad 14)$$

where P refers to a point and V to a vector. x, y and z represent the coordinates of a point or the components of a vector in the three Cartesian directions. n and m represent respectively the total number of points and vectors considered in the definition of the mechanical model.

In a multibody formulation with fully Cartesian coordinates, the generalized coordinates of a vector $\boldsymbol{q}$ are dependent, as they are related by algebraic expressions defining the topology of the problem. These expressions, usually called kinematic constraints, define the proprieties of the joints, rigid bodies and the driver actuators of the system (vide section 5.3). The presented model is holonomic, as all kinematic constraints of the system are holonomic. i.e., they only depend on the coordinates and the time variable t. The holonomic constraints are considered scleronomic when the kinematic constraints do not include time as an explicit variable (the position does not depend explicitly on time; used to define rigid body proprieties and to define joints), and rheonomic otherwise (used to guide the rigid bodies – driving actuators).

The vector of kinematic constraints ($\boldsymbol{\Phi}$) is represented by the following expression:

$$\boldsymbol{\Phi}(\boldsymbol{q}, t) = \{\boldsymbol{\Phi_i}(\boldsymbol{q}) \dots \boldsymbol{\Phi_{ns}}(\boldsymbol{q})\ \boldsymbol{\Phi_{ns+1}}(\boldsymbol{q}, t) \dots \boldsymbol{\Phi_{ns+nr}}(\boldsymbol{q}, t)\}^T = \boldsymbol{0} \qquad 15)$$

where $\boldsymbol{\Phi_i}$ represents the ith kinematic constraint. ns and nr represents respectively the number of scleronomic constraints and the number of rheonomic constraints.

5.2. Kinematic Analysis

As previously referred, kinematic analysis allows obtaining the position, velocity and acceleration of every element of the mechanical system. This information is useful in the context of gait analysis, since some of the gait patterns are related with velocities and accelerations of body members and these results represent inputs for the inverse dynamic analysis.

To obtain kinematic consistent positions (the positions that satisfy the equation of kinematic constraints), it would be necessary to solve the equation (15). However, their non-linear behavior requires the use of numerical methods, such as the Newton-Raphson method (NR). The results obtained with this method present a quadratic convergence in the neighborhood of the solution, i.e. the error in each iteration is proportional to the square of the error in the previous iteration. The NR method is based on the linearization of equation (15) – the equation of kinematic constraint is replaced by the first two terms of its expansion in Taylor series, evaluated around an initial approximation of the solution **q**. Thus, for the instant t, the application of the NR results in:

$$\boldsymbol{\Phi}(\boldsymbol{q}, t) \cong \boldsymbol{\Phi}(\boldsymbol{q}_i, t) + \boldsymbol{\Phi_q}(\boldsymbol{q}_i)(\boldsymbol{q} - \boldsymbol{q}_i) = 0 \qquad 16)$$

where $\boldsymbol{\Phi_q}(\boldsymbol{q}_i)$ represents the Jacobian matrix of the constraints, composed of the partial derivatives of each kinematic constraint with respect to the generalized coordinates vector (n_h is the number of constraint equations and n_c the number of dependent coordinates).

$$\boldsymbol{\Phi}_{\mathbf{q}} = \begin{bmatrix} \dfrac{\partial \boldsymbol{\Phi}_1}{\partial \mathbf{q}_1} & \dfrac{\partial \boldsymbol{\Phi}_1}{\partial \mathbf{q}_2} & \cdots & \dfrac{\partial \boldsymbol{\Phi}_1}{\partial \mathbf{q}_{n_{\mathrm{c}}}} \\ \dfrac{\partial \boldsymbol{\Phi}_2}{\partial \mathbf{q}_1} & \dfrac{\partial \boldsymbol{\Phi}_2}{\partial \mathbf{q}_2} & \cdots & \dfrac{\partial \boldsymbol{\Phi}_2}{\partial \mathbf{q}_{n_{\mathrm{c}}}} \\ \vdots & \vdots & \ddots & \vdots \\ \dfrac{\partial \boldsymbol{\Phi}_{n_{\mathrm{h}}}}{\partial \mathbf{q}_1} & \dfrac{\partial \boldsymbol{\Phi}_{n_{\mathrm{h}}}}{\partial \mathbf{q}_2} & \cdots & \dfrac{\partial \boldsymbol{\Phi}_{n_{\mathrm{h}}}}{\partial \mathbf{q}_{n_{\mathrm{c}}}} \end{bmatrix} \qquad \text{17)}$$

The system defined by equation (16) allows obtaining an approximation of the solution in (15). Considering this approximation as $\mathbf{q}_{i+1}$, a recursive equation is formulated:

$$\boldsymbol{\Phi}(\boldsymbol{q}_i) + \boldsymbol{\Phi}_{\mathbf{q}}(\boldsymbol{q}_i)(\boldsymbol{q}_{i+1} - \boldsymbol{q}_i) = 0 \qquad \text{18)}$$

Considering to $\Delta \boldsymbol{q}_i = \boldsymbol{q}_{i+1} - \boldsymbol{q}_i$, as the residual for the current iteration, equation (12) becomes:

$$\boldsymbol{\Phi}_{\mathbf{q}}(\boldsymbol{q}_i)\Delta \boldsymbol{q}_i = -\boldsymbol{\Phi}(\boldsymbol{q}_i) \qquad \text{19)}$$

The iterative equation (19) is applied repeatedly until the norm of $\Delta \boldsymbol{q}_i$ reaches a tolerance value defined by the user.

To calculate the velocity of each element of the system, the velocity constraint equations are used, obtained through derivation of equation (15) with respect to time:

$$\dot{\boldsymbol{\Phi}}(\mathbf{q}, \dot{\mathbf{q}}, t) = \frac{\mathrm{d}\boldsymbol{\Phi}(\mathbf{q}, t)}{\mathrm{d}t} = \frac{\partial \boldsymbol{\Phi}(\mathbf{q}, t)}{\partial t} + \frac{\partial \boldsymbol{\Phi}(\mathbf{q}, t)}{\partial \mathbf{q}}\frac{\mathrm{d}\mathbf{q}}{\mathrm{d}t} = \mathbf{0} \qquad \text{20)}$$

where $\frac{\partial \boldsymbol{\Phi}(q,t)}{\partial t}$ represents the vector of partial derivatives of the constraints with respect to time, $\frac{\partial \boldsymbol{\Phi}(q,t)}{\partial \mathbf{q}}$ is the Jacobian matrix of constraints (equation (17)) and the term $\frac{\mathrm{d}\mathbf{q}}{\mathrm{d}t}$ is the vector of generalized velocities (containing the velocities of each point and unit vectors that define the mechanical system), also represented as $\dot{q}$. Defining the vector *v(t)* as the right-hand-side of the velocity equation, equation (20) can be rewritten as:

$$\boldsymbol{\Phi}_{\mathbf{q}}\dot{\mathbf{q}} = -\frac{\partial \boldsymbol{\Phi}}{\partial t} = \boldsymbol{v} \qquad \text{21)}$$

The steps to calculate the vector of generalized acceleration (containing the acceleration of each point and unit vector that define the mechanical system) are similar to the ones used for velocity analysis. The velocity constraint equations (equation (21)) are derived with respect to time obtaining:

$$\ddot{\boldsymbol{\Phi}}(\mathbf{q}, \dot{\mathbf{q}}, \ddot{\mathbf{q}}, t) = \frac{\mathrm{d}\dot{\boldsymbol{\Phi}}(\mathbf{q}, \dot{\mathbf{q}}, t)}{\mathrm{d}t} = \boldsymbol{\Phi}_{\mathbf{q}}\ddot{\mathbf{q}} + \left(\boldsymbol{\Phi}_{\mathbf{q}}\dot{\mathbf{q}}\right)_{\mathbf{q}}\dot{\mathbf{q}} + \boldsymbol{v}_t = 0 \qquad \text{22)}$$

where $\boldsymbol{v}_t$ represents the vector of partial derivatives of $\boldsymbol{v}$ with respect to time. Defining the vector $\boldsymbol{\gamma}(\mathbf{q}, \dot{\mathbf{q}}, t)$ as the right-hand-side of the acceleration equation, the previous equation can be rewritten as:

$$\boldsymbol{\Phi}_{\mathbf{q}}\ddot{\mathbf{q}} = \boldsymbol{v}_t - \left(\boldsymbol{\Phi}_{\mathbf{q}}\dot{\mathbf{q}}\right)_{\mathbf{q}}\dot{\mathbf{q}} = \boldsymbol{\gamma} \qquad \text{23)}$$

In some mechanical systems, problems related with linear dependence in the lines of the Jacobian matrix may cause difficulties in calculating **q**. Usually, these problems are originated by the formulation of redundant constraint equations (constraint equations with the same topological information). Some

methods had been developed to circumvent this; the least-squares formulation is an example (used in Apollo software) and its application in equation (15) results in the following expression:

$$\Phi_q^T(q_i)\Phi_q(q_i)\Delta q_i = -\Phi_q^T(q_i)\Phi(q_i) \qquad 24)$$

5.3. Definition of Constraint Equations

To define mechanical systems, several kinematic constraint equations can be considered. In this section only the constraints with interest in this type of analysis will be presented. Essentially, one can consider three groups: 1) Rigid body constraints – permit defining and maintaining the proprieties of the elements in analysis. 2) Joint constraints – define the kinematic pairs and the topology of the mechanism. 3) Driver constraints –control the movement of the elements of the system.

5.3.1. Rigid body constraints and rotational driver constraints

The rigid body constraints are used to define and preserve proprieties of rigid bodies. If the element is defined with fully Cartesian coordinates (a set of points and unit vectors), this type of constraints is based in the maintenance of the distance between two points of the element or/and the preservation of the angle between two vectors. The number of expressions necessary to define correctly these constraints is equal to the difference between the number of Cartesian coordinates used to define the element and the number of DOF. For instance, considering the humerus (Figure 27 b)) as a rigid body defined by two basic points and two unit vectors, the number of constraint equations needed to its characterization is six: 12 Cartesian coordinates and 6 DOF (3 rotations in turn of the spatial frame axes and 3 translations in the direction of the spatial frame axes). In Figure 28 is represented an element defined with these characteristics. The six constraint conditions are: one constant distance between i and j, three constant angle conditions (between $\mathbf{u}$ and $\mathbf{r}_{ij}$, $\mathbf{v}$ and $\mathbf{r}_{ij}$ and $\mathbf{u}$ and $\mathbf{v}$) and two unit vector module conditions ($\mathbf{u}$ and $\mathbf{v}$).
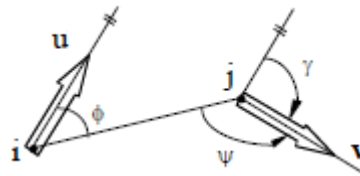
Figure 28 – Element defined with two basic points and two unit vectors
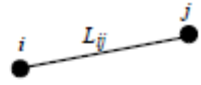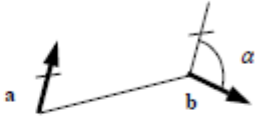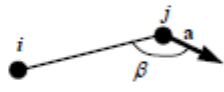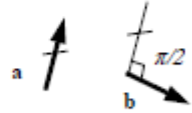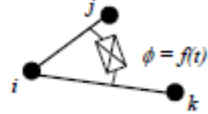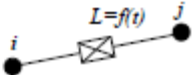
The rotational drivers are rheonomic constraints that allow the control of the angular movement of two articulated elements during the time of analysis. Usually, this type of element is used in joints to describe the angle formed by two bones (two rigid bodies).

These constraints, as several others (*vide* Table 1), can be defined by a generic expression that relates two vectors by means of the scalar product:

$$\Phi^{SP}(\mathbf{q}, t) = \mathbf{v}^T\mathbf{u} - L_v L_u \cos(\langle\mathbf{v}, \mathbf{u}\rangle(t)) = 0 \qquad 25)$$

where $\mathbf{u}$ and $\mathbf{v}$ are two generic vectors, L_v and L_u are their norms and $\langle\mathbf{v}, \mathbf{u}\rangle(t)$ is the angle between them.

Table 1 – applications of the scalar product constraint. $\mathbf{r}_i$, $\mathbf{r}_j$, $\mathbf{r}_k$ and $\mathbf{r}_l$ represent the Cartesian coordinates of points *i, j, k* and *l*, **a** and **b** are the unit vectors used to define the rigid bodies. (Silva 2003)

Constraint Description	v	u	L_v	L_u	<v,u>	Graphical representation
Constant distance between points *i* and *j*.	$(\mathbf{r}_j\text{-}\mathbf{r}_i)$	$(\mathbf{r}_j\text{-}\mathbf{r}_i)$	L_{ij}	L_{ij}	0	
Unit vector.	a	a	*1*	*1*	0	
Constant angle between unit vectors a and b.	a	b	*1*	*1*	α	
Constant angle between segment $\mathbf{r}_{ij}$ and unit vector a.	$(\mathbf{r}_j\text{-}\mathbf{r}_i)$	a	L_{ij}	*1*	β	
Constant angle between segments $\mathbf{r}_{ij}$ and $\mathbf{r}_{kl}$.	$(\mathbf{r}_j\text{-}\mathbf{r}_i)$	$(\mathbf{r}_l\text{-}\mathbf{r}_k)$	L_{ij}	L_{kl}	γ	
Orthogonal unit vectors.	a	b	*1*	*1*	$\pi/2$	
Rotational driver about a revolute joint located in point *i*, using segments $\mathbf{r}_{ij}$ and $\mathbf{r}_{ik}$.	$(\mathbf{r}_j\text{-}\mathbf{r}_i)$	$(\mathbf{r}_k\text{-}\mathbf{r}_i)$	L_{ij}	L_{ik}	$\phi=f(t)$	
Translational driver defined between point *i* and point *j* belonging to different rigid bodies.	$(\mathbf{r}_j\text{-}\mathbf{r}_i)$	$(\mathbf{r}_j\text{-}\mathbf{r}_i)$	$L=f(t)$	$L=f(t)$	0	

Due to the quadratic dependency on the generalized coordinates, the contribution of the scalar product constraint to the Jacobian matrix is linear:

$$\mathbf{\Phi}_{\mathbf{q}}^{\mathrm{SP}} = \frac{\delta(\mathbf{v}^{\mathrm{T}}\mathbf{u})}{\delta\mathbf{q}} = [\mathbf{0}^{\mathrm{T}} \quad \dots \quad \mathbf{u}^{\mathrm{T}} \quad \dots \quad \mathbf{0}^{\mathrm{T}} \quad \dots \quad \mathbf{v}^{\mathrm{T}} \quad \dots \quad \mathbf{0}^{\mathrm{T}}] \qquad 26)$$

Applying the equations (21) and (23) in (25) results that the contribution of the scalar product constraint to the right-hand side of the velocity and acceleration are, respectively:

$$\boldsymbol{v}^{\mathrm{SP}}(t) = -L_{\mathbf{v}}L_{\mathbf{u}} \sin\big(\langle\mathbf{v},\mathbf{u}\rangle(t)\big)\frac{\delta\langle\mathbf{v},\mathbf{u}\rangle(t)}{\delta t} \qquad 27)$$

$$\boldsymbol{\gamma}^{\mathrm{SP}}(t) = -L_{\mathbf{v}}L_{\mathbf{u}}\left[\cos\big(\langle\mathbf{v},\mathbf{u}\rangle(t)\big)\left(\frac{\delta\langle\mathbf{v},\mathbf{u}\rangle(t)}{\delta t}\right)^{2} + \sin\big(\langle\mathbf{v},\mathbf{u}\rangle(t)\big)\frac{\delta^{2}\langle\mathbf{v},\mathbf{u}\rangle(t)}{\delta t^{2}} - 2(\dot{\mathbf{v}}^{\mathrm{T}}\dot{\mathbf{u}})\right] \qquad 28)$$

Although most rigid bodies can be defined by the formulation presented, when the elements have complex forms it is necessary to recur to other types of rigid body formulations, which are beyond the scope of this thesis (Silva).

5.3.2. Joint Constraints

The joint constraints are used to define kinematic pairs and enable the relative movement between their elements. These vary according to the DOF permitted and, consequently, their formulations will be different, depending if the joint is spherical, revolute, universal, prismatic, and so on. Essentially, the first three joints types are enough to define biomechanical models of interest in gait, which is why these will be elaborated along the following sections.

5.3.2.1. *Spherical Joint*

The spherical joint is used to define socket ball joint (hip and shoulder) and only enable three DOFS (the three rotations). When a shared point is used to define a spherical joint, it is not necessary to generate a constraint equation, because this is implicitly defined, i.e. when two elements share the same point, the only motion that is enabled is the rotation around this point.

On the other hand, if an explicit definition of joints is used (hip case), it is necessary to generate a constraint equation that ensures the union of the two points defining it. Considering m and n these points, and $\mathbf{r}_n$ and $\mathbf{r}_m$ their position vector, the constraint equation for spherical joint is given by:

$$\mathbf{\Phi}^{\mathbf{SPH}}(\mathbf{q}) = \mathbf{r}_n - \mathbf{r}_m = \mathbf{0} \tag{29}$$

5.3.2.2. *Revolute joint*

The revolute joint enables only one rotation between two rigid bodies, i.e. it restrains three translations and two rotations. It is used to define hinge joints as the elbow or knee.

If the two rigid bodies, defining the joint share a basic point and a unit vector (Figure 27a)), the revolution joint is automatically defined. However, if an explicit model is used (Figure 27b)), it is necessary to generate two sets of constraint equations. The first ensures that the two points share the same spatial position (according to (29)). The other set considers that the two unit vectors that define the two elements have the same spatial components. Using the notation of Figure 27b), the second set of constraint becomes:

$$\mathbf{\Phi}^{\mathbf{REV}}(\mathbf{q}) = \mathbf{v} - \mathbf{u} = \mathbf{0} \tag{30}$$

5.3.2.3. *Universal Joint*

The universal joint, also called cardan joint, restricts four DOF, enabling only two rotations around two orthogonal vectors. In the adopted biomechanical model, this joint is used in the definition of the ankle (see Figure 29).
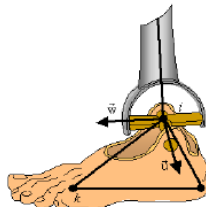
Figure 29 – representation of the ankle joint using a universal joint. **u** is the unit vector that defines the foot (3 basic points and 1 unit vector) and **w** is one of the two unit vectors that define the leg (2 basic points and 2unit vectors) (Silva 2003).

Using the notation of Figure 29, the point *i* can be shared by the two elements – foot and leg. In this case, it is only necessary to generate an expression that guarantees the orthogonality between **w** and **u** (vide Table 1). If the joint is defined explicitly, an additional constraint equation must be considered, in order to ensure that the two points that define the kinematic pair share the same spatial position (as in (29)).

5.4. Dynamic Analysis

5.4.1. The principle of virtual power

The starting point of this analysis is to deduce the equations for motion to a multibody system; although Jalon and Bayo present several different ways of obtaining them, in this work only the formulation deduced by the principle of virtual power will be presented. Such principle states that the sum of the virtual power produced by the external and inertial forces in the system to each instant is zero. Considering *nc* the number of generalized coordinates the principle can be formulated as:

$$P^* = \sum_{i=1}^{nc} f_i \dot{\mathbf{q}}_\mathbf{i}^* \equiv \dot{\mathbf{q}}_\mathbf{i}^{*\mathrm{T}} \mathbf{f} = \mathbf{0} \tag{31}$$

where $\dot{\mathbf{q}}_\mathbf{i}^*$ is the virtual velocity vector that represents a set of imaginary velocities and is consistent with the homogeneous form of the velocity constraint equations at a stationary time:

$$\boldsymbol{\Phi}_\mathbf{q}^\mathrm{T} \dot{\mathbf{q}}^* = \mathbf{0} \tag{32}$$

f is the vector of all the forces that produce virtual power (external and inertial forces), and it is defined as:

$$\mathbf{f} = \mathbf{M}\ddot{\mathbf{q}} - \mathbf{g} \tag{33}$$

where **Mq̈** is the vector of inertial forces (**M** represents the global mass matrix and **q̈** the vector of generalized accelerations) and **g** is the vector of generalized forces, which includes the external forces and the velocity-dependent inertial forces (centrifugal and Coriolis forces). In vector **f**, the internal forces associated to kinematic constraints are not included, since these do not produce virtual power because they exist in action/reaction pairs. Thus, to calculate these internal forces, it is necessary to make use of the Lagrange multipliers method:

$$\mathbf{g}^* = \boldsymbol{\Phi}_\mathbf{q}^\mathrm{T} \boldsymbol{\lambda} \tag{34}$$

where $\mathbf{g}^*$ represents the generalized force vector that contains the internal constraint forces and $\boldsymbol{\lambda}$ is the vector of Lagrange multipliers. The columns of the Jacobian matrix indicate the direction of the internal forces vector, while the Lagrange multipliers correspond to its magnitude. Considering equations (33) and (34) associated to the fact that internal constraint forces do not produce virtual power, the equation can be formulated as:

$$P^* = \dot{\mathbf{q}}_\mathbf{i}^{*\mathrm{T}}(\mathbf{M}\ddot{\mathbf{q}} - \mathbf{g} + \boldsymbol{\Phi}_\mathbf{q}^\mathrm{T}\boldsymbol{\lambda}) = \mathbf{0} \tag{35}$$

5.4.2. Equations of Motion

Equation (35) can be rewritten, resulting in the equations of motion of a constrained multibody system:

$$\mathbf{M}\ddot{\mathbf{q}} + \boldsymbol{\Phi}_\mathbf{q}^\mathrm{T}\boldsymbol{\lambda} = \mathbf{g} \tag{36}$$

Expression (36) represents a second-order ordinary differential equation with (*nc*+*nh*) unknowns and *nc* equations. To enable solving the problem, it is necessary to add *nh* equations, which can be achieved by considering the kinematic equations. Despite being more adequate to apply equation (15) to this problem, the achievement of a solution becomes difficult. Equation (23) can be applied instead, so as to provide the additional necessary equations. The system in matrix form becomes:

$$\begin{bmatrix} \mathbf{M} & \mathbf{\Phi_q^T} \\ \mathbf{\Phi_q} & \mathbf{0} \end{bmatrix} \begin{Bmatrix} \ddot{\mathbf{q}} \\ \boldsymbol{\lambda} \end{Bmatrix} = \begin{Bmatrix} \mathbf{g} \\ \boldsymbol{\gamma} \end{Bmatrix} \tag{37}$$

To solve the system of equations of motion, several methods can be used, It was chosen to use the direct integration method (De Jalon and Bayo 1994). However, to guarantee its convergence, a stabilization method is required, such as the Baumgarte stabilization that allows converting differential algebraic equations in ordinary differential equations (De Jalon and Bayo 1994). Thus, the convergence and stability of the system is guaranteed.

The right-hand-side of the acceleration equation results in an instable differential equation:

$$\mathbf{\Phi_q}\ddot{\mathbf{q}} = \boldsymbol{\gamma} \implies \ddot{\mathbf{\Phi}} = \mathbf{0} \tag{38}$$

By means of the Baumgarte method, it is possible to obtain a more stable system recurring to the following equation:

$$\ddot{\mathbf{\Phi}} + 2\alpha\dot{\mathbf{\Phi}} + \beta^2\mathbf{\Phi} = \mathbf{0} \tag{39}$$

As the first and second derivatives of the constraints equations are given by:

$$\begin{cases} \ddot{\mathbf{\Phi}} = \mathbf{\Phi_q}\ddot{\mathbf{q}} - \boldsymbol{\gamma} \\ \dot{\mathbf{\Phi}} = \mathbf{\Phi_q}\dot{\mathbf{q}} - \boldsymbol{v} \end{cases} \tag{40}$$

Substituting (40) in (39):

$$\boldsymbol{\gamma}^* = \boldsymbol{\gamma} - 2\alpha(\mathbf{\Phi_q}\dot{\mathbf{q}} - \boldsymbol{v}) - \beta^2\mathbf{\Phi} \tag{41}$$

Replacing $\boldsymbol{\gamma}$ by $\boldsymbol{\gamma}^*$ in equation (37) results in a stabilized system:

$$\begin{bmatrix} \mathbf{M} & \mathbf{\Phi_q^T} \\ \mathbf{\Phi_q} & \mathbf{0} \end{bmatrix} \begin{Bmatrix} \ddot{\mathbf{q}} \\ \boldsymbol{\lambda} \end{Bmatrix} = \begin{Bmatrix} \mathbf{g} \\ \boldsymbol{\gamma} - 2\alpha(\mathbf{\Phi_q}\dot{\mathbf{q}} - \boldsymbol{v}) - \beta^2\mathbf{\Phi} \end{Bmatrix} \tag{42}$$

The constants α and β are parameters of the model and should be adjusted for each analysis. Their values must be included in the range from 0 to 20.

5.4.3. Integration of the Motion Equations

As referred, the method used to solve the motion equations is the direct integration algorithm. It allows studying the evolution of the system over time ($\mathbf{q}, \dot{\mathbf{q}}, \ddot{\mathbf{q}}, \boldsymbol{\lambda}$), knowing the initial position and velocity, and the external forces applied. This type of problem is designated as initial-value problem and the integrating processes are represented in Figure 30:
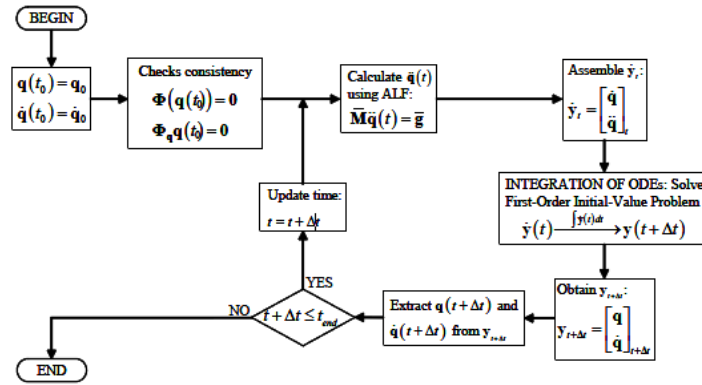
Figure 30 – Schematic representation of the initial-value problem (Silva 2003)

5.4.4. Mass matrix for 3D rigid bodies

The number of rigid bodies of a multibody mechanical system suggests that it is necessary to develop a mass matrix for each of them. Although, it is true that each rigid body has its own mass matrix, but its determination can be obtained from a basic mass matrix (constructed for a basic rigid body – see Figure 31) through a simple coordinate transformation.
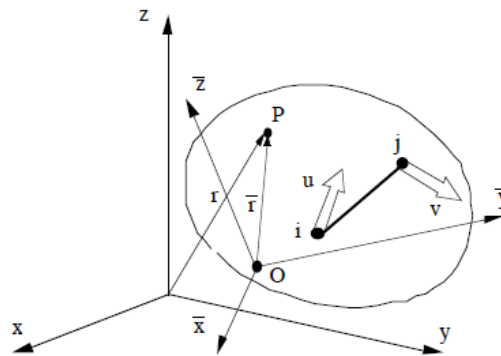
Figure 31 – Representation of the inertial and local system for a basic rigid body in 3D. It is made by two points (i and j) and two non-coplanar unit vectors (**u** and **v**). The reference frame (*x,y,z*) represents the inertial reference frame; the reference frame $(\overline{x},\overline{y},\overline{z})$ represents the local reference attached to the rigid body that has is origin in the point O. The point *P* consists of a generic point of the element, and its localization is defined by the position vector **r** in the inertial reference and $\overline{\mathbf{r}}$ in the local frame.

Using the principle of virtual power of the inertial forces, it is possible to calculate the mass matrix for a rigid body. This expression can be described in the integral form as:

$$P^* = -\rho \int_{\Omega} \dot{\mathbf{r}}^{*T}\ddot{\mathbf{r}} \ d\Omega$$

43)

where ρ is the density of the rigid body, Ω is the body's volume, $\dot{\mathbf{r}}$ and $\ddot{\mathbf{r}}$ are the virtual velocity and acceleration of the generic point P, respectively. The latter can be calculated by means of a coordinate transformation, but before it is necessary to define the vector **r**. Since the element is rigid, the local relative position $(\mathbf{r} - \overline{\mathbf{r}})$ remains constant. Considering the element defined by the Cartesian coordinates (points *i* and *j* and the unit vectors **u** and **v**), the position of point P relative to point *i* can be expressed as:

$$\mathbf{r} - \mathbf{r_i} = c_1(\mathbf{r_j} - \mathbf{r_i}) + c_2\mathbf{u} + c_3\mathbf{v}$$

44)

72

where c_1, c_2 and c_3 represents the components of $(\mathbf{r} - \overline{\mathbf{r}})$ in the 3D base formed by the vectors $(\mathbf{r} - \overline{\mathbf{r}})$, **u** and **v**. Through manipulation of (44) to the matrix form results:

$$\mathbf{r} = \begin{Bmatrix} x \\ y \\ z \end{Bmatrix} = [(1 - c_1)\mathbf{I_3} \quad c_1\mathbf{I_3} \quad c_2\mathbf{I_3} \quad c_3\mathbf{I_3}] \begin{Bmatrix} r_i \\ r_j \\ u \\ v \end{Bmatrix} = \mathbf{C}\mathbf{q}_e \qquad 45)$$

where $\mathbf{I_3}$ is the identity matrix of order (3x3), and **C** represents the transformation matrix (independent of the system's motion – constant in time). $\mathbf{q}_e$ is the vector of generalized coordinates of the rigid body. Deriving equation (45) twice with respect to time, one obtains:

$$\mathbf{r} = \mathbf{C}\dot{\mathbf{q}}_e \qquad 46)$$

$$\mathbf{r} = \mathbf{C}\ddot{\mathbf{q}}_e \qquad 47)$$

where $\dot{\mathbf{q}}_e$ and $\ddot{\mathbf{q}}_e$ are respectively, the generalized velocity and acceleration of the basic rigid body. The coefficients c_1, c_2 and c_3 can be obtained by rewriting equation (44) in the local reference frame of the rigid body:

$$\overline{\mathbf{r}} - \overline{\mathbf{r_i}} = c_1(\overline{\mathbf{r_j}} - \overline{\mathbf{r_i}}) + c_2\overline{\mathbf{u}} + c_3\overline{\mathbf{v}} \qquad 48)$$

Expressing equation (48) in matricial form yields:

$$\overline{\mathbf{r}} = [\overline{\mathbf{r}} - \overline{\mathbf{r_i}} \quad \overline{\mathbf{u}} \quad \overline{\mathbf{v}}] \begin{Bmatrix} c_1 \\ c_2 \\ c_3 \end{Bmatrix} = \overline{\mathbf{X}}\mathbf{c} \qquad 49)$$

where **c** is the vector that contains the coefficients c_1, c_2 and c_3 and $\overline{\mathbf{X}}$ represents the matrix containing the components of the vector $(\overline{\mathbf{r}} - \overline{\mathbf{r_i}})$, $\overline{\mathbf{u}}$ and $\overline{\mathbf{v}}$. By definition these vectors are non-coplanar, so $\overline{\mathbf{X}}$ can always be inverted; this fact allows solving equation (49) in order to **c** :

$$\mathbf{c} = \overline{\mathbf{X}}^{-1}(\overline{\mathbf{r}} - \overline{\mathbf{r_i}}) \qquad 50)$$

Replacing the expressions (46) and (47) in the expression of the virtual power of the inertial forces (43) results in:

$$P^* = -\rho \int_\Omega \dot{\mathbf{q}}_e^{*T}\mathbf{C}^T\mathbf{C}\ddot{\mathbf{q}}_e \ d\Omega = -\dot{\mathbf{q}}_e^{*T}(\rho \int_\Omega \mathbf{C}^T\mathbf{C} \ d\Omega)\ddot{\mathbf{q}}_e \qquad 51)$$

where $\dot{\mathbf{q}}_e^{*T}$ and $\ddot{\mathbf{q}}_e$ are independent of Ω, and, consequently, can be moved outside the integral. Comparing (51) with (35) yields in the expression of mass matrix:

$$\mathbf{M} = -\rho \int_\Omega \mathbf{C}^T\mathbf{C} \ d\Omega \qquad 52)$$

Through integration (vide (De Jalon and Bayo 1994)), expression (52) results in the following matrix:

$$\mathbf{M} = \begin{bmatrix} (m - 2ma_1 - z_{11})\mathbf{I_3} & (ma_1 - z_{11})\mathbf{I_3} & (ma_2 - z_{12})\mathbf{I_3} & (ma_3 - z_{13})\mathbf{I_3} \\ (ma_1 - z_{11})\mathbf{I_3} & z_{11}\mathbf{I_3} & z_{12}\mathbf{I_3} & z_{13}\mathbf{I_3} \\ (ma_2 - z_{21})\mathbf{I_3} & z_{21}\mathbf{I_3} & z_{22}\mathbf{I_3} & z_{23}\mathbf{I_3} \\ (ma_3 - z_{31})\mathbf{I_3} & z_{31}\mathbf{I_3} & z_{32}\mathbf{I_3} & z_{33}\mathbf{I_3} \end{bmatrix} \qquad 53)$$

where m is the total mass of the rigid body and a_i is the first area moments of the rigid body. This moment can be calculated with respect to the reference frame with origin at i and the axes defined by the generalized coordinated of ($\overline{\mathbf{r}} - \overline{\mathbf{r_i}}$) and unit vectors **u** and **v**. The matrix **M** is constant and symmetric in time, so during a dynamic analysis it is only necessary to compute it in the beginning. (It

depends of a set of ten values: total mass of the rigid body, the coordinates of center of gravity, and the six different elements of the inertial tensor).

The presented mass matrix corresponds to an element with two basic points and two unit vectors. Generally, it is possible to identify these two conditions in an element; however, in case this is not possible, it is necessary to recur to another notations. These vary essentially in the number of basic points and unit vectors considered (e.g. element with three basic points and a unit vector, element with two basic points and a unit vector, etc.). The deductions are similar to the ones presented, but fall off the scope of the work and as such will not be presented. This deductions can be found in (De Jalon and Bayo 1994).

Chapter VI

Protocol Definition

In this chapter, the protocols established to analyze gait in a experimental environment are introduced and explained. These suggested protocols make use of the knowledge on anatomo-physiology presented in chapter 2, the gait concepts of chapter 3 and the study of some gait pathologies presented in chapter 4 and are meant to be used in the LBL for the analysis of pathologic and non-pathologic gait.

6.1. Marker Set Protocol

The present work has been developed in LBL – Biomechatronic Research Group of Instituto Superior Técnico. The acquisition of kinematic data is made by means of four IR cameras – Qualisys ProReflex (QUALYSIS 2010) and two video cameras. The acquisition software is Qualisys Track Manager (QTM) (QUALYSIS 2010).

The adopted protocol must be robust and fast setting, since one of this work's objectives is the application of this study in a clinical context. At the same time, the number of markers and their body location setting must be compatible with the software used for data treatment - Visual3D^{TM} (c-motion 2010) and Apollo (Silva 2003).

The markers used in the trials are spherical passive markers with flat base and 19mm of diameter. They are made of polystyrene hemispheres covered in special retro-reflective tape, manufactured by Qualysis®.

The Apollo software has been developed in IDMEC/IST – Institute of Mechanical Engineering of IST. It is a software for three-dimensional dynamic analysis of mechanical systems and permits an inverse dynamic multibody analysis. This software recurs to a biomechanical model of the human body, which considered 33 rigid bodies to model sixteen anatomical segments. A total of 25 anatomic points used to define the fifteen kinematic joints and the anatomical segments (23 measured and 2 calculated). It is important refer that the notation used in developed routines follows the numeration presented in Figure 32 c) (Silva 2003).

Visual3D^{TM} is biomechanical analysis software for performing kinematic and kinetic analysis as well as a three-dimensional observation of the movement. Visual3D's modeling flexibility allows a variety of marker sets, requiring at least three markers to define a body segment. Visual3D^{TM} considers two

different types of markers: (1) Calibration markers – define the body segments and should be placed in anatomical references of interest. (2) Tracking markers – should be placed in strategic and geometrically relevant positions of the segments, used for computing the movements. Calibration markers can be used as tracking markers, although the markers placed in segment extremities can be easily affected by skin movement artifacts, which is a very important issue (Collins, Ghoussayni et al. 2009; c-motion 2010).
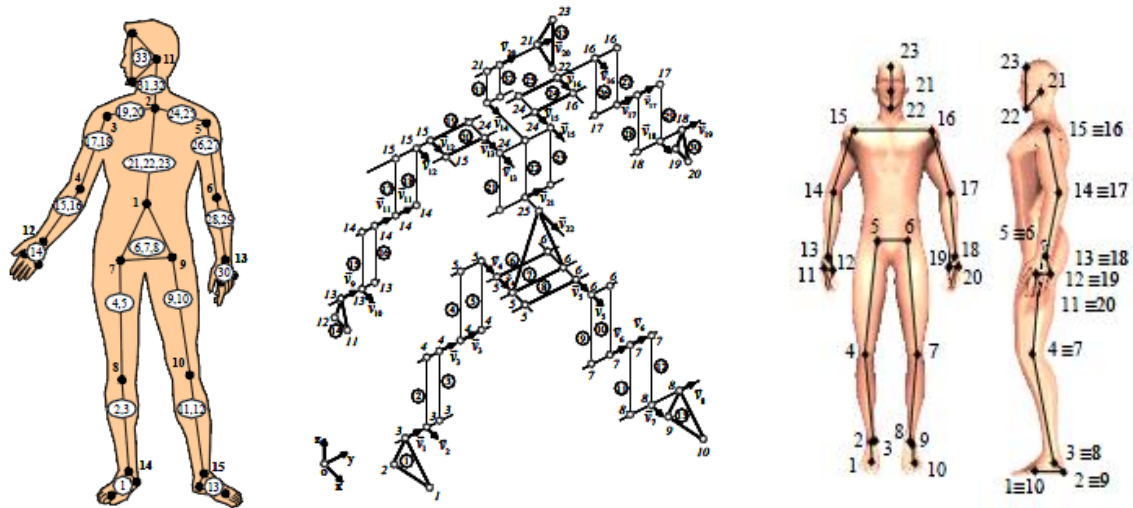
Figure 32 – Inverse biomechanical model used in Apollo Software. a) Representation of the 33 rigid bodies (numbers inside the circle) used to define the sixteen anatomical segments. b) Representation of the same model of a), but considering also the points (italic notation) and unit vectors used to define the model. c) Set of the anatomical points used to define the model presented in a) and b) (Silva 2003)

According to Cappozzo et al., these artifacts are the most critical source of error in kinematic/kinetic studies. Since the frequency of skin movement artifacts and bone movements in locomotion is the same; there is no way of filtering such artifact from data of interest. To mitigate this problem Cappozzo et al. suggest a careful marker placement in anatomical landmarks whose relative displacement is minimal, and an efficient algorithm to estimate the position and orientation of the desired segment from the positions of the skin markers (Cappozzo, Catani et al. 1996).

In order to be applied in academic and clinical studies, the developed model should consider several definitions proposed by (Cappozzo, Catani et al. 1995):

Bone-embedded frames – the experimental data should be repeatable and applicable both for the same subject and for different subjects. The model should enable the determination of suitable axes with respect to all movements of each joint (rotations and translations). Moreover, it should also enable a practical implementation of techniques for the estimation of the center of mass and of the principal inertial axes of body segments. Finally, it should consider the muscle and ligament line of action, as well as its location and orientation.

Marker points – the light emitted or reflected from markers should be oriented within a field of view of at least two cameras. The three markers defining a body segment should be sufficiently large so as to minimize the error propagation during reconstruction of marker coordinates. The markers should be easily implantable and applicable in anatomical objects (orthoses, prostheses, etc.) and their relative movement should be minimal.

Markers can be placed directly on the skin surface or assembled on components (plates and elastic bands) attached to the body. Cappozzo suggests preferentially the use of the latter, since their placement is easier and fast. Moreover, wide elastic bands help to reduce soft-tissue movement artifacts (Cappozzo, Catani et al. 1995).

Hence, in this work a set of clothing accessories was conceived in order to be applicable in academic and clinical locomotion studies. This set consists of a pair of socks, lycra shorts, sleeveless sweater, a pair of cycling gloves and a lycra swim cap. To avoid clothes movement, it is important that each accessory tightly fits into the body and for that reason several clothes sizes were developed.

It was pretended that the clothes accessories to be applicable for a large number of people, which demanded clothes to be washable. After some locomotion tests, the use of a sewed Velcro's band proved to be the most effective mechanism for marker attachment, as it permits an easy and fast marker placement and it is washable and durable. Furthermore, while it is in perfect conditions, it does not allow small displacements and vibrations of markers. In appendix C the photos and the projects of clothing developed accessories can be consulted.

6.1.1. Extensive Marker set Protocol

The first developed protocol, extensive marker set protocol (EMSP), takes into account all the aspects above. The EMSP consists of a model of 59 markers (22 tracking markers and 37 calibration markers) based on the model proposed by Visual3D (c-motion 2010). However, the obtained results are not good enough. Due to the low number of cameras (four), many marker trajectories were misinterpreted as the same one, and some markers were not visible by cameras. In order for QTM to consider a valid point; the corresponding marker has to be seen by at least 2 cameras at the same time (QUALYSIS 2010).

The proposed model can be consulted in appendix B. Although EMSP will not be used in this thesis, it can be applicable in a biomechanics laboratory with more cameras, making this protocol preferable to the one presented in 6.1.2.

6.1.2. Marker Set Protocol

Due to the problem related to the insufficient number of cameras in the laboratory, it was necessary to develop a new protocol – Marker Set Protocol (MSP). MSP is based in Helen Hayes Marker Set (HH) developed by Kadaba at Helen Hayes Hospital (Kadaba, Ramakrishnan et al. 1991). Essentially, marker set protocols used in clinic represent variations of HH, as these are adapted for low resolution imaging systems, with as few markers as possible (Collins, Ghoussayni et al. 2009).

The total number of markers in MSP is 33, distributed amongst the body. To standardize the data, the markers were placed in anatomical landmarks of each body segment. Several published works suggests different anatomical landmarks for each marker; the positions adopted for this thesis is based in the works of (Cappozzo, Catani et al. 1995; Collins, Ghoussayni et al. 2009) (vide Table 2).

Unlike the previous protocol (EMSP), MSP considers all calibration markers as tracking markers, for the reasons explained in 6.1.3. The problem of skin movement artifact was attenuated, by using a set of tight clothes and carefully defining the placement of markers in locations of low skin displacement. The Apollo software, that will be the main tool of kinetic analysis, does not consider the

hypothesis of clusters of marker as tracking markers; the model input considered just 23 calibration markers that are at the same time tracking markers (vide Figure 32c)).
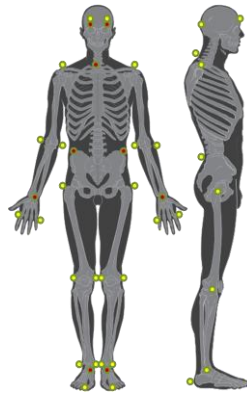
Figure 33– marker set protocol (yellow – markers seen in the anterior view; red – markers seen in the posterior view)

Table 2 – Location and Anatomical Landmark of markers in MSP

Maker Nº	Location	Anatomic Landmark	Maker Nº	Location	Anatomic Landmark
0	Anterior left Skull	Temporal line of frontal bone	17	Pelvis	Left iliac crest (LIC)
1	Anterior Right Skull	Temporal line of frontal bone	18	Pelvis	Right iliac crest (RIC)
2	Posterior Left Skull	Occipital protuberance (left)	19	Left Distal Knee	Most prominent point of lateral femoral epicondyle
3	Posterior Right Skull	Occipital protuberance (Right)	20	Left Medial Knee	Most prominent point of medial femoral epicondyle
4	neck	Spinous Process of C7	21	Left Distal Ankle	Most prominent point of lateral malleolus
5	Left Shoulder	Clavicle – Acromion	22	Left Medial Ankle	Most prominent point of medial malleolus
6	Right Shoulder	Clavicle – Acromion	23	Left Foot	Upper ridge of the calcaneus posterior surface
7	Left Distal Elbow	Lateral epicondyle of humerus	24	Left Foot	II metatarsal heads
8	Left Medial Elbow	Medial epicondyle of humerus	25	Right Distal Knee	Most prominent point of lateral femoral epicondyle
9	Left Wrist	Medial position between styloid process of radius and ulna	26	Right Medial Knee	Most prominent point of medial femoral epicondyle
10	Left Hand	Distal head of II Metacarpus	27	Right Distal Ankle	Most prominent point of lateral malleolus
11	Left Hand	Distal head of V Metacarpus	28	Right Medial Ankle	Most prominent point of medial malleolus
12	Right Distal Elbow	Most prominent point of lateral epicondyle of humerus	29	Right Foot	Upper ridge of the calcaneus posterior surface
13	Right Medial Elbow	Most prominent point of medial epicondyle of humerus	30	Right Foot	II metatarsal heads
14	Right Wrist	Medial position between styloid process of radius and ulna	31	Left Hip Joint	Center of acetabulum
15	Right Hand	Distal head of II Metacarpus	32	Right Hip Joint	Center of acetabulum
16	Right Hand	Distal head of V Metacarpus			

To define a pelvic coordinate system, several models have been developed. One of the most used is HH (Sacrum, Right ASIS and Left ASIS). However, these anatomical landmarks, especially the ASIS, are not easily palpable in some subjects (as in overweight subjects) and during locomotion these may be occluded several times due to arm movement and by skin tissue from the abdominal area. An alternative model is CODA (Right PSIS, Left PSIS, Right ASIS and Left ASIS), but has the same limitations as the HH model (placement in ASIS). (c-motion 2010; Fukuchi, Arakaki et al. 2010)

Yet, an additional method uses 4 markers (RIC, LIC, Right Hip Joint Center and Left Hip Joint Center); and c-motion designates this method as Visual3D Pelvis. Some advantages can be pointed out: 1) easy identification of anatomic landmarks 2) these locations are not easily occluded by arm movement and skin tissue (c-motion 2010; Fukuchi, Arakaki et al. 2010).

Comparing the three presented methods, in this work, it was has chosen to adopt the last one because it requires fewer markers, it can be used in a wider range of subjects and can be applied both in Apollo software as in Visual3D^{TM}.

One last aspect to be considered was the use of two markers in some joints (ankle, knee and elbow). Although this method implies more markers, it enables an easy and more precise determination of articular center by computing the medial point of the two markers (Collins, Ghoussayni et al. 2009). The other joints are estimated by varying the distance of marker to respective joint center. The wrist joint is not calculated by the first method, due to the low number of cameras and the small distance between markers. The trajectories of hand-wrist are easily confused and the author preferred to consider only one marker in wrist to avoid blunders.

6.2. Spatial Arrangement of Cameras and Force Plates

As already referred, the LBL has presently four IR cameras (Qualisys ProReflex) and four video cameras. The present chosen configuration for the cameras had in consideration the several problems caused by the small number of cameras.

In the first tested arrangement, the IR cameras were placed in the four corners of the laboratory. The results were not good enough, since the medial markers of the lower limbs, especially the knee markers, were in many instances occluded during the swing phase. As, the subject has only two cameras in front of him, the swing leg hides the stance leg during the mid swing and terminal swing from the camera disposed in the side of, which led to loss of information.

The presence of markers in medial and lateral position in the lower limbs joints is essential to calculate of their articular center. The kinetic analysis of gait focuses on the study of the lower limbs, so it was preferred to modify the previous cameras arrangement to a different one which allowed the acquisition of medial markers with minimum occlusion. Hence, while the two cameras behind the subject and one of the cameras in front of him maintained their position, the other fourth camera was placed directly in front of subject, over the imaginary line of progression (vide Figure 34). Such arrangement solved the problem of occlusion of the medial markers of lower limbs. However, the maker trajectories of the hand and the elbow of the opposite side of the anterior corner camera lost some quality since the period of occlusion slightly increased; nonetheless, as these trajectories are relatively easy interpolated and not essential for kinetic analysis, this arrangement was considered as the most adequate for the present laboratory the conditions.

In what concerns the use of video cameras, these represent a qualitative method to visualize the trial and to take some notes. Hence, these were placed to record the sagittal and coronal view of the trial.

To acquire de data from external forces, LBM is equipped with three AMTI-OR6-7 force platforms (508mm x 464mm). The software used to treat this data is essentially QTM. Since the data yielded by the force plates represents voltage, it was necessary to use an algorithm developed in MATLAB in order to obtain the corresponding forces and moments of force. The spatial arrangement of the force plates used is represented in Figure 34 and was the adopted by the LBL. The arrangement was fixed for all subjects and it is based in one of the configurations presented by (Richards 2008).
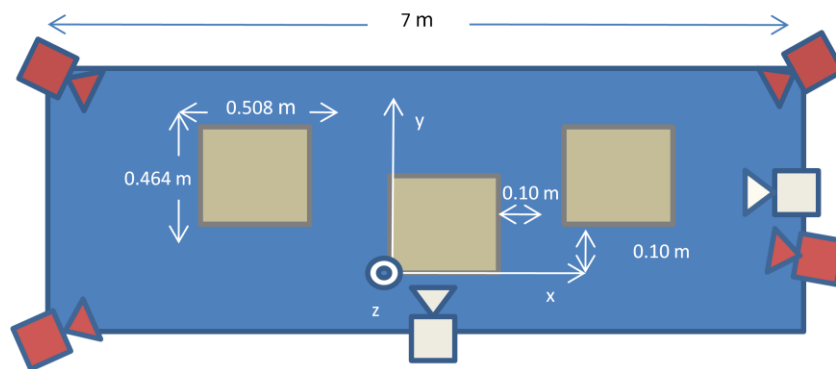
Figure 34 - Representation of arrangement in space of the four IR cameras (red) and the two video cameras (white) used to acquire the motion and the three force plates used to acquire the GRF during the stride period (gray)

6.3. Superficial Electromyography

In order to perform a complete study of normal and pathologic gait, it is essential to understand the pattern of muscular activation. Monitoring sEMG can play an important role, especially during the study and detection of neurological injuries (Ricamato and Hidler 2004).

Electromyography (EMG) is a technique that permits the study of muscles by recording and analyzing the myoelectric signals. These signals are generated by physiological variation in the state of membranes of the muscle fiber. It serves as an indicator for muscle activation (when muscular excitation begins and ends), enables the estimation of the force produced by the muscle and allows the study of the index of the rate at which a muscle fatigues (Perry and Bekey 1981 a); Cholewicki and McGill 1994; Delsys 2010)

Typically, a detected and unprocessed signal is called a raw EMG Signal, as can be seen in the following figure:
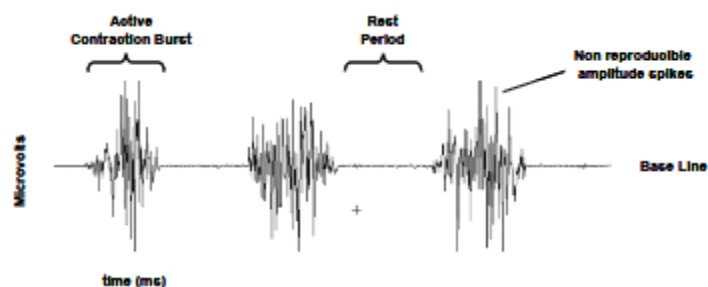
Figure 35 – The raw EMG recording for 3 contraction bursts of the M. Biceps (Konrad 2005)

The raw EMG baseline noise varies with several factors, as the quality of EMG amplifier, environmental noise and the quality of the conditions of detection. During contraction, spikes present a random shape, and thus cannot be precisely reproduced in exact shape. Usually this type of signal has a range of amplitudes between +/- 5000 µV and a range of frequency between 6 and 500 Hz (showing most of the frequency power between 20 and 150 Hz).(Konrad 2005)

The EMG signal can be influenced by several factors as (Merletti 1999; Konrad 2005):

Tissue characteristics – the electrical conductivity of the human body can vary with tissue type, thickness, physiological changes and temperature. For example, a subject with more fat tissue will have less EMG Magnitude due to the greater distance between the muscle and the electrodes. The number and size of muscle fibers also influence the amplitude of EMG signal.

Cross Talk (physiological) – During a contraction of the muscle under study, its neighbors may also produce contraction, which can be detected at the site of local electrodes. The selection of the appropriate electrode size, inter-electrode distance and location should be carefully planned to avoid this phenomenon. In the study of some muscles (especially on the upper trunk and shoulder muscles) ECG spikes can also be observed.

Geometry changes provoked by variations of the muscle belly – during contraction, some muscles change their geometry, altering the distance between signal source and detection site and thus causing variations in EMG reading.

Electrode/Amplifiers – The selection and the quality of the EMG devices can also influence the quality of the recorded signal.

The noise in EMG can be divided in 4 groups: 1) noise inherent to the electronic components of EMG device (0 Hz to several thousand Hz); 2) Ambient Noise – it is originated from sources of electromagnetic radiation (electric-power wires, light bulbs, etc.). The human skin is also a source of this type of noise; it is constantly embedded with electro-magnetic radiation from the surrounding space. (50/60 HZ) 3) Motion artifacts –comes from the displacement between the surface of the electrode and the skin, and also from the movement of the cable connecting the electrode to the amplifier. (0 to 20 Hz) 4) Inherent instability of signal – occurs essentially to frequency components between 0 and 20 Hz, due the quasi-random nature of the firing rate of motor units (De Luca 2002).

A wide variety of electrodes can be found, with different shapes, sizes, materials and assemblies. The choice depends essentially on the objective of the study and on the muscle of interest (Soderberg 1992). In electromyography studies two types of electrodes can be considered essentially (Winter 1991):

Indwelling electrodes (invasive) – mainly for the study of small and deeper muscles layers (but also superficial layers);

Superficial electrodes (non invasive) – only for the study of superficial muscles, as these detect signals approximately 2cm below the skin tissue.

Conflicting views emerge on which method is more susceptible to the cross-talking phenomenon. Winter considers that since an indwelling electrode acquires all the signals in a sphere of 2 cm radius, it is more susceptible to cross-talking phenomenon of deeper muscles (Winter 1991). Conversely, Perry, in a study where the differences between the surface and fine-wire electrodes in EMG were

compared, concluded that the results obtained by sEMG had tendency to present more cross-talking (Perry, Easterday et al. 1981 b)).
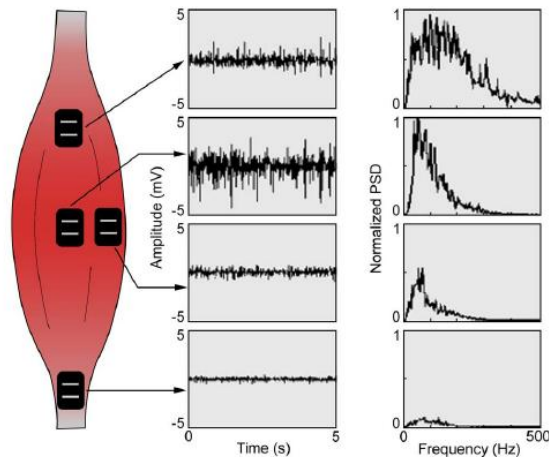
Figure 36 - the amplitude and frequency spectrum of the EMG signal to different location in same muscle. (De Luca 1997)

As can be seen in Figure 36, the location of the electrodes has significant influence on the resulting EMG signal. While in indwelling electrodes are placed directly in the muscle belly, in sEMG the right place for electrode is much less clearer (Soderberg 1992). Luca advocates that the electrode should be placed approximately in the middle line of the belly of the muscle between the nearest innervations zone and the myotendonous junction (De Luca 1997). The Orientation of electrodes is defined as the line between the 2 bipolar electrodes. Surface ElectroMyoGraphy for the Non-Invasive Assessment of Muscles (SENIAN), European recommendations for sensor placement procedures and signal processing for sEMG, recommends the placement of the electrodes with the orientation parallel to the muscle fibers. The placement of the reference changes according to the muscle to study, always aiming at minimizing the common mode disturbance signal (bony prominence, larger size, good adhesive properties) (Merletti, Rau et al. 2010). Motion artifacts are avoided essentially with an appropriate electrode and cable fixation, although it is recommended not to directly tape over the electrodes, so as to keep a constant pressure of application (Konrad 2005). A correct placement of electrodes in sEMG requires a previous skin preparation. In order to improve the sEMG-recordings, reduce the number and intensity of artifacts, decrease the risk of electrodes imbalance and, lastly improve the S/N ratio. The skin preparation should consist in two procedures: 1) remove the hair (best electrode adhesion) and 2) Clean the skin surface with alcoholic/abrasive pastes (Konrad 2005; Merletti, Rau et al. 2010).

EMG signal processing can make use of several algorithms. To study the amplitude of EMG signal, the International Society of Electrophysiology and Kinesiology (ISEK) recommends (Merletti 1999):

Smoothing – using low-pass filters, typically digital non causal FIR linear phase filters.

Average Rectified Value (ARV) or Mean Amplitude Value (MAV) – represents the mean value of the rectified EMG over a time interval T; it is computed as the integral of the rectified EMG signal over the time interval T, divided by the value of T.

Root Mean Square (RMS) –the square root of the mean square value.

Integrated EMG (IEMG) – the signal is integrated over a time interval, representing the area under a voltage curve measured in $V.s^{-1}$.

For studying gait, the analysis of amplitude provides information on the patterns of muscular activation. However, studies in the frequency and temporal domain can also provide important results. For instance, the frequency domain permits the study of fatigue, while the time domain allows the study of events such as foot-step pace and cadence.

6.3.1. Superficial Electromyography Set Protocol (SESP)

For the acquisition of sEMG signals, the LBL is equipped with Myomonitor® III Wireless EMG System and Bagnoli™ EMG System, both provided by DELSYS®. The acquisition and treatment of results, uses the EMGworks® 3.7 software, also provided by DELSYS®.

This thesis has two main objectives – the study of non-pathologic and pathologic gait. Hence, the developed protocol should be both robust and quickly implemented so as to be used in the clinical context. Some works, as from Winter and Vaughan, present the muscular pattern activation for several muscles (Winter 1991; Vaughan, Davis et al. 1999). However the used protocol is very complex, making the assembly very slow. To circumvent this fact it was opted for the study of the principal muscular groups of the lower limbs with greater relevance in gait analysis (see chapter 3).

Table 3 shows the muscles considered in the protocol and the correct placement of electrodes. The location is based on the SENIAN recommendations and should be done in both limbs (Merletti, Rau et al. 2010).

Before the electrodes placement, a skin preparation procedure should be done as explained in section 6.3.

If the results are inconclusive for SESP an exhaustive analysis can be done, studying the several muscles of each muscular group; the correct placement of electrodes can be consulted in Winter or SENIAN (Winter 1991; Merletti, Rau et al. 2010).

Table 3 – Electrode placement of the SESP

Muscular Group	Muscle	Electrode placement (see Figure 37)
Triceps Surae Muscles	Gastrocnemius Lateralis	1/3 of the line between the head of the fibula and the heel
	Gastrocnemius Medialis	Most prominent bulge of the muscle
	Soleus	2/3 of the line between the medial condyles of the femur and the medial malleolus
Anterior Leg Muscles	Tibialis Anterior	1/3 on the line between the tip of fibula and the tip of the medial malleolus
Posterior Thigh Muscles	Biceps Femoris	Middle of the line between anterior spina iliaca and superior part of patella
Anterior Thigh Muscles	Rectus Femoris	Middle of the line between the ischial tuberosity and the lateral epicondyle of tibia
Gluteus	Gluteus Maximus	Middle of line between the sacral vertebrae and the greater trochanter. The orientation should be the direction of the line from the PSIS to the middle of the posterior aspect of the thigh.
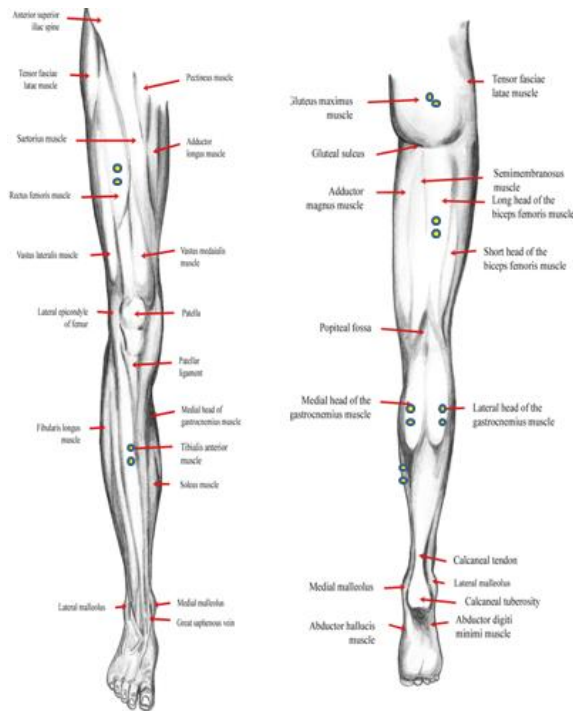
Figure 37 – Anatomical positions of the selected electrodes sites (Left – anterior view, Right – posterior view)

6.4. Non-Pathological Acquisition Protocol

6.4.1. Considerations

Since the main objectives of this work is the study of the patterns of normal gait for 3 distinct groups, the selected subjects (children, men and women) were all healthy, presenting no gait abnormalities neither a family record of gait disorders.

Each subject was asked to walk with his own natural cadence through a treadmill. One of the factors that may increase the number of rejected trials is the incorrect placement of feet in the force plate during the stance phase. As referred, each foot must be placed entirely on a force plate for a trial to be considered valid. Although most gait researchers do not inform subjects about the exact localization of the plates or ask them to not look to the ground, some studies were performed in order to understand if targeting the plates has significant influence on the results. Grabiner et al. performed several trials, asking the subjects to specifically target a force plate during the gait analysis or not informing their location. The authors concluded that targeting the force plates did not increase the variability of the GRF and as a consequence does not alter the variability of calculated joint kinetics (Grabiner, Feuerbach et al. 1995). Conversely, Paul considered this conclusion unjustified, since the study was focused solely on kinetic data, not considering the influence of targeting in the kinematic results; the author indicated that targeting the force platform results in lengthening or shortening of the stride length (Paul 1996). Wearing and al. reached the same conclusions. The researchers observed that subjects, when asked to not target the plate force, developed visual control strategies to correctly hit it. They also concluded that developing a specific protocol with an optimized start point for each subject, enabled his natural cadence, not affecting the GRF parameters (Wearing, Urry et al. 2000).

6.4.2. Acquisition Protocol

Each subject was asked to perform a set of ten trials without knowing the localization of the force plates and when subjects identify their localization, it was asked not to look to the ground. After each trial, the kinematic results were analyzed and the start point was optimized, as suggested by (Wearing, Urry et al. 2000). The start point corresponded to the exact position located three steps behind the point of hitting the first force plate with the left foot.

A test was considered valid when the subject walked along the entire treadmill with his natural cadence, hitting correctly the three platforms (left, right, left foot), performing three steps before the IC of the left foot with the first force plate and performing at least three steps after the TO of the third force plate. A minimum of 5-6 valid trials is suggested, since these allow a subsequent selection of the best data, excluding those that have seem valid but present failures at the time of analysis; if necessary, other set with a variable number of trials should be performed.

All the acquisition systems (IR cameras, video cameras, force plates and sEMG) should be triggered in synchrony, so as to avoid errors of data inconsistency caused by different start times. In the present work, the EMGWorks 3.7 software was responsible for triggering these systems.

6.5. Data Treatment Protocol

6.5.1. Data treatment using QTM

In order to perform a kinematic and kinetic analysis, it is necessary to previously process the acquired data. The treatment of kinematic data is performed primarily with QTM. Although this software can be used to perform kinematic analysis, in this work it is used only to acquire the markers and treat the trajectories. An AIM model of 33 markers was defined for a rapid assignment of the trajectories; the order of the markers is the same as in Table 2. These assignments require attention, especially when many markers are used or the distance between them is relatively small (EMSP case); some markers can be considered as the same or can be confused (if the software considers marker x as marker y and vice-versa, which can happen when two markers pass simultaneously in the same area) leading to an incorrect definition of trajectories (examples of usual trajectory errors – occur with the hip markers when the hand passes close to the hip, medial knee markers during middle swing and the three markers defining the hand, during all the trial) (QUALYSIS 2010).

Depending on the stride to be analyzed (right or left), one should consider at least 10 frames before the IC of the foot in analysis and at least 10 frames after the second IC of the same foot. This measure is essential to a correct data filtering in the Apollo software. The first event must be equal to all subjects in order to enable the posterior analyses with Apollo software and to be subsequently used in the database. The IC was chosen as the first event, in agreement with most of gait researchers.

The interpolation of gaps in trajectories is also performed by QTM; this software makes use of the NURBS interpolation (Non-Uniform Rational B-Splines), an algorithm used to define free-form curves and surfaces through more simplistic geometry (Terzopoulos and Qin 1994).

In case the analysis uses Visual3D software, data must be exported to a *.C3D file (a binary file format used in some biomechanics software). If the objective is a kinematic and kinetic analysis using

Apollo or the inclusion of a trial in the developed database, both kinematic and force data should be exported to a *.tsv file (tab-separated values) (Motion Lab Systems 2010; QUALYSIS 2010).

6.5.2. Preparing data to be used in Apollo

The Apollo software requires four input files: *.kin (file with kinematic information), *.frc (file with the GRFs and their applications points), *.sml and *.mdl (input files with information about the biomechanical model, acquisition frequencies, number of frames, filter design and file inputs). Apollo was developed to receive kinematic and force inputs from other motion acquisition software (Ariel Dynamics), which differs significantly from the outputs of QTM.

To prepare these four file inputs, a series of routines were developed in MATLAB. The file GaitAnalysis.fig allows the user to convert the *.tsv files from the QTM software to the required *.kin and *.frc formats. This file also permits the creation of simulation files (*.sml and *.mdl). (vide Appendix D - Figure 70 a)).

6.5.3. Read the kinematic, kinetic and electromyographic results

The interface GaitAnalysis.fig serves as a main menu where other routines can be called, such as ApolloAnalysis.fig, semgdatabase.fig and Analisedatabase.fig.

ApolloAnalysis.fig is a tool to analyze the kinematic and kinetic results provided by Apollo for each subject. It permits the visualization of kinematic plots and kinematic data of interest, as the position, consistent position, velocity, acceleration of each marker and the angular variations in joints of interest. It also displays the anthropometric data and the three components of GRFs, as well as their application points. Additionally, the kinetic results, as the moments of forces and their application points, the mechanical power and the positive/negative work can also be plotted and consulted in this routine.

As for the Analisedatabase.fig routine, it consists of a menu of the developed database, providing the same results as ApolloAnalyis.fig, although considering the results for a group of analysis (children, men, women and elderly). This routine also permits comparing the data of a particular subject with the data of his respective group. The plots and matrices presented are the mean values and standard deviation for all the Apollo outputs (*.BMI) contained in the folder of analysis. To correctly compare the results, the data of each subject is interpolated (with a cubic splines algorithm – MATLAB function) to a number of frames adopted for the entire group (the thesis used 200 frames). The mean value is calculated to all frames using the "mean" function and the standard deviation using the "std" function of MATLAB. To perform this statistic treatment MATLAB considers equations (54) and (55) (MathWorks 2010):

$$\overline{x} = \frac{1}{n}\sum_{i=1}^{n} x_i \qquad\qquad 54)$$

$$s = \left(\frac{1}{n-1}\sum_{i=1}^{n}(x_i - \overline{x})^2\right)^{\frac{1}{2}} \qquad\qquad 55)$$

where x_i is the value of the of the frame of interest of subject i (position, velocity, etc…), n is the number of elements in the sample (number of subjects), $\overline{x}$ is the arithmetic mean for the frame of

interest to all subjects in analysis and *s* is the sample standard deviation for the frame of interest to all subjects in analysis.
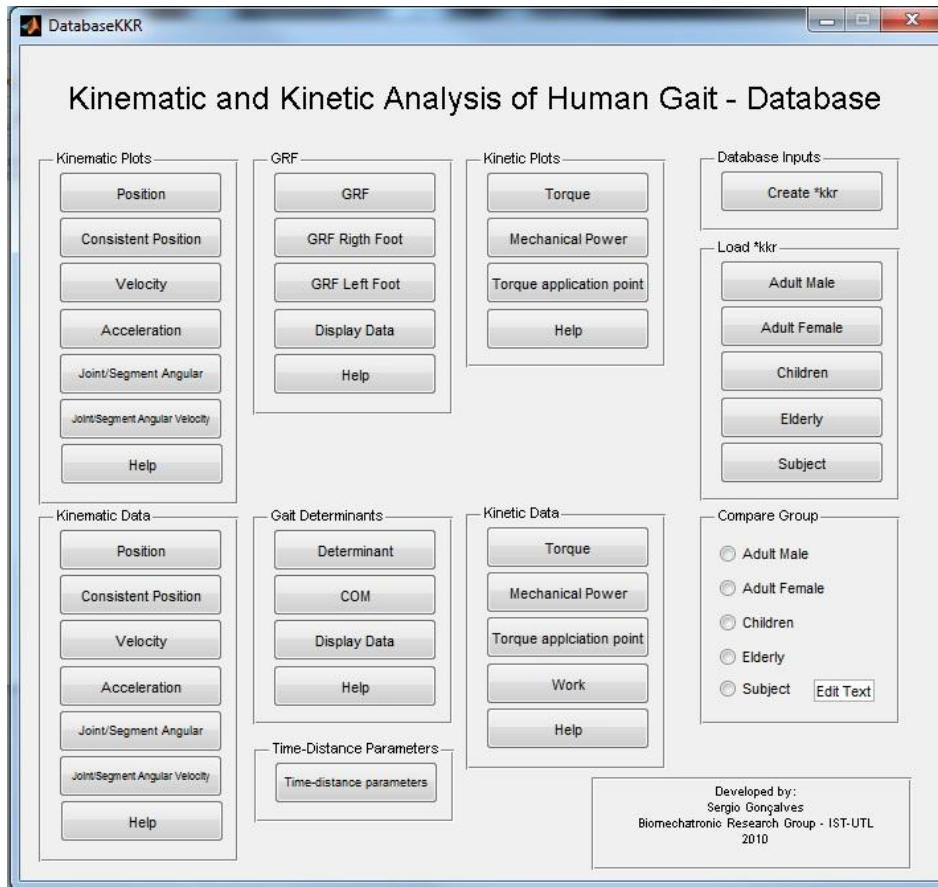
Figure 38 – Developed database for the analysis of the time-distance, kinematic and kinetic parameters

The semgdatabase.fig routine consists in a interface which allows the study of the sEMG patterns for each group considered in this thesis, as well as it allows to comparison of the obtained results for a given subject with his respective group of analysis. The underlying ideas to its development are the same as those presented for the Analisedatabase.fig routine, i.e. the mean and standard deviation values are calculated after the data being interpolated to a fixed number of samples.
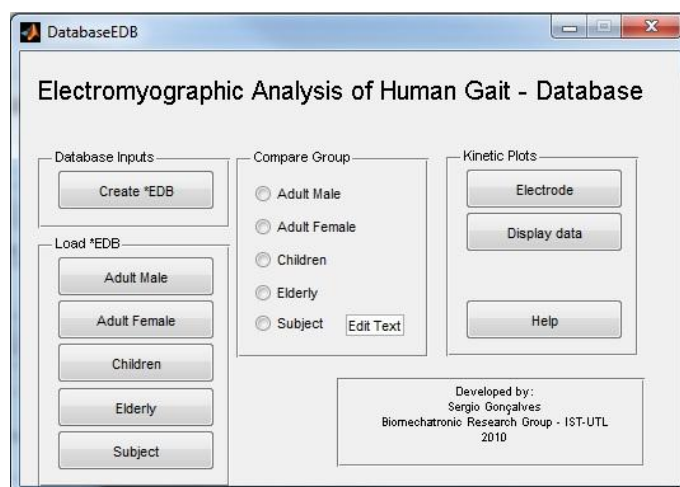
Figure 39 - Developed database for the analysis of sEMG patterns

Chapter VII

Results for non-pathological gait

7.1. Method

In the present study, ten men ($\bar{x}$=23.8±1.75 years old), nine women ($\bar{x}$=23.40±0.52 years old) and two children ($\bar{x}$=9.5±2.12 years old), with no history of gait disorders were selected. People were asked to walk across a treadmill without knowing the presence of the plate forces. The used marker set, sEMG and acquisition protocol are the MSP, SESP and NPAP respectively, presented in chapter VI. Concerning the spatial distribution of the cameras and forces plates, these parameters followed the configuration presented in previous chapter. It was used a sampling frequency of 100 Hz to the IR cameras and force plates. To the acquisition of sEMG was used the Myomonitor$^{®}$ III Wireless EMG System, with a sampling frequency of 1000 Hz and a gain of 4000. This system was placed inside of a belt pack in the abdomen anterior position.

The kinematic, kinetic and electromyographic results presented in this section were treated with the routines explained in 6.5.

In the next sections the obtained results for the three groups considered will be presented. In this thesis it was opted for presenting in each section the results for only one of the group, though the graphical representation for the remaining can be consulted in Appendix E. Since one of the main goals of this thesis is to develop a database with kinematic, kinetic and electromyographic data for normal Portuguese subjects, the obtained results will be compared with other studies to validate the protocol's applicability and the routines developed. The results of this study are also presented in Appendix E. The graphical representation of results is presented in function of % of GC (stride period). Zero percent corresponds to the heel strike (IC) of right foot and the 100% corresponds to the next heel strike of the same limb.

Another goal in this work is the applicability of these protocols and routines to clinical practice, in next sections it will be only discussed the results that can provide useful information, i.e. the parameters that allow to understand the principal deviations of normal pattern.

7.2. Kinematic Results

7.2.1. Time distance Parameters

In Table 4 the results obtained for the principal time parameters presented in section 3.5 are presented. Comparing the cadence results, children present the highest value, followed by women; whereas, men group presents the lowest value. These variations between groups are consistent with the values expected, i.e. the literature show that men tend to present slower cadences while children present higher cadences. However, these values are relatively smaller than those presented in section 3.5. These results are consistent with the idea presented by Öberg et al., that exists variations between trials performed in short and long treadmills (Öberg, Karsznia et al. 1993).

Another fact that may influence the time-distance parameters is the fixed spatial distribution of the force plates and the necessity of hitting it. The assembly used is designed to try covering all the three groups considered, as well as to enable its utilization with subjects with different gait disorders. During the analysis, it was observed that the necessity of hitting the force plates may have distorted these parameters; e.g. in first trials, men presented a stride length and velocity that did not allow hitting correctly the plates, because of that, it was asked to reduce their velocity slightly. This effect can be observed in the small difference between men's stride length and women's stride length, as well as in the difference between their cadences. Winter stated that in general, this difference varies between 6 and 11 steps/min (a difference of 18 steps/min was obtained) and Murray concluded that the difference between stride lengths for the two groups is approximately 0.26m (the stride length obtained for the two groups is practically equal) (Murray, Drought et al. 1964; Murray, Kory et al. 1970; Winter 1991).

During children analysis, it had to be asked to increase slightly their stride length to allow hitting correctly the force plates and as a result, this parameter presents higher values than those observed in literature (approximately 1m) (Sutherland 1997).

Despite being an important tool to analyze the human walking, the measurement of time-distance parameters should be performed without considering the necessity of hitting the force plates as those indicators have a purely kinematic nature

.

Table 4 – Time-distance parameters. Stride time, stride length, cadence and velocity were calculated taking the right IC as the reference point. The remaining parameters were calculated between the right IC and left IC

	Men		Women		Children	
	$\overline{x}$	s	$\overline{x}$	s	$\overline{x}$	s
Stride Time [s]	1.2850	0.1227	1.0829	0.1104	1.0500	0.0990
Stride Length [m]	1.2512	0.0614	1.2533	0.0589	1.1114	0.0140
Step Time [s]	0.7190	0.0799	0.6286	0.0398	0.6300	0.0566
Step Length [m]	0.6133	0.0222	0.6171	0.0372	0.5496	0.0140
Cadence [steps/min]	94.1882	9.4190	111.7962	11.2526	114.7959	10.8231
Velocity [m.s^{-1}]	0.9832	0.1202	1.1675	0.1278	1.0626	0.0868
Width [m]	0.0580	0.0400	0.0760	0.0202	0.0219	0.0509
Right Foot Angle [º]	9.4155	5.6260	-1.1048	0.0202	6.0226	1.4502
Left Foot Angle [º]	5.5130	5.2233	-3.5493	3.2047	3.3794	7.0867

7.2.2. Foot displacement and velocity

The developed routines allow analyzing the displacement, the velocity and the acceleration of each marker of the model presented in Figure 32. However, in this section, it will only be presented the results for the right foot markers (toe and heel). The study of these two markers is important to understand the mechanisms of foot, enabling the detection of several gait disorders. The graphical representation of these results can be consulted in Appendix E - Figure 71.

For these three parameters, both groups present a graphical pattern that is very similar with the ones found in literature (Winter 1991). However, especially in men, the magnitude of these values (graphical peaks) is more consistent with those obtained by Winter for slow cadence. In Table 5 the obtained results for men are presented and, as it can be seen, the values are inclusive smaller than those obtained for slow cadence. It is a fact that both time-distance parameters and these results are in concordance with the theory presented by Öberg et al. (vide 3.5), which states that the environment of study influences the normal cadence of a subject.

The vertical displacement of heel starts with HO. The maximum value is achieved during middle swing, when the knee is at its maximum extension. Both vertical and antero-posterior velocity may present a non-zero value during IC events (HC by assumption), which results from the position of the marker, placed few centimeters over the heel. During WA, while the foot is spinning over the calcaneus, the precise location of the marker has a slight movement that causes this apparent non-zero velocity (Winter 1991).

The pattern of vertical displacement of toe is characterized by a small peak (approximately 2cm) after the TO, which results from the angular configuration of leg and foot. The critical phase of toe clearance happens after the first peak, when the toe passes few centimeters over the ground with an antero-posterior velocity of approximately 3.278 m/s. The second peak (approximately 14 cm) occurs instants before new IC, when the knee extends and the foot dorsiflexes.

Table 5 – Results obtained for vertical displacement and antero-posterior and vertical velocity of foot markers (men)

	Vertical displacement (m)		Vertical Velocity (m/s)				Sagittal Velocity (m/s)	
	% GC	Maximum	% GC	Maximum	% GC	Minimum	% GC	Maximum
Heel	66.3%	0.2046	57.79	0.9567	77.39	-1.053	81.91	2.881
Toe	95.98%	0.1427	88.94	0.5577	2.513	-0.6069	76.88	3.278

7.2.3. Joint Angles

The analysis of joint angular displacement is probably one of the most used methods to detect and correct gait disorders. This study is essential to design personalized devices that compensate deviations from typical patterns. Thus, in this section the normal patterns of the joint angular displacements will be addressed and compared with the gait description performed in section 3.4. The obtained results were calculated using the formulation presented in 3.1.6. In order to calculate the body segment angles (thigh, leg, trunk, foot), the inner product approach was used. Considering θ_i the angle of the ith body segment, **o** a unit vector with relevance in the analysis and $\mathbf{p_i}$ the vector which defines the orientation of the body segment i, the segment angle can be calculated as (Hefferon 2006):

$$\theta_i = arccos\left(\frac{\mathbf{o} \cdot \mathbf{p}_i}{|\mathbf{o}||\mathbf{p}_i|}\right) \qquad 56)$$

where $\mathbf{o} \cdot \mathbf{p}_i$ is the dot product of vectors [$\mathbf{o}$, $\mathbf{p}_i$], and $|\mathbf{o}|$ and $|\mathbf{p}_i|$ are respectively the norm of the vector $\mathbf{o}$ and $\mathbf{p}_i$. Since the codomain of the function arcos is [0-π], the direction of the vector $\mathbf{o}$ is chosen to enable obtain values in this range, e.g. the thigh rotates approximately between 75⁰-120⁰, so the chosen vector was the (1,0,0).

Although most joints have some importance in the mechanisms of progression and balance, (e.g. the shoulder/elbow mechanisms have an important role in maintaining the body balance and minimizing the torque in joints – vide 3.4) it was opted for presenting only the obtained results that are the most relevant and the most discussed in literature – hip flexion/extension, knee flexion/extension and ankle dorsi-plantar flexion. However, the developed routines allow the calculation of many other joint angular displacements: a) sagittal plane – foot, leg, thigh, trunk, shoulder, elbow and neck b) horizontal plane – foot rotation and pelvic rotation c) coronal plane – hip abduction/adduction and pelvic tilt.

It is important to mention that several studies present results for these three parameters, obtaining for ankle and knee angle similar results. Whereas, the hip joint angle varies depending on the author, i.e. the curve patterns are similar but the values of maximum extension and flexion are relatively different. This fact is caused by the different definitions of the hip angle, e.g. some authors consider the maximum extension as 0⁰ and therefore the maximum flexion is approximately 40⁰, while other authors consider the vertical thigh in quiet standing to be zero position. The present study used this last definition – ($\theta_h = \theta_{th} - \theta_{tr}$). In the Table 6 is compared the results obtained in present study with previous works. Figure 40 shows the graphical representation obtained for men groups.

Table 6 – Comparison of joint angle (⁰) with previous works [(Sutherland, Olshen et al. 1980; Kadaba, Ramakrishnan et al. 1991; Winter 1991; Perry 1992)]

	Maximum	Present study (men)	Winter	Perry	Kadaba et al.	Sutherland et al
Ankle	Plantar flexion	-2.157	-19.77	~-20	~-13	~-20
Knee	Flexion – stance phase	13.21	21.67	~18	~17.5	~18
	Flexion – swing phase	59.44	64.86	~58	~60	~62
Hip	Extension	-9.83	-10.95	~-10	~-3	~-2
	Flexion	24.59	21.87	~32	~37.5	42

Analyzing the results, it is observed that Men, women and children groups showed similar results among them. Both hip and knee joints present an angular displacement similar with the values found in literature. The only exception is the hip angle for children; contrarily to the expected, this parameter presented no hip extension, since the joint angle varies between 3⁰ and 35⁰. Comparing the children thigh and trunk angle with other groups, a significant difference is observed in the second parameter. Both men and women presented small oscillations around 90⁰ (erect posture), while the children presented the same pattern of oscillations, but around 84ª-85⁰ (forward flexion of trunk) (vide Figure 72 – Appendix E). This difference may be related with the use of the wireless EMG system in an abdomen anterior position. This system has a considerable weight, which, especially in children, may affect the posture, causing a slightly anterior flexion of the trunk. Since, it is used the trunk angle in the

calculation of the hip angle, an error is introduced by this abnormal flexion causing the differences observed.

Also, the results obtained for ankle joint present a pattern slightly different in comparison with expected values. Particularly, during TO event, an angular magnitude of approximately -20⁰ (vide 3.4.5) was expected, which is considerably different from the value obtained (-3⁰). A possible explanation for this is the incorrect development of the marker set protocol. The EMSP considered two markers in an anterior position of the foot – II metatarsal heal and V metatarsal head. The first enables the study of foot angle (horizontal plane) and toes displacement, while the second is used to calculate the foot angle (sagittal plane). As referred in section 6.1, the EMSP presented several problems in data treatment caused by the few number of IR cameras used, and as result the protocol had to be adapted. It was chosen only the first marker for the calculation of the foot angle in sagittal and horizontal plan. In order to avoid this error in the future it is advisable to use an additional marker in the V metatarsal, and make use of this data to calculate the ankle joint angle.
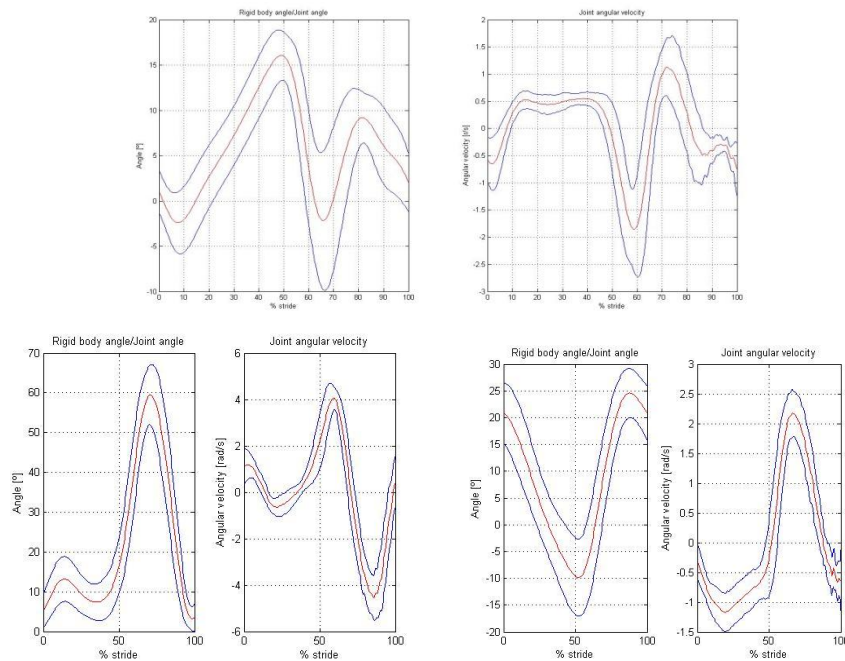
Figure 40 – Joint angles obtained for men group: a) ankle (on the top) b) knee (left) c) hip (right)

In the scope of the study of joint angles, it is also necessary to address the parameters related with angular velocities. This study is necessary to the calculation of the mechanical power (vide 7.3.3). This parameter is obtained as the derivative of angle with respect to time:

$$\omega = \frac{d\theta}{dt} \qquad\qquad 57)$$

where ω is the angular velocity and θ the joint angle. In appendix E, the hip, knee and ankle angular velocities (sagittal plane) are showed for the three analyzed groups. The obtained results presented the expected behavior; the only exception is the lower value of the ankle angular velocity during the PO. However, these results were expected, since their calculation was based on the derivative of a parameter with a systematic error (ankle angle).

7.3. Kinetic Results

7.3.1. Ground Reaction Forces and Center of Pressure

As mentioned in the section 3.6.2, for subjects with no pathologies the measurement of GRF and COP usually present a characteristic graphical representation. For each group the obtained standard deviations are relatively small, attesting the idea that the three components of the GRF present a well-defined curve in these cases. In both cases a stride period of approximately 63% of GC (37% swing period) was observed, which is in concordance with the results from literature. Once more, the men group presented a pattern of values more consistent with slow cadence results. As can be seen in Figure 41; the first peak of Fz has a value almost equal to the BW (approximately 1). Generally, this behaviour is observed in slow cadence studies. On the other hand, the children group presented values more consistent with the observed in fast cadence, the first peak of Fz present a normalized value of 1.305 (Winter 1991).

Recurring to equation (11), it is possible to study the evolution of COP during the stance phase. Significant differences were not observed between the three groups, presenting a pattern in concordance with literature (vide 3.6.2.1).

As mentioned, the study of these two parameters is extremely important, since most of gait disorders produce considerable deviations in these patterns, and understanding these variations is essential to develop prostheses/orthoses adaptable to each patient. The analysis of two subjects suffering from neuromuscular pathologies allowed the observation that sometimes their prostheses/orthoses originate foot sores, often caused by the poor design of the insoles used.
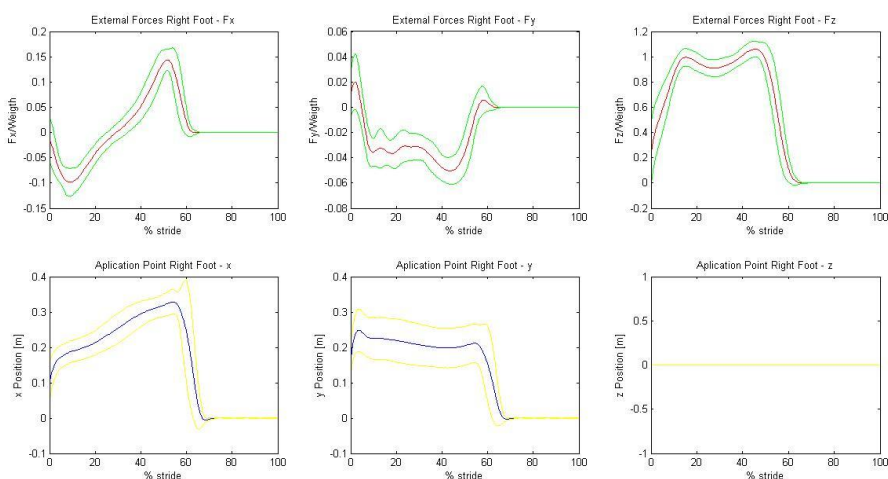
Figure 41 – GRF components and COP obtained for men group

7.3.2. Joint Moments of Forces

Moment of force, also denominated as torque, is an external solicitation that causes a body rotation about a specific point or axis. It is defined as the product of a force acting at a given distance and, as a result an angular acceleration over the point or axis of rotation is generated. It is possible to apply this concept to joints, where the applied force is the set of the internal forces that act in that joint. Thus, this parameter includes the moments caused by muscles and ligaments, joint friction and other structural constraints. The value of this parameter varies substantially with the joint angle and angular

velocity, caused by the subject intrinsic muscle characteristics – force-length and force-velocity (Winter 1991; Anderson, Madigan et al. 2007).

The formulation of inverse dynamic analysis, presented in chapter V, allows the calculation of the internal forces in kinematic pairs (Lagrange multipliers methods). Adding a driving actuator (constraint equation) for each DOF of the model, the simulation enables the calculation of the Lagrange multipliers associated to each joint torque (Silva 2003).

In Figure 74, the model used in Apollo software is represented. Although the routines presented in chapter VI allow the analysis of the torques for all forty four DOFs of the model, in this section only the torques with relevance in the human walking will be presented: the ankle, knee and hip, respectively M1, M4 and M7.

The data presented in this section are normalized by bodymass. The signs convention follows the Winter notation. Commonly, two different conventions are considered, the one used in this thesis considers as positive the extensor torques, due to the fact that they push away the members of the ground. Other usual notation, such as Perry's notation, considers the moment caused by the action of the GRF – physiological torque. Essentially, these two conventions vary in the signal values, presenting symmetrical graphics. Thus, in this thesis a hip extension and an ankle plantar flexion moment are represented as negative, while a knee extension moment is represented as positive (Winter 1991).

The ankle torque presents a characteristic graphical representation. At IC the GRF vector is located behind the ankle causing a physiologic plantar flexion torque, therefore the body counteracts generating a dorsiflexor torque to control this. Due to the rapid advancement of COP, and the localization of this vector on an ankle anterior position, a physiological dorsiflexion torque is generated (5% of GC), hence, the body responds producing a plantar flexion torque. With the continuous advancement of COP, the value of ankle torque magnitude decreases (more negative), having a maximum value in late terminal stance. Until TO, the ankle torque magnitude increases (less negative), being null in swing phase (Perry 1992).

Both knee and hip moments also present a characteristic pattern, although the variability is considerable higher comparing with the ankle torque. The knee torque pattern is characterized by 5 peaks (2 extension peaks and 3 flexion peaks). The two extensor torques are caused by the knee anterior location of the GRF vector – instants after IC (0-3% GC) and between MS and middle of TS (20-42% GC) (vide - Figure 6). On the other hand, the first two flexion peaks are a result of the knee posterior location of the GRF vector. – WA-MS (3-20% GC) and middle of TS till PO (42-60%). The third flexion peak occurs in the terminal swing (Winter 1991; Perry 1992).

The hip torque graphic is characterized by a first extension peak in the first instants of the GC. After this phase, the torque magnitude decreases and approximately at 30% of GC the hip torque reverses from extension to flexion. The hip torque magnitude continues to increase having a maximum torque value at the beginning of pre-swing phase. The torque magnitude decreases again, having a minimum torque (extension peak) in terminal swing (Winter 1991).

In Figure 42 the obtained results for the women group are presented. The graphic patterns for the three groups are in accordance with literature (Appendix E). The small differences in magnitude of

graphic peaks between groups (children – higher values, men – lower values) are consistent with the bibliographic results for different cadences. As expected, the hip and knee torques presented higher standard deviation values than those obtained for the ankle torque. However, these values are still relatively small and thus, indicate the proper application of the protocol.

Analyzing the men hip plot, some noise can be observed during late swing phase. This may have been originated by instabilities in the calculation of Jacobian matrix, caused by total extension of knee.
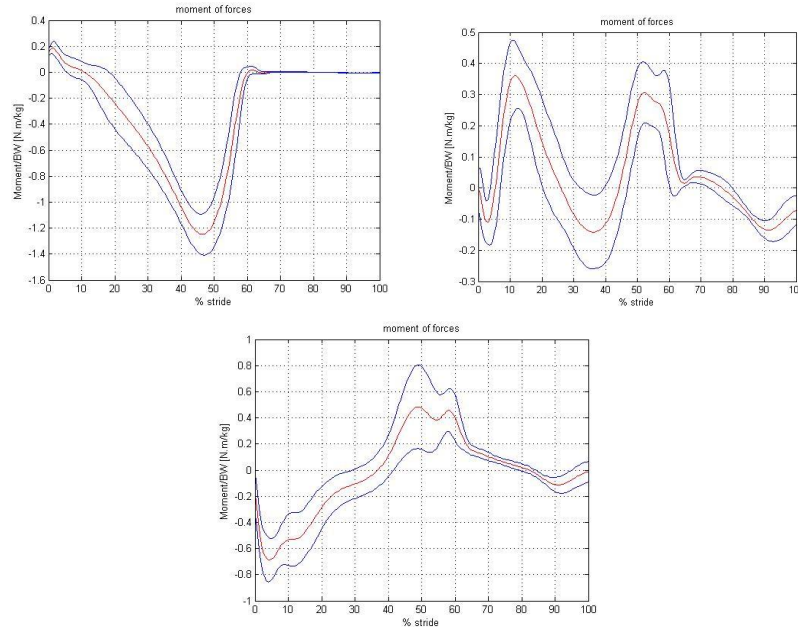
Figure 42- Moment of force obtained for women group a) right ankle moment (left) b) right knee ankle (right) c) right hip angle (down)

7.3.3. Mechanical Power and Work

The dynamic analysis is not complete without the study of the mechanical power. This measurement is sometimes used for the detection of gait disorders, such as cerebral palsy. Mechanical power is defined as the work performed per unit time and it is calculated as:

$$P_j = M_j . \omega_j \qquad \text{58)}$$

where M_j is the flexion-extension moment and ω_j the joint angular velocity of joint j. P_j is the mechanical power, it is defined as positive when a concentric contraction is performed and as negative for eccentric contractions. Equation (58) is applicable assuming that the torque generator in joint j is independent of the events in other joints. This assumption is not always valid, like in the case of biarticulated muscles that can perform isometric contractions, transferring energy between segments (Winter 1991; Chen, Kuo et al. 1997).

From the calculation of the mechanical power is possible to estimate the positive and negative work done in a given joint. Considering a gait cycle, the positive (W^+) and negative work (W^-) is calculated as (Gutierrez, Bartonek et al. 2005):

$$W^+ = \int_{t_i}^{t_f} P_j \ dt \ \text{ for } P \geq 0 \qquad \text{59)}$$

$$W^- = \int_{t_i}^{t_f} P_j \ dt \ \text{ for } P < 0 \qquad \text{60)}$$

where the t_i and t_f are respectively the initial and final gait cycle times.

The graphical pattern of mechanical power presents several characteristics that are common to all groups. Figure 43 shows the obtained normalized results for the women group (the magnitude of the mechanical power are divided by subjects' body mass). The small differences of power magnitude between men, women and children are related with the different cadences observed in these groups. Once more, the pattern of ankle power presented significant differences in the magnitude of values during the PO. This is expected since the angular velocity, for this period, showed a lower value than the ones of literature. (vide - 7.2.3).
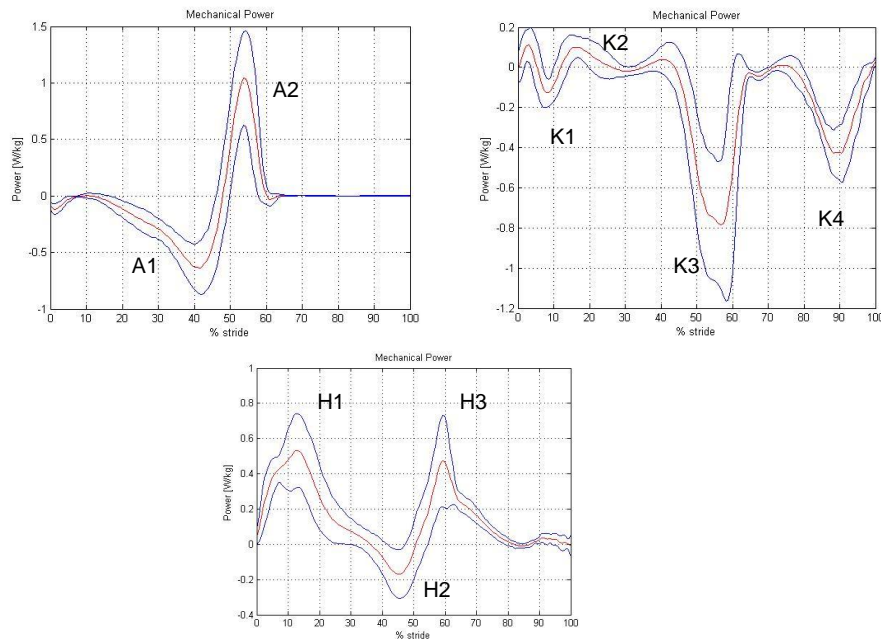
Figure 43 – Mechanical power obtained for women group a) right ankle (left) b) right knee (right) c) right hip (down)

The analysis of the mechanical power provides an idea of the energy expenditure during the gait cycle. The ankle graphic presents two important phases. The first (A1) occurs between 5-40% of GC and corresponds to a phase of power absorption (negative work), when the ankle dorsiflexes under control of an increasing plantar flexion torque. The second phase (A2) is characterized by an abrupt power generation (positive work) during PO. Almost 80-85% of the generated energy in a GC is expended in this action. A third phase can also be considered that corresponds to the dorsiflexion of the foot after PO (until MSw), though the magnitude of this values is extremely small (low mass ballistic movement) (Winter 1983; Winter 1991).

The knee power plot presents four relevant phases: 1) Negative work (K1) – K1 occurs during WA phase while the knee flexes controlled by the action of quadriceps. 2) Positive work (K2) – K2 occurs between 15-40% of GC, while the knee extends by the action of quadriceps. Almost 10-15% of the generated energy in a GC is expended to perform this action. 3) Negative work (K3) – K3 begins with PO and continues until 70% of GC. it is characterized by the flexion of the knee controlled by the action of quadriceps. During this phase, there is no positive work, since the energy used for swing the leg comes from the pendulum action. 4) Negative work (K4) – K4 begins approximately in the MSw

phase, when the knee begins to extend controlled by the action of the hamstrings (for leg control and deceleration) (Winter 1983; Winter 1991).

In general terms, the hip power graph present higher variability than those of the knee and ankle. However, three power phases can be distinguished: 1) Positive work (H1) – H1 begins with the IC of ipsilateral foot and continues approximately till 20% of GC, when the hip starts extending controlled by the action of the hip extensors. 2) Negative work (H2) – begins after H1, when the hip continues extending (backward rotation of the thigh) controlled by the action of the hip flexors. This muscular action helps to control and decelerate this rotation. 3) Positive work (H3) – H3 begins few instants before the TO, the action of hip flexors helps to accelerate the leg to perform the swing phase (Winter 1983; Winter 1991).

In order to solve the equations (59) and (60), a routine was developed which calculate automatically this value. The integral was computed using the trapezoidal method defined in MATLAB (MathWorks 2010). Table 7 shows the positive and negative work for all groups. The adult male group presented the lowest value, which are in concordance with the fact that these tended to present a slow cadence. In the same way, the children group presented the highest value. However, the obtained results for the ankle work are affected by the reported differences in the calculation of the mechanical power for this joint.

Table 7 – Positive and negative work for men, women and children groups

	Men			Women			Children		
	W^+ [J/kg]	W^- [J/kg]	W^+-W^- [J/kg]	W^+ [J/kg]	W^- [J/kg]	W^+-W^- [J/kg]	W^+ [J/kg]	W^- [J/kg]	W^+-W^- [J/kg]
Ankle	0.0980	-0.1934	-0.0954	0.1282	-0.1983	-0.0701	0.1019	-0.1898	-0.0879
Knee	0.0173	-0.1776	-0.1777	0.0258	-0.2684	-0.2426	0.0585	-0.2794	-0.2209
Hip	0.1872	-0.0174	0.1692	0.2813	-0.0252	0.2561	0.3461	-0.0021	0.3461
Total	0.3025	-0.3884		0.4353	-0.4919		0.5065	-0.4716	

7.4. Gait Determinants

In section 3.8 three theories were presented to explain the mechanisms of human walking – inverted pendulum, gait determinants and dynamic walking. In this section the results obtained for the three groups of analysis will be compared with the six ideas proposed by (Saunders, Inman et al. 1953).

7.4.1. COM

Figure 44 represents the horizontal and vertical displacement of COM for the men group, assuming that it is located in the middle position of the two hip markers. The graphical representation is consistent with the pattern presented by Saunders et al. The total amount of vertical and horizontal displacements (Table 8) is also in concordance with the values presented by the same author. It is important to mention that the graphical representation of the COM horizontal displacement can be subject to a small error, like verified in children, caused by the fact that sometimes subjects do not walk parallel to the direction of progression axis and, hence, the horizontal position of COM is not equal in the first and last instant of analysis.
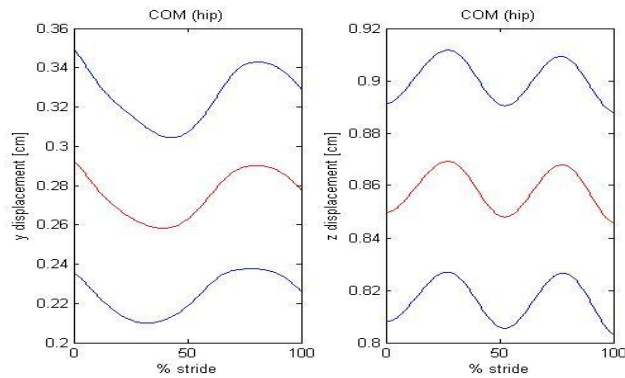
Figure 44- horizontal and vertical displacements of the COM during a GC.

Table 8 – Total amount of vertical and horizontal displacements of the COM, assuming that the COM located in the middle position of the two hip markers

	Vertical displacement [cm]	Horizontal displacement [cm]
Men	2.13	3.2
Women	1.76	3.22
Children	2.55	1.81

7.4.2. Six gait determinants

The 1st and 2nd determinant cannot be computed using the outputs files of the Apollo software, since its biomechanical model does not consider markers in the anatomical positions that are used in the calculation of these parameters (RIC and LIC). For simplicity of the data treatment, it would be important to consider a new model in Apollo, which receives these markers in its input files, and yields in their output files.

However, an approximation was performed and using the hip markers to calculate the lateral pelvic tilt (2nd determinant) is possible observe the expected pattern (Figure 45 a)), i.e. a positive tredelenburg during the first 50% of the GC, and a negative tredelenburg during the last 50% of the GC.
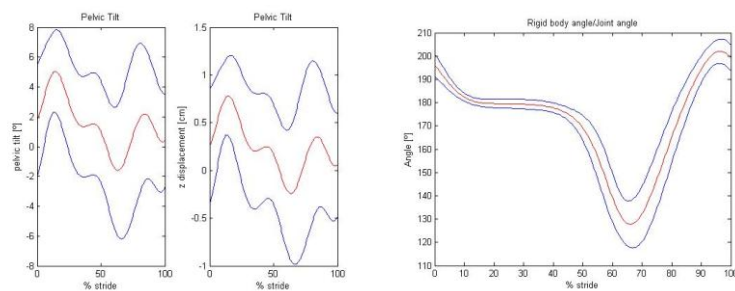
Figure 45 – a) Lateral pelvic tilt for men group. b) Foot angle for men group.

Using the RIC and LIC markers to calculate the lateral rotation (1st determinant), the pelvic rotation presented the expected pattern (Figure 17).

The 3rd determinant considers the existence of a knee flexion of approximately 20º, during early support phase. Such fact allows both the absorption of impact energy and reducing the reduction of COM's vertical displacement. Analyzing the knee angle graphics (Figure 40) and data presented in Table 9, the pattern presented by Saunders et al. is observed. The highest value observed in the

children group is consistent with the faster cadence observed in this group, as well as the lowest value in men group.

Table 9 – maximum knee flexion during early stance phase.

	Knee Flexion [º]	stride period [%]
Men	13.21º	14.07
Women	16.21	12.06
Children	26.86	14.02

Considering the graphical representation of the foot angle (sagittal) (vide Figure 45 b)), the two arcs that define the 4th and 5th determinants identify can be identified. The first arc begins with IC event and continues until the foot is flatted (~10% GC). A decrease in the foot angle from 195º to 180º can be observed, resulting from the foot rotation over the heel. During this phase, the idea of a restrained plantar flexion is also observed through the analysis of the ankle torque graphic (Figure 42) and sEMG pattern of the tibialis anterior (Figure 79). A dorsiflexor torque is generated to control the plantar flexion caused by the location of the GRF vector in an ankle posterior position (vide 7.3.2).

The second arc begins with the HO event, when a decrease in the foot angle from 180º to 128º is clearly observed, corresponding to the rising of the heel. The idea of a powered plantar flexion can also be visualized in the ankle torque graphic and in the sEMG pattern of the triceps surae muscles. Both graphs present a distinct peak in this phase (vide Figure 43a) and Figure 76-78).

In order to minimize the horizontal displacement of COM, Saunders considers the existence of a hip adduction angle during the stance phase (the knees are medial to the hips) – the 6th determinant. Analyzing the results obtained for all groups (Table 10), this behavior is observed. The highest value of hip adduction angle observed in women is natural, anatomically, the female pelvis is wider (vide 2.1.3).

Table 10 – Maximum hip adduction angle during stance phase (right limb)

	Hip adduction angle [º]	stride period [%]
Men	3.88	33.17
Women	7.627	15.58
Children	6.098	20.1

7.5. Marker set protocol and Acquisition Protocol – considerations

All the kinematic and kinetic results, with the exception of the ankle angle, were consistent with the literature. The designed clothes helped to decrease substantially the time spent on markers placement. The clothes conferred stability to the markers, since the Velcro attachment caused the markers to drop fewer times than when scotch tape was used in skin.

The cameras arrangement, presented in section 6.2, allowed to acquire with success all the markers from lower limbs, even though some problems were detected in acquisition of metacarpal markers. As mentioned, it was preferred to guarantee a good acquisition of medial markers from lower limbs because they allow the calculation of the articular centers with more precision.

In general terms, the developed marker set protocol is robust and allows a fast assembly. For these reasons it is considered that it can be easily applied in clinical practice, considering two

changes. The first one is the use of another marker in V metatarsal, allowing the correct calculation of the ankle angle. The second one is to develop a new protocol, which enables the study of the time-distance parameters without considering the necessity of hitting the force plates. As mentioned, men results showed slow cadence, while children present faster cadence results. Although subjects are asked to walk with natural cadences, in some cases their stride has been adapted to properly hit the force plates.

7.6. sEMG patterns

The protocol used to obtain the sEMG pattern is presented in section 6.3.1. Although the electrode placement was optimized to avoid the cross-talk artifacts, this effect can be observed in some subjects (especially in women and children). In some cases during placement of the soleus electrode, an activation signal from the muscles responsible for the foot dorsiflexion was observed. The measurement of Tibialis anterior may also contain this artifact caused by the activation of Triceps surae muscle, however, it is observed that if the electrode is placed in a location where the muscle is anterior to the tibia, this effect is reduced. One last note to retain is the fact that, in some subjects, significant variations in Gluteus maximus signal were not observed, most likely caused by the amount of adipose tissue in this body region.

The results processed with MAV and normalized using peak value normalization (the maximum value is considered as 100% and the lowest as 0%) can be consulted in appendix E (Figure 76-82). Generally, these results are in accordance with the muscular pattern described in section 3.4. However, small differences can be observed in the Soleus. The soleus graphic presents three distinct peaks (0-10%, 20-60% and 90-100% of GC), though the expected results predict only one peak between 20% and 60% of GC. The first and third peaks correspond to artifacts introduced by muscle cross-talking. Although it was tried to avoid such artifact by choosing carefully the location for placing the electrode, such effort was not sufficient in some subjects, resulting in these artifacts.

As expected, the inter-subject variance is considerable (vide 6.3), especially in the Gluteus maximus, rectus femoris and biceps femoris, where more adipose tissue exists. Although at first sight there do not seem to be great variations, a careful analysis allows to a clearly identification of the expected pattern of these muscles.

The SESP achieved the desired objective, since it allowed the analysis of the patterns of activation of the principal lower limb muscular groups. However, this protocol presented a problem, which was the time that took to place all the electrodes. For this reason and if the objective is the clinical application, this protocol should be adapted to each pathological case.

Chapter VIII

Results for Pathological Gait

In this chapter the results obtained results for two subjects with different motor disabilities will be presented and analyzed. Firstly, intra-subject variability with and without prosthesis and orthosis will be studied. In a second section, pathological results will be compared with normal pattern results. The results presented were obtained using the protocol explained in section 6.4.2. Configuration parameters such as the cameras and force plates sampling frequency were the same as those of section 7.1. In this chapter, the option was put in presenting only the results that express significant differences.

A male subject (13 years old) with Spina Bifida will be analyzed in section 8.1, and in section 8.2 a female subject (14 years old) with muscular weakness of lower limbs (leg) will be studied.

8.1. Subject 1 – Spina bifida

8.1.1. Remarks on subject preparation

It is important to mention two points regarding the preparation of this subject. The first aspect is related to the placement of foot markers; in trials where the AFO was not used, foot markers were placed in the anatomical positions explained in section 6.1.2, and the subject walked through the treadmill with socks on. However, in trials where the AFO was used, the subject had to wear tennis shoes to avoid slipping, and so the toe and heel markers were placed directly on these shoes. As the toe markers were placed a few millimeters over the toe, the heel markers had to be placed approximately at the same height, so that the foot angle (sagittal plane) would be null when the foot was flat. This aspect caused a small increase in toe and heel vertical displacement in the trials where the AFO was used (vide 8.1.4.1). On the other hand, the ankle markers were placed on the metallic structure medially/laterally to the malleolus (see Figure 46 a)).

The second note is related to placement of electrodes. As referred in section 7.6 their placement is optimized to obtain the best signal possible with minimum cross-talking artifacts. During electrode placement of subject 1, an incapability of the subject to perform an ankle dorsiflexion was observed, as well as only small variations were observed in sEMG signal of tibialis anterior. The triceps surae muscles presented very small variations the subject was asked to perform a plantar flexion motion. Both tibialis anterior and triceps surae muscles presented clear evidence of muscular atrophy, which contrasted with the thigh muscles that demonstrated good muscle strength. While standing up static, the subject was observed to tend to flex his knees controlled by the action of knee extensors. A tendency to present a slight forward flexion of the trunk when the subject was standing up or walking through the treadmill was observed (vide Figure 46 a)-c)).

Figure 46 – Subject 1: a) Static position, b) Initial swing of right limb without AFO, c) IC of left foot without AFO, d) IC of right limb with AFO.

8.1.2. Visual Observation

The study will consider a first part comprising the analysis of results obtained without an ankle foot orthosis (AFO) and posteriorly of results obtained with a hinged AFO (free ankle dorsiflexion, free or restricted plantar flexion and medial lateral stabilization of subtalar joint) (ICRC 2006). It is important to mention that in visual terms the trials for the two cases presented significant differences. When the subject walked on the treadmill, he presented difficulties in maintaining body balance, using his arms and balancing the trunk (coronal plane) to try to maintain the stability (vide Figure 46 b) and c)). The subject also tended to walk with spread legs, as well as to present a higher foot angle (horizontal plane) than observed for normal subjects. Both external observation and the patient's experience suggested an increase in stability with the use of the AFO.

Table 11 - Time-distance parameters. Stride time, stride length, cadence and velocity were calculated taking the right IC as the reference point. The remaining parameters were calculated between the right IC and left IC

	Men		Children		With no AFO		With AFO	
	$\bar{x}$	s	$\bar{x}$	s	$\bar{x}$	s	$\bar{x}$	s
Stride Time [s]	1.2850	0.1227	1.0500	0.0990	1.1340	0.09456	1.260	0.0887
Stride Length [m]	1.2512	0.0614	1.1114	0.0140	1.1312	0.0979	1.1909	0.0748
Step Time [s]	0.7190	0.0799	0.6300	0.0566	0.6460	0.0270	0.6340	0.0680
Step Length [m]	0.6133	0.0222	0.5496	0.0140	0.6262	0.0415	0.5486	0.0998
Cadence [steps/min]	94.1882	9.4190	114.7959	10.8231	105.9548	4.1864	95.4442	6.3214
Velocity [m.s^{-1}]	0.9832	0.1202	1.0626	0.0868	0.9984	0.0914	0.9454	0.0586
Width [m]	0.0580	0.0400	0.0219	0.0509	0.1436	0.0519	0.1571	0.0408
Right Foot Angle [º]	9.4155	5.6260	6.0226	1.4502	20.4926	8.0665	11.5078	4.0759
Left Foot Angle [º]	5.5130	5.2233	3.3794	7.0867	36.8766	5.2067	20.9708	3.2361

Table 11 shows the results obtained for the subject under study and for children and men with normal patterns. The differences between these and normal pattern results for width and foot angle parameters are evident, as are the differences between trials with and without AFO for these parameters. As mentioned in section 7.2.1, the values of time-distance parameters were affected by

the error introduced by the need of hitting the force plates. However, it is easily observed that the utilization of AFO helps to decrease foot angle values significantly.

8.1.3. Intra-subject Variability

The study of intra-subject variability allows for the understanding of the behavior and repeatability of patterns in a given subject. These results were obtained using the same principles as those behind the development of the database, which was used to study the gait patterns of normal subjects. The results were calculated using the mean of five valid trials (6.4.2). In appendix F the graphical representation of the main gait analysis parameters for subject 1 can be consulted. All of these graphs presented the same behavior, i.e. the obtained results for the trials where the AFO was not used showed higher standard deviation values than those obtained using the AFO. These results are consistent with what was observed during the trials, the use of AFO conferred stability and helped to control body balance.

Especially in the trials where the AFO was not used, toe and heel displacement graphs, as well as joint angular displacement graphs showed a higher variability during the swing phase. These results were as expected given the subject's tendency to perform an abrupt leg swing with excessive hip muscular tension, instead of the regular pendular behavior of the leg in normal subjects. This effect can be also observed in the major variability of hip moment during stance phase.

8.1.4. Comparison between Subject 1 patterns and non-pathological patterns

8.1.4.1. Foot displacement and velocity

Comparing subject results for these parameters with those of normal patterns important differences are observed. The patient presented a lower value of toe vertical displacement during late swing, especially when the AFO was not used. This fact is related to the incapacity of the subject to perform foot dorsiflexion – drop foot; this same idea can be obtained observing the ankle angle graph (Figure 48). The analysis of medial-lateral foot displacement corroborates the idea presented regarding the tendency of the subject to walk with spread legs. It is important to mention that the use of AFO helped to stabilize the foot, since it allowed the toe clearance during swing phase. However, the use of this orthosis did not yield improvements in the tendency of walking with spread legs, although the importance of its utilization in the control of foot angle (horizontal plane) is notorious – the values of toe medial-lateral displacement are closer to the normal pattern data, confirming the already presented idea that the use of AFO helps to stabilize this parameter.

The analysis of these parameters also enables understanding important differences in the contact of the foot with the ground. Instead of being made with the heel, the contact appears to be made with the flat foot. During WA, for the trials where subject 1 did not use the AFO, toe vertical velocity does not present the typical decrease resulting from the controlled plantar flexion that occurs in this phase. Heel vertical velocity also tends to decrease in absolute value, being approximately null at 7% of GC. This fact shows that the heel was still in the air when foot contact with the ground happened. This analysis allows for the conclusion that the IC for subject 1 was made with the forefoot; this fact is expected since the subject presents symptoms of drop foot. On the other hand the trials where the

AFO was used presented significant improvements, with the foot hitting the ground with the heel and the parameters for this event being similar to the results obtained for normal male patterns.
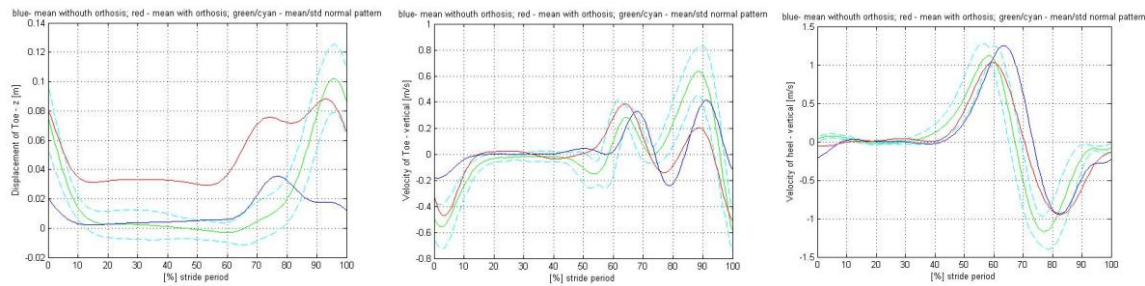

Figure 47 – Representation of displacement and velocity for Subject 1 without orthosis (blue), and with orthosis (red), and for a normal pattern (green/cyan): a) Vertical displacement of Toe; b) Vertical velocity of Toe c) Vertical velocity of Heel

8.1.4.2. Joints Angles

From a clinical point of view, the study of the joint angle during a gait cycle is important, since this enables extracting essential information about the effect of the disease in locomotion. After processing, this information allows helping the prosthesis/orthosis designers to develop biomedical correctives adapted to each patient. The joint angle patterns were compared with the normal patterns presented in section 7.2.3. Some differences were found between the plot obtained for the ankle and literature, caused by the use of the marker in the II toe instead of the V metatarsal. However, to enable the comparison of subject's ankle angle with the normal patterns, the used apparatus was the same, so that the error introduced by this marker placement is approximately equal in both cases, allowing the direct comparison of the graphic curves.

In the first instants of the ankle plot where the AFO was not used important differences are observed. At IC the foot does not present the slight dorsiflexion angle characteristic, of the foot-ground contact with the heel.

No dorsiflexion angle is observed, and this angle usually generated to avoid the contact of the foot with the ground during the swing phase. This difference is related to the inability of the subject to perform the dorsiflexion, i.e. unless the foot is on the floor, it drops.

The knee angle presented an abnormal pattern during the stride phase. The graphical representation of this parameter shows a first peak of approximately 35º with AFO and 30º without it, which remains approximately constant until the TO. This higher value is related to the necessity of the patient to flex the knees to help maintaining the balance, as mentioned in 8.1.1.

In section 7.2.3 it was mentioned a difference in the children hip angle pattern caused by the forward flexion of the trunk, and the same effect was also visible for subject 1. Figure 48 shows the variation of the trunk angle for patient 1 during the stride period, and it is easily observed that, while this parameter for adult male and children varies respectively between ~88º - ~92º and ~83º - ~87º, this parameter for subject 1 presents a larger amplitude of variation (~73º - ~87º) The thigh pattern is relatively similar between children and patient 1, so that the plateau observed in the subject hip angle plot during the first 40% of the gait cycle is related with the higher value of trunk forward flexion during this phase.

The analysis of these three parameters shows that the use of AFO only helped improving the ankle angle pattern. Nevertheless, it is important to retain that the AFO only avoids the foot drop, it does not lead to a dorsiflexion of the foot.
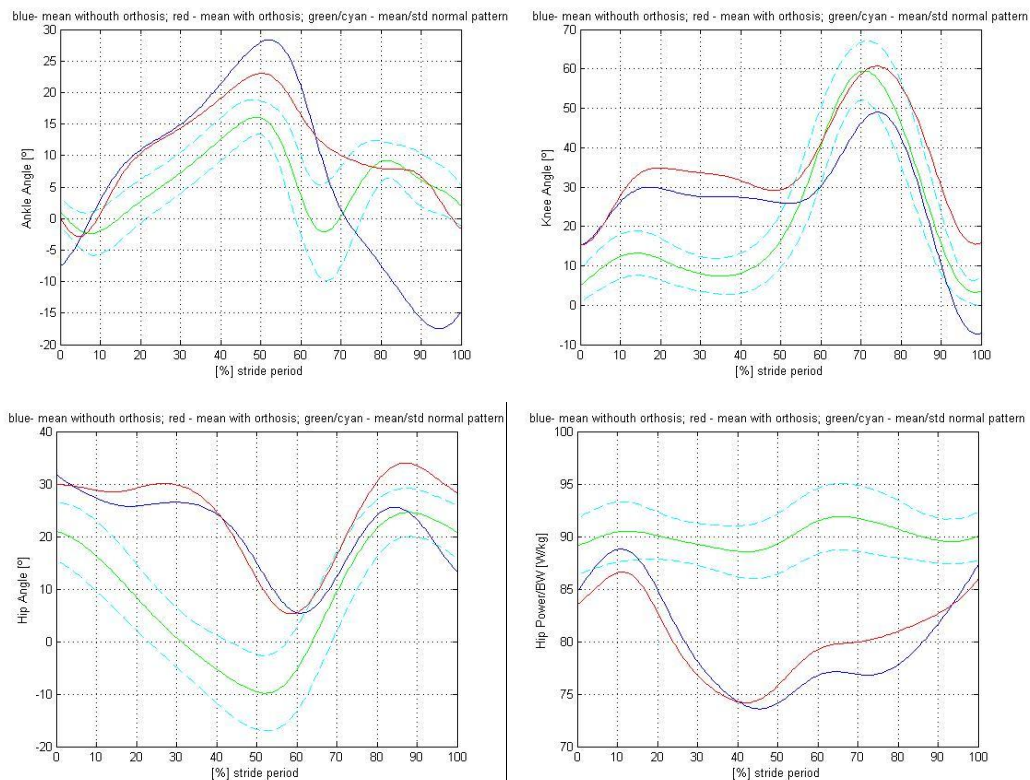

Figure 48 – Representation of joint angles for subject 1 without orthosis (blue), and with orthosis (red), and for a normal pattern (green/cyan): a) ankle; b) knee; c) hip d) trunk

8.1.4.3. *Ground Reaction forces and Center of Pressure*

As mentioned previously, subject 1 presented a tendency to perform an abrupt leg swing. As result, important differences are observed in the three components of GRF, especially in the range between 0% and 20% of GC. This lack of leg control in the swing phase results in an abrupt impact with the ground, leading to higher magnitude values of reaction forces (vide Figure 49 a) b) c)).

The study of COP is important to understand how the forces are acting in the subject's feet. In trials where the AFO was not used it is easily observed that the COP advances by the medial arch of the foot, which contrasts with the pattern for non-pathological gait. Considering that the extremities of colored line segments of Figure 49 d) represent the heel and toe markers, it is evident that the COP begins in an anterior position when comparing with the normal pattern. The distance between the extremity of the line segment that represents the heel and the beginning of COP is clearly higher in the trials in which the AFO was not used. This is caused by the differences observed in the contact of foot with the ground during IC event.

Although the AFO does not appear to improve these parameters (though its use decreased the magnitude of antero-posterior component of GRF, it increased the value of medial-lateral component of GRF), this fact is not true, since clear improvements are observed for the distribution of COP in the foot. The COP is clearly shifted to a lateral position and its action starts in a foot posterior position (heel).

It is important to highlight the idea presented by Perry and mentioned in section 3.6.2.1, which indicates that sometimes the analysis of vertical forces provides unreliable results, since the influence of the pathology in this parameter can be smaller than the decrease in speed inherent to the pathology or pain (Perry 1992). Due to this fact, it is advised to perform a small set of questions in which it is asked if the subject feels pain, where he feels it and if he usually changes his walking style to avoid this sensation. Subject 1 complained that sometimes the AFO induces him pain in the feet, probably caused by imperfections in the development of this device.
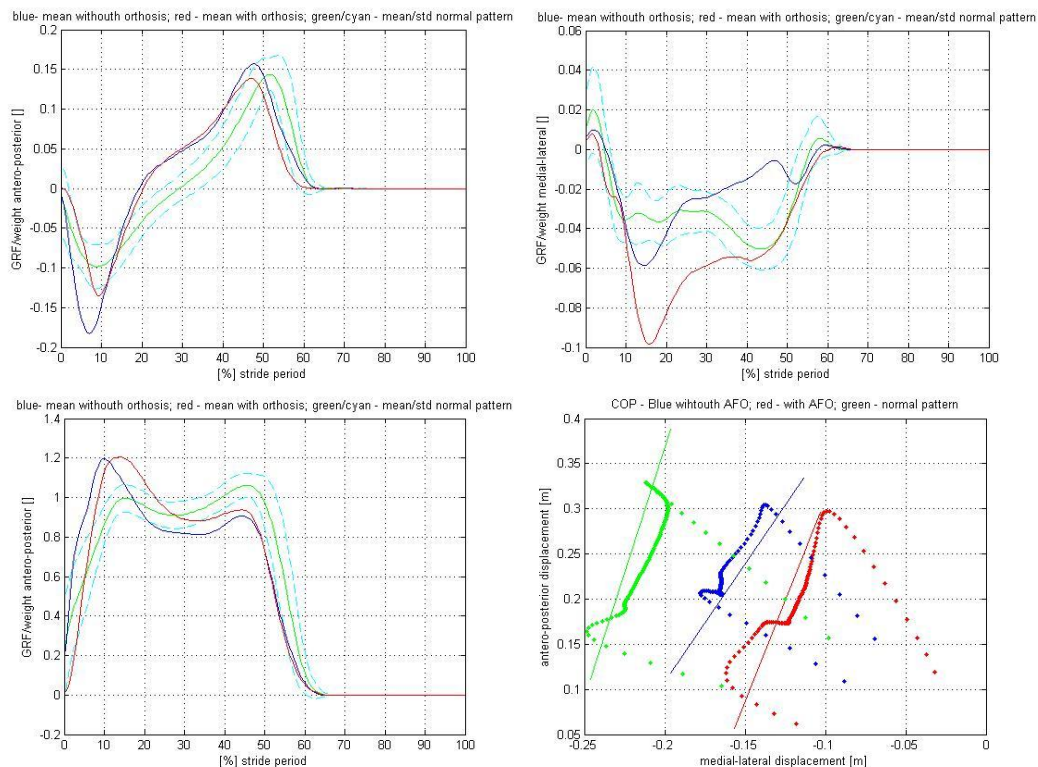

Figure 49 – Ground Reaction forces and COP for subject 1 without orthosis (blue), and with orthosis (red) and for a normal pattern (green/cyan): a) Antero-posterior; b) medial-lateral; c) vertical d) COP – the color line segments represent the foot angle in horizontal place (end points – heel marker and toe marker)

8.1.4.4. *Joint Moments of Forces and Mechanical Power*

The analysis of these parameters for subject 1 allows understanding that his gait presents important differences from the normality, which results in patterns of expenditure energy quite different from those obtained in non-pathological gait. The obtained results are consistent with the literature; the weakness in dorsiflexors and plantar flexors tends to be compensated by the loading alteration in the other joints, especially the knee and hip. The torque and power pattern for the trials where the AFO is used are similar, since it does not alter the weakness of muscles, only conferring some stability to the ankle joint and foot (Gutierrez, Bartonek et al. 2005).

The obtained results are consistent with the evidences observed during the subject preparation. The dorsiflexors paresis and the plantar flexors weakness result in lower torque values and less power generated in the ankle joint. These evidences are easily observed in the lower peak of these parameters during PO. The ankle torque results in the AFO absence do not present a small dorsiflexion torque for the first instants of WA, because as the foot hits the ground with its anterior part, the GRF vector is not applied in a posterior ankle position, as it happens when the contact with

the ground is done with the heel. Since the AFO avoids the drop foot during the swing phase, the foot hits the ground with the heel and therefore a small dorsiflexion toque is observed at the beginning of WA.

It is important to note that 80-85% of the energy generated in a gait cycle is expended in the ankle during the PO, thus if the ankle movement presents abnormalities, as it happens for patient 1, this energy is compensated by the other joints. The plots of hip and knee mechanical power show this idea, and the results for both trials where the AFO was used or not, present in general higher peaks than those obtained for healthy gait. Other important observation is the fact that although the use of AFO increased the positive work generated in the knee, it also helped to decrease the positive work performed in the hip and consequently the total positive work.
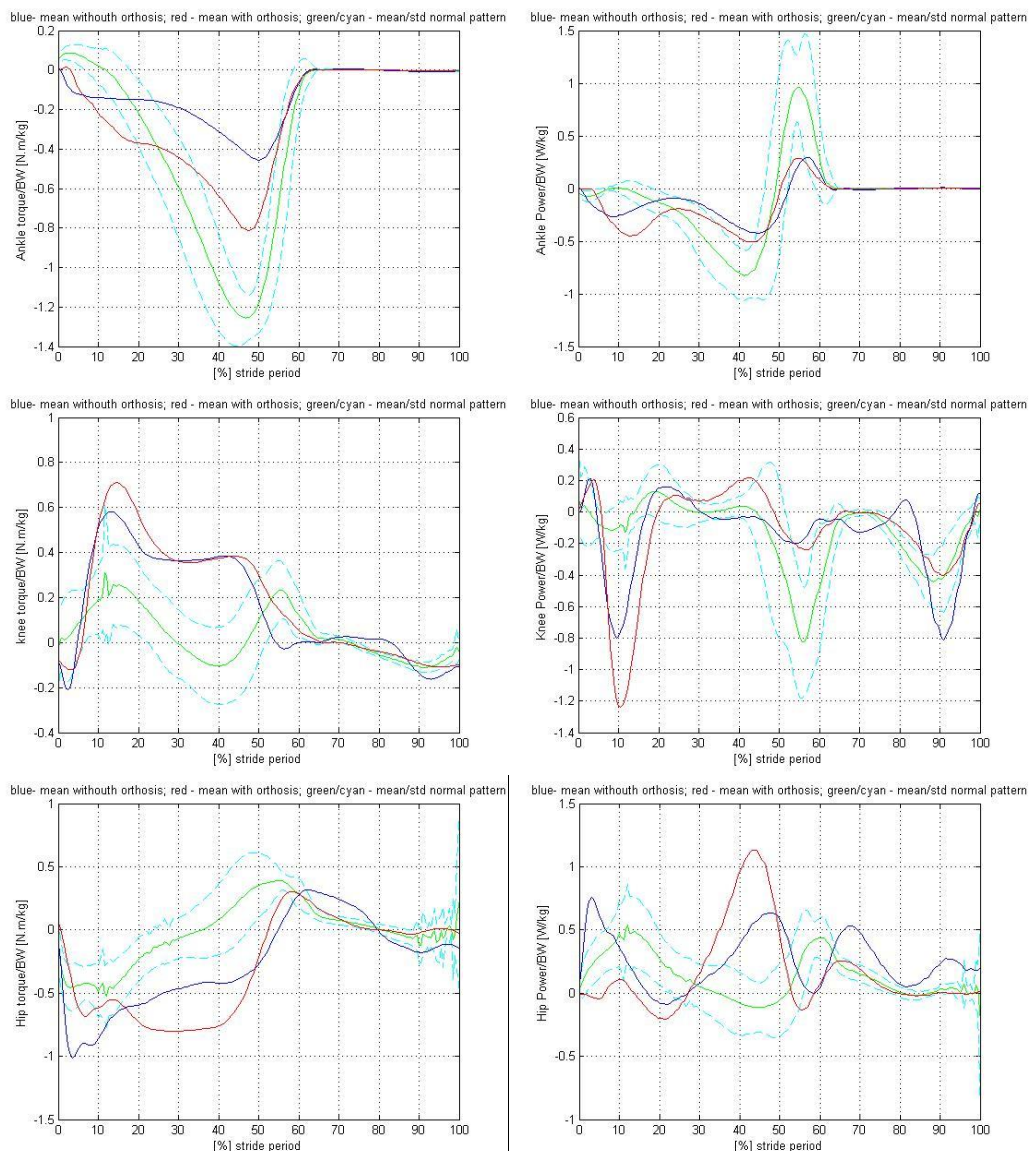

Figure 50 - Representation of torques and mechanical power for subject 1 without orthosis (blue), and with orthosis (red) and for a normal pattern (green/cyan): a) ankle torque; b) ankle power; c) knee torque; d) knee power; e) hip torque; f) hip power

Table 12 – Positive and negative work for subject 1

	Normal pattern			Without AFO			With AFO		
	W$^+$ [J/kg]	W$^-$ [J/kg]	W$^+$-W$^-$ [J/kg]	W$^+$ [J/kg]	W$^-$ [J/kg]	W$^+$-W$^-$ [J/kg]	W$^+$ [J/kg]	W$^-$ [J/kg]	W$^+$-W$^-$ [J/kg]
Ankle	0.0980	-0.1934	-0.0954	0.0214	-0.1299	-0.1085	0.0254	-0.1892	-0.1638
Knee	0.0173	-0.1776	-0.1777	0.0257	-0.1846	-0.1589	0.0516	-0.2123	-0.1607
Hip	0.1872	-0.0174	0.1692	0.2950	-0.0061	0.2889	0.2411	-0.0319	0.2092
	0.3025	-0.3884		0.3421	-0.3206		0.3181	-0.4334	

8.1.4.5.   *Electromyographic Results*

The obtained results for sEMG patterns can be consulted in appendix G. The comparison of these results with the ones obtained for men show significant differences. Although subject 1 could not perform the ankle dorsiflexion, small peaks of sEMG signal were observed in Tibialis anterior during the first and last 10% of GC, which are consistent with the pattern observed in the adult male. Another peak was observed between the 50% and 70% of GC.

The sEMG signal for Gastrocnemius medialis and Soleus does not present great variations during the whole gait cycle. This fact is consistent with the absence of signal variation observed during the subject preparation and his inability to perform an ankle plantar flexion. The Gastrocnemius lateralis graph presented a motion artifact typical curve caused by relative movement between the electrode and the skin, and so it will not be considered in this analysis.

The sEMG pattern of Biceps femoris shows two peaks during the first and the last 20% of GC, which are in concordance with normal pattern. Park et al. studied the EMG pattern for children with myolomeningocele and also obtained activity during these intervals. However, these authors did not obtain the uncharacteristic peak observed in subject 1 during the terminal stance. This difference is probably related with a subject mechanism to help performing the act of walking (Park, Song et al. 1997).

In section 8.1.1 it was mentioned a tendency of the subject to flex the knees controlled by the action of knee extensors. Since the knees were never locked, caused by this flexion, and due to the localization of the COM in a knee posterior position, the knee extensors had to be activated in order to avoid the total flexion of the knees. This action could be observed when the subject was standing up, the sEMG signal presented a pattern of muscular activation during this phase. This fact influenced the sEMG signal of the trials, since the muscle was always active only small variations are observed during the typical peak phases (0-20%, 55-80% and 90-100%). Due to this fact the subject got tired quickly, supporting his weight on something in the interval between trials.

The Gluteus maximus for subject 1 presented an abnormal pattern, no signal variation was observed during the entire GC. Although, the comparison of sEMG magnitudes is not used, since the sEMG signal varies significantly with the analyzed subject (vide 6.3), in this case it will be considered. Higher values are observed in the Gluteus maximus graph in comparison with normal patterns. This fact may be related with the constant activation of Gluteus maximus, as happened with Rectus femoris. As mentioned in chapter II, the Gluteus maximus, in addition to being a hip extensor, has also a function of assistance of the knee extension. For this reason, Gluteus maximus might have presented this pattern of activation, to help the quadriceps in the action of avoiding the total flexion of knee.

The analysis of the sEMG signal of Triceps surae muscles for the trials with AFO was not possible. This can be justified by the fact that the AFO was tightly attached to the leg, which caused friction on the electrodes, and consequently, movement artifacts on the analysis. On the other hand, the Tibialis anterior presented the same peak between the 50-70% of the GC, although the two characteristic peaks of the first and last 10% of GC were not observed. This fact may be related with the support given by the AFO for these phases. The subject might feel safer, and his control system did not send the electric impulses to try to perform the ankle dorsiflexion.

The sEMG signal for Biceps femoris shows a pattern similar to those obtained without AFO, however, the uncharacteristic peak observed during terminal stance presents a lower value.

The sEMG signal of the Rectus femoris of the right limb presented motion artifacts. However, analyzing the pattern for the left limb is clearly possible to observe a decrease of the magnitude of the values for the trials where the orthosis was used. The same result was obtained for the left gluteus maximus. These results are consistent with Park et al. and with the kinetic results for this subject. The use of the orthoses conferred stability to the subject, which decreased the demand on knee extensors (Park, Song et al. 1997).

Figure 51 - Representation of sEMG signal of Rectus femoris (left limb) for subject 1 without orthosis (blue/black), and with orthosis (red/magenta) and for a normal pattern (green/cyan): a) MAV b) Normalized
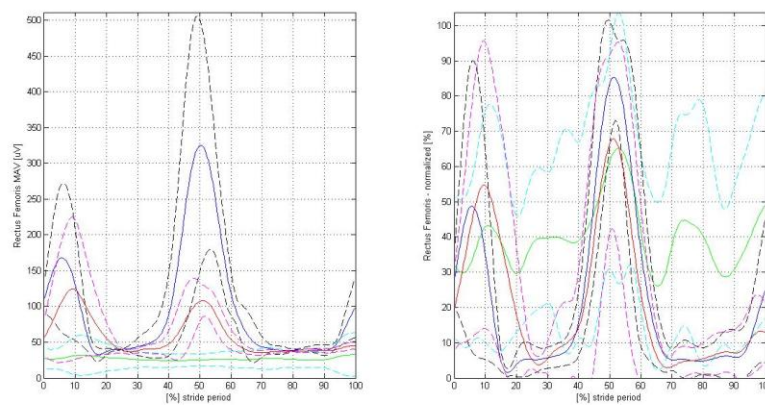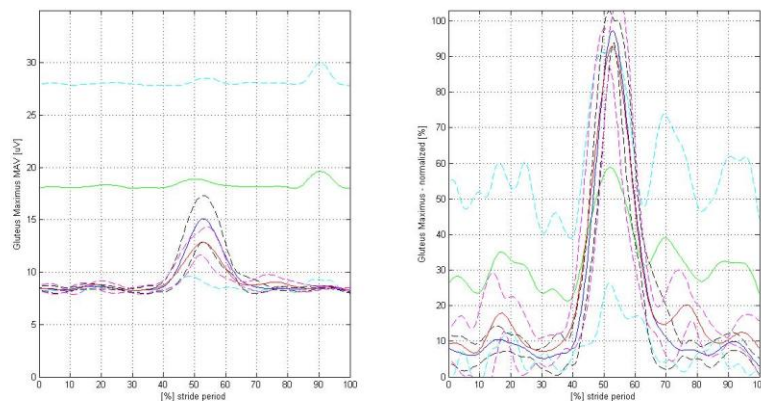

Figure 52 - Representation of sEMG signal of Gluteus Maximus (left limb) for subject 1 without orthosis (blue/black), and with orthosis (red/magenta) and for a normal pattern (green/cyan): a) MAV b) Normalized

8.2. Subject 2 – Muscle weakness of lower limbs (leg)

8.2.1. Remarks on subject preparation

It is important to mention that during the placement of sEMG electrodes no sEMG signal was observed in Tibialis anterior for both legs, as well as the inability of performing a voluntary foot dorsiflexion. The Triceps surae muscles presented very small variations when asked to perform a plantar flexion. Inclusively, the right soleus electrode did not detect any signal for this muscle. It is also noted that although the patient could make a foot plantar flexion, the range of motion and the produced force are relatively reduced in comparison to what is observed in healthy subjects.

Figure 53 – Subject 2: a) IC of right foot without AFO b)MSw of right limb c) IC of right foot with rigid AFO d) IC of right foot with flexible AFO

8.2.2. Visual Observation

The analysis of subject 2 will consider three different parts. First, a comparative intra-subject variability study will be performed between the trials where the orthoses were and were not used. Two different orthoses are considered – hinged AFO (Figure 53 c)) and foot-up orthosis (Figure 53 d)). It is important to mention that the foot-up orthosis provides dorsiflexion assistance, helping to avoid the drop and slap foot. On the other hand, the hinged AFO allows free ankle dorsiflexion and free or restricted ankle plantar flexion, conferring also medial-lateral stabilization of the subtalar joint and the possibility of controlling the adduction/abduction of forefoot.(ICRC 2006)

Visually, the trials where the AFOs were not used presented a drop foot symptom (vide Figure 53 a) and b)). In order to enable the toe clearance, a tendency of the subject to a greater flexion of the knee is more prevalent that in normal gait. Another observed aspect was the great pelvic rotation during the swing phase, possibly as a mechanism used by the patient to improve the comfort while walking. Comparing the observed deviation with the abnormal gaits presented in chapter IV, subject 2 presented clear symptoms of a steppage gait.

The trials where the orthoses were used presented clear improvements; the symptom of drop foot was corrected conferring stability to the gait. It is also noted that the subject stated to feel safer with the hinged AFO than with the foot-up orthosis.

Table 13 shows the time-distance parameters calculated for subject 2. The obtained results for stride/step length showed values inferior to those obtained for children and women. On the other hand, the stride/step time presented considerably higher values than that of these control groups. The

conjugation of these factors resulted in a cadence and velocity values lower than normal, as well as in the observed difficulty in hitting the force plates, supporting the idea already presented that the spatial arrangement of the force plates should be adapted to each subject, especially when an analysis is performed with a pathological individual. One last note to mention is the fact that the analysis of time-distance parameters for the three types of trials performed did not show significant differences.

Table 13 - Time-distance parameters. The stride time, stride length, cadence and velocity were calculated taking right IC as the reference point. The remaining parameters were calculated between the right IC and left IC

	Women		Children		Without AFO		With hinged AFO		With foot-up AFO	
	$\overline{x}$	s	$\overline{x}$	s	$\overline{x}$	s	$\overline{x}$	s	$\overline{x}$	s
Stride Time [s]	1.0829	0.1104	1.0500	0.0990	1.3633	0.0924	1.3267	0.0379	1.3033	0.0513
Stride Length [m]	1.2533	0.0589	1.1114	0.0140	1.0210	0.0497	1.0577	0.0608	1.0465	0.0416
Step Time [s]	0.6286	0.0398	0.6300	0.0566	0.7900	0.0458	0.7733	0.0231	0.7467	0.0462
Step Length [m]	0.6171	0.0372	0.5496	0.0140	0.5078	0.0288	0.5115	0.0398	0.5039	0.0270
Cadence [steps/min]	111.7962	11.2526	114.7959	10.8231	88.2796	5.7564	90.5007	2.5441	92.1655	3.5793
Velocity [m.s^{-1}]	1.1675	0.1278	1.0626	0.0868	0.7496	0.0159	0.7972	0.0380	0.8044	0.0589
Width [m]	0.0760	0.0202	0.0219	0.0509	0.0408	0.0714	0.0700	0.0410	0.0853	0.0858
Right Foot Angle [º]	-1.1048	0.0202	6.0226	1.4502	14.0498	3.1674	15.7714	2.7092	13.6227	3.0278
Left Foot Angle [º]	-3.5493	3.2047	3.3794	7.0867	1.0391	8.3935	-7.5646	1.9808	-3.6452	2.7297

8.2.3. Intra-subject Variability

Due to the difficulty in performing a valid test and the limited time, the results are calculated using the mean for three valid trials. The graphical representation of the main parameters can be consulted in Appendix F.

The obtained results for kinematic analysis followed the expected, i.e. the trials where the AFOs were not used presented, in general, standard deviation values higher than those obtained using orthoses. However, these differences are relatively small in comparison with those observed in subject 1. Comparing the obtained results for hinged AFO and foot-up orthosis, no significant differences were found.

The intra-subject variability of GRF components did not present significant differences between the three trials. The standard deviation values were relatively small, except for the medial-lateral component during the second half of the stride phase.

The study of torques and mechanical power of joints has to be carried on separately. Analyzing the ankle, a decrease of the standard deviation values is observed in trials where the AFOs were used. Both orthoses presented similar standard deviation values, having an important role in the stabilization of this parameter.

The obtained results for torque and power of the knee present a higher variability than those obtained for the ankle, especially during the MS and TS events. Comparing the three types of trials performed, it is possible to identify a clear stabilization of these parameters by the use of hinge AFO. The values of standard deviation are clearly lower than those obtained in the other trials. Similar

results were obtained for torque and power of the hip, i.e. a higher variability is observed during MS and TS events, while the use of hinge AFO contributed to the stabilization of hip kinetic parameters.

Summarizing, differences between the three types of trials can be identified. The hinge AFO helped to stabilize all the kinetic and kinematic parameters. The foot-up orthosis seemed to have an important role in the stabilization of the ankle, but its use did not contribute substantially for improvements in variability of the hip and the knee kinetic parameters.

8.2.4.   Comparison between Subject 2 patterns and non-pathological patterns

8.2.4.1.   Foot displacement and velocity

Comparing the obtained results of subject 2 for this parameter with those of subject 1, similarities were found in the contact of foot with the ground. The results of vertical toe velocity for the trials where the AFO was not used did not present the decrease in WA, resulting of the controlled plantar flexion that typically occurs in this phase. Observing the heel vertical velocity, an increase (less negative) of vertical velocity is noted, which is caused by the fact that at IC the heel is still in the air. It is also possible to observe that during the MSw and terminal swing phases, the subject presented a lower value of vertical toe displacement. These two evidences are a clear symptom of drop foot.

Analyzing the results for the trials where the hinged AFO was used, a clear improvement in these parameters is observed. The contact of the foot with the ground was corrected, to be performed with the heel. On the other hand, the results for the trials where the foot-up orthosis was used also present some improvements. The contact is done with the heel (At IC, the heel presents a vertical velocity and vertical displacement almost null). Nevertheless, the toe vertical displacement and velocity show a similar pattern to the trials where the AFOs were not used. i.e., although the contact was done with the heel, the foot did not present a dorsiflexion angle as marked as the observed in tests with hinge AFO and in normal pattern. Possibly, one of the reasons that lead the subject 2 to feel safer with hinge AFO may be related with this difference.

8.2.4.2.   Joint Angle

The analysis of the joint angles for subject 2 enables the identification of a set of deviations from the normality. The first difference is visualized on the ankle plot, which presents a typical pattern of drop foot. I.e. at IC event, the ankle is plantar flexed; the foot does not present a dorsiflexion angle. After TO, a dorsiflexion angle is also not observed.

The second difference is observed in the knee angle plot. Although, generally, a knee flexion during the stance phase is observed – 2nd determinant of gait, the subject 2 presented a plateau during this phase (~8º). On the other hand, a higher value of knee flexion is observed during swing phase.

The hip presented a pattern relatively similar to the one obtained for normal subjects, though, during MSw and terminal swing events, this parameter presented values of hip flexion higher than those obtained for a normal pattern. This fact is consistent with the visual observation of the trials; the subject presented a tendency to flex the hip more than what is observed for normal subjects. These higher values of knee and hip flexion appear to be a mechanism presented by subject to ensure the toe clearance during this phase.

The analysis of the trials in which the AFOs were used shows they have an important role on the ankle stabilization. Both orthoses supported the foot during the periods in which it was not on the floor. However, small differences were observed between orthoses. While the use of the hinged AFO led to a clear foot dorsiflexion (vide Figure 53c), the foot-up orthosis only avoided the drop foot, i.e. when the foot hits the ground, it is almost flat (vide Figure 53d)). The obtained results for the trials in which the orthoses were used also show a decrease of the knee and hip flexion during the MSw and terminal swing. Nonetheless, these values are still higher than for normal pattern.
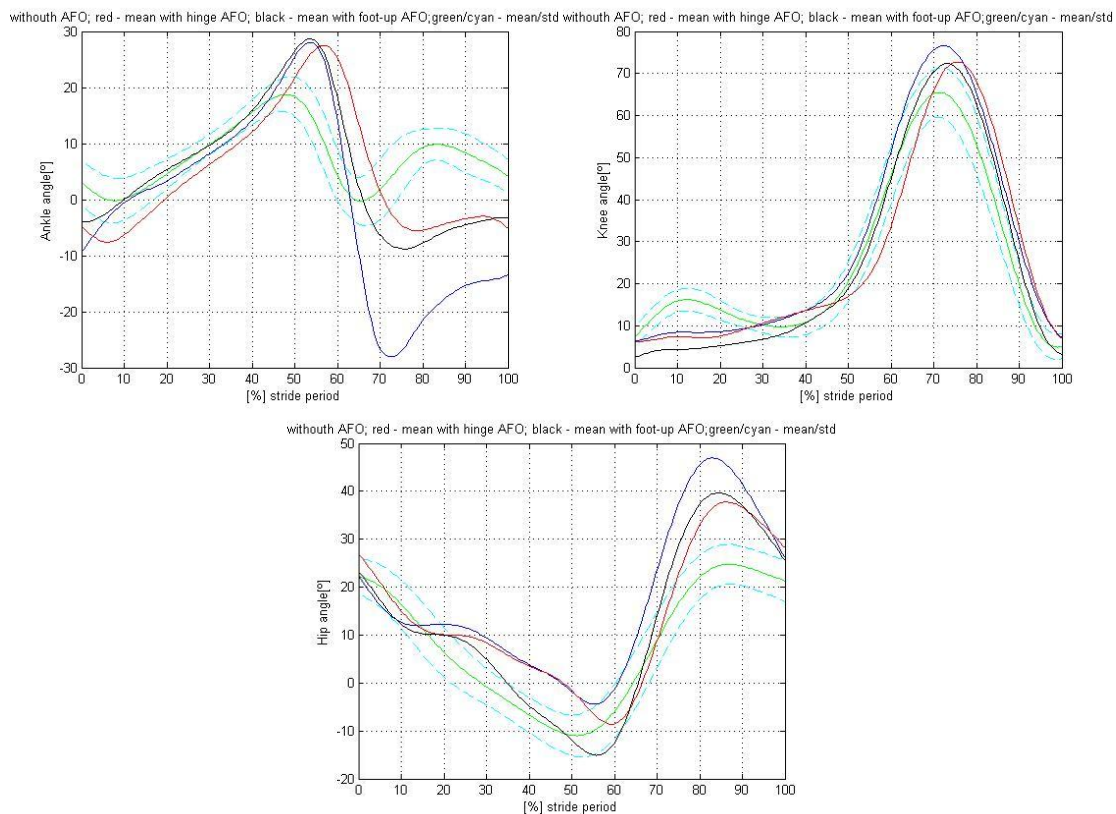

Figure 54 - Representation of joint angles for subject 2 without orthosis (blue), with hinge AFO (red), and with foot-up orthosis (black) and for a normal pattern (green/cyan): a) ankle; b) knee; c) hip

8.2.4.3. Ground Reaction Forces and Center of Pressure

For all the different types of analyses, the antero-posterior component of GRF presents a pattern much similar to the obtained for normal subjects, However, differences were observed in vertical and medial-lateral components, causing an abnormal pattern of the COP(vide Figure 56).

The analysis of medial-lateral component shows a lateral peak at 10% of GC higher than the observed for a normal pattern. On the other hand, the vertical component does not present the typical "m" curve; instead of two peaks (at ~13% and ~46% of GC), three peaks are observed, two in accordance with the normal pattern and another one at 25% of GC, where a minimum is usually observed (vide Figure 55 b) and c)).

As afore mentioned, the COP pattern for subject 2 presented great differences from the normality. The obtained results for the trials where the orthoses were not used show that the application of the GRF vector does not start on the heel, beginning approximately in the middle of the foot (consequence of drop foot observed in this subject). The results obtained with the hinge AFO show that this problem

was, in part, corrected, i.e. although the application of the GRF vector starts approximately at the heel, abnormalities in the COP curve are still observed in the middle of the foot. When the foot-up orthosis was used, it is possibly to observe that the COP starts in an anterior position in relation to the starting point of the trials where no orthosis was used. This fact appears to be an apparent improvement, but it is also obvious that this parameter does not begin at the heel, as it would be expected for a corrective orthopedic device.
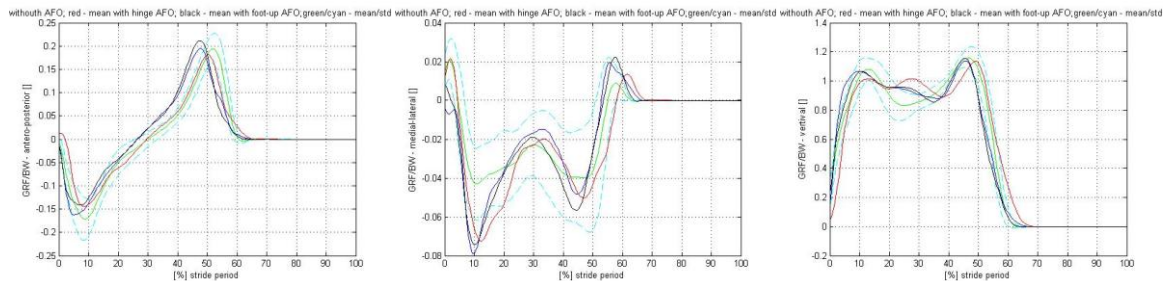

Figure 55 - Ground Reaction forces for subject 2 without orthosis (blue), with hinge AFO (red), and with foot-up orthosis (black) and for a normal pattern (green/cyan): a) Antero-posterior; b) medial-lateral; c) vertical
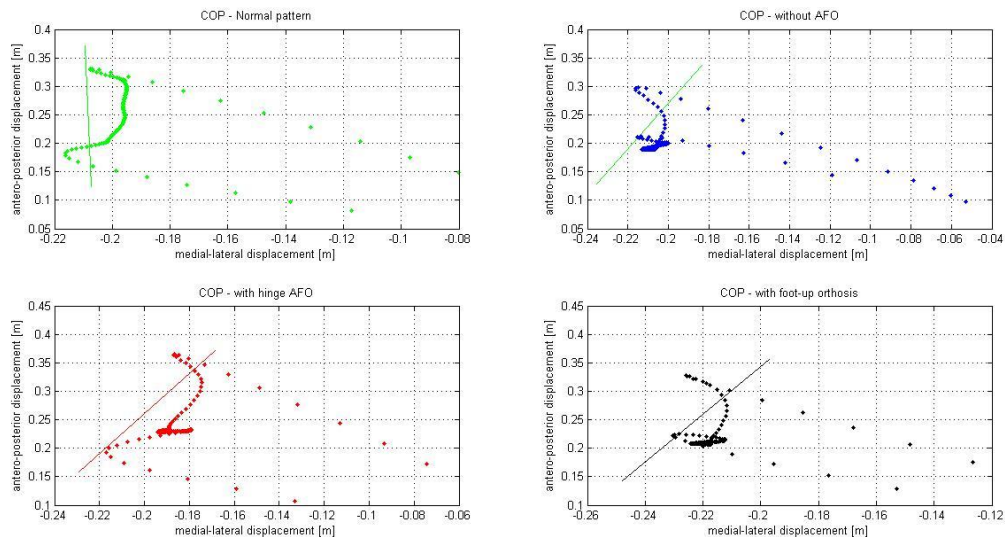

Figure 56 - COP for subject 2 without orthosis (blue), with hinged orthosis (red), and with foot-up orthosis (black) and for a normal pattern (green/cyan); the color line segments represent the foot angle in horizontal place (end points – heel marker and toe marker)

8.2.4.4. *Joint Moments of Forces and Mechanical Power*

The torque and mechanical power of the joints present patterns that are quite different from those observed in normal subjects. This fact was already expected, since the analysis of kinetic and GRF results allowed finding important deviations from the normality, which have repercussions in the calculation of these parameters.

The ankle moment revealed a similar pattern to the one observed for subject 1, concordant with the muscular anomalies addressed in section 8.2.2. Once more, lower torque and power values are observed during PO, and the small dorsiflexion torque that is usually observed for the first instants of WA is nonexistent. Similar curves were observed in the different trials, which were already expected, since the orthoses only support the foot, not interfering with the generation of muscular contraction responsible for the ankle angular movements.

On the other hand the knee mechanical power presented a plateau during the first 40 % of GC. This fact is related in part with the differences observed in knee angle plot, where a plateau is also observed for this interval. Since the mechanical power is calculated from the multiplication of the torque by the angular velocity, if the angle is constant in this phase, the power will be null.

No significant differences were observed in the kinetic parameters of the hip and knee between trials, with or without orthoses. Thus, the use of orthoses does not appear to have improved these parameters. In fact, as afore mentioned, the use of the orthoses has substantially decreased the intra-variability for the hip and knee torque/power. This is an important observation, since it provided stability to the subject's gait.
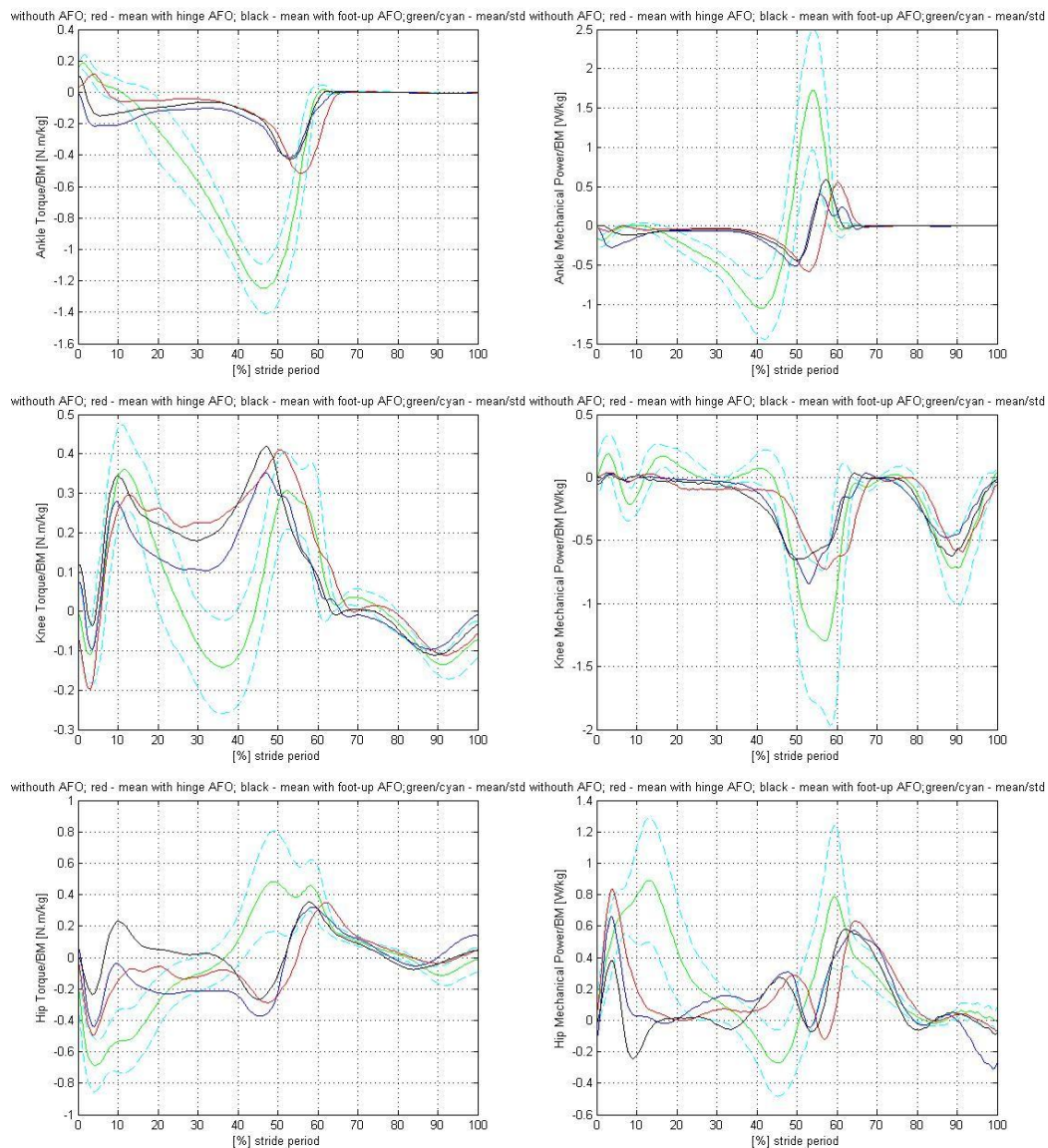

Figure 57 - Representation of torques and mechanical power for subject 2 without orthosis (blue), with hinged orthosis (red) and with foot-up orthosis (black), and for a normal pattern (green/cyan): a) ankle torque; b) ankle power; c) knee torque; d) knee power; e) hip torque; f) hip power

Table 14 – Positive and negative work for subject 1

	Normal pattern			Without AFO			With hinge AFO			With Foot-up AFO		
	W^+	W^-	W^+-W^-	W^+	W^-	W^+-W^-	W^+	W^-	W^+-W^-	W^+	W^-	W^+-W^-
	[J/kg]	[J/kg]	[J/kg]	[J/kg]	[J/kg]	[J/kg]	[J/kg]	[J/kg]	[J/kg]	[J/kg]	[J/kg]	[J/kg]
Ankle	0.1282	-0.1983	-0.0701	0.0305	-0.1213	-0.0908	0.0354	-0.0915	-0.0561	0.0337	-0.0838	-0.0501
Knee	0.0258	-0.2684	-0.2426	0.0020	-0.2558	-0.2538	0.0031	-0.2587	-0.2556	0.016	-0.2617	-0.2600
Hip	0.2813	-0.0252	0.2561	0.2262	-0.0280	0.1982	0.2297	-0.0060	0.2237	0.1539	-0.0286	0.1253
Total	0.4353	-0.4919		0.2587			0.2682			0.2036		

8.2.4.5. Electromyographic Results

Once more the results obtained for sEMG can be consulted in appendix G. As expected, these results presented significant differences in comparison to the normal patterns. The first appointment is related with the incapability of the subject to perform an ankle dorsiflexion. However, in line with the results of subject 1, signal variations were observed in Tibialis anterior plot during the first and last 10% of the GC. In the same way, the trials where the orthoses were used presented lower values. This fact shows that exists a muscular activation, though such activation does not generate the desired movement. This last aspect may be related with the feeling of security provided by the orthoses, which leads to a lower muscular activation.

The second difference was observed in the Triceps surae muscles. During the preparation subject 2, it was observed that when asked to perform an ankle plantar flexion, she could only move few degrees and the sEMG signal variations were very small. However, the analysis of triceps surae muscles during the trial showed no signal variation during the entire gait cycle. This aspect is in concordance with the low value observed in the ankle power graph during the PO.

Once more, the pattern obtained for Biceps femoris presented results similar to those obtained for subject 1. Two peaks during the first and last 10% of GC, which are in concordance with the normal pattern, and another during PO event. This abnormal activation may be related with a compensatory mechanism of the two subjects to help performing the ankle plantar flexion during the PO event, since there is no activity of the plantar flexors.

The graphical representation of the Rectus femoris activation shows an abnormal pattern during the entire cycle for the different performed trials (with and without orthoses). An abnormal peak was observed between the 30-40% of the GC. This aspect may be related with the abnormal plateau observed in the knee angle graph during the stance phase (Figure 54). The Rectus femoris is activated, maintaining the knee extended. The Gluteus maximus pattern also presents this peak, and probably for the same reason, i.e. its action helps to maintain the knee extended.
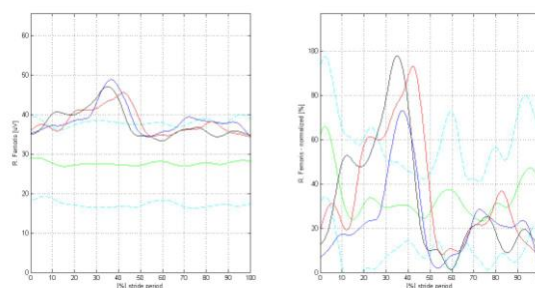

Figure 58 - Representation of sEMG signal of rectus femoris for subject 2 without orthosis (blue), with hinged AFO (red) and with foot-up orthosis (black), and for a normal pattern (green/cyan): a) MAV b) normalized

Chapter IX

Conclusions and Future Developments

9.1. Conclusions

In this thesis, the author's proposal is to achieve four main objectives. The first consisted in the development of a gait acquisition protocol for LBL, which would enable the analyses of the principal time-distance, kinematic, kinetic and electromyographic parameters for non-pathological and pathological subjects. In order to apply in future clinical analysis, the protocol would consider two important aspects: robustness and fast assembly. The second objective aimed the development a set of routines, which would allow the data processing with the academic software – Apollo, and to create a database of non-pathologic gait. The third objective consisted in the acquisition of a population of subjects for three distinct groups – adult male, adult female and children. This step was very important, since it allowed to validate the protocols developed, comparing the obtained results with previous works, and it also allowed to acquire a set of data to use in future clinic analyses as normal pattern. Lastly, the fourth objective was aimed at the study of the gait of two pathological subjects with and without orthoses, comparing the deviations observed with other studies in order to help validating the designed protocol to future applications in study of pathological subjects.

In order to achieve these four main objectives, several topics related with the non-pathological and pathological gait analysis were addressed. Chapter II presented the anatomy and terminology of articular movement. In chapter III addressed several topics related with the human gait, as well as methodologies used to its study. Chapter IV presented typical abnormal gaits, which are generally used to describe the gait of pathological individuals. Both chapter III and IV have been essential to the development of the protocol presented in chapter VI, since these allowed to understand the gait patterns that should be analyzed to obtain conclusive results. Chapter V presented the mathematic formulation of multibody system dynamic behind the kinematic and kinetic analysis performed in this thesis. The multibody formulation used to define the biomechanic model followed the methodologies presented by (De Jalon and Bayo 1994; Silva 2003), which are the basis of the Apollo software. This biomechanical model considers thirty three rigid bodies and twenty five anatomical points to define the sixteen anatomical segments (Figure 32).

Chapter VI addressed important works related with the marker placement for visual motion acquisition systems. The designed marker set protocol used the ideas extracted for this analysis such

as that the first presented protocol (EMSP) considered the utilization of calibration markers to define the body segments and tracking markers to compute the movements, since this setting would tend to present better results, because it would be less affected by skin movement artifacts. Another aspect read in the literature was related with the use of plates and elastic bands to reduce the skin motion artifact and increase the subject's time preparation. Hence, the thesis author designed a set of clothing accessories. After some locomotion tests, the utilization of a sewed velcro's band proved to be the most effective mechanism used, since it allows an easy and fast marker placement, as well as it is washable and durable, and more importantly, its utilization does not allow small displacements or vibration, while it is in perfect condition. However, due to the problems related to the insufficient number of cameras in the laboratory, a new protocol had to be developed (MSP). This protocol was based in HH marker set protocol, and it was designed to have the smallest number of possible markers (33), allowing also its utilization both in Apollo software as in Visual3D^{TM}.

In chapter VI some issues related with the acquisition and processing of electromyographic data were also discussed. The choice of muscular groups to analyze was based on the normal and abnormal gait patterns discussed in chapter III and IV respectively. The choice considered the principal joint motions: ankle dorsiflexion – tibialis anterior; ankle plantar flexion – triceps surae muscles; knee flexion – biceps femoris (long head); knee extension – quadriceps femoris (rectus femoris) and hip extension – gluteus maximus.

Chapter VI also approached the acquisition protocols, as well as the routine developed to analyze experimental data and generate the database. The database interface fulfilled the considered assumptions, since it allowed the analysis of all the principal parameters with importance in gait analysis, as well as it allowed to compare the results of a given subject with the normal patterns, enabling a quick and easy interpretation of the results.

The analysis of time-distance parameters, such as stride/step length/time, cadency and velocity, for natural cadence of the non-pathological groups showed that these values were affected by the necessity of hitting correctly the force plates. During men trials, in order to allow the correct hitting of feet with force plates, it had to be asked to decrease slightly their stride/step length and their velocity. The inverse had to be asked to children. This resulted in values that were not in concordance with the expected, e.g. the difference between men and women cadence was higher than the expected, while the stride/step length presented practically the same value (due to the fixed force plate arrangement). Since one of the most important indicator of gait abnormalities are the study of these parameters, a different protocol should be considered to analyze these parameters. The author suggests including a set of trials in which it should not be considered the necessity of hitting the force plates.

The analysis of displacement and velocity of feet markers, along with the study of COP, allowed understanding the mechanisms of toe clearance and ground contact, especially in pathological subjects. The observed differences between the obtained results for normal pattern and other studies were related with the different group velocities caused by the necessity of hitting the force plates. However, the observed patterns presented the expected behavior.

Another important parameter, and widely used in clinics, is the study of joint angular displacement. Once more, small differences were observed between the obtained results and the literature.

Analyzing men joint angle and foot velocity, values more in agreement with those presented by Winter for slow cadence were observed. The analysis of the remaining kinematic and kinetic patterns also presented this tendency.

Both knee and hip graphs presented the expected pattern, as well as the expected values. The only exception was observed in hip graph of children. Although, the pattern was similar, a maximum extension value of approximately 0º instead the normal -10º and a maximum flexion value of 35º instead the normal 25º was observed. This fact was caused by the anterior flexion of the trunk observed for the subjects of this group, which probably was caused by the use of the wireless EMG system in an abdomen anterior position. Equally, the study of joint angular velocities for knee and hip was in concordance with the expected pattern.

On the other hand, the analysis of joint angular displacement and joint angular velocity of ankle presented some differences in relation with the literature, especially during plantar flexion events. This fact was caused by the use of the II phalange marker to calculate the foot angle (sagittal plane) instead of the V metatarsal head. In order to avoid this error in the future, it is advisable to adapt the MSP, considering one extra marker in V metatarsal head.

The analysis of the three GRF components and COP showed values consistent with the expected, as well as low standard deviation values. The obtained duration of the stance phase and swing phase were respectively 63% and 37%, values that fit with those observed in the literature.

One of the goals of performing a kinetic analysis is the calculation of the articular torques, since this analysis allows the understanding of how the forces are being applicable in joints, and it enables the calculation of the joint mechanical power and work. The obtained results for torque are consistent with the literature, as well as the idea that the inter-variability is higher in the hip joint. The mechanical power of the hip and the knee presented the pattern expected for all the groups. On the other hand, although the ankle results presented the same pattern, the magnitude of the characteristic peak during the PO presented a value slightly inferior than observed in literature. This difference came from the differences observed in the calculation of angular velocity of the ankle.

The analysis of the six gait determinants presented the expected patterns. However, in order to improve the simplicity of the data treatment, it would be important to consider a new biomechanical model in Apollo, which considers the RIC and LIC markers (usually used to calculate the rotation and lateral tilt of the pelvis).

Lastly, the obtained results for sEMG presented the patterns expected, allowing detect all the characteristics peaks.

In general terms, the methodology used in this work presented consistency, robustness and fast applicability, generating results in concordance with the literature. The protocols enabled the analyses of all the important parameters, the designed clothes obtained good results and at the same time helped decreasing substantially the time of subject preparation. The database interface allowed an easy and quick consult to the pretended data, as well as to compare a given subject with his respective group.

In order to achieve the fourth objective of this work, it was analyzed the gait of two subjects suffering from two neuromuscular diseases (subject 1 – male subject suffering from Spina Bifida (13

years old); subject 2 – female subject suffering from muscular weakness of lower limbs (leg) (14 years old)). For both subjects was studied the intra-subject variability with and without their orthoses (subject 1 – hinge AFO; subject 2 – hinge AFO and foot-up orthosis) and, in a second section, these results were compared with those obtained for non-pathologic subjects.

Subject 1 showed clear improvement in the trials where the AFO was used. In general terms, almost all kinematic and kinetic parameters presented standard deviations values lower in these trials.

On the other hand, subject 2 presented slightly improvements in kinematic parameters for the trials where the orthoses were used. Comparing the results obtained for the two orthoses, it was not observed significant differences for these parameters. However, the same result was not observed for kinetic parameters. The standard deviation of GRF components presented relatively low values for the three trials of trials, so no significant differences were observed between these trials. The obtained results for torque and mechanical power of ankle showed clear improvements in trials where the orthoses were used, as well as no significant differences were observed between the standard deviations values of these trials. On the other hand, the use of hinge AFO also helped to stabilize the knee and hip kinetic parameters, while the use of foot-up orthosis did not contributed substantially with improvements in these parameters.

Visually, subject 2 presented symptoms characteristics of a steppage gait: inability of performing an ankle dorsiflexion, drop foot symptom during swing phase, an increased flexion of hip and knee during swing phase, a decrease in step length and an increase of stride time. The kinematic data collected matches of the observations performed, suggesting that the guidelines established are in accordance with the clinical cases found in this thesis. This fact is an example of possible applications of the developed protocols in further studies of pathological gait.

Comparing the three types of performed trials with normal patterns, it is possible observe a decrease in the maximum hip flexion and knee flexion in the trials where the orthoses were used. These results were expected, since the orthoses avoided the drop of foot during the swing phase, the subject did not need to flex these joints that much to ensure the toe clearance. Another important difference was the inexistence of a knee flexion during the stance phase, which was constant to the three types of trials.

The analysis of GRF showed significant differences in vertical component for the trials with and without the orthoses. Instead of two peaks, three were observed, two in accordance with the normal pattern and another where it is usually observed a minimum, which resulted in significant differences in COP. Analyzing this last parameter and the displacement and velocity of foot, it was possible to confirming that the contact of foot with the ground was made with the forefoot (typical symptom of an equine gait). The use of hinge AFO allowed the correction of this symptom, passing the contact to be made by the heel. However, the same result was not observed when the foot-up orthosis was used.

The analyses of the torque and mechanical power for the ankle showed significant differences. Lower torque and power values are observed during the PO event, which is in concordance with the incapability of the subject to perform an ankle plantar flexion. Similar curves were observed in the different trials, with and without orthoses, which were already expected, since the orthoses only support the feet and allow the toe clearance during the swing phase.

The analyses of the knee and hip torque also presented important differences. However, no significant differences were observed in the kinetic parameters of these joints between trials, with and without orthoses. Although the use of orthoses did not appear to have improved these parameters, this fact is not true, since its use contributed to decrease substantially the intra-variability of the hip and knee kinetic torque/mechanical power, which provided stability to the subject's gait.

On the other hand, subject 1 presented symptoms of different pathological gaits. Visually, his gait was characterized by a wide base of walking, difficulties in controlling the body balance, drop foot symptom, crouched gait among others. Clear improvements were observed when the AFO was used. The same results were achieved through the performed analysis, attesting again the robustness of the developed protocol and its possible application in further clinical studies.

The analysis of joint angles for subject 1 showed significant differences. The ankle graph presented a typical drop foot curve, i.e. during swing phase the foot is plantar flexed due to the impossibility of subject performing the ankle dorsiflexion. The knee angle graph presented a higher knee flexion during stance phase; this difference is probably related with a mechanism used by subject to help maintain the balance of the body. It was observed that while the subject was standing, he presented a tendency to flex the knees and trunk to maintain this static posture. The hip angle graph also presented a small variation similar to those obtained for the children pattern and, once more, this difference was caused by the excessive anterior flexion of the trunk. It is important to mention that the use of orthosis did not show significant differences in knee and hip angle graph, though its utilization contributed to stabilize the ankle angle, supporting the foot during the swing phase.

Subject 1 presented a tendency to perform an abrupt leg swing instead of the regular pendular behaviour of the leg observed in normal subjects. As a result, an abrupt impact of foot to the ground was observed during IC event. This fact resulted in significant differences in GRF components, all the components presented higher values, especially during the first 20% of GC. Similar results were observed for the trials where the AFO was not used. However, the use of the orthosis contributed significantly to improve the distribution of the COP in foot. In the trials where the AFO was not used, the COP began in a foot anterior position, progressing through the medial arch of the foot. On the other hand, in trials where the AFO was used, significant improvements were observed, the beginning of COP action started in heel and advanced through the lateral arch of the foot.

The obtained results for kinetic parameters presented similar to those obtained in the literature, confirming the idea that the weakness or incapability in dorsiflexors and plantar flexors muscles tends to be compensated by the loading alterations in other joints, especially in the knee and the hip joints. The graphical representation of the ankle torque and mechanical power did not present the characteristic peak during PO, where in non-pathological gait is generated approximately 85% of energy generated in a GC. On the other hand, the graphical representation of the torques and mechanical power of the knee and hip showed significant differences in these parameters which resulted in higher values of generated positive work in these joints. Small differences were observed between the trials with and without AFO, though the positive work generated in the trials where the AFO was not used was higher.

Both subject 1 and subject 2 presented significant differences in sEMG patterns, though presented some similarities: 1) The triceps surae muscles showed no signal variation during the entire gait cycle, which is in concordance with the low value observed in the ankle power graph during the PO for the two cases. 2) Both subjects presented an incapability to perform the ankle dorsiflexion. However, in both cases, two peaks were observed in the first and last 10% of the GC of the tibialis anterior (consistent with the normal pattern). This fact shows that exists an muscular activation, though such activation does not generate the desired movement. Another aspect is related with the lower values observed in this muscle when the orthoses were used. This last aspect may be related with the feeling of security provided by the orthoses, which appear have influence in the gait control system (no electric impulses are generated to try to perform the ankle dorsiflexion). 3) In both cases, an abnormal activation was observed during the PO event. This pattern may be related with a mechanism of both subjects to help performing the ankle plantar flexion during this phase.

Other differences were observed in the sEMG patterns of rectus femoris and gluteus maximus, which seem being consistent with the kinetic and kinematic parameters. This fact helped to validate the applicability of the SESP at a clinical level.

In general terms, the thesis author thinks that the developed method achieved all the goals proposed at the beginning. The developed protocol proved to be robust and quick, as well as applicable at a clinical level. The methodology of data treatment showed efficacy, enabling quickness and easiness in the analysis of a given subject.

9.2. Future Developments

In order to improve the results obtained for the time-distance parameters, the author recommends the development of another protocol. One possible idea would be to consider the use of pressure sensors in the foot and systems of motion acquisition, allowing the principal parameters to be calculate, such as the stride/step length, stride/step time, cadence, velocity and width. Using this protocol would also be possible to analyze the asymmetries in these parameters between the two legs.

In this work was used the torque, mechanical power and work in joints as a mechanism of analyzing the energy in gait. However, it would be interesting to consider the utilization of experimental methods, such as the metabolic gas analysis systems or metabolic measurement carts, as well as electrocardiograms and sphygmomanometer. This information would allow the calculation of metabolic rates, relating these values with the kinetic results, as well as to compare the metabolic rates between pathological and non-pathological subjects.

The second point would be to continue the study of non-pathological subjects, in order to increase the number of pattern subjects, and if possible to consider subjects from different regions of Portugal, ethnicities and social classes, with the aim of having a representative sample of the Portuguese population. Although the database is prepared to receive results of elderly population, this work did not perform any analysis for this group. Since, several works reported some differences in the gait of elderly (Hageman and Blanke 1986; Blanke and Hageman 1989; Winter 1991; Ostrosky, VanSwearingen et al. 1994); it would be enriching to acquire the data of this population. Sutherland et al. reported differences in the gait of children for different ages (Sutherland, Olshen et al. 1980;

Sutherland 1997); it would also be interesting to consider in the future not just one group but different groups according to their age.

The third point would be the systematic application of the work developed in this thesis in the study of pathological subjects. However, it would be important to get a feedback from the medical community, about other possible parameters to acquire in order to improve the potentialities of the performed analysis. The obtained results may be used to help diagnose certain condition, but it will essentially be a source of information for physical rehabilitation, developing corrective biomedical devices (prosthesis, orthoses, active orthoses, etc.) adapted to the needs of each patient. Many subjects, who use these devices, usually complain of problems related with the lack of comfort, pain caused by imperfections in the development of these and fragility of the structure. In these cases, the thesis author suggests the development of a questionnaire that covers some issues related with the comfort of used prosthesis/orthosis, pain (e.g. if he feels pain when he uses the device, when and where), walking style (e.g. if he usually changes his walking style to avoid the sensation of pain), etc.

The developed methodology may also be applicable in the study of patterns of a given pathology, considering not only the data of a single subject, but instead the data from a population of subjects with such pathology. This information can be posteriorly used to generate a database of pathological gaits, enabling the study of the characteristic deviations of this pathology and the comparison of pathological subjects with different pathological patterns. The information of this database can also be applied in physical rehabilitation, enabling the design of biomedical correctives with the capability of being used simultaneous in a set of different pathologies.

It would be interesting to develop a routine that would allow to generate reports automatically in which it is described the principal time-distance, kinematic, kinetic and electromyographic parameters for a given subject, in order to be submitted to the medical community or prosthetist/orthotist.

Another idea would be to develop a series of routines that allows automatically the detection of deviations from normality, and if possible relating these with a database containing information of the main pathological gaits. Thus, it would be possible the comparison of the results with the normal patterns and with similar pathologies, and to obtain information not only of the subject but also of the subject condition. This information could also be presented in the report that is addressed in the preceding paragraph.

Eventually, the developed model may be used to the development of a database of human movements, i.e. use the methodologies developed in this work to study the pattern of other human movements, such as jumping, running, pushups, climbing stairs, etc. After being processed the data would be used as inputs for biomechanical computational models.

Another application of the methodology developed in this work is the study of movements in elite sports, with the aim of perfecting these movements by improving their scores. For example, this methodology can be used to improve the technical skills of some athletic disciplines, such as shot put, javelin throw, discus throw, long jump and running.

The final suggestion for further developments is the development of another biomechanical model in the Apollo software. This software has presented itself as a powerful tool to calculate the torques in joints. However, in order to enable the calculation of other parameters in the database, this new model

should consider four markers to define the foot (ankle, heel, II metatarsal head and V metatarsal head) and pelvis (left and right hip joint, LIC and RIC). Therefore, it makes it possible to calculate simultaneously in database various parameters such as the foot angle in sagittal and horizontal plane, inversion and eversion of foot, lateral pelvic tilt and pelvic rotation.

Chapter X

References

Accardo, N. (1975). "Orthopaedic problems in children." <u>Journal of the National Medical Association</u> **67**(3): 250.

Agur, A. M., V. Ng-Thow-Hing, et al. (2003). "Documentation and Three-Dimensional Modelling of Human Soleus Muscle Architecture." <u>Clnical Anatomy</u> **16**(4): 285-293.

Ambrósio, J. A. and M. T. d. Silva (2005). A Biomechanical Multibody Model with a Detailed Locomotion Muscle Apparatus. <u>Advances in Computational Multibody Systems,</u>, Springer.

Anderson, D., M. Madigan, et al. (2007). "Maximum voluntary joint torque as a function of joint angle and angular velocity: Model development and application to the lower limb." <u>Journal of Biomechanics</u> **40**(14): 3105-3113.

Anderson, F. C. and M. G. Pandy (2001). "Dynamic Optimization of Human Walking." <u>Journal of Biomechanical Engineering</u> **123**(5): 381-390.

Arsenault, A., D. Winter, et al. (1986). "Bilateralism of EMG profiles in human locomotion." <u>American journal of physical medicine</u> **65**(1): 1.

Arsenault, A., D. Winter, et al. (1986). "Is there a 'normal'profile of EMG activity in gait?" <u>Medical and Biological Engineering and Computing</u> **24**(4): 337-343.

Arsenault, A., D. Winter, et al. (1986). "Treadmill versus walkway locomotion in humans: an EMG study." <u>Ergonomics</u> **29**(5): 665-676.

Arsenault, A., D. Winter, et al. (1986 a)). "Is there a 'normal'profile of EMG activity in gait?" <u>Medical and Biological Engineering and Computing</u> **24**(4): 337-343.

Arsenault, A., D. Winter, et al. (1986 b)). "Bilateralism of EMG profiles in human locomotion." <u>American journal of physical medicine</u> **65**(1): 1.

Ayyappa, E. (1997). "Normal human locomotion, part 1: Basic concepts and terminology." <u>Journal of Prosthetics and Orthotics</u> **9**(1).

Basmajian, J. and G. Stecko (1962). "A new bipolar electrode for electromyography." <u>Journal of Applied Physiology</u> **17**(5): 849.

Basmajian, J. V. and C. J. De Luca (1985). <u>Muscles alive: their functions revealed by electromyography</u>, Williams & Wilkins.

Bauby, C. and A. Kuo (2000). "Active control of lateral balance in human walking." <u>Journal of Biomechanics</u> **33**(11): 1433-1440.

Blanke, D. and P. Hageman (1989). "Comparison of gait of young men and elderly men." Physical Therapy **69**(2): 144.

Borelli, G., J. Bernoulli, et al. (1743). De motu animalium, Petrum Gosse.

Borghese, N. A., L. Bianchi, et al. (1996). "Kinematic determinants of human gait." Journal of Physiology **494**(3): 863-879.

Braune, W. and O. Fischer (1887). Untersuchungen über die Gelenke des menschlichen Armes, Hirzel.

Braune, W. and O. Fischer (1889). Über den Schwerpunkt des menschlichen Körpers mit Rücksicht auf die Ausrüstung des deutschen Infanteristen, Hirzel.

Braune, W. and O. Fischer (1890). Die rotationsmomente der Beugemuskeln am Ellbogengelenk des Menschen, Hirzel.

Braune, W., O. Fischer, et al. (1987). The human gait, Springer-Verlag Berlin.

Bresler, B. and J. Frankel (1950). "The forces and moments in the leg during level walking." Trans. Asme **72**(27): 25-35.

c-motion (2010). "Visual3D Movement Analysis Software Features (software help)." Retrieved 01-08-2010, 2010, from http://www.c-motion.com/help/whnjs.htm.

Cappozzo, A. (1984). "Gait analysis methodology." Human movement science **3**(1-2): 27-50.

Cappozzo, A., F. Catani, et al. (1995). "Position and orientation in space of bones during movement: anatomical frame definition and determination." Clinical Biomechanics **10**(4): 171-178.

Cappozzo, A., F. Catani, et al. (1996). "Position and orientation in space of bones during movement: experimental artifacts." Clinical Biomechanics **11**(2): 90-100.

Carlet, G. (1872). Essai expérimental sur la locomotion humaine: étude de la marche, Sc. nat.: Paris: 1872; 340.

Cavagna, G. A. and R. Margaria (1963). "External work in walking." Journal of Applied Physiology.

Cavagna, G. A. and R. Margaria (1966). "Mechanics of walking." Journal of Applied Physiology.

Cavanagh, P. and M. Lafortune (1980). "Ground reaction forces in distance running." Journal of Biomechanics **13**(5): 397-406.

Chao, E. Y., R. K. Laughman, et al. (1983). "Normative data of knee joint motion and ground reaction forces in adult level walking." Journal of Biomechanics **16**(3): 219-223.

Chen, I., K. Kuo, et al. (1997). "The influence of walking speed on mechanical joint power during gait." Gait & Posture **6**(3): 171-176.

Cho, C., W. Chao, et al. (2009). "A vision-based analysis system for gait recognition in patients with Parkinson's disease." Expert Systems with Applications **36**(3): 7033-7039.

Cholewicki, J. and S. McGill (1994). "EMG assisted optimization: a hybrid approach for estimating muscle forces in an indeterminate biomechanical model." Journal of Biomechanics **27**(10): 1287-1289.

Cioni, M., C. Richards, et al. (1997). "Characteristics of the electromyographic patterns of lower limb muscles during gait in patients with Parkinson's disease when OFF and ON L-Dopa treatment." The Italian Journal of Neurological Sciences **18**(4): 195-208.

Close, J. (1964). Motor function in the lower extremity: analyses by electronic instrumentation, Thomas.

Close, J. and F. Todd (1959). "The phasic activity of the muscles of the lower extremity and the effect of tendon transfer." The Journal of Bone and Joint Surgery **41**(2): 189.

Collins, J. J. and C. J. D. Luca (1992). "Open-loop and closed-loop control of posture: A random-walk analysis of center-of-pressure trajectories." Experimental Brain Research **95**(2): 308-318.

Collins, T. D., S. N. Ghoussayni, et al. (2009). "A six degrees-of-freedom marker set for gait analysis: Repeatability and comparison with a modified Helen Hayes set." Gait & Posture **30**(2): 173-180.

Correa, T. A., K. M. Crossley, et al. (2010). "Contributions of individual muscles to hip joint contact force in normal walking." Journal of Biomechanics **43**(8): 1618-1622.

Croskey, M. I., P. M. Dawson, et al. (1922). "The Height of the Center of Gravity in Man." american Journal of Physiology **61**(171-185).

De Jalon, J. and E. Bayo (1994). Kinematic and dynamic simulation of multibody systems, Springer New York.

De Luca, C. J. (1997). "The Use of Surface Electromyography in Biomechanics." Journal of Applied Biomechanics **13**(2): 135-163.

De Luca, C. J. (2002). "Surface Electromyography:Detection and Recording." 2010, from http://www.delsys.com/KnowledgeCenter/KnowledgeCenter.html.

DeLisa, J. and C. Kerrigan (1998). Gait analysis in the science of rehabilitation, Diane Publishing.

Della Croce U, Riley P.O., et al. (2001). "A refined view of the determinants of gait." Gait & Posture **14**(2): 79-84.

Della Sala, S., H. Spinnler, et al. (2004). "Walking difficulties in patients with Alzheimer's disease might originate from gait apraxia." Journal of Neurology, Neurosurgery & Psychiatry **75**(2): 196.

Delsys (2010). "EMGworks® Software - Advanced Signal Processing (User Guides)." 2010, from http://www.delsys.com/KnowledgeCenter/KnowledgeCenter.html.

DeLuca, P., S. Õunpuu, et al. (1998). "Effect of hamstring and psoas lengthening on pelvic tilt in patients with spastic diplegic cerebral palsy." Journal of Pediatric Orthopaedics **18**(6): 712.

Don, R., M. Serrao, et al. (2007). "Foot drop and plantar flexion failure determine different gait strategies in Charcot-Marie-Tooth patients." Clinical Biomechanics **22**(8): 905-916.

Donelan, J. M., R. Kram, et al. (2002). "Mechanical work for step-to-step transitions is a major determinant of the metabolic cost of human walking." The Journal of Experimental Biology **205**: 3717-3727.

Du Bois-Reymond, E. (1848). "Untersuchungen iiber thierische Elektricitat." Berlin, Reimer **1849**: 1-24.

Duysens, J. and H. W. A. A. V. d. Crommert (1998). "Neural control of locomotion; The central pattern generator from cats to humans." Gait Posture **7**(2): 131-141.

Eberhart, H. and V. Inman (1947). "Fundamental studies of human locomotion and other information relating to design of artificial limbs." Report to the National Research Council.

Elftman, H. (1934). "A cinematic study of the distribution of pressure in the human foot." The Anatomical Record **59**(4): 481-491.

Elftman, H. (1938). "The measurement of the external force in walking." Science (New York, NY) **88**(2276): 152.

Elftman, H. (1939). "Forces and energy changes in the leg during walking." american Journal of Physiology **125**(2): 339.

Fauci, A., L. Kasper, et al. (2008). Harrison's principles of internal medicine, McGraw-Hill New York:.

Figueroa, P., N. Leite, et al. (2003). "A flexible software for tracking of markers used in human motion analysis." Computer Methods and Programs in Biomedicine **72**(2): 155-166.

Fischer, O. and C. Braune (1899). Der gang des menschen, BG Teubner.

Fong, D., Y. Chan, et al. (2008). "Estimating the complete ground reaction forces with pressure insoles in walking." Journal of Biomechanics **41**(11): 2597-2601.

Forner Cordero, A., H. Koopman, et al. (2004). "Use of pressure insoles to calculate the complete ground reaction forces." Journal of Biomechanics **37**(9): 1427-1432.

Fukuchi, R. K., C. Arakaki, et al. (2010). "Evaluation of alternative technical markers for the pelvic coordinate system." Journal of Biomechanics **43**(3): 592-594.

Fukunaga, T., K. Kubo, et al. (2001). "In vivo behaviour of human muscle tendon during walking." Proceedings of the Royal Society **268**(1464): 229-233.

Gage, J. and S. Society (1991). Gait analysis in cerebral palsy, Mac Keith Press London.

Gage, J. R., P. A. Deluca, et al. (1995). "Gait Analysis: Principles and Applications. Emphasis on Its Use in Cerebral Palsy." The Journal of Bone and Joint Surgery **77**(10): 1607-1623.

Galvani, L. and R. Green (1953). De viribus electricitatis in motu musculari commentarius, Elizabeth Licht, Publisher.

Gard, S. A. and D. S. Childress (1996). "The influence of stance-phase knee flexion on the vertical displacement of the trunk during normal walking." Archives of Physical Medicine and Rehabilitation **80**(1): 26-32.

Gard, S. A. and D. S. Childress (1997). "The effect of pelvic list on the vertical displacement of the trunk during normal walking." Gait & Posture **5**(3): 233-238.

Gard, S. A. and D. S. Childress (2001). "What determines vertical motion of the human body during normal walking." Journal of Prosthetics and Orthotics **13**(3): 64-67.

Gleicher, M. (1999). "Animation from observation: Motion capture and motion editing." ACM SIGGRAPH Computer Graphics **33**(4): 51-54.

Gonçalves, C. (2003). "Enquadramento familiar das pessoas com deficiência: uma análise exploratória dos resultados dos Censos 2001 - 2003." 2010, from www.ine.pt.

Graaff, V. D. (2001). Human Anatomy, McGraw-Hill.

Grabiner, M., J. Feuerbach, et al. (1995). "Visual guidance to force plates does not influence ground reaction force variability." Journal of Biomechanics **28**(9): 1115-1117.

Gray, H. (1918). Anatomy of the Human Body.

Gundersen, L., D. Valle, et al. (1989). "Bilateral analysis of the knee and ankle during gait: an examination of the relationship between lateral dominance and symmetry." Physical Therapy **69**(8): 640.

Gurney, B. (2002). "Leg length discrepancy." Gait & Posture **15**(2): 195-206.

Gutierrez, E., A. Bartonek, et al. (2005). "Kinetics of compensatory gait in persons with myelomeningocele." Gait & Posture **21**(1): 12-23.

Hageman, P. and D. Blanke (1986). "Comparison of gait of young women and elderly women." Physical Therapy **66**(9): 1382.

Hall, S. (2003). Basic biomechanics, McGraw-Hill Boston.

Hasan, S., D. Robin, et al. (1996 a)). "Simultaneous measurement of body center of pressure and center of gravity during upright stance. Part I: Methods." Gait & Posture **4**(1): 1-10.

Hasan, S., D. Robin, et al. (1996 b)). "Simultaneous measurement of body center of pressure and center of gravity during upright stance. Part II: Amplitude and frequency data." Gait & Posture **4**(1): 11-20.

Hefferon, J. (2006). Linear Algebra, 2006.

Herr, H. (2009). An Introduction to human Gait (Presentation). E5. Biomedical Devices and Technologies Course Module. IST - Lisbon.

Hill, A. V. (1938). "The Heat of Shortening and the Dynamic Constants of Muscle." The Royal Society **126**: 136-195.

Hughes, J., S. Bowes, et al. (1990). "Parkinsonian abnormality of foot strike: a phenomenon of ageing and/or one responsive to levodopa therapy?" British journal of clinical pharmacology **29**(2): 179.

ICRC, I. C. o. t. R. C. (2006). "Ankle-Foot Orthosis - Physical Rehabilitation Programme." 2010, from http://www.icrc.org/.

Inman, V., H. Ralston, et al. (1952). "Relation of human electromyogram to muscular tension." Electroencephalography and Clinical Neurophysiology **4**(2): 187-194.

Inman, V., H. Ralston, et al. (1981). Human walking, Williams & Wilkins.

Jamshidi, N., M. Rostami, et al. (2010). "Differences in center of pressure trajectory between normal and steppage gait." JRMS **15**(1): 33-40.

Kadaba, M. P., H. K. Ramakrishnan, et al. (1991). "Measurement of Lower Extremity Kinematics During Level Walking." Journal of Orthopaedic Research **8**(3): 383-392.

Kettelkamp, D., R. Johnson, et al. (1970). "An electrogoniometric study of knee motion in normal gait." The Journal of Bone and Joint Surgery **52**(4): 775.

Kim, C. and J. Eng (2003). "Symmetry in vertical ground reaction force is accompanied by symmetry in temporal but not distance variables of gait in persons with stroke." Gait & Posture **18**(1): 23-28.

Knutsson, E. (1972). "An analysis of parkinsonian gait." Brain **95**(3): 475.

Konrad, P. (2005). The ABC of EMG - A Pratical Introduction to Kinesiological Electromyography, Noraxon INC.

Kuo, A. D. (2007). "The six determinants of gait and the inverted pendulum analogy: A dynamic walking perspective." Human movement science.

Kuo, A. D., J. M. Donelan, et al. (2005). "Energetic Consequences of Walking Like an Inverted Pendulum: Step-to-Step Transitions." Exercise and sport sciences reviews **33**(2): 88-97.

Lam, W., J. Leong, et al. (2005). "Biomechanical and electromyographic evaluation of ankle foot orthosis and dynamic ankle foot orthosis in spastic cerebral palsy." Gait and Posture **22**(3): 189-197.

Lee, C. R. and C. T. Farley (1998). "Determinants of the center of mass trajectory in human walking and running." The Journal of Experimental Biology **2001**(21): 2935-2944.

Lee, P., S. Yong, et al. (2005). "Correlation of midbrain diameter and gait disturbance in patients with idiopathic normal pressure hydrocephalus." Journal of neurology **252**(8): 958-963.

Lewis, J. L. and w. D. Lew (1977). "A note on the description of articulating joint motion." Journal of Biomechanics **10**(10): 675-678.

Lin, C., L. Guo, et al. (2000). "Common abnormal kinetic patterns of the knee in gait in spastic diplegia of cerebral palsy." Gait & Posture **11**(3): 224-232.

Liu, X., G. Fabry, et al. (1998). "Kinematic and kinetic asymmetry in patients with leg-length discrepancy." Journal of Pediatric Orthopaedics **18**(2): 187.

Macfarlane, D. J. (2001). "Automated Metabolic Gas Analysis Systems: A Review." Sports Medicine **31**(2): 841-861.

Marey, E. (1994). Le mouvement, Editions J. Chambon.

MathWorks (2010). "R2010b MathWorks Documentation." 2010, from http://www.mathworks.com/help/.

Matteucci, C. and P. Savi (1844). Traite des phenomlenes electro-physiologiques des animaux, Fortin, Masson & Cie.

Medved, V. (2001). Measurement of human locomotion, CRC.

Menz, H., S. Lord, et al. (2003). "Age-related differences in walking stability." Age and Ageing **32**(2): 137.

Merletti, R. (1999). "Standards for Reporting EMG data." Journal of Electromyography and Kinesiology **9**(1).

Merletti, R., G. Rau, et al. (2010). "Surface ElectroMyoGraphy for the Non-Invasive Assessment of Muscles." 2010, from http://www.seniam.org/.

Miller, N., O. Jenkins, et al. (2004). Motion capture from inertial sensing for untethered humanoid teleoperation. Humanoid Robots, 2004 4th IEEE/RAS International Conference on Humanoid Robotics, Santa Monica, CA.

Mitoma, H., R. Hayashi, et al. (2000). "Characteristics of parkinsonian and ataxic gaits: a study using surface electromyograms, angular displacements and floor reaction forces." Journal of the neurological sciences **174**(1): 22-39.

Mochon, S. and T. A. McMahon (1980). "Ballistic walking." Journal of Biomechanics **13**(1): 49-57.

Morris, M., R. Iansek, et al. (1996). "Stride length regulation in Parkinson's disease." Brain **119**(2): 551.

Motion Lab Systems (2010). "The 3D Biomechanics Data Standard." 2010, from http://www.c3d.org/.

Mündermann, L., S. Corazza, et al. (2006). "The evolution of methods for the capture of human movement leading to markerless motion capture for biomechanical applications." Journal of NeuroEngineering and Rehabilitation **3**(1): 6.

Murray, M., A. Drought, et al. (1964). "Walking patterns of normal men." The Journal of Bone and Joint Surgery **46**(2): 335.

Murray, M., R. Kory, et al. (1969). "Walking patterns in healthy old men." The Journal of Gerontology **24**(2): 169.

Murray, M., R. Kory, et al. (1970). "Walking patterns of normal women." Archives of Physical Medicine and Rehabilitation **51**(11): 637-650.

Muybridge, E. (1979). Complete human and animal locomotion (All 781 Plates from the 1887 Animal Locomotion). DOVER PUBLICATIONS.

Netter, F. (2006). Atlas of human anatomy, Saunders.

Newton, I. (1833). Philosophiae naturalis principia mathematica perpetuis commentariis, Brookman.

Nigg, B. M. and W. Herzog (1994). Biomechanics of the musculo-skeletal system, Wiley.

Norkin, C. C. and P. K. Levange (1992). Joint Structure and Function. A Comprehensive Analysis., F. A. Davis Company.

Nussbaum, M. (1985). Aristotle's De motu animalium, Princeton Univ Pr.

O'Brien, J., B. Bodenheimer, et al. (2000). "Automatic joint parameter estimation from magnetic motion capture data." To appear in the proceedings of Graphics Interface: 1.

Öberg, T., A. Karsznia, et al. (1993). "Basic gait parameters: reference data for normal subjects, 10-79 years of age." Journal of rehabilitation research and development **30**: 210-210.

Orendurff, M. S., A. D. Segal, et al. (2004). "The effect of walking speed on center of mass displacement." Journal of Rehabilitation Research & Development **41**(6A): 829-834.

Ostrosky, K., J. VanSwearingen, et al. (1994). "A comparison of gait characteristics in young and old subjects." Physical Therapy **74**(7): 637.

Õunpuu, S. (1994). "Terminology for clinical gait analysis." Rep. Amer. Acad. Cerebral Palsy Developmental Medicine Gait Lab Committee.

Ounpuu, S., R. Davis, et al. (1996). "Joint kinetics: methods, interpretation and treatment decision-making in children with cerebral palsy and myelomeningocele." Gait and Posture **4**(1): 62-78.

Ounpuu, S., J. Gage, et al. (1991). "Three-dimensional lower extremity joint kinetics in normal pediatric gait." Journal of Pediatric Orthopaedics **11**(3): 341&hyhen.

Õunpuu, S. and D. A. Winter (1989). "Bilateral electromyographical analysis of the lower limbs during walking in normal adults." Electroencephalography and Clinical Neurophysiology **72**(5): 429-438.

Palliyath, S., M. Hallett, et al. (1998). "Gait in patients with cerebellar ataxia." Movement Disorders **13**(6): 958-964.

Park, B., H. Song, et al. (1997). "Gait electromyography in children with myelomeningocele at the sacral level." Archives of Physical Medicine and Rehabilitation **78**(5): 471-475.

Park, J. (2008). "Synthesis of natural arm swing motion in human bipedal walking." Journal of Biomechanics **41**(7): 1417-1426.

Paul, J. (1996). "Visual guidance to forceplates does not influence ground reaction force variability " Journal of Biomechanics **29**(6): 833.

Perry, J. (1992). Gait analysis: normal and pathological function, SLACK incorporated.

Perry, J. and G. Bekey (1981 a)). "EMG-force relationships in skeletal muscle." Crit Rev Biomed Eng **7**(1): 1-22.

Perry, J., C. Easterday, et al. (1981 b)). "Surface versus intramuscular electrodes for electromyography of superficial and deep muscles." Physical Therapy **61**(1): 7.

Petrofsky, J. (2001 a)). "Microprocessor-based gait analysis system to retrain Trendelenburg gait." Medical and Biological Engineering and Computing **39**(1): 140-143.

Petrofsky, J. (2001 b)). "The use of electromyogram biofeedback to reduce Trendelenburg gait." European journal of applied physiology **85**(5): 491-495.

Pina, J. A. E. (1999). Anatomia Humana da Locumação, Lidel.

Pizzi, A., G. Carlucci, et al. (2007). "Gait in hemiplegia: evaluation of clinical features with the Wisconsin gait scale." Journal of Rehabilitation Medicine **39**(2): 170-174.

Pratt, F. (1917). "The all-or-none principle in graded response of skeletal muscle." american Journal of Physiology **44**(4): 517.

QUALYSIS, A. (2010). Qualisys Track Manager User Manual.

Ralston, H., F. Todd, et al. (1976). "Comparison of electrical activity and duration of tension in the human rectus femoris muscle." Electromyography and clinical neurophysiology **16**(2-3): 271.

Redi, F. (1671). Esperienze intorno a diverse cose naturali.

Ricamato, A. L. and J. M. Hidler (2004). "Quantification of the dynamic properties of EMG patterns during gait." Journal of Electromyography and Kinesiology **15**(4): 384-392.

Richards, J. (1999). "The measurement of human motion: a comparison of commercially available systems." Human movement science **18**(5): 589-602.

Richards, J. (2008). Biomechanics in Clinic and Research, Churchill Livingstone.

Riggs, B. L., L. J. Melton, et al. (2004). "Population-Based Study of Age and Sex Differences in Bone Volumetric Density, Size, Geometry, and Structure at Different Skeletal Sites." Journal of Bone and Mineral Research **19**(12): 1945-1954.

Rose, S., P. DeLuca, et al. (1993). "Kinematic and kinetic evaluation of the ankle after lengthening of the gastrocnemius fascia in children with cerebral palsy." Journal of Pediatric Orthopaedics **13**(6): 727.

Sabir, M. and D. Lytlle (1984). "Pathogenesis of Charcot-Marie-Tooth Disease. Gait analysis and electrophysiologic, genetic, histopathologic, and enzyme studies in a kinship." Clinical Orthopaedics and Related Research **184**: 223.

Sadeghi, H., P. Allard, et al. (2000). "Symmetry and limb dominance in able-bodied gait: a review." Gait & Posture **12**(1): 34-45.

Saunders, M., T. Inman, et al. (1953). "The Major Determinants in Normal and Pathological Gait." The Journal of Bone and Joint Surgery **35**(3): 543-558.

Schiehlen, W. and M. Ackermann (2005). Estimation of Metabolical Costs for Human Locomotion. 5th International Conference on Multibody Systems, Nonlinear Dynamics, and Control, Parts A, B, and C. **6:** 299-315.

Segers, V. (2006). A biomechanical analysis of the realization of actual human gait transition, Universiteit Gent.

Silva, M. T. d. (2003). Human Motion Analyisis using Multibody Dynamics and Optimization Tools. IDMEC/IST. Lisboa, Instituto Superior Técnico. **PhD**.

Soderberg, G. L. (1992). Selected Topics in Surface Electromiography for Use in the Occupational Setting: Expert Perspectives, U.S. Department of Health and Human Services.

Stauffer, R., E. Chao, et al. (1977). "Biomechanical gait analysis of the diseased knee joint." Clinical Orthopaedics and Related Research **126**: 246.

Stein, R. B. and V. Mushahwar (2005). "Reanimating limbs after injury or disease." TRENDS in Neurosciences **28**.

Stolze, H., S. Klebe, et al. (2002). "Typical features of cerebellar ataxic gait." Journal of Neurology, Neurosurgery & Psychiatry **73**(3): 310.

Sutherland, D. (1966). "An electromyographic study of the plantar flexors of the ankle in normal walking on the level." The Journal of Bone and Joint Surgery **48**(1): 66.

Sutherland, D. (1984). Gait disorders in childhood and adolescence, Williams & Wilkins Baltimore.

Sutherland, D. (1997). "The development of mature gait." Gait & Posture **6**: 163-170.

Sutherland, D. (2001). "The evolution of clinical gait analysis part l: kinesiological EMG." Gait & Posture **14**(1): 61-70.

Sutherland, D. (2002). "The evolution of clinical gait analysis-Part II Kinematics." Gait and Posture **16**(2): 159-179.

Sutherland, D. (2005). "The evolution of clinical gait analysis part III-kinetics and energy assessment." Gait and Posture **21**(4): 447-461.

Sutherland, D., F. Bost, et al. (1960). "Electromyographic study of transplanted muscles about the knee in poliomyelitic patients." The Journal of Bone and Joint Surgery **42**(6): 919.

Sutherland, D., R. Olshen, et al. (1988). The development of mature walking, Cambridge University Press.

Sutherland, D., R. Olshen, et al. (1980). "The development of mature gait." The Journal of Bone and Joint Surgery.

Sutherland, D., R. Olshen, et al. (1980). "The development of mature gait." The Journal of Bone and Joint Surgery **62**(3): 336.

Sutherland, D., E. Schottstaedt, et al. (1969). "Clinical and electromyographic study of seven spastic children with internal rotation gait." The Journal of Bone and Joint Surgery **51**(6): 1070.

Terzopoulos, D. and H. Qin (1994). "Dynamic NURBS with geometric constraints for interactive sculpting." ACM Transactions on Graphics **13**(2): 103-136.

Thackeray, C. and P. Beeson (1996). "In-toeing gait in children. A review of the literature." The Foot **6**(1): 1-4.

Tortora, G. J. and S. R. Grabowsky (2004). Introduction to the human body, Wiley.

Tyrrell, P. (1994). "Apraxia of gait or higher level gait disorders: review and description of two cases of progressive gait disturbance due to frontal lobe degeneration." Journal of the Royal Society of Medicine **87**(8): 454.

Umberger, B. R., K. G. M. Gerristen, et al. (2003). "A Model of Human Muscle Energy Expenditure." Computer Methods in Biomechanics and Biomedical Engineering **6**(2): 99-111.

Vanneste, J. (2000). "Diagnosis and management of normal-pressure hydrocephalus." Journal of neurology **247**(1): 5-14.

Vaughan, C. L., B. L. Davis, et al. (1999). Dynamics of Human Gait, Kiboho Publishers.

Walsh, M., P. Connolly, et al. (2000). "Leg length discrepancy--an experimental study of compensatory changes in three dimensions using gait analysis." Gait & Posture **12**(2): 156-161.

Washburn, S. L. (1948). "Sex differences in the pubic bone." American Journal of Physical Anthropology **6**(2): 199-208.

Waters, R. L. and S. Mulroy (1999). "The energy expenditure of normal and pathologic gait." Gait & Posture **9**(3): 207-231.

Wearing, S., S. Urry, et al. (2000). "The effect of visual targeting on ground reaction force and temporospatial parameters of gait." Clinical Biomechanics **15**(8): 583-591.

Weber, W. and E. Weber (1836). Mechanik der menschlichen Gehwerkzeuge: Eine anatomisch-physiologische Untersuchung, Dietrich.

Whittle, M. (2002). Gait analysis: an introduction, Butterworth-Heinemann Medical.

Winter, D. (1979). "A new definition of mechanical work done in human movement." Journal of Applied Physiology **46**(1): 79.

Winter, D. (1981). "Use of kinetic analyses in the diagnostics of pathological gait." Physiotherapy Canada **33**: 209-214.

Winter, D. (1983). "Energy generation and absorption at the ankle and knee during fast, natural, and slow cadences." Clinical Orthopaedics and Related Research **175**: 147-154.

Winter, D. (1984). "Kinematic and kinetic patterns in human gait: variability and compensating effects." Human movement science **3**(1-2): 51-76.

Winter, D. (1990). Biomechanics and motor control of human movement, Wiley.

Winter, D., C. MacKinnon, et al. (1993). "An integrated EMG/biomechanical model of upper body balance and posture during human gait." Progress in brain research **97**: 359-367.

Winter, D., A. Patla, et al. (1990). "Biomechanical walking pattern changes in the fit and healthy elderly." Physical Therapy **70**(6): 340.

Winter, D., A. Quanbury, et al. (1975). "Instantaneous power and power flow in body segments during walking." Journal of Human Movement Studies **1**: 59-67.

Winter, D., A. Quanbury, et al. (1976). "Analysis of instantaneous energy of normal gait." Journal of Biomechanics **9**(4): 253-257.

Winter, D. and D. Robertson (1978). "Joit torque and energy patterns in normal gait." Biological cybernetics **29**(3): 137-142.

Winter, D. and H. Yack (1987). "EMG profiles during normal human walking: stride-to-stride and inter-subject variability." Electroencephalography and Clinical Neurophysiology **67**(5): 402-411.

Winter, D. A. (1991). The Biomechanics and Motor Control of Human Gait: Normal, Elderly and Pathological, University of Waterloo Press.

Wu, G., F. C. T. v. d. Helm, et al. (2005). "ISB recommendation on definitions of joint coordinate systems of various joints for the reporting of human joint motion—Part II: shoulder, elbow, wrist and hand." Journal of Biomechanics **35**(5): 981-992.

Wu, G., S. Siegler, et al. (2002). "ISB recommendation on definitions of joint coordinate system of various joints for the reporting of human joint motion—part I: ankle, hip, and spine " Journal of Biomechanics **35**(4): 543-548.

Yang, J. and D. Winter (1984). "Electromyographic amplitude normalization methods: improving their sensitivity as diagnostic tools in gait analysis." Archives of Physical Medicine and Rehabilitation **65**(9): 517.

Yang, J. and D. Winter (1985). "Surface EMG profiles during different walking cadences in humans." Electroencephalography and Clinical Neurophysiology **60**(6): 485-491.

Yokochi, K. (2001). "Gait patterns in children with spastic diplegia and periventricular leukomalacia." Brain and Development **23**(1): 34-37.

Zhou, H. and H. Hu (2004). "A survey-human movement tracking and stroke rehabilitation." University of Essex, Colchester United Kingdom.

Appendix A – Anatomy
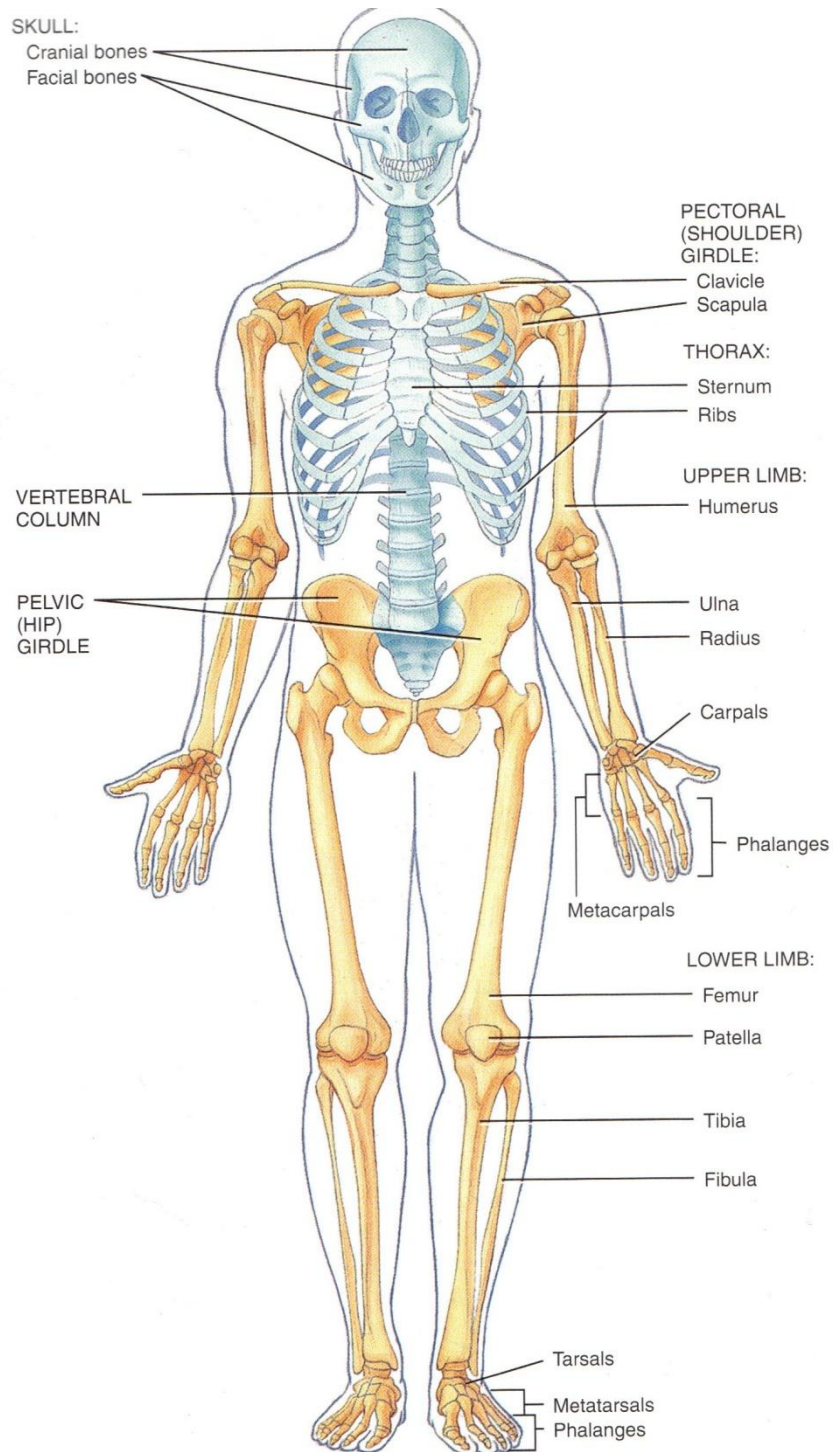
Figure 59 – representation of human adult skeleton (Anterior View): Axial skeletal (Blue) and Appendicular Skeleton (yellow) (Tortora and Grabowsky 2004)
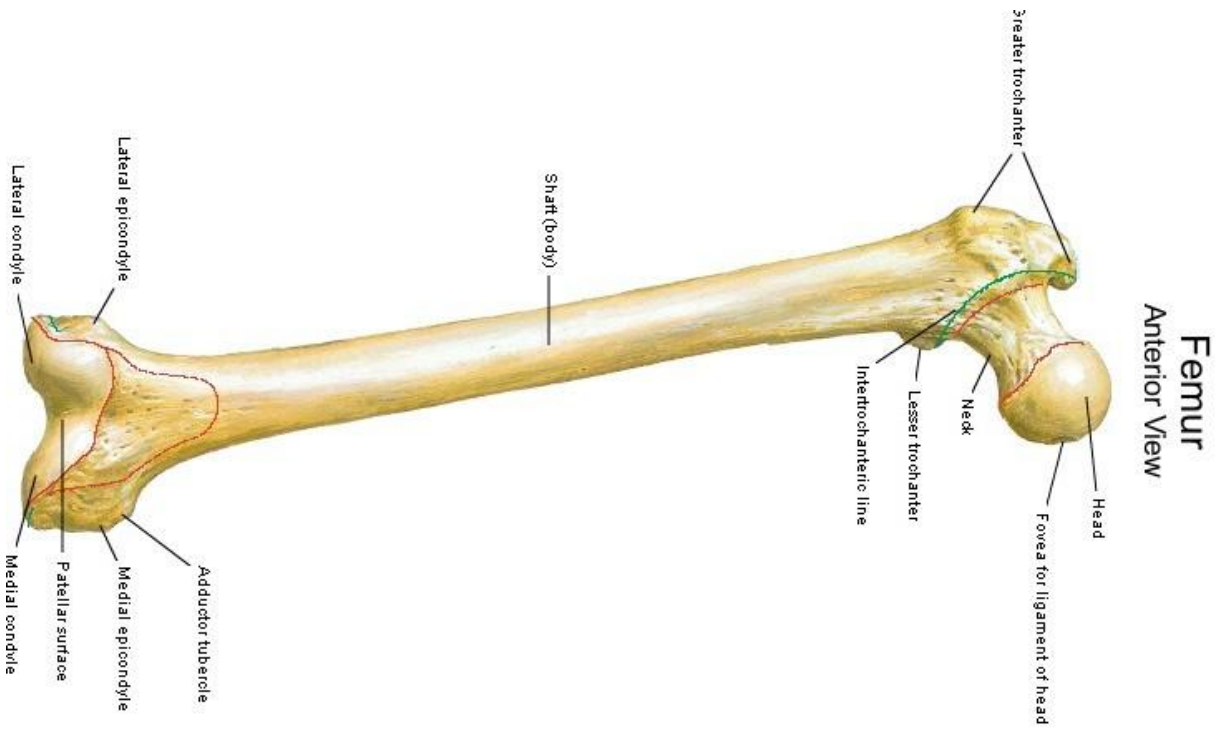
Figure 60 – Femur – Anterior View (Netter 2006)
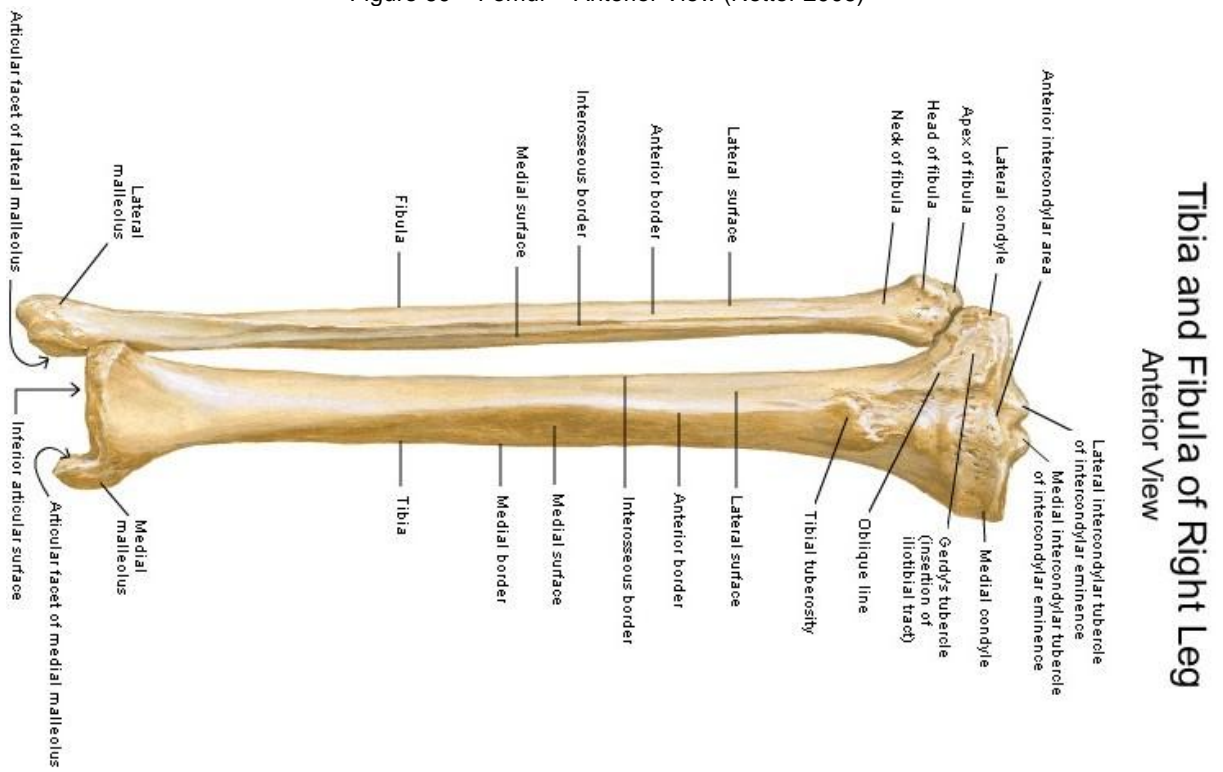
Figure 61 – Tibia and Fibula – Anterior View (Netter 2006)
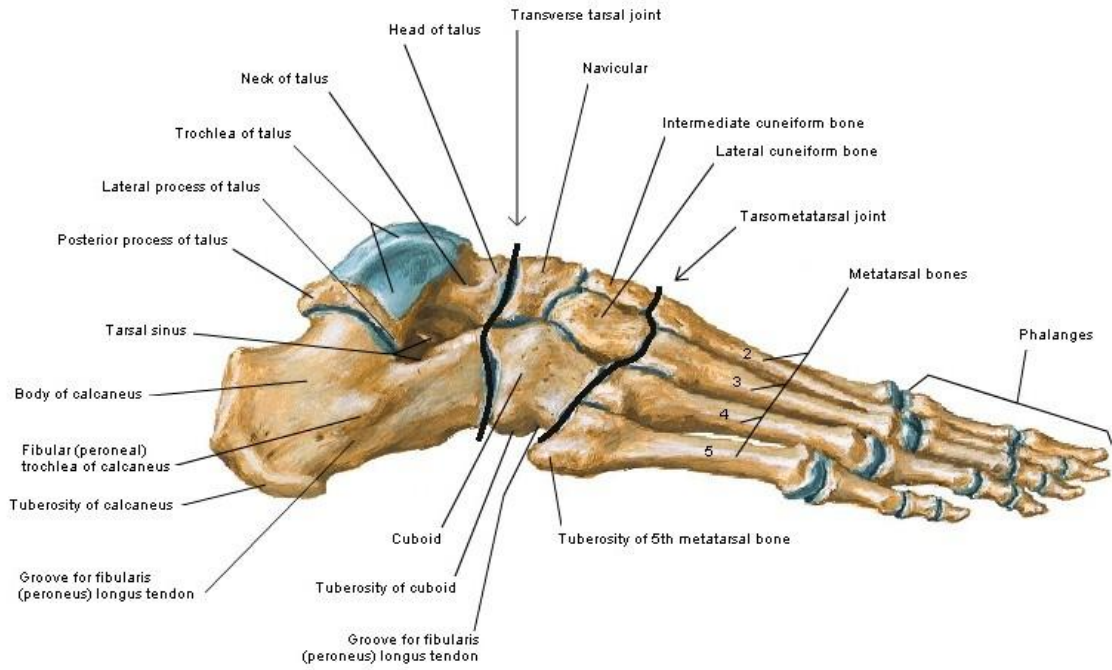
Figure 62 – Foot bones: a) Lateral View (above) b) Dorsal View (below) (Netter 2006)
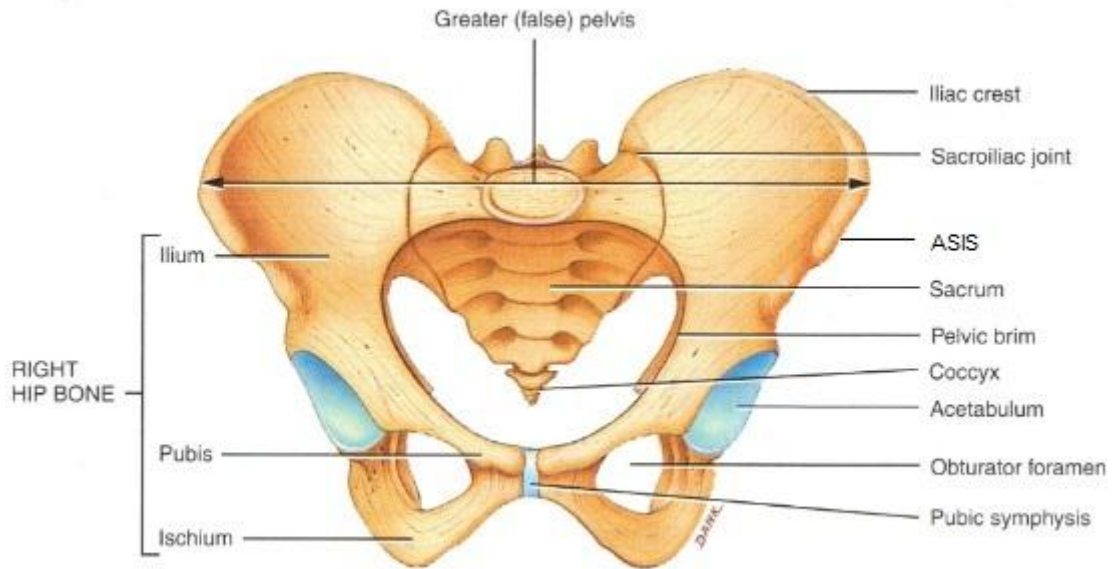
Figure 63 – representation of Women Pelvic girdle (Tortora and Grabowsky 2004)
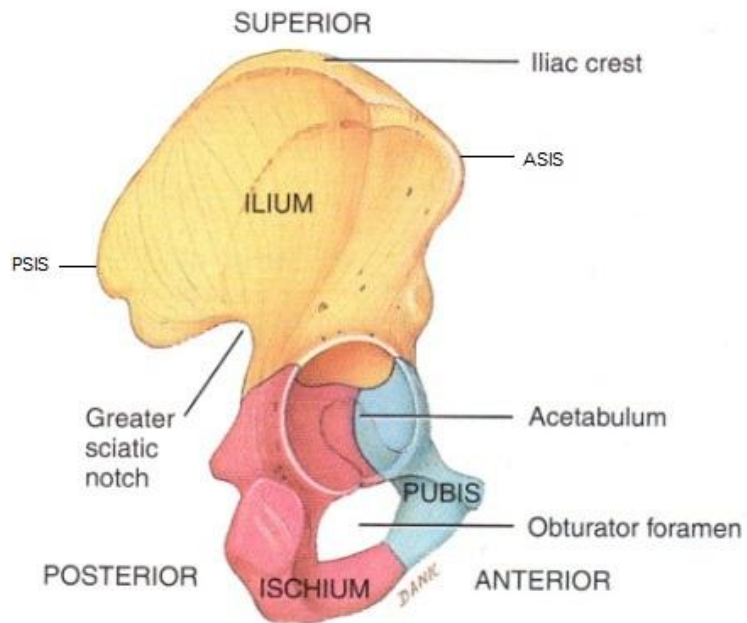
Figure 64 – representation of right hip bone (Tortora and Grabowsky 2004)

Anterior superior iliac spine

Sartorius muscle (origin)

Tensor fasciae latae muscle (origin)

Rectus femoris muscle (origin)

Greater trochanter

Iliopsoas muscle (cut)

Adductor longus muscle

Gracilis muscle

Vastus lateralis muscle

Vastus intermedius muscle

Vastus medialis muscle

Anteromedial intermuscular septum

Iliotibial tract (cut)

Rectus femoris tendon (cut)

Quadriceps femoris tendon

Lateral patellar retinaculum

Medial patellar retinaculum

Patella

Lateral patellar retinaculum

Head of fibula

Patellar ligament

Tibial tuberosity

Sartorius tendon

Anterior inferior iliac spine

Ligaments of hip joint

Pectineus muscle

Iliac crest

Gluteal aponeurosis over
gluteus medius muscle

Gluteus maximus muscle

Semitendinosus muscle

Biceps femoris muscle (long head)

Adductor minimus part of
adductor magnus muscle

Semimembranosus muscle

Iliotibial tract

Gracilis muscle

Short head of biceps femoris muscle

Long head of biceps femoris muscle

Semimembranosus muscle

Semitendinosus muscle

Popliteal vessels and tibial nerve

Common fibular (peroneal) nerve

Plantaris muscle

Medial head of gastrocnemius muscle

Lateral head of gastrocnemius muscle

Sartorius muscle

Soleus muscle

Figure 65 – Superficial Muscles of Hip and Thigh: a) Anterior View b) Posterior View (Netter)

143

Muscles of Leg (Superficial Dissection)
Anterior View
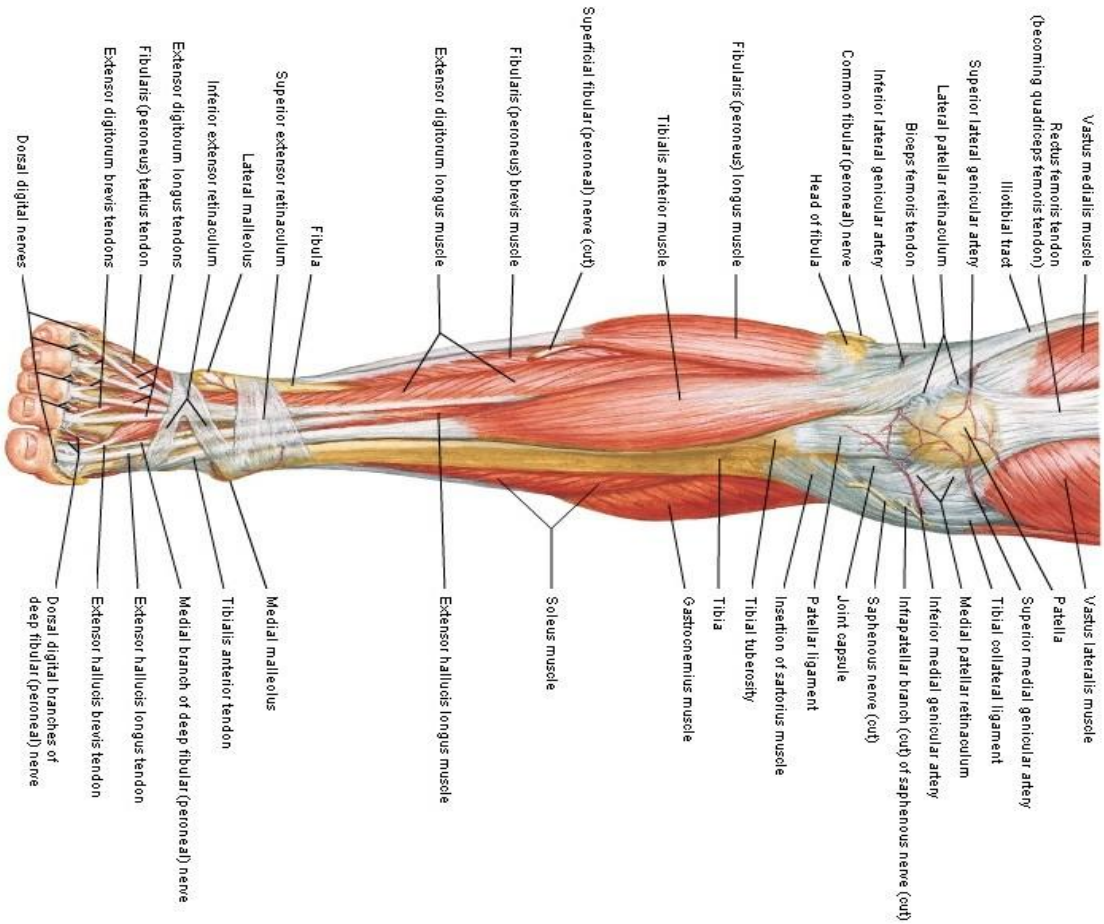
Muscles of Leg (Superficial Dissection)
Posterior View
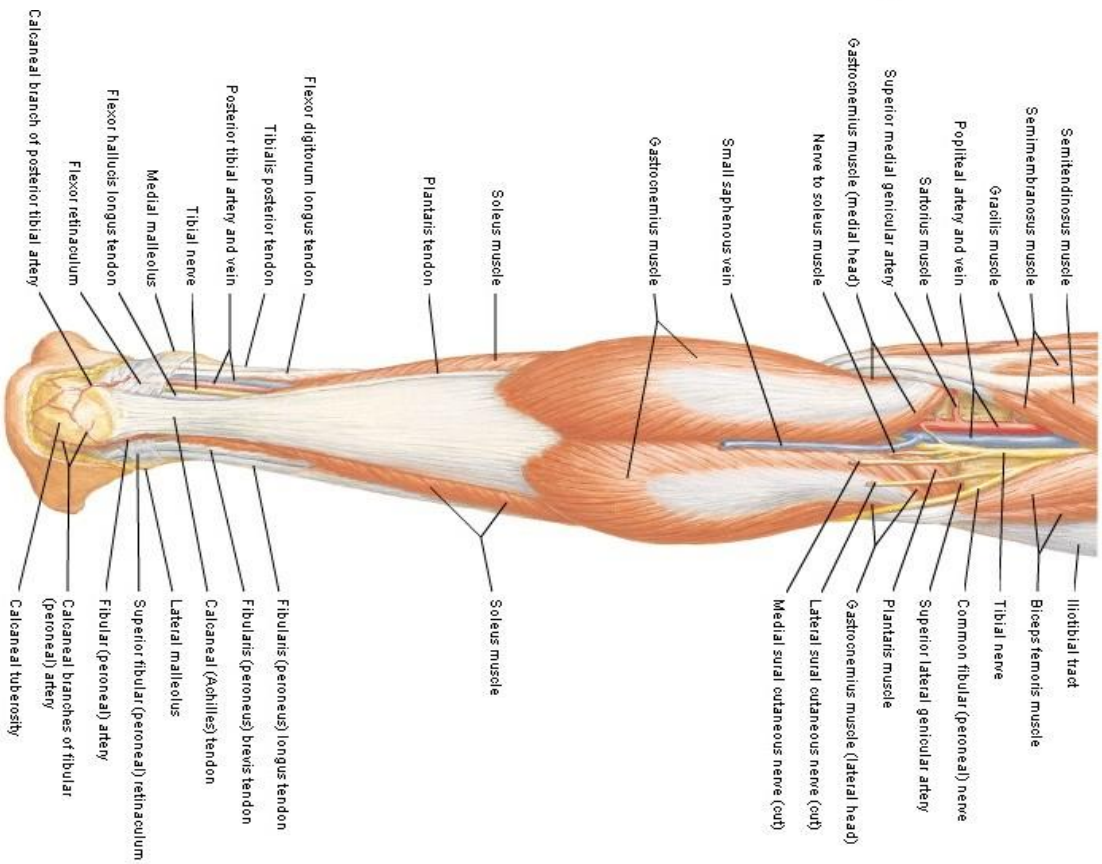
Figure 66 – Superficial muscles of leg: a) Anterior view b) Posterior view (Netter)
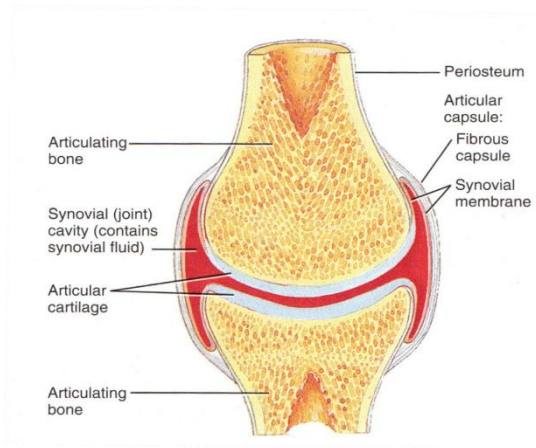
Figure 67 – Structure of a typical synovial joint
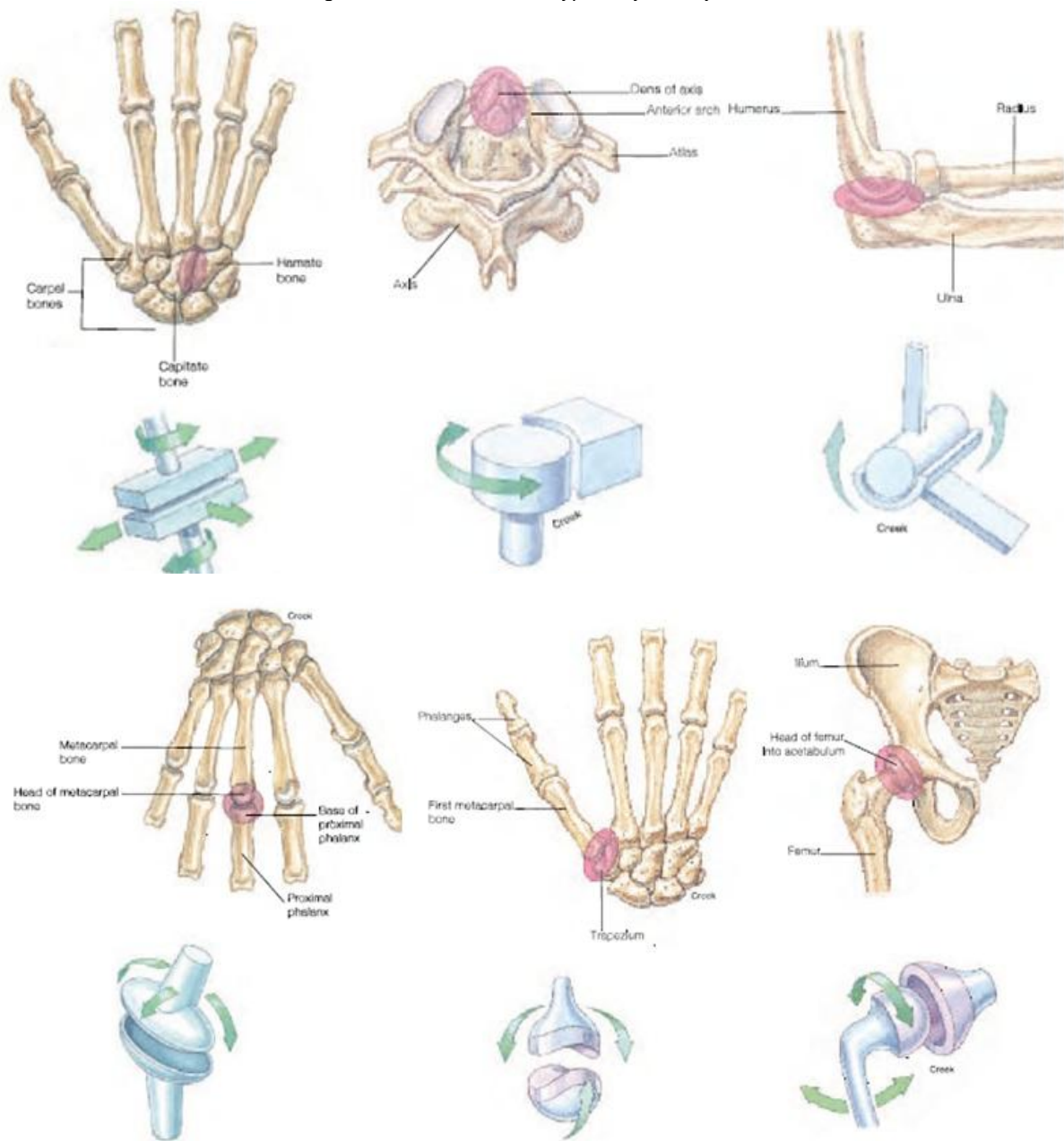
Figure 68 – Types of synovial joints: a) gliding (intercarpal articulation) b) pivot (atlas) c) hinge (elbow) d) condyloid (metacarpophalangeal articulations) e) saddle (trapezium articulates) f) ball-and-socket (hip joint)
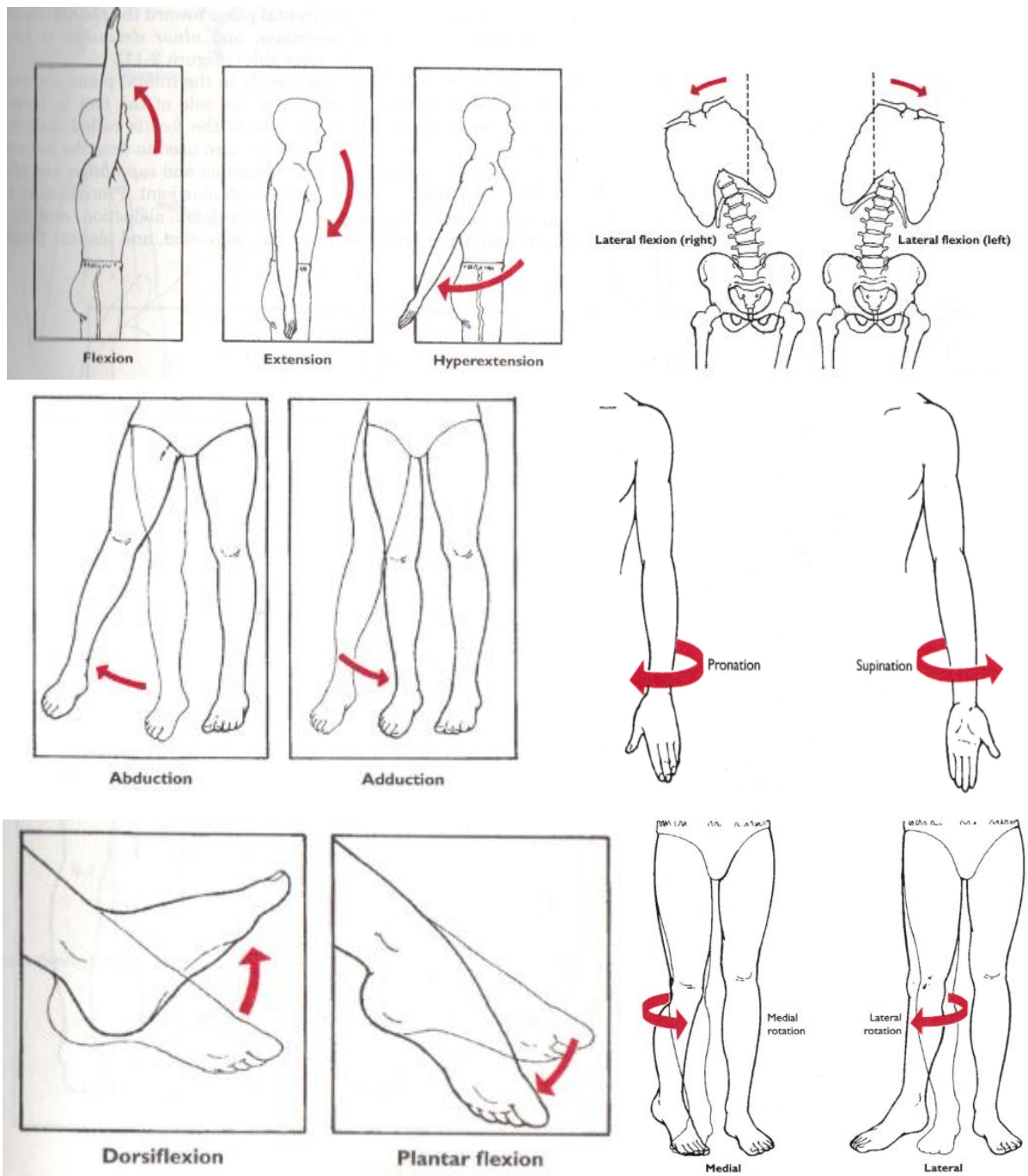
Figure 69 – Joint movement terminology

Appendix B – Extensive Marker Set Protocol

Maker Nº	Location	Anatomic Landmark	Maker Nº	Location	Anatomic Landmark
0	Anterior left Skull	Temporal line of frontal bone	24	Pelvis	Right PSIS
1	Anterior Right Skull	Temporal line of frontal bone	25	Left Distal Knee	Most prominent point of lateral femoral epicondyle
2	Posterior Left Skull	Occipital protuberance (left)	26	Left Medial Knee	Most prominent point of medial femoral epicondyle
3	Posterior Right Skull	Occipital protuberance (Right)	27	Left Distal Ankle	Most prominent point of lateral malleolus
4	neck	Spinous Process of C7	28	Left Medial Ankle	Most prominent point of medial malleolus
5	Left Shoulder	Clavicle – Acromion	29	Left Foot	Upper ridge of the calcaneus posterior surface
6	Right Shoulder	Clavicle – Acromion	30	Left Foot	II metatarsal head
7	Left Distal Elbow	Lateral epicondyle of humerus	31	Left Foot	V metatarsal head
8	Left Medial Elbow	Medial epicondyle of humerus	32	Left Foot	V metatarsal base
9	Left Wrist	styloid process of radius	33	Right Distal Knee	Most prominent point of lateral femoral epicondyle
10	Left Wrist	styloid process of ulna	34	Right Medial Knee	Most prominent point of medial femoral epicondyle
11	Left Hand	Distal head of II Metacarpus	35	Right Distal Ankle	Most prominent point of lateral malleolus
12	Left Hand	Distal head of V Metacarpus	36	Right Medial Ankle	Most prominent point of medial malleolus
13	Right Distal Elbow	Most prominent point of lateral epicondyle of humerus	37	Right Foot	Upper ridge of the calcaneus posterior surface
14	Right Medial Elbow	Most prominent point of medial epicondyle of humerus	38	Right Foot	II metatarsal head
15	Right Wrist	styloid process of radius	39	Right Foot	V metatarsal head
16	Right Wrist	styloid process of ulna	40	Right Foot	V metatarsal base
17	Right Hand	Distal head of II Metacarpus	41	Left Hip Joint	Center of acetabulum
18	Right Hand	Distal head of V Metacarpus	42	Right Hip Joint	Center of acetabulum
19	Pelvis	Left iliac crest (LIC)	43-46	Left Thigh	Cluster
20	Pelvis	Right iliac crest (RIC)	47-50	Left Leg	Cluster
21	Pelvis	Left ASIS	51-54	Right Thigh	Cluster
22	Pelvis	Right ASIS	55-58	Left Leg	Cluster
23	Pelvis	Left PSIS			

Appendix C – Developed Clothes
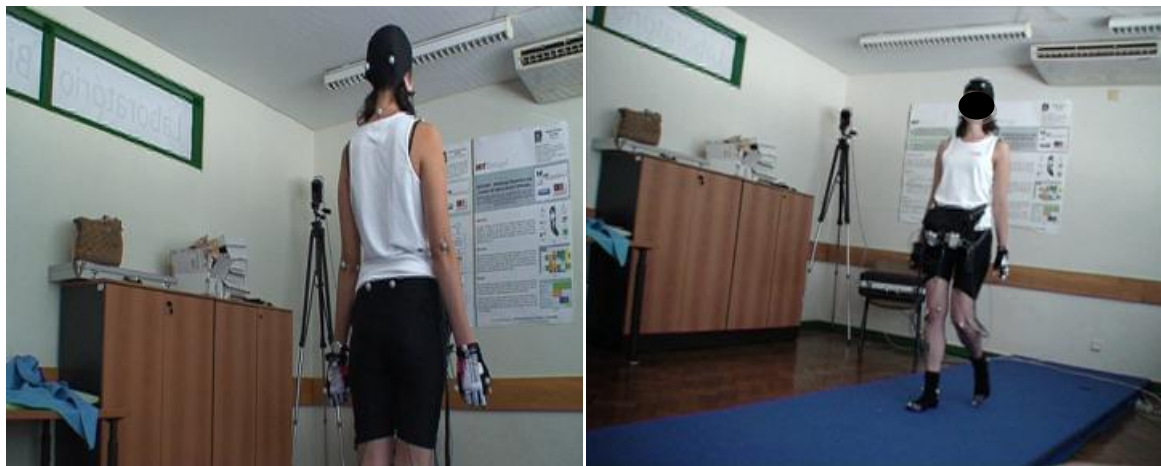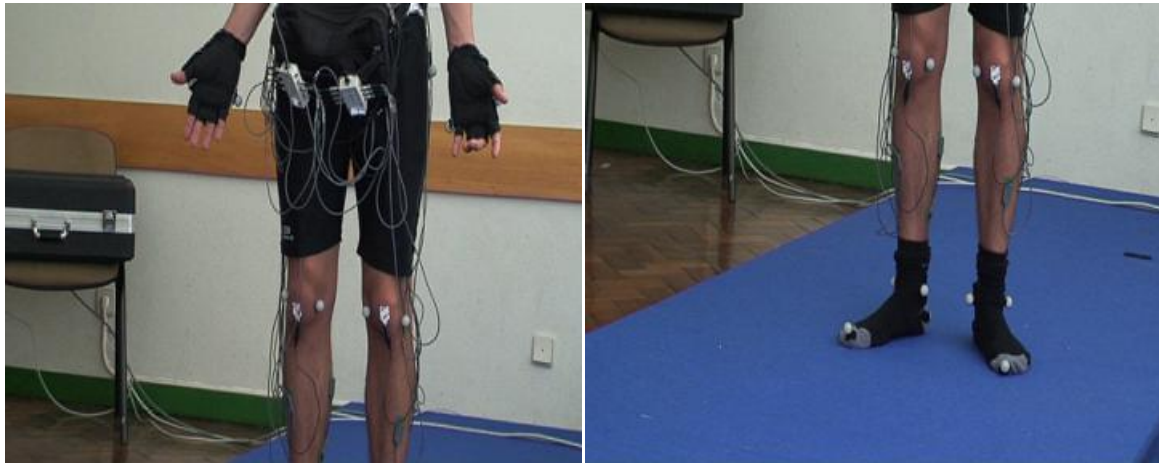
Appendix D – Database Interface
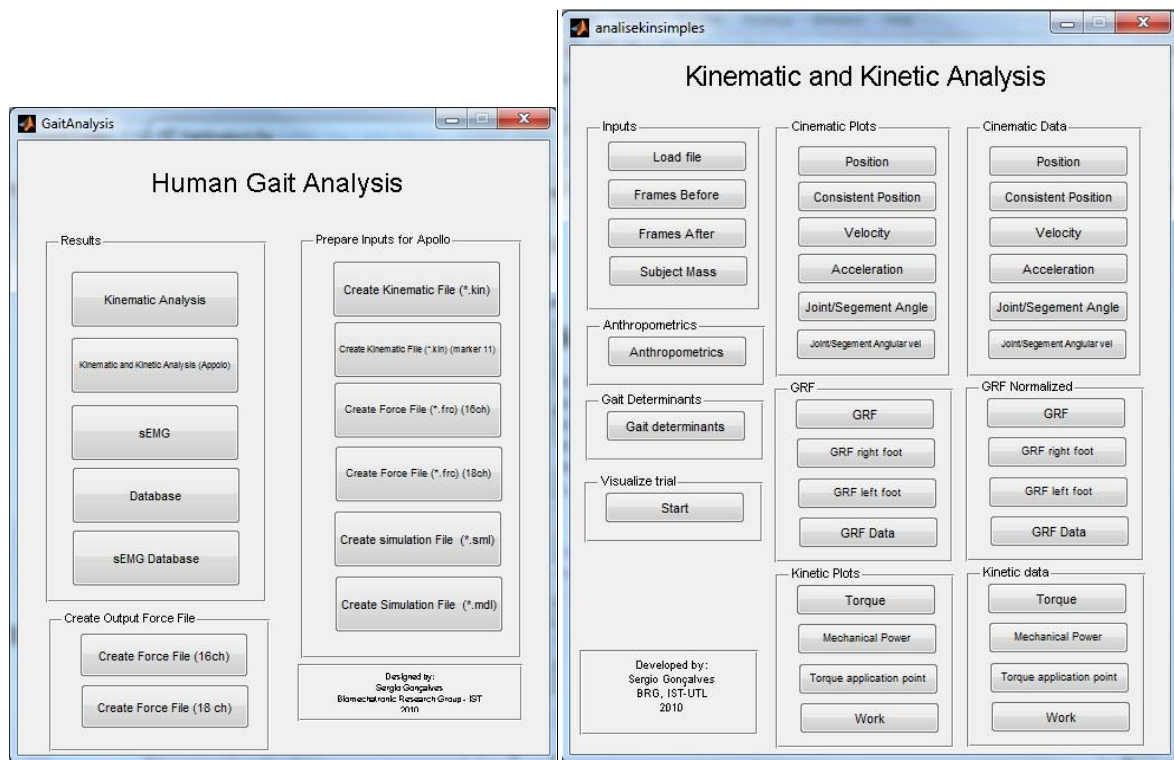
Figure 70 – Representation of the developed interfaces: a) Main menu (GaitAnalysis.fig) b) Analysis of a single file (ApolloAnalysis.fig)

Appendix E – Graphical representation of normal patterns
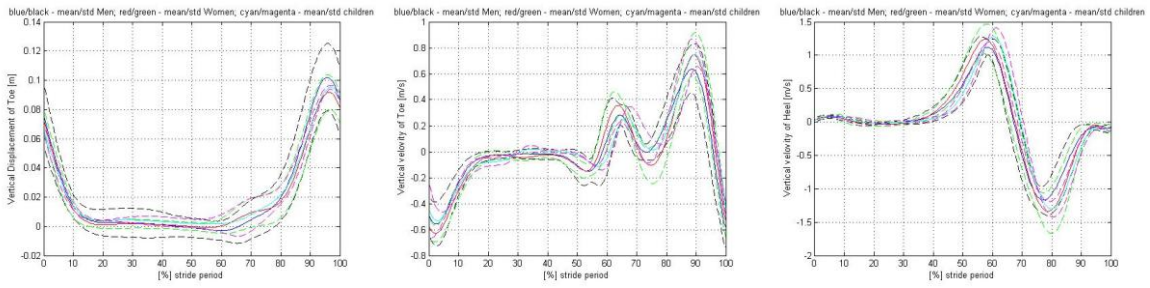
Figure 71 – Representation of displacement and velocity for men (blue/black), women (red/green), and children (cyan/magenta): a) Vertical displacement of Toe; b) Vertical velocity of Toe c) Vertical velocity of Heel
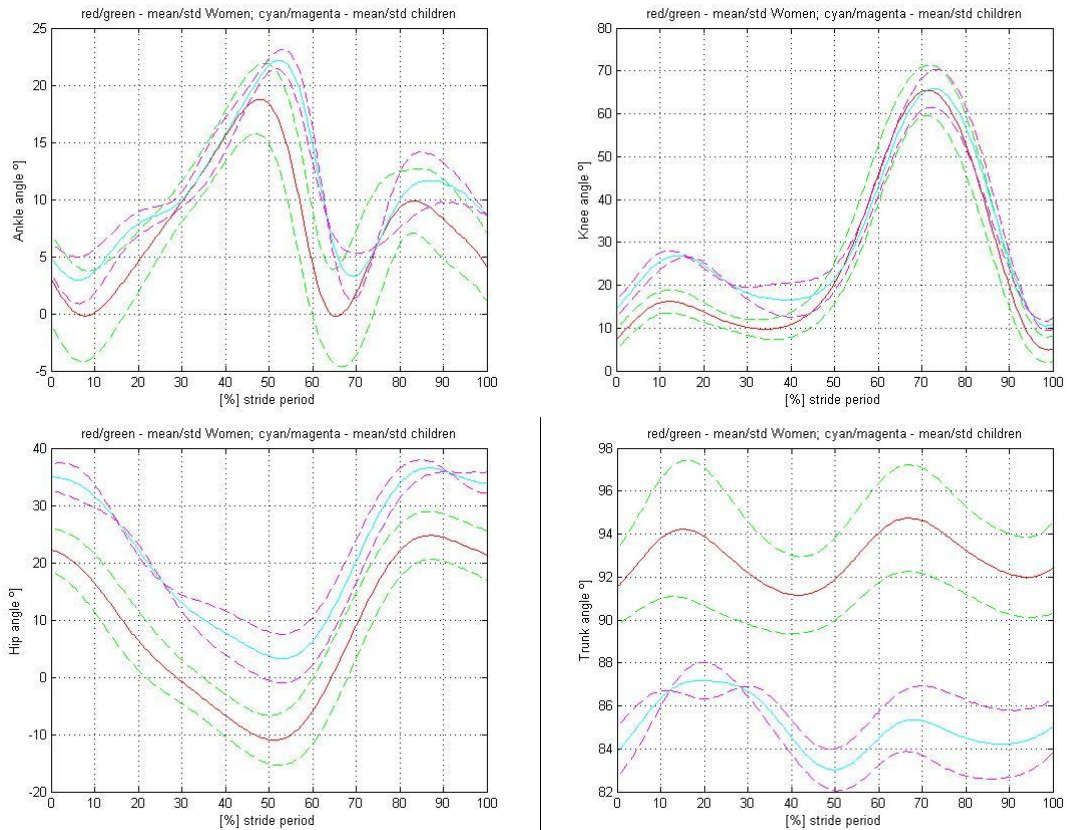
Figure 72 - Representation of joint/segment angles for women (red/green), and children (cyan/magenta): ankle; b) knee; c) hip d) trunk
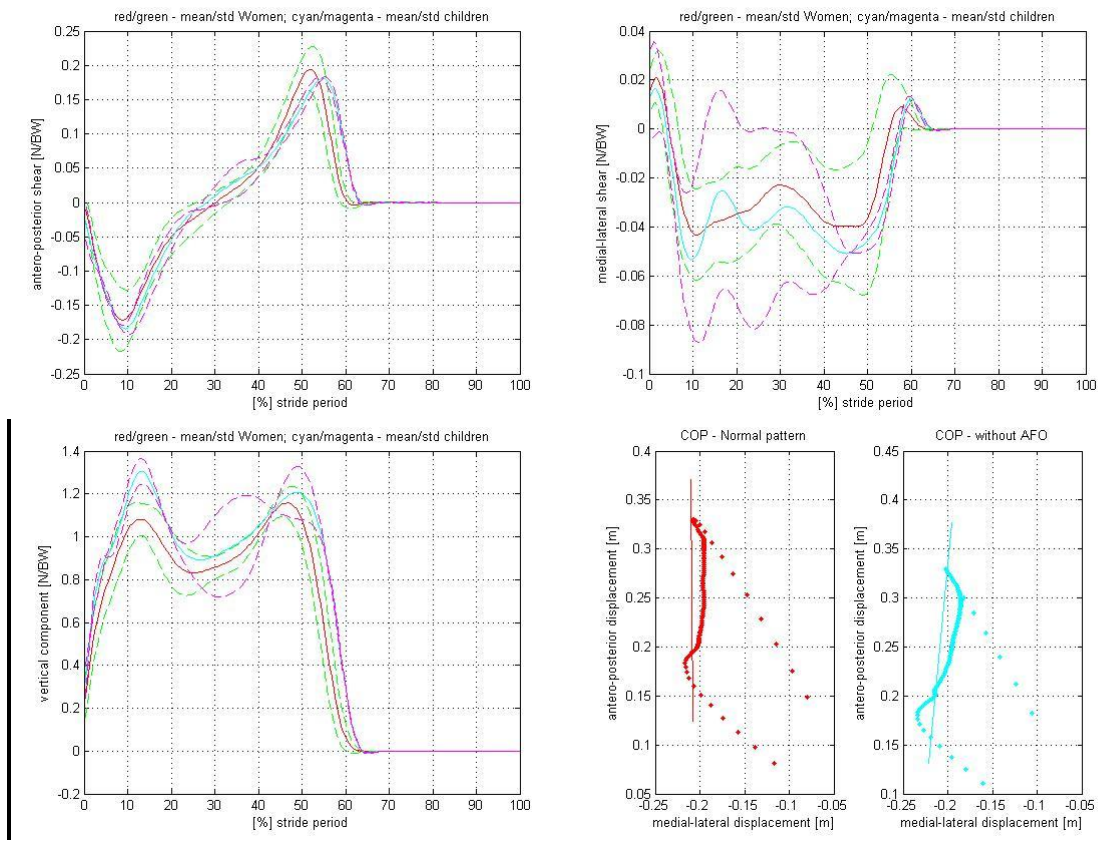
Figure 73 – Representation of the GRF and COP for women (red/green), and children (cyan/magenta): a) Antero-posterior; b) medial-lateral; c) vertical d) COP – the color line segments represent the foot angle in horizontal place (end points – heel marker and toe marker)
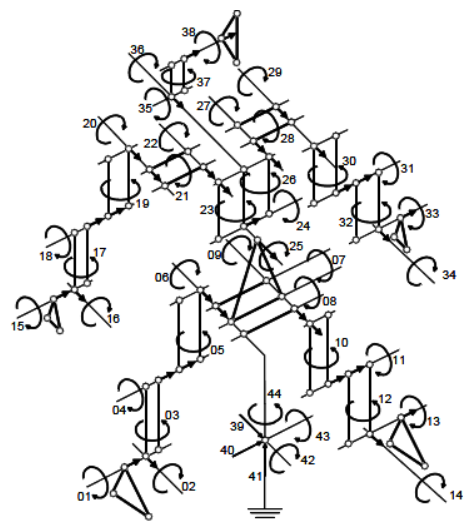
Figure 74 – Schematic representation of the 44 DOF of the biomechanical model used in the Apollo Software (Silva 2003)
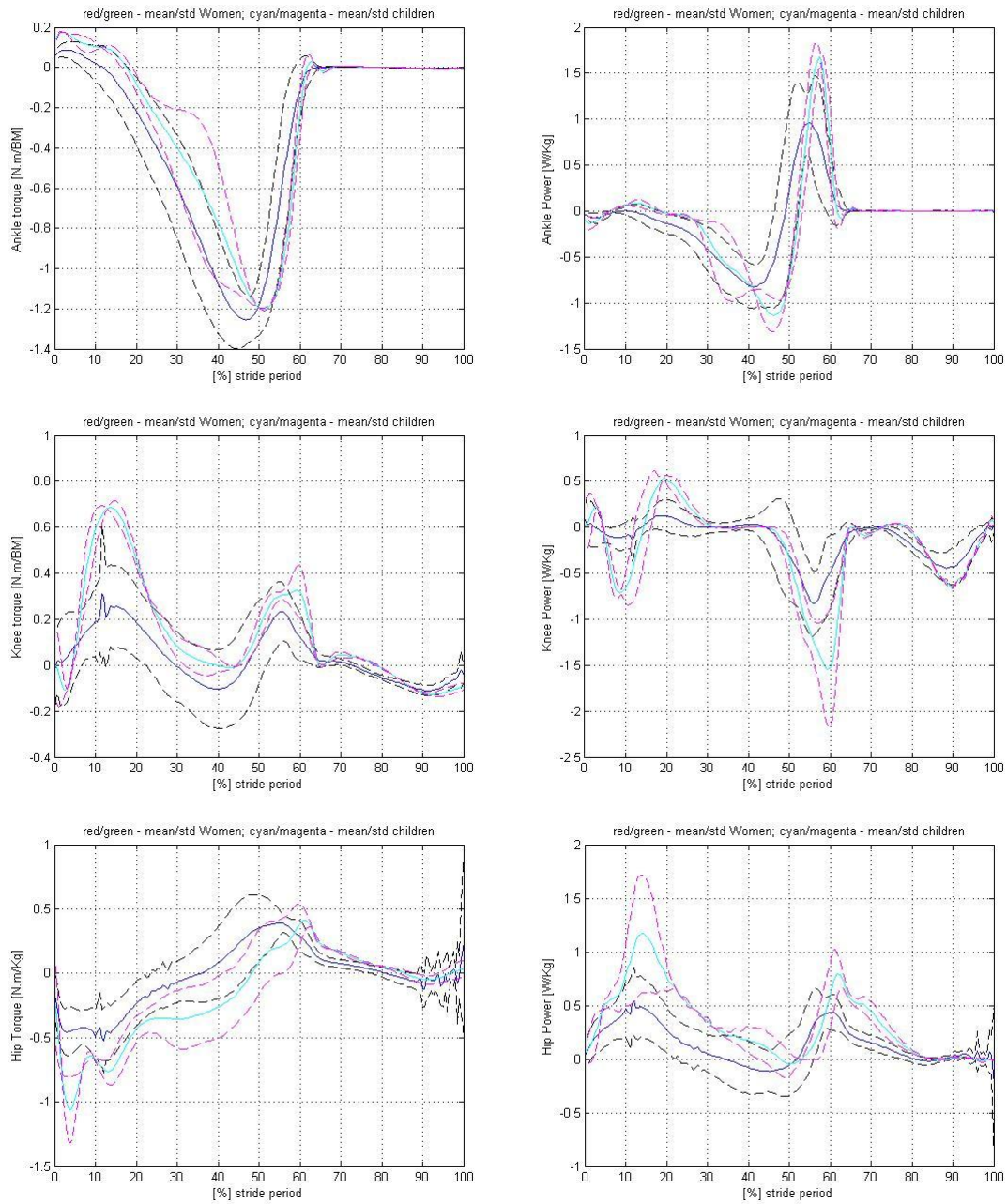
Figure 75 - Representation of torques and mechanical power for men (blue/black), and children (cyan/magenta):
a) ankle torque; b) ankle power; c) knee torque; d) knee power; e) hip torque; f) hip power
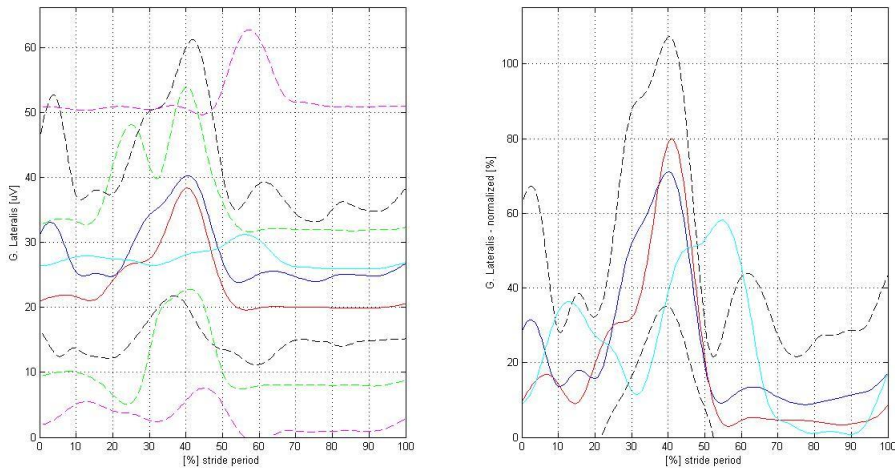
Figure 76 - Representation of sEMG signal of Gastrocnemius Lateralis for men (blue/black), women (red/green), and children (cyan/magenta): a) MAV b) Normalized
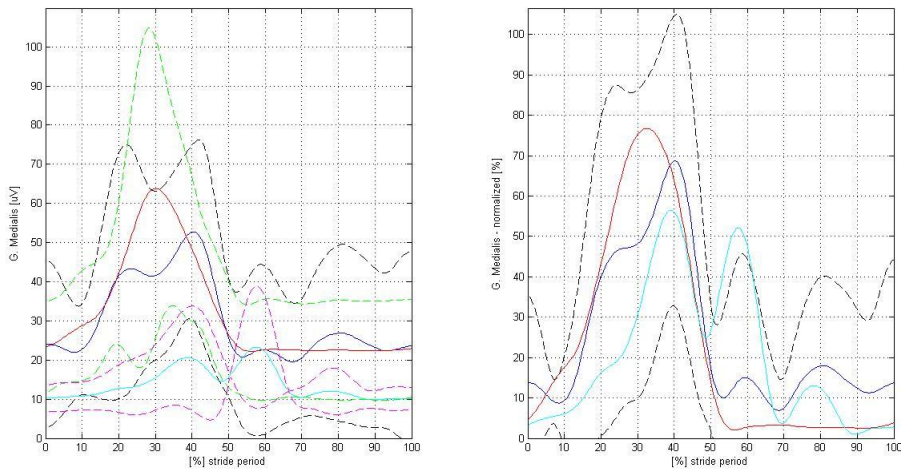
Figure 77 - Representation of sEMG signal of Gastrocnemius Medialis for men (blue/black), women (red/green), and children (cyan/magenta): a) MAV b) Normalized
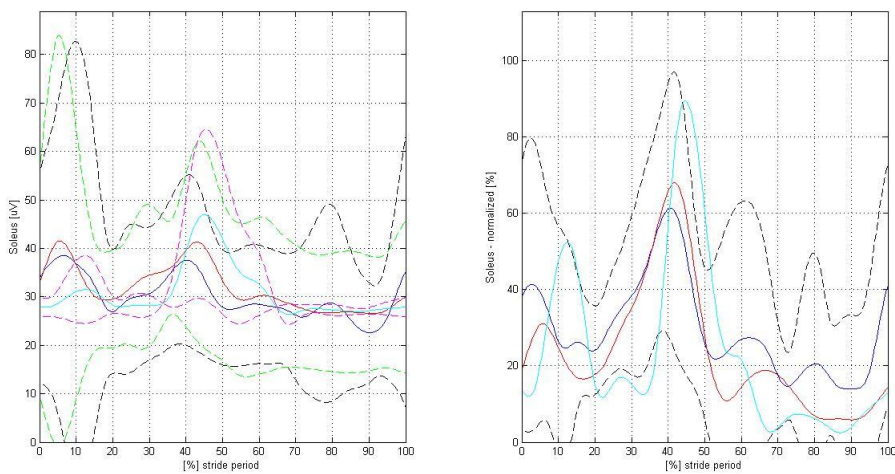
Figure 78 - Representation of sEMG signal of Soleus for men (blue/black), women (red/green), and children (cyan/magenta): a) MAV b) Normalized

153
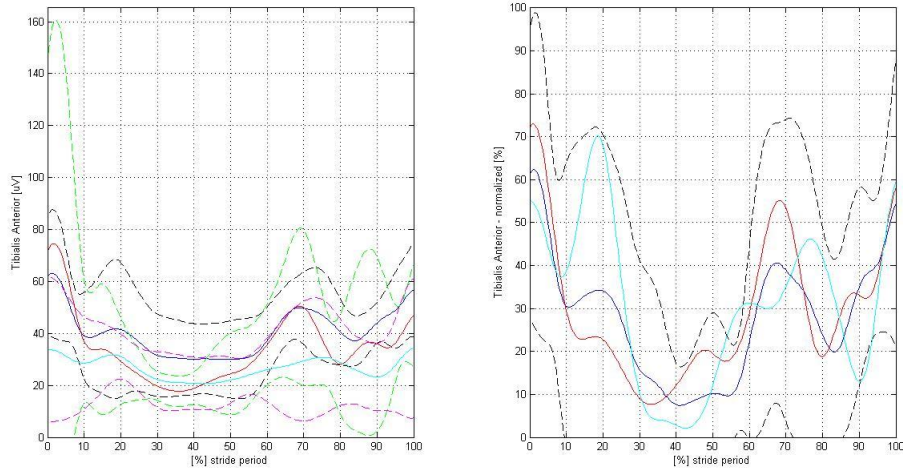
Figure 79 - Representation of sEMG signal of Tibialis Anterior for men (blue/black), women (red/green), and children (cyan/magenta): a) MAV b) Normalized
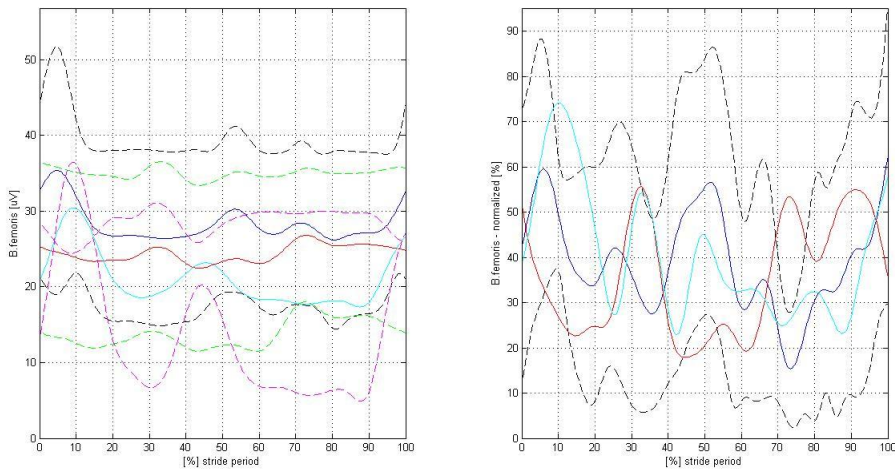
Figure 80 - Representation of sEMG signal of Biceps Femoris for men (blue/black), women (red/green), and children (cyan/magenta): a) MAV b) Normalized
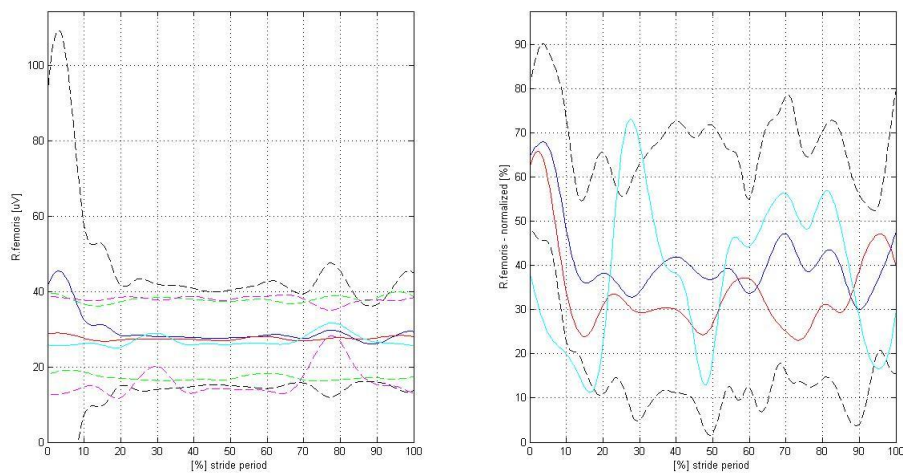
Figure 81 - Representation of sEMG signal of Rectus Femoris for men (blue/black), women (red/green), and children (cyan/magenta): a) MAV b) Normalized

154
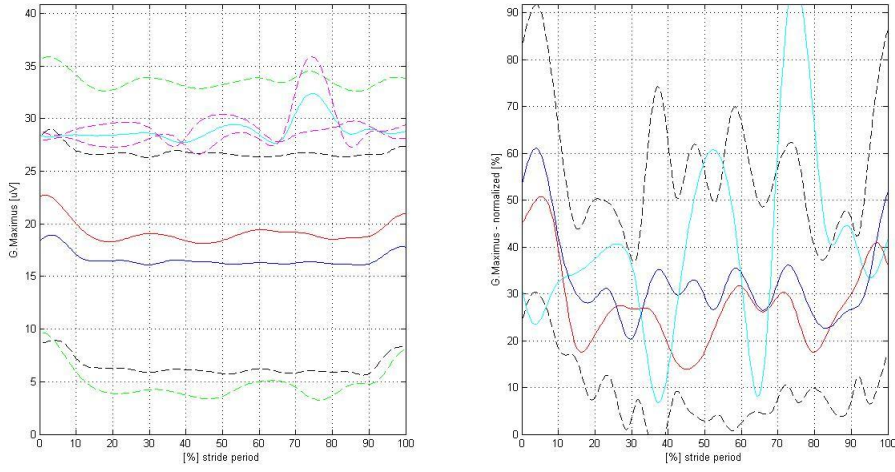
Figure 82 - Representation of sEMG signal of Rectus Femoris for men (blue/black), women (red/green), and children (cyan/magenta): a) MAV b) Normalized

Appendix F - Intra-subject Variability – Subject 1 and 2
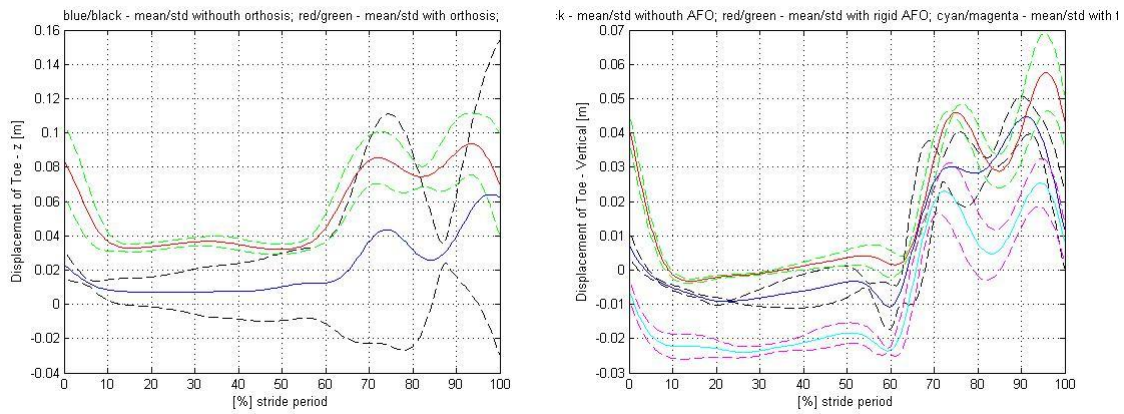
Figure 83 – Vertical displacement of Toe for: a) subject 1 (blue/black – without orthosis, red/green with hinged AFO b) subject 2 (blue/black – without orthosis, red/green with hinged AFO and cyan/magenta with foot-up orthosis)
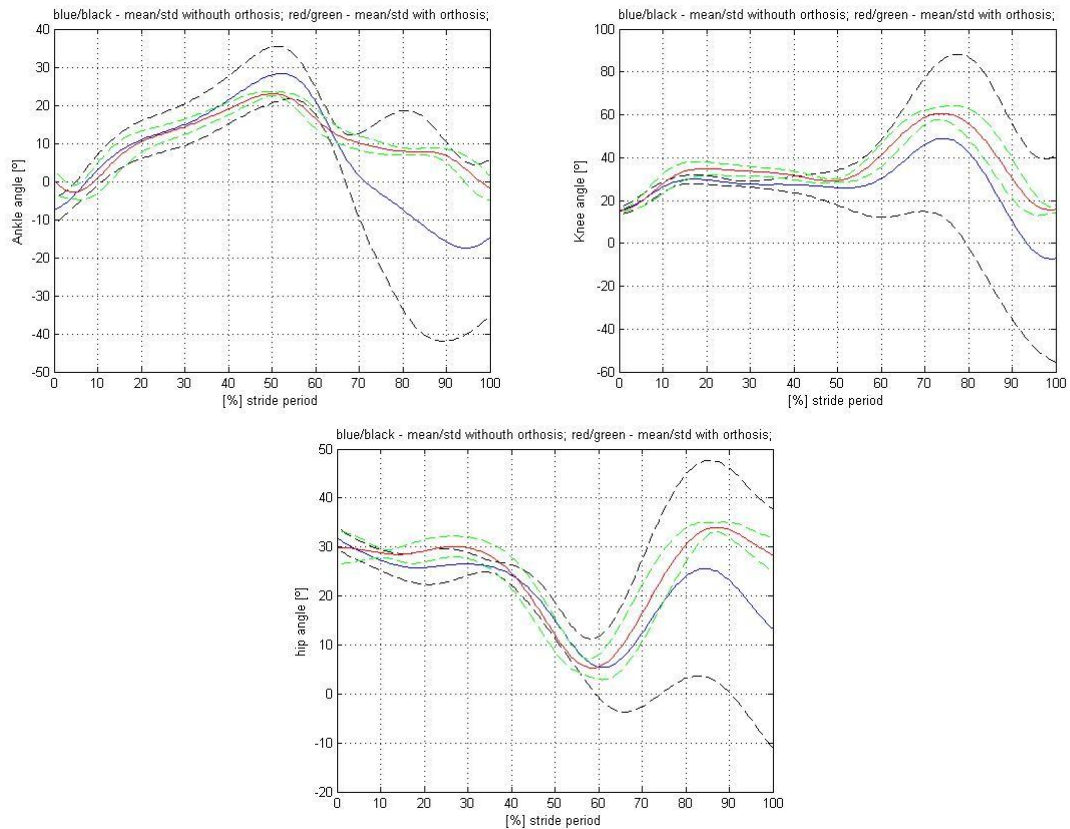
Figure 84 – Representation of joint angles for subject 1 without orthosis (blue/black), and with orthosis (red/green): a) ankle; b) knee; c) hip
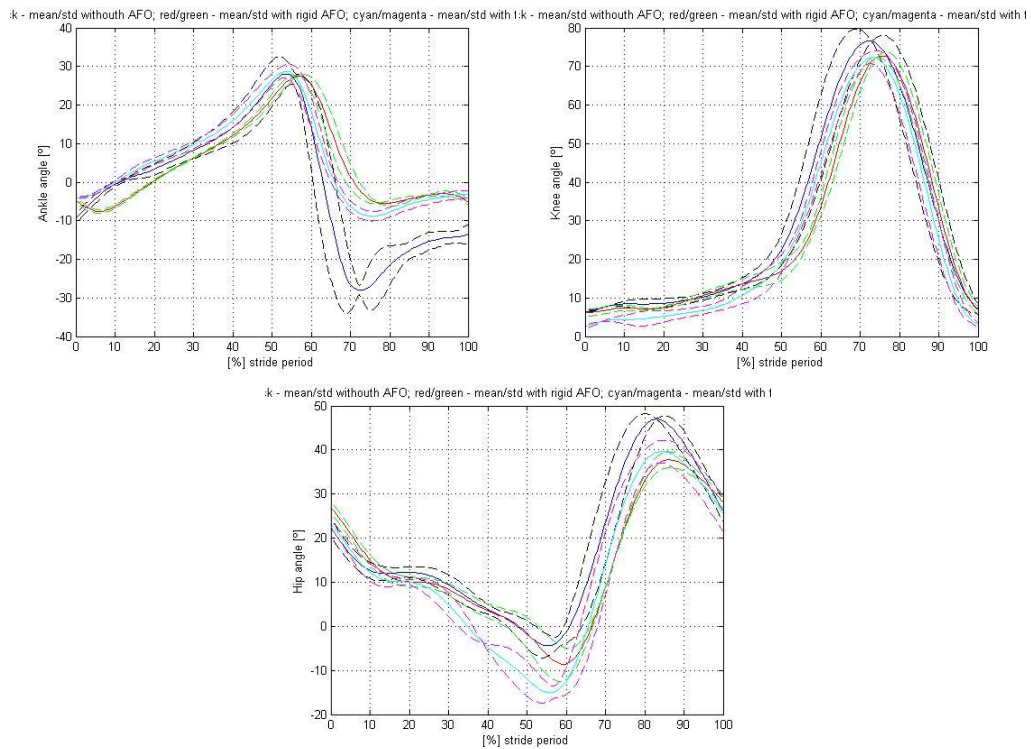
Figure 85 - Representation of joint angles for subject 2 without orthosis (blue/black), with hinged orthosis (red/green) and with foot-up orthosis: a) ankle; b) knee; c) hip
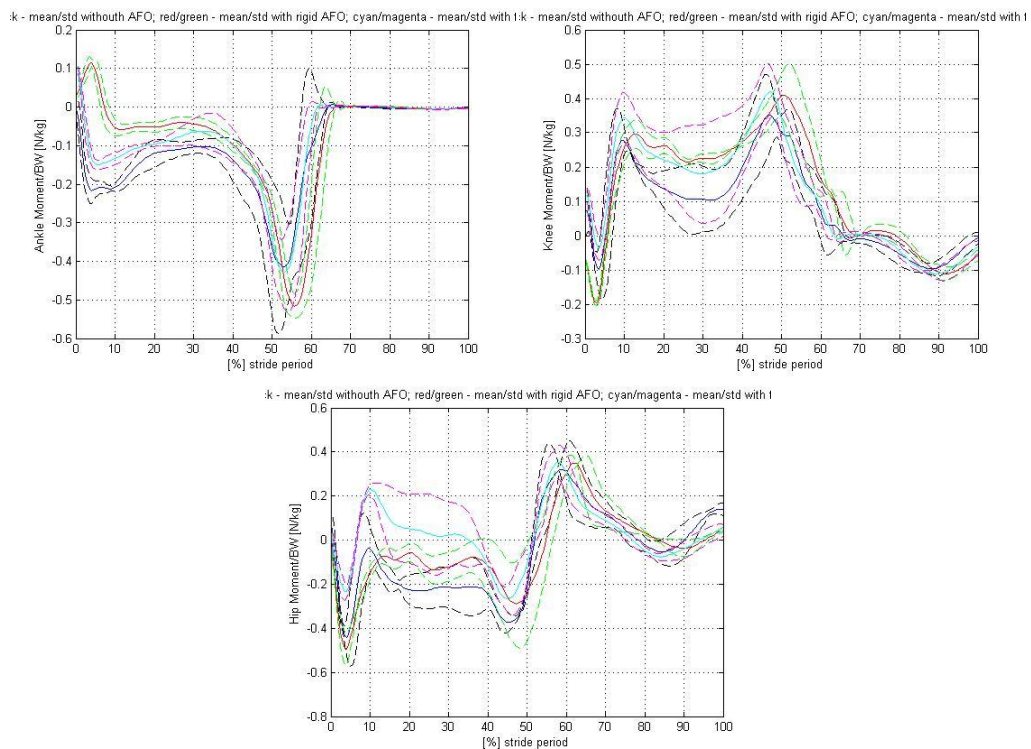
Figure 86 - Representation of joint moment of forces for subject 2 without orthosis (blue/black), with hinged orthosis (red/green) and with foot-up orthosis: a) ankle; b) knee; c) hip

157

Appendix G – Electromyographic results for subject 1 and 2
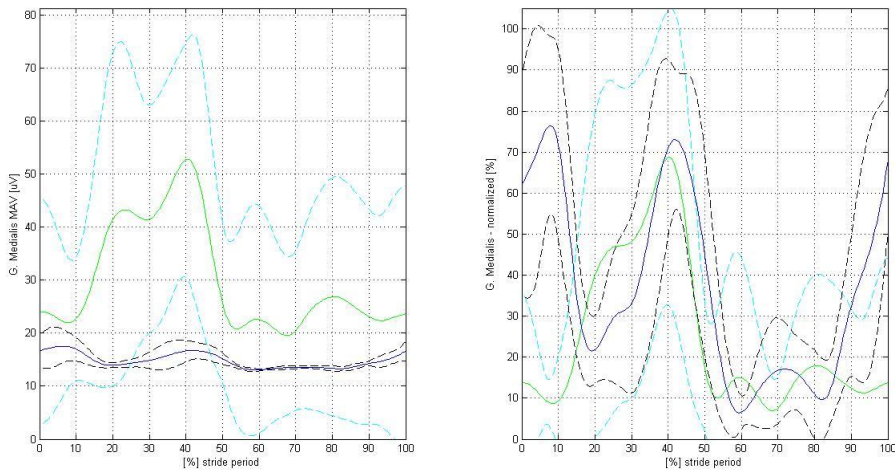
Figure 87 - Representation of sEMG signal of Gastrocnemius Medialis for subject 1 without orthosis (blue/black), and for a normal pattern (green/cyan): a) MAV b) Normalized
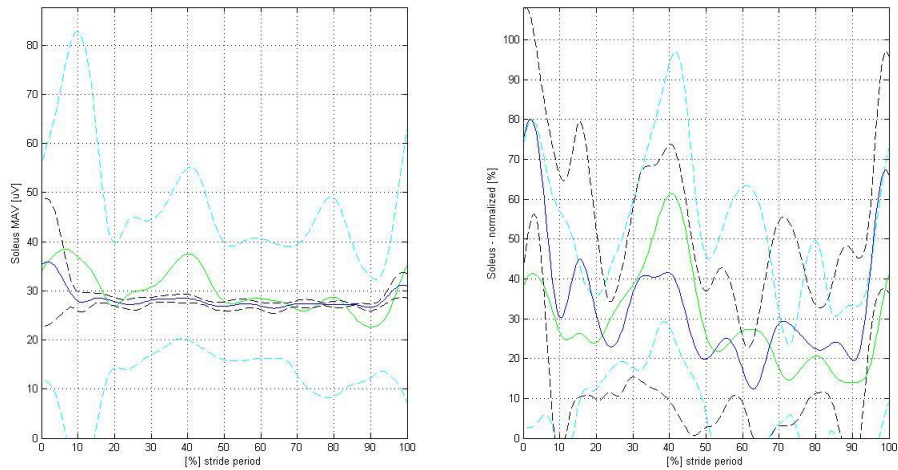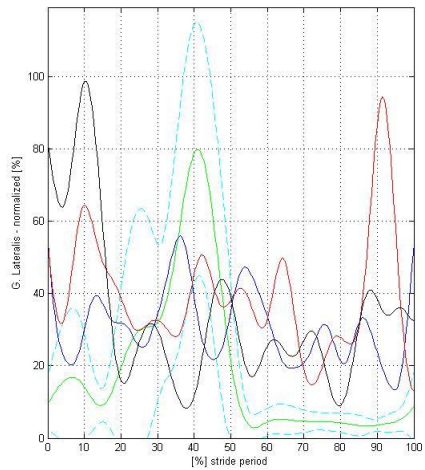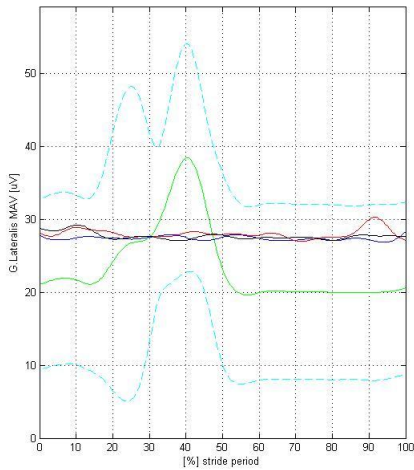

Figure 88 - Representation of sEMG signal of Soleus for subject 1 without orthosis (blue/black), and for a normal pattern (green/cyan): a) MAV b) Normalized
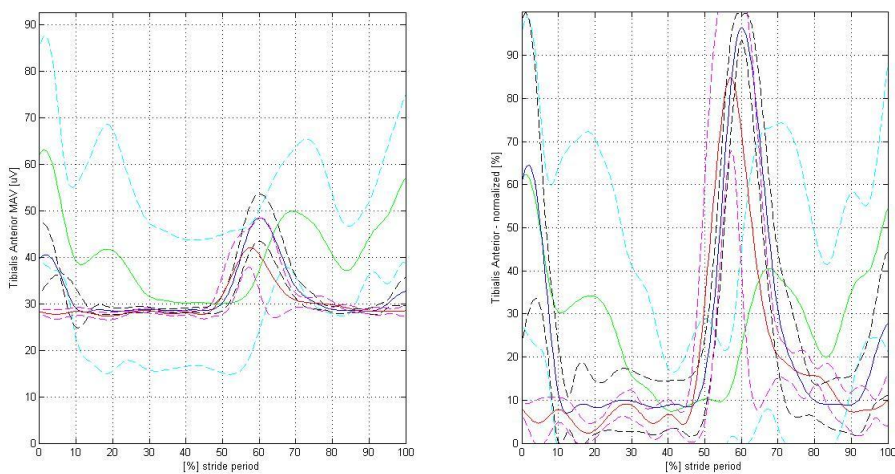
Figure 89 - Representation of sEMG signal of Tibialis anterior for subject 1 without orthosis (blue/black), and with hinged AFO and for a normal pattern (green/cyan): a) MAV b) Normalized
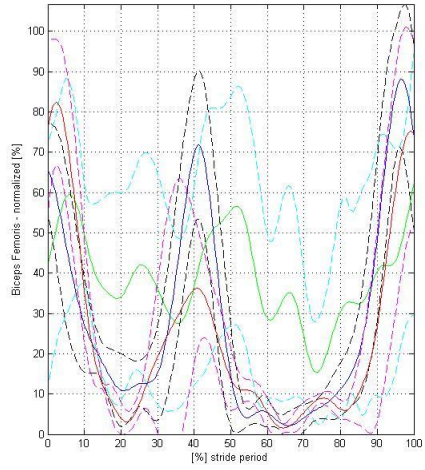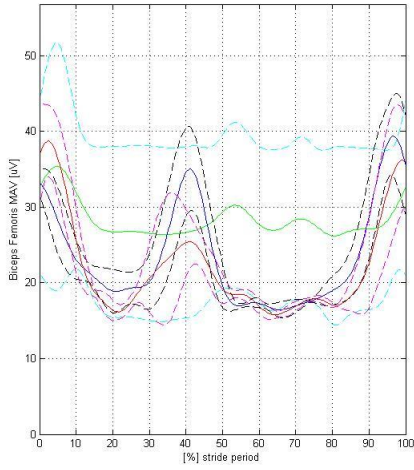
Figure 90 - Representation of sEMG signal of Biceps femoris for subject 1 without orthosis (blue/black), and with hinged AFO and for a normal pattern (green/cyan): a) MAV b) Normalized
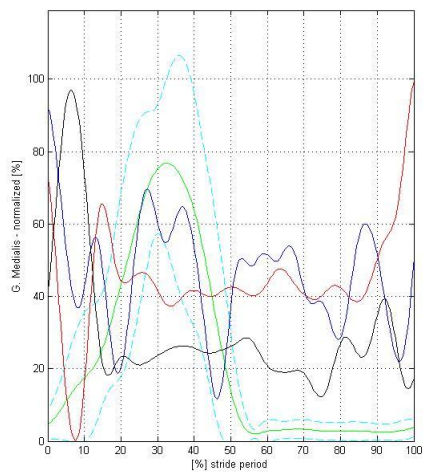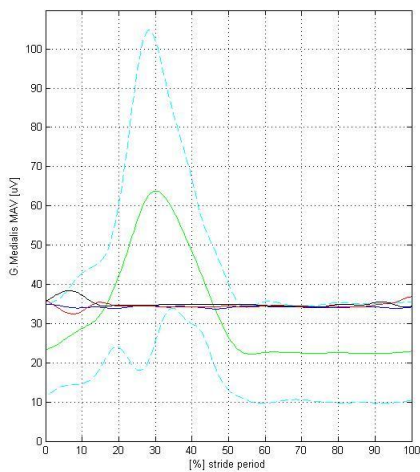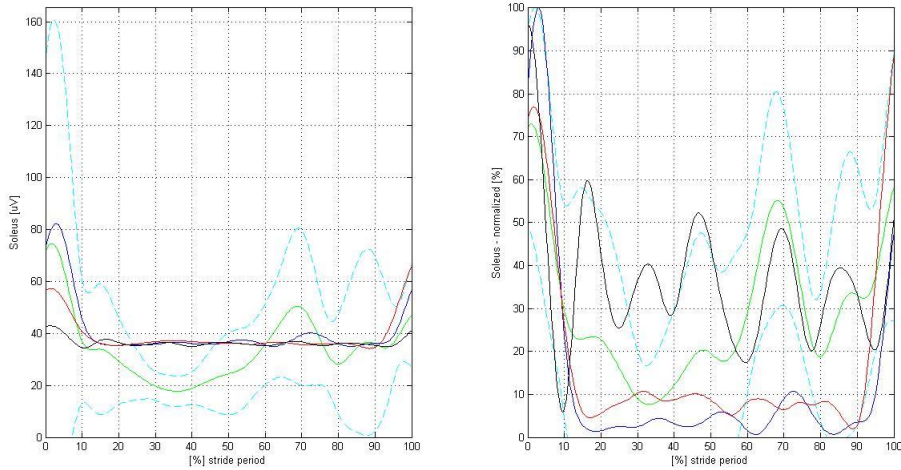
Figure 91 - Representation of sEMG signal of triceps surae muscles for subject 2 without orthosis (blue), with hinged AFO (red) and with foot-up orthosis (black), and for a normal pattern (green/cyan): a) Gastrocnemius Lateralis - MAV b) Gastrocnemius Lateralis –Normalized c) Gastrocnemius Medialis - MAV d) Gastrocnemius Medialis –Normalized e) Soleus - MAV f) Soleus –Normalized
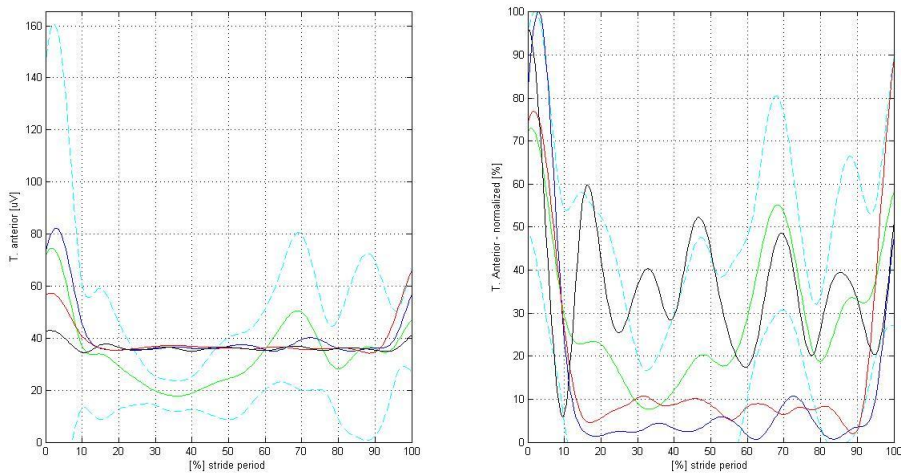

Figure 92 - Representation of sEMG signal of Tibialis anterior muscles for subject 2 without orthosis (blue), with hinged AFO (red) and with foot-up orthosis (black), and for a normal pattern (green/cyan): a) MAV b) normalized
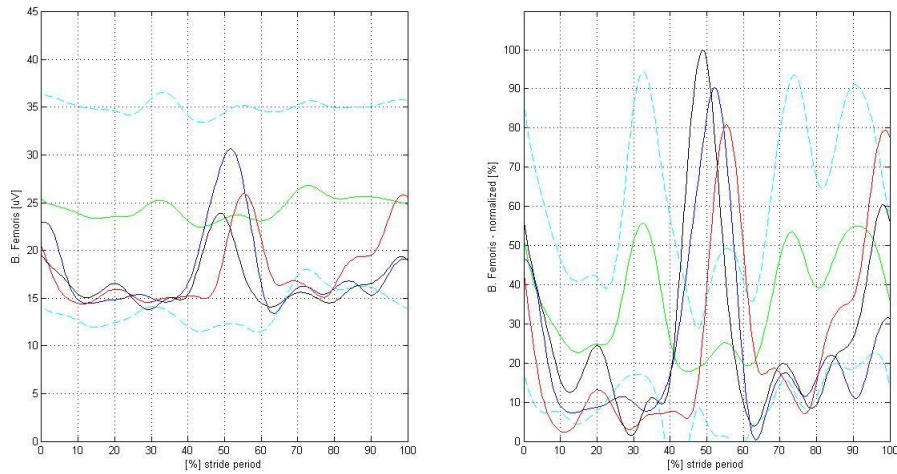
Figure 93 - Representation of sEMG signal of Biceps femoris muscles for subject 2 without orthosis (blue), with hinged AFO (red) and with foot-up orthosis (black), and for a normal pattern (green/cyan): a) MAV b) normalized
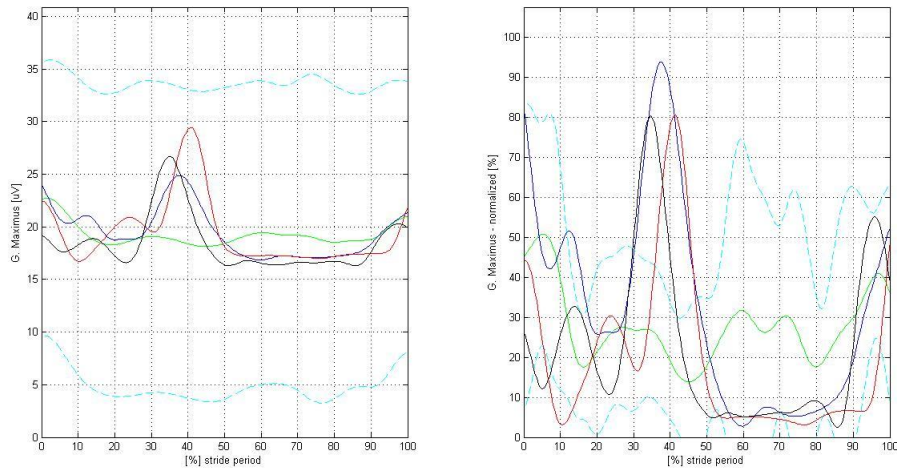

Figure 94 - Representation of sEMG signal of Gluteus maximus muscles for subject 2 without orthosis (blue), with hinged AFO (red) and with foot-up orthosis (black), and for a normal pattern (green/cyan): a) MAV b) normalized

161